Journal of Engineering

ISSN 1726-4073

A Scientific Refereed Journal Published by College of Engineering University of Baghdad

February 2014

Number 2

Volume 20

مجلة الهندسة

ISSN 1726-4073

مجلة علمية محكمة تصدرها
كلية الهندسة ـ جامعة بغداد

شباط
2014

العدد 2

المجلد 20

JOURNAL ENGINEERING

College of Engineering Baghdad University Baghdad

List of Contents

English Section: Page

Visual Continuity of Traditional Vocabulary in contemporary urban Development Projects

Dr. Wahda Shuker Al-Hinkawi
University of Technology
Dep. Of Architecture
Inana-ar@yahoo.com

Nada Abdul Mueen Hassan
University of Technology
Dep. Of Architecture
nadaabdulmueen@ahoo.com

ABSTRACT:
The sustainability of the individual and society get great interest in contemporary studies, Considering the rebuilding of the society cultural values as the most important goals, which prompted many researchers to explore ways and social elements of sustainability and the most important urban and architectural vocabulary achieving it, thus, the search will be directed towards the human being within the social dimensions of sustainability, his belonging and awareness of identity through the employment of local heritage in the contemporary product.
The literatures confirmed the continuity of heritage vocabulary in the contemporary product, accordingly the research problem was defined as: "**The visual continuity of the heritage vocabulary in achieving social sustainability**".
To deal with the research problem a theoretical framework was built for the concept of continuity in general, and visual continuity, in particular, and the application of concluded theoretical framework in a contemporary urban projects adopted the heritage vocabulary and expressed sustainable social identity, the results of the analysis showed that the visual continuity of traditional vocabulary achieved At highest level in the continuity of the surfaces organization in terms of optical properties and elevations treatments, and the continuity of formal relations in terms of scale and proportion, when ever the continuity of the local architectural style appears in the heritage formal elements.

Key words: Visual Continuity, Heritage Vocabulary, Social Sustainability, contemporary Urban Developments.

الاستمرارية البصرية للمفردات التراثية في مشاريع التطوير الحضري المعاصر

أ.م.د.وحدة شكر الحنكاوي
قسم الهندسة المعمارية/ الجامعة التكنولوجية

م.ندى عبد المعين حسن
قسم الهندسة المعمارية/ الجامعة التكنولوجية

المستخلص

تحظى استدامة الفرد والمجتمع باهتمام كبير في الدراسات المعاصرة، باعتبار ان اعادة بناء القيم الحضارية للمجتمع من اهم اهدافها، الامر الذي دفع كثير من الباحثين الى استقصاء سبل ومقومات الاستدامة الاجتماعية واهم المفردات المعمارية والحضرية التي تعزز ذلك، عليه فأن توجه البحث سيكون نحو الانسان ضمن ابعاد الاستدامة الاجتماعية وانتمائه وادراكه للهوية عبر توظيف التراث المحلي في النتاج المعاصر.

اكدت الطروحات ضرورة استمرارية المفردات التراثية في النتاج المعاصر، وعليه حددت مشكلة البحث بـ " **الاستمرارية البصرية للمفردات التراثية في مشاريع التطوير الحضري المعاصر**"". ولمعالجة مشكلة البحث تم بناء اطار نظري لمفهوم الاستمرارية

بصورة عامة والاستمرارية البصرية بصورة خاصة، وتطبيق الاطار النظري المستخلص في عينة قصدية من المشاريع الحضرية المعاصرة التي اعتمدت مراعاة أن تكون تلك النتاجات قد وظفت المفردات التراثية وعبرت عن هويتها الاجتماعية المستدامة، وقد اظهرت نتائج التحليل ان تحقيق الاستمرارية البصرية للمفردات التراثية يتحقق بنسبة اعلى في المشاريع المنتخبة في استمرارية تنظيم السطوح من حيث الخصائص البصرية ومعالجة الواجهات، واستمرارية العلاقات الشكلية من حيث المقياس والتناسب، اما استمرارية النمط المعماري المحلي فيظهر في العناصر الشكلية التراثية.

الكلمات المفتاحية: الاستمرارية البصرية، المفردات التراثية، الاستدامة الاجتماعية، التطوير الحضري المعاصر.

المقدمة

يتناول البحث الاستدامة الاجتماعية بابعادها المختلفة وصولا الى دور المفردات التراثية في تحقيق الاستدامة الاجتماعية، من خلال خلق نتاج حضري معاصر يتسم باستثمار المفردات التراثية وخلق بيئة حضرية تعزز الهوية الحضارية والانتماء المكاني وهي احد صيغ تحقق الاستدامة الاجتماعية.

اعتمد البحث فرضية استمرارية (يقصد بالاستمرارية هنا ليس التواصل ولكن الاستمرارية البصرية للتكوين الحضري سواء كان على مستوى المشهد او النسيج الحضري.) المفردات التراثية في النتاج لخلق صورة حضرية متكاملة، لهذا يسعى البحث الى تحديد ابعاد الاستمرارية البصرية في العمارة ، واستمرارية المفردات التراثية في النتاج المعاصر، اعتمد البحث تعريف الاستدامة الاجنماعية وتحديد ابعادها المختلفة وصيغ تحقيقها في النتاج الحضري المعاصر، وصولا الى صيغ تحقيق الاستمرارية في المفردات التراثية في النتاج الحضري المعاصر.

1. المحور الاول: الاستدامة الاجتماعية

يرى بعض الباحثين إن العمارة المستدامة "هي اعادة توجيه الاطار المفاهيمي للعمارة لتتجاوب مع الاهتمامات المتعددة لتاثيرات الفعاليات الانسانية على البيئة، بما يؤكد البعد الاخلاقي للعمارة والذي يعنى بكيفية معيشة الانسان من خلال تعامله مع الاخرين والعالم بحيث يكون السلوك الانساني نحو البيئة بشكل اكثر مسؤولية"؛ فالعمارة التي تحقق مبادئ الاستدامة والتي لها اقل تأثيرات سلبية على

البيئة الطبيعية والمشيدة سواء على مستوى البيئة المحلية او الاقليمي والعالمي، هي العمارة التي تكرس القيمة التكاملية للاداء الاقتصادي والاجتماعي والبيئي.(الزبيدي،2006،ص ج).

ان التعامل مع فكر الاستدامة في العمارة يضع في مقدمة اولوياته الرجوع الى الجوانب الاجتماعية المرتبطة بالقيم والعادات والتقاليد والاعراف، فضلا عن الاعتبارات الثقافية والرمزية التي لايمكن اغفالها ضمن توجهات العمارة، وان ارتباط مفهوم الاستدامة بكل هذه الامور يفتح الباب امام تطبيقات ناجحة تدعم التواصل الحضاري وتزيد التقارب بين الاجيال (الأحبابي،2010، ص102). وان تحقيق الحل الامثل للتخطيط والتصميم الحضري المستدام يكمن في احياء مفاهيم قديمة أثبتت نجاحها في البنية الحضرية التقليدية مثل (المدينة المتراصة، الاستخدام المختلط للارض وتعزيز حركة المشاة) (عن المصدر: نعمة والاحبابي،2011، ص 135).

بينت الدراسات تجاوب التخطيط العام للمدينة التقليدية ووحدة الجيرة والمسكن التقليدي مع البيئة المحيطة، على وفق مفهوم الاستدامة،التي تحقق عبر مواءمتها مع القيم

الاجتماعية وعادات وتقاليد المجتمع (نعمة والاحبابي،2011، ص 148).

1.1.المفهوم العام للاستدامة الاجتماعية

عكف برنامج الامم المتحدة الانمائي (UNDP) في نشاطه على الجوانب البشرية للاستدامة، نتيجة لأزمات التنمية[1] المستعصية، مشجعا على بروز رؤية جديدة للاستدامة، تم توضيح هذه الرؤية الجديدة من خلال التقارير السنوية التي يصدرها البرنامج منذ عام (1990)، وبحلول عام (1993)، اطلق البرنامج هذه الرؤية الجديدة للاستدامة تحت عنوان "**الاستدامة الاجتماعية**" التي تضع الانسان في قمة سلم اولوياتها من خلال التاكيد على ان "الناس هم الثروة الحقيقة للامم".

جاء في تقرير التنمية البشرية لعام (1990) تعريف الاستدامة الاجتماعية على انها "عملية توسيع خيارات الناس"، ومن بين هذه الخيارات: (الحريات السياسية والاجتماعية والاقتصادية والثقافية، وكذلك التمتع باحترام الذات، والتمكين بالاحساس بالانتماء الى المجتمع، وتاكيد الهوية الاجتماعية)،(Human Development Report, 1990,P.10). اما تقرير الاستدامة الاجتماعية لعام (1993) يعرف الاستدامة الاجتماعية على انها "استدامة الناس، من اجل الناس، بواسطة الناس". فاستدامة الناس تعني الاستثمار في قدرات البشر في المجالات المختلفة وإدامة قيمهم المجتمعية حتى يمكنهم من العمل على نحو منتج وخلاق، والاستدامة من اجل الناس معناها كفالة الاجتماعية والعدالة والمساواة الاجتماعية، والاستدامة بواسطة الناس معناها إعطاء كل امرئ فرصة المشاركة فيها. (تقرير التنمية البشرية،1993،ص3). ويشير تقرير التنمية البشرية لعام (1994) الى ان الاستدامة الاجتماعية: "هي نموذج للتطور يمكّن جميع الافراد من توسيع نطاق قدراتهم البشرية الى اقصى حد ممكن وتوظيف تللك القدرات افضل توظيف لها في جميع المجالات، وهو يحمي ايضا خيارات الاجيال التي لم تولد بعد، ولا يستنزف قاعدة الموارد الطبيعية اللازمة لدعم التنمية في المستقبل" (Human Development Report،1994,P.4).

وتتجلى أهمية الاستدامة الاجتماعية في انها "تعترف بالتنوع، وتقبل بامكانية وجود عدة انماط متوازية تؤدي كلها الى الاستدامة"، وبامكانية اختيار كل بلد للنهج التطوري الذي يراه صالحا له رغم تبني الجميع لنفس الاهداف التطويرية البعيدة المدى، وهي مقاربة تعطي الاولوية للاستنباط والاستحداث المتجذر في التجارب السابقة، وهكذا تصبح التقاليد والاعراف والخصوصيات والهوية الاجتماعية– الثقافية مصدرا للثراء والإثراء وليس حاجزا في طريق الاستدامة الاجتماعية (حمزة،1999،ص1). وتلتقي الاستدامة الاجتماعية مع حقوق الانسان، حيث تؤكد على الحرية الثقافية بوصفها جزءا لايتجزأ من حقوق الانسان. وتعرف الحرية الثقافية بأنها الحرية التي ينعم بها الناس لاختيار هوياتهم، ولان يكونوا ما يشاؤون والعيش دون استبعاد من خيارات اخرى، ذات اهمية لهم (تقرير التنمية البشرية،2004،ص22).

2.1.أبعاد الاستدامة الاجتماعية

تناولت الدراسات المعمارية ابعاد الاستدامة الاجتماعية وأهم المحاور التي يمكن تحقيقها من خلالها، فقد اشارت (الزبيدي،2006) الى التنمية المستدامة والابعاد الاجتماعية كجزء من الاهتمام بالبيئة الانسانية من النواحي الاجتماعية والنفسية والحضارية. فالنمو السكاني المستمر لفترة طويلة وبمعدلات شبيهة بالمعدلات الحالية أصبح يشكل ضغوط حادة على الموارد الطبيعية وعلى قدرة الحكومات في توفير الخدمات، كما ان النمو السريع للسكان في بلد أو منطقة ما يحد من التنمية ويقلص من قاعدة الموارد الطبيعية المتاحة

[1] تعرف التنمية على انها: حصيلة تفاعلات سياسية واقتصادية واجتماعية وادارية متداخلة ومستمرة تشكل كل منها، وبدرجة متفاوتة، عاملا مستقلا وتابعا في آن واحد، كما يمكن تعريفها على انها: كل ما يحيط بالجوانب المتصلة بالسكان، واستخدام الموارد الطبيعية وادارة البيئة. او هي كافة المتطلبات الاساسية، وتوفير الرفاهية لجميع البشرية لانجاز تطلعاته من اجل حياة افضل (قنطقجي،2009،ص3).

لكل فرد. ان أهم أهداف التنمية الاجتماعية هو تحقيق التمكين الاجتماعي[2] والاستقرارية لمختلف المجتمعات الانسانية من خلال تحقيق مبدأ المساواة وتوفير فرص العمل والتواصل مع الاخرين دون فقدان الهوية الحضارية لكل مجتمع ضمن البيئة والمؤثرات المحيطة (الزبيدي،2006،ص32،35). وجاء في دراسة (بابان،2004) ان الابعاد الاجتماعية تعني الحفاظ على المجتمع والانسان بصورة رئيسة، أي الحفاظ على المجتمع والانسان بصورة سليمة. مغزى المجتمع الرئيسي احتوائه على أو ضمه للهوية والتراث، المساواة، التماسك الاجتماعي، التنوع، القدرة على التحمل، التعددية، الاصالة، والنظام (بابان،2004،ص10).

وبينت دراسة (Stenberg,1999) الشروط الأساسية لتحقيق الاستدامة الاجتماعية ضمن أي محيط خلال توفير مكان جيد للعيش يتضمن مسكناً جميلاً ومريحاً، صيانة وأماناً، وعلاقات جيدة مع الجيران، ورعاية صحية، ومميزات ثقافية، ووسائط نقل مريحة، وعمل مناسب يدر دخلا كافيا، وإمكانية التطور والنمو الشخص (P2 Stenberg,1999,).

وبصورة عامة لا يكون النظام مستداما اجتماعيا إلا إذا كان متبنيا لمجموعة من الأهداف والمعايير والتي تشمل حماية الصحة العقلية والبدنية لجميع أصحاب المصلحة (Greenwood,2004,P.2) والحفاظ عليها لتحقيق الدور التربوي (Yung,2011) وتشجيع التفاعل والفعاليات الاجتماعية وتوفير الخدمات الاساسية لبناء مجتمع صحي وتحقيق العدالة والمسؤولية الشخصية والجماعية اللازمة للمجتمع للحيلولة دون تحوله الى حالة من الفوضى، كما تشمل توزيع الخدمات الاساسية على نحو فعال لجميع من يحتاج اليها وتوفير فرص التطوير الشخصي والاجتماعي متضمنة تشجيع إمكانية الوصول الى وسائل ومؤسسات التعليم، اضافة الى خلق أماكن ذات هوية فريدة تجمع الثقافة مع التراث (Greenwood,2004,P.2) وتعزيز الإحساس بالمكان والثقافة المحلية والذاكرة الجماعية (Yung,2011) حيث يعيش أفراد من خلفيات مختلفة ويتطورون معا الى مجتمعات متكاملة ومزدهرة لها القدرة على التربية وتعليم عائلاتهم والاستفادة من فرص التوظيف والاستجمام المتنوعة وذات الجودة العالية، وخلق بيئة تعزز الصحة والسعادة والأمن وتحترم الخصوصية وتشجيع النفاذ الى الطبيعة والفضاءات الخارجية المفتوحة وتعزيز جودة الحياة فيها وتأسيس طرق اتصال سهلة ومريحة بحيث تعتبر أماكن تواصل، وإيجاد الحلول المثلى لمعالجة أية تطورات أو تعقيدات في المجتمع (Greenwood,2004, P.2).

إذ شخصت دراسة نعمة والاحبابي أثر المنظومة الاجتماعية في استدامة البنية الحضرية التقليدية، وفيما يتعلق بالمستوى التخطيطي للمدينة التقليدية (المستوى الحضري)، فأن الخصوصية التي تتمتع بها الفضاءات الحضرية ودرجة الاحتواء العالية تساهم في صياغة هوية مميزة للمنظومة بامكانها التعبير عن جوانب كثيرة اجتماعية ووظيفية وبيئية ذات صلة بالاستدامة، ومن هذه الجوانب ما يأتي: (مفهوم الأحتواء، الفضاء الانتقالي الرابط، عنصر المفاجأة، **الامتداد البصري والحركي**، المحاور الرمزية، ومفهوم الخصوصية) (نعمة والاحبابي، 2011، ص138).

أفرزت الطروحات الدراسات السابقة جملة من الابعاد الخاصة بمفهوم الاستدامة الاجتماعية والتي اهتمت في رسم ملامح المفهوم التي يمكن اعتمادها لتحقيق العمارة المستدامة وكما مبين في الجدول (1).

[2] يعتبر مفهوم التمكين المستدام إعادة صياغة لمفهوم التمكين في عمليات العمارة المستدامة، فهو يعني اتاحة الفرصة للمجتمع للقيام بدور فعال في جميع مراحل عملية الاستدامة، بكل من الجوانب العمرانية والادارية والاجتماعية والاقتصادية من حيث اتخاذ القرار، التخطيط، التنفيذ، المتابعة، والتقييم. ويعتمد التمكين المستدام على آليات تفعيل مفاهيم مثل المشاركة الشعبية وبناء القدرات من أجل تحقيق الاستدامة الاجتماعية في البيئة العمرانية والحضرية (الأحبابي،2010، ص72-71).

جدول (1): أبـــعاد الاستدامة الاجتماعية/ المصدر: الباحثتان

	المفردات الرئيســـــة	المفردات الثانويـــــــــة	
أبعاد الاستدامة الاجتماعية	مميزات المجتمع المستدام	التنوع	التعددية
		الاصالة	النظام
		التجديد	القدرة على التحمل
	مستويات الاستدامة الاجتماعية	الاستدامة المحلية	**استدامة الهوية الحضارية- الثقافية**
			استدامة المكان
		استدامة النظام الاجتماعي	العدالة الاجتماعية: المساواة
			التفاعل الاجتماعي: الفعاليات الاجتماعية
			التماسك الاجتماعي: الخصوصية
		التمكين الاجتماعي	المشاركة الاجتماعية: المسؤولية الشخصية والاجتماعية
			بناء القدرات: امكانية التطور والنمو الشخصي والاجتماعي
	أهداف ومعايير الاستدامة الاجتماعية	توفير مكان جيد للعيش (جميل،مريح،آمن)	رعاية وحماية الصحة العقلية والبدنية
		توفير فرص التوظيف والاستجمام	توفير وتوزيع الخدمات الرئيسة بشكل فعال
		تعزيز جودة الحياة	العلاقة مع الطبيعة والفضاءات الخارجية المفتوحة
		ايجاد الحلول المثلى	تأسيس طرق اتصال سهلة ومريحة- اماكن تواصل

مما تقدم يتضح تاكيد مفاهيم الاستدامة الاجتماعية على خصوصية الهوية الاجتماعية – الثقافية والتراث، والتأكيد عل الانفتاح على باقي الشعوب بما يحقق الاستدامة الاجتماعية.

وسوف تناقش الفقرة **التالية استدامة الهوية الحضارية– الثقافية** كونها إحدى مقومات الاستدامة الاجتماعية وتوضيح العلاقة بين الاستدامة والتعبير عن الهوية الاجتماعية– الثقافية من جهة وعلاقتها بالعمارة والبيئة المبنية من جهة اخرى.

3.1. علاقة الهوية (الاجتماعية – الثقافية) والاستدامة الاجتماعية في العمارة

وتشمل هذه الفقرة التعريف بالهوية الاجتماعية والثقافية وتعبيرها عن التراث

1.3.1. الهوية الاجتماعية – الثقافية والتراث

أن ما يمنح العمارة سماتها هي الفوارق الواسعة في المناخ والظروف الاقتصادية والعادات والتقاليد، وهي فوارق معمارية يؤكد وجوب الاحتفاظ بها، لأنها تمنح العمارة هويتها المحلية، وتؤكد نزعتها للتكيف المكاني من أجل الاستعمال الأفضل للأحيزة والتمتع بها من قبل الناس (Corea,1990,P.25). وتعرف الهوية المعمارية بأنها امتلاك العمارة لجوهر خاص، لتمثل التناغم المثالي المتواصل بين الشكل، والثقافة، والمكان، والمناخ (Able,1997,146-167). ويعرف (النعيم،2002) الهوية العمرانية بأنها "اطار بنيوي يتحقق عبر التفاعل بين الافراد والجماعات، وبين عناصر البيئة العمرانية، وبهذا تصبح الهوية في حالة تشكل مستمر، اي ان الهوية العمرانية جزء من الهوية الثقافية لمجتمع من المجتمعات" (النعيم،2002 ،ص98-104). اما تعريف (Hall,1996) للهوية الثقافية فهي موضوع الكينونة والارتباط بالمستقبل والماضي على حد سواء، حسب (Hall) هناك طريقتين للتفكير بالهوية الثقافية: الاولى، يعرف **الهوية الثقافية كهوية تعكس موروث المجتمع**. انها تبدو كخطوة تتجاوز الزمن كما يدعم **التراث** من اجيال عدة. والثانية، يفكر بالهوية الثقافية كإطار من محورين: الاول (التشابه والاستمرارية) والثاني (الاختلاف والانقطاع) (Hall, 1996, P.13). أكدت دراسة (أمين،2007) على استغلال التراث للحفاظ على الهوية الاجتماعية، حيث يلعب التراث دورا هاما في صياغة ذاكرة الامم وعمقها الحضاري وتمايز ثقافتها المحلية، وقد اشار العديد من المعماريين الى أهميته، فتشير الدراسة الى ان الجادرجي في مقالته "التراث ضرورة،1981" قد عرف التراث على انه: "الرصيد والمخزون المتميز الذي يتميز بالثبات والاستمرارية ويجمع بين القيمة الروحية والجمالية بالاضافة الى كونه حقيقة مادية ملموسة فرضت قبولها واحترامها لكونها تسجيلا صادقا لثقافة المجتمع ووحدة منهجه وملامحه الانسانية والفكرية عبر العصور فهو تعبير عن اسلوب ومنهج التعامل مع المحيط وضواغط الماديات خلال فترات متباينة الظروف وبالتالي هو ضرورة اجتماعية (أمين،2007،ص300).

ان **التراث المعماري** كائن حي نابض ومؤثر في المجتمع فهو "مصدر للافكار ومرجعية لها". كما يشير (التوني، 1988) الى ان التراث هو "التجسيد المتميز لثقافة الجماعة في حقبة أو حقب بعينها فهو تعبير صادق عن محققات الثقافات المحلية والقومية" (التوني،1988،ص24). لذا يعتبر التراث المعماري والعمراني رمزا للتطور الانساني عبر التاريخ وتعبيرا عن القدرات التي وصل اليها الانسان في التغلب على مشاكل البيئة المحيطة، وكلمة التراث تعني الشئ الموروث عبر الاجيال وهي تعني الاهمية الاجتماعية أو الحضارية أو السياسية أو الدينية للشئ المتوارث والتراث المعماري مرتبط بتجربة عمرانية قد مر بها الانسان وتولدت عن هذه التجربة معان وقيم وهوية عمرانية ارتبط بها الانسان وقد لخصت الدراسات الى ان التراث العمراني هو تتابع لتجربة وقيم

حضارية واجتماعية ودينية بين الاجيال (الأحبابي،2010، ص102).

وبتحليل الرؤى السابقة يجد البحث ان التراث (الموروث) المعماري أو العمراني تجسيدا وانعكاسا حقيقيا لثقافة المجتمعات وهويتها وعنصر مهم من عناصرها، ونظرا لامتلاكه خصائص متجددة ناتجة من امكانية حل مشاكل البيئة المحيطة بصورة مستمرة، لذا فالاعتماد عليه يعني في واقع الامر استدامة اجتماعية من خلال استدامة الهوية والثقافة المحلية.

2.3.1. التطبيقات الاجتماعية في العمارة المستدامة (الهوية المعمارية المستدامة):

ان جوهر آلية خلق مدينة مبدعة ومميزة ومتفردة هو استغلال القوة الكامنة للعوامل الثقافية والاجتماعية، كما شهد منتصف التسعينات التحول نحو مفردات مثل "المؤشرات الثقافية" والتي تضمنت (العوامل التاريخية، والتراث الفني، والعمارة، والمعالم الاثارية) (Charles P.xxxi landry,2008,). والدعوة الى توظيف العوامل الثقافية والاجتماعية لخلق مدن مستدامة وفي مقدمتها استيعاب الحراك الاجتماعي والفكري والتراث الثقافي للمجتمع الذي يمثل الذاكرة الجمعية. فهي استدامة الشعور بالانتماء للمدينة وسبيل لمواجهة المستقبل، في ظل الأثر السلبي للعولمة على الاستقرار الاجتماعي والجذور المحلية، فالتراث الثقافي هو: "ابداع الماضي ومن نتائج هذا الابداع الحفاظ على المجتمع في حركة دائمة (Charles landry,2008,P.16).

وفيما يخص حفظ الهوية الثقافية والإقليمية فأن الأنماط المعمارية الموجودة في الوقت الحالي تستجيب إلى العوامل الثقافية والمناخية، وتشير الأدبيات المتعلقة بهذا الموضوع إلى أن جميع المعلومات يجب أن تستغل في بناء التصميم ليس فقط من وجهة نظر الطاقة الكفوءة ولكن في خلق الحيوية عبر الحفاظ على الثقافة المحلية للمنطقة والعادات وخلق الإحساس بالمكان، وهذا يتحقق من خلال: استعمال مواد منتجة محليا قدر الإمكان مما يبقي على الهوية الإقليمية ويعزز الاقتصاد المحلي ويساعد البيئة كما تنخفض الحاجة لعملية نقل المواد؛ استخدام العمال المحليين قدر الإمكان، إذ يخلق الإحساس بالاهتمام باليد العاملة المحلية وبلورة الإحساس بالملكية لدى أفراد المجتمع؛ استخدام العناصر المعمارية والملامح المميزة في المنطقة المحلية، إذ يوجد توجهان فكريان لهذا الموضوع: الأول: استخدام العناصر المعمارية المحلية والمواصفات التي تصمم عموما بوصفها استجابة للبيئة والمناخ الإقليمي والثاني: استخدام العناصر المعمارية التي تبقي الثقافة والهوية المحلية وتخلق الإحساس بالمكان؛ اختيار مواد البناء التي تستعمل في الهيكل الإنشائي (بثيون،2005،ص ص34-36).

أفرزت المعرفة السابقة مجموعة من المؤشرات الممكن تحقيق الاستدامة الاجتماعية واستدامة الهوية المعمارية من خلالها:

- **توظيف العوامل الثقافية والاجتماعية.**
- **تغلال التراث للحفاظ على الهوية الاجتماعية- الثقافية.**
- **استخدام مواد وتقنيات البناء المحلية.**
- **استخدام الانماط والعناصر المعمارية المحلية.**

ولكن ان هذه الدراسات لم تحدد صيغ استثمار المفردات التراثية في تكوين المشهد الحضري المعاصر. ولهذا يفترض البحث ان الاستمرارية البصرية للمفردات التراثية في المشهد الحضري احد صيغ تحقيق الاستدامة الاجتماعية.

مما يتطلب دراسة خاصية الاستمرارية (الامتداد) البصرية للمفردات التراثية التي تساهم في صياغة هوية مميزة وعلى مستوى النسيج العمراني القديم منه والحديث.

2. المحور الثاني: مفهوم الاستمرارية

يتناول البحث مفهوم الاستمرارية من خلال استعراض التعريف اللغوي والاصطلاحي أولا، والاستمرارية في

الطروحات والدراسات المعمارية والحضرية ثانياً، وأخيرا يتناول البحث الاستمرارية من وجهة النظر السايكولوجية.

1.2. الاستمرارية لغوياً

الاستمرارية فى اللغة العربية: من مرر والمرار، يقال: فلان يصنع الأمر ذات المرار، أي يصنعه مراراً ويدعه مراراً. ومر عليه وبه يمر مراً ومر ومراً: ذهب واستمر مثله. ويقال استمر مريرة، أي استحكم عزمه (البردي). وترد الاستمرارية تحت مصطلح (Continuity) باللغة الانكليزية، وكما جاء في معجم (Webster) والتي من معانيها:

- اتصال بدون انقطاع (متواصل)، متعاقب، أو توحيد.

Uninterrupted connection, succession, or union.

- استمرار بدون تغير اساسي.

Persistence without essential change.

- ما يميز خاصية الوظيفة المستمرة.

The property characteristic of a continuous function. (Webster, P.243)

- خاصية أو حالة كونه مستمر.

The quality or state of being continuous.

- شئ يملك أو يوفر الاستمرارية.

Something that has or provides continuity

(Webster, 2010 Ultimate DVD)

وتحت مصطلح (Continuous):

Marked by Uninterrupted extension in space, time, or sequence (Webster, P.243).

- امتداد متواصل(بدون انقطاع) في الفضاء،الوقت،أومتتابع.

2.2. الاستمرارية اصطلاحاً:

أشارت الطروحات الى الاستمرار (continuation) بأنه طريقة التي تحقق الوحدة. ويعني ايضا أن شيئا "يستمر" – عادة ما يكون خط، حافة، أو اتجاه من شكل إلى آخر. وتنتقل عين المشاهد بسلاسة من عنصر إلى آخر (Lauer& Pentak, 2008, P.38). فالاستمرار هو ترتيب المخطط لأشكال مختلفة بحيث تصطف حوافها بالتالي (Ibid, P.40). و يستخدم مصطلح الاستمرارية (Continuity) غالبا للدلالة على العلاقة البصرية بين اثنين أو أكثر من التصاميم الفردية (Ibid,P.41).

مما تقدم من تعريفات لغوية واصطلاحية يمكن تحديد أهم الجوانب المعرفة للاستمرارية بصورة عامة كما يأتي:

- **صيغة لتحقيق الوحدة والترتيب.**
- **تكرار أو تعاقب لعلاقة بين شيئين أو أكثر ممكن ان يكون خط، حافة، اتجاه، أو أشكال مختلفة.**
- **التأكيد على الجوانب البصرية التي تحكم العلاقة بين الاشياء.**

3.2. الاستمرارية في العمارة والتصميم الحضري

تناولت الطروحات والدراسات مفهوم الاستمرارية من خلال تركيزها على جانبين اساسيين، الاول يتعلق بتحليل وتفحص التكوين الحضري وفق مفردات مبادئ التصميم الاساسية، والثاني يرتبط بالخصائص البصرية، وحسب توجهاتها النظرية والفكرية.

تناولت طروحات (يوسف، 1983) استمرارية المباني– عناصر التشكيل (وظيفيا وتشكيليا) كأبرز المعالجات البصرية في تشكيل المدينة، وهي إما استمرارية في حدود التشكيلات أو في اسطحها .. (مثل خط السماء والارتداد في المباني) مع تقارب الأجزاء بحيث تحقق وحدة أو وحدات في المجموعة المتكاملة من التشكيلات، وتحقيق التكرار الإيقاعي لفواصل التشكيل، والتجانس، والتماثل، والمحاكاة في الاسطح والأشكال والاستخدامات، فكل هذه المعالجات في الاستمرارية تعمل على تأكيد ادراك التكوينات الفيزياوية كعنصر بصري واحد، أو كعدة عناصر متداخلة العلاقة وذات طابع أو شخصية واحدة متميزة (يوسف،1983).

فيما بينت طروحات (Amin,1988) الامتداد المستمر والمتجانس للمكونات الفيزياوية لبنية الفضاءات المفتوحة الذي ينتج عن التناغم في العلاقات بين المكونات البصرية وبالتالي يقود الى الاستمرارية البصرية – من حيث المقياس، التناسب، الارتفاع ،الصلادة والفراغ، استمرارية اللون ومواد البناء، استمرارية خط السماء. (Amin,1988,p82)

واشار (الحيدري،2010) الى الاستمرارية والتجانس كمبادئ معتمدة في تنظيم المشهد الحضري، ويتبلور الامتداد المستمر والمتجانس في تكوينات المشهد الحضري نتيجة التناغم في العلاقات بين مكوناته البصرية، وبالتالي تحقيق الحفاظ على وحدة التكوين وتجنب التناقض بين مكونات النسيج العمراني القديم منه والحديث (الحيدري،2010،ص 12).

وتناولت دراسة (القره غولي، 1999) صيغة تحقق الوحدة الشكلية ضمن التعددية المتناغمة، وبما يحقق التناغم والتجانس من خلال مفهوم الترابط الذي يشير الى الكل المتماسك ويعرف من خلال الاستمرارية والتشابه والتجاور. حيث تشير الاستمرارية الى علاقات التراصف، التكرار والتتابع، الايقاع المتناسب (المنتظم وغير المنتظم)، حركة العين المستمرة ما بين الاجزاء، بالاضافة الى علاقة الاحتواء لاكمال الاشكال الناقصة (القره غولي،1999،ص116-117).

واختصت دراسة (علي،2012) توضيح الخصائص الشكلية للفضاءات المفتوحة المدينة التقليدية التاريخية وتاثيرها على الشكل الحضري العام للمدينة. وإن أهم مايميز الفضاءات المفتوحة والميادين التاريخية عن بقية عناصر المشهد هو الاستمرارية البصرية لعناصر التكوين المحيطة المحددة للفضاء المفتوح، للحفاظ على مستوى الاتصال والارتباط في التكوين الكتلي العام المحدد والموجه للفضاء وان الترابط بين العناصر التكوينية يساهم في رسم ملامح الوحدة البصرية للفضاء المفتوح من خلال الحفاظ على مستوى التكوين الكتلي المنتظم للواجهة والحفاظ على النمط المعماري ومواد انهائها ولونها (علي،2012، ص181).

بناءاً على ما تقدم يمكن تحديد أهم مفردات الاستمرارية البصرية في التصميم الحضري على وجه الخصوص بكل من:

- **أهداف الاستمرارية: الوحدة، الترتيب أو النظام، التجانس، التماثل، المحاكاة.**
- **عناصر الاستمرارية: أسطح، أشكال، واستخدامات.**
- **أدوات الاستمرارية: تناغم العلاقات الشكلية، وتعددية العناصر، والتكرار الإيقاعي لفواصل التشكيل.**
- **مستويات تحقق الاستمرارية:**

-مستوى التكوين الكتلي: الحجم، الشكل، الاتجاه، والصلادة والفراغ.

- مستوى تنظيم السطوح: خط السماء، ارتداد المباني، والخصائص البصرية (مواد البناء والانهاء، الالوان،..).

- مستوى العلاقات الشكلية: التكرار والتتابع، التناسب، التناغم، المقياس، الايقاع (المنتظم وغير المنتظم).

- مستوى النمط المعماري: عناصر معمارية، ومواد البناء والانهاء.

كما شملت الطروحات اشارة الى مفردات الاستمرارية في المدينة العربية التقليدية، ولكن الاشارة الى هذه النقطة كانت ضمنية، وسيتم التوجه الى الفقرة القادمة نحو مجموعة من الدراسات التي تناولت مفردات الاستمرارية في المدينة التقليدية تحديدا.

4.2. الاستمرارية في المدينة العربية التقليدية

بالرغم من ان العمارة الاسلامية للمدينة العربية القديمة تعتبر مرآة للبيئة الحضارية لسكان ذلك العصر سواء كانت من الناحية الاجتماعية والثقافية او من الناحية الطبيعية

والمناخية الا انها تحمل في اجمالها وتفاصيلها كثيرا من القيم المعمارية التي ترتبط في عصورها المختلفة.

ان سمة التكامل والتماسك للعمارة التقليدية والنسيج الحضري التقليدي لم تبرز عن طريق الصدفة وانما جاءت انعكاس لتماسك طبيعي ينتج عن الانماط الاجتماعية المركبة. حيث يتكون الهيكل الحضري للمحلات السكنية من نسيج متضام (Compact urban fabric)؛ **فالوحدات السكنية في معظمها متشابهة حجماً، متناسقة كتلة وتصميماً، بحيث تبدو في مجملها متسلسلة ومتجانسة** ضمن اطارها الكلي (الكناني،2006، ص90). **وتتساوى المباني في الارتفاعات** وتتلاحم في كتلة بنائية واحدة "كالبنيان المرصوص" ولا يرتفع عنها غير مآذن المساجد لذلك يمثل المسجد والمئذنة علامة بارزة في تشكيل صورة المدينة. لذلك فقد تميزت المدينة الاسلامية بالامتداد الافقي المتواضع مع محدودية الاتجاه العمودي لعناصر النسيج الحضري، **وبتناغم خط الافق لهذه العناصر** (العنبكي، 1999، ص17)، شكل (1).

وان **اعتماد المقياس الانساني** في فضاءات المدينة العربية التقليدية ساعد على زيادة القدرة على ادراكها وفهمها شاملا بذلك **جميع مستويات بنية المدينة الحضري من وحدات بنائية وشوارع** حتى لا يحدث انفصال بين الساكن ومدينته ويأتي ذلك لمراعاة الدين الاسلامي للانسان ومقياسه (الطالب، 1990، ص40).

يمتاز النسيج التقليدي في المدينة العربية والاسلامية بالفضاءات اللا إتجاهية فيه، فالشوارع والازقة يراها الناظر **كفضاءات مستمرة لا إتجاهية** وهذه الفضاءات تعمل على الربط بين الابنية المنفردة وعلاقتها بذلك الزقاق وكيفية التعبير عن نفسها داخل الزقاق. وهكذا فإن تخطيط المدينة العربية التقليدية لا يسمح بتكوين مشهد مستمر لمسافة طويلة فالطريق الذي يتغير اتجاهه بزوايا مختلفة يعطي أثراً تتابعياً للمشهد من خلال الانقطاع والتواصل في انكشاف المشهد بصورة مستمرة حيث نلاحظ أن تغير زاوية الطريق في كل مرة وما يترتب عليها من تغير زاوية سقوط أشعة الشمس عليها وتغير الظل والضوء يعطي شعورا بتجدد المشهد بعد المرور من التواء إلى آخر مما يجدد عنصر المفاجأة لدى المتلقي، ويشعره بالتناغم الدائم دون انقطاع (المظفر، 2005، ص79)، شكل (2).

ويعتبر توجيه المباني إلى الداخل إحدى المكونات الأساسية في الهيئة الحضرية لمجاميع الأبنية ذات **الواجهة المستمرة والمغلقة** للشارع التي اتسمت **بالبساطة من ناحية المعالجات المعمارية**، ومن خلال وحدة الجيرة والوحدة العمرانية فأنها تؤدي إلى الوحدة في النسيج الحضري (Wheatly, 1976, P.42).

وبذلك تتمثل الاستمرارية البصرية في المدينة العربية التقليدية من خلال:

- **على مستوى الوحدات السكنية: التشابه الحجمي، التناسق الكتلي، التساوي بالارتفاعات، التلاحم الكتلي، الواجهة المستمرة والمغلقة للشارع، بساطة المعالجات المعمارية.**
- **على مستوى الزقاق أو الشارع: فضاءات مستمرة لا إتجاهية، وتتابعية المشهد من خلال الانقطاع والتواصل.**
- **على مستوى النسيج الحضري: الامتداد الافقي ومحدودية الاتجاه العمودي وبتناغم خط الافق.**
- **اعتماد المقياس الانساني على جميع مستويات بنية المدينة.**

5.2. الاستمرارية في الدراسات السايكولوجية:

تناولت العديد من الطروحات مبادئ النظرية الكشتالتية وتطبيقاتها في العمارة والتصميم الحضري، ويعتبر مبدأ التشاكل (Isomorphism) من أهم مبادئ النظرية المتعلقة بتنظيم العناصر. فالتشاكل هو المماثلة الصورية بين النظائر المتشابهة الأجزاء مع اختلاف الاصل (Al-Katib, 1989, P.503)، وعلى هذا المبدأ توجد ثلاثة قوانين تؤثر

في استيعاب الشكل تشمل: قانون التقارب (Proximity)، قانون التشابه (Similarity)، وقانون الاستمرارية (Continuity). فالكل الحسي حسب هذ القوانين هو أكثر من مجرد حاصل جمع الأجزاء، حيث يعتمد الكل على موقع الأجزاء (قانون التقارب)، وخواص الأجزاء (قانون التشابه)، وعدد الأجزاء بالإضافة الى خواصها وموقعها (قانون الاستمرارية) (Park, 1977, P.67).

ويشير قانون الاستمرارية الى الميل لاستيعاب العناصر المستمرة كوحدة واحدة والى الظاهرة المشتقة من تأثير ما بعد التصور والتي تعتمد على الخبرة السابقة للمتلقي، واتجاه ومقدار أجزاء الموضوع المرئية، فالخط المنكسر يدرك بانه ايقاع من التكسرات باتجاه معين، والخط المستقيم المقطع يدرك بانه اتجاه مستقيم، والخط المنحني المقطع يدرك باتجاه منحني، الا ان الخطوط المتقطعة والتي تكون فيها الفجوات بين القطع أكبر من طول القطعة الواحدة، ربما تفقد خاصية الاستمرارية وتدرك كخطوط منفصلة عن بعضها (Park, 1977, PP.18-20) (Issac, 1971, P.40). وبذلك تلعب الاشكال دورا في تنظيم حركة العين من خلال التراصف والتتابع وبما يخلق حركة مستمرة غير متقطعة، فتبدو الخطوط كأنها تسير وراء نهاياتها، والسطوح تمتد الى حافاتها وهكذا (Meggs, 1989, P.70,93). اذ

اشار (Issac) الى اهمية الاستمرارية في الفكرة التصميمية وذلك لشد الانتباه عن طريق استخدام التفاصيل

وفي ذلك اشارة الى ضرورة وجود انقطاعات محددة تعمل على تحفيز الادراك وشد الانتباه، وهذا ما نجده في الأزقة التقليدية التي يتغير اتجاهها بزوايا مختلفة يعطي أثراً تتابعياً للمشهد من خلال الانقطاع والتواصل ويشعر بالتناغم الدائم دون انقطاع.

يتضح مما تقدم أهمية قوانين التشاكل (قانون الاستمرارية) في خلق التكوين الشكلي الكلي كوحدة واحدة بالاعتماد على عدد الأجزاء، خواصها، اتجاهها، موقعها (الفواصل بين الأجزاء)، والخبرة السابقة للمتلقي.

من خلال ما اشارت اليه المفاهيم العامة والادبيات المعمارية يمكن استخلاص الاطار النظري للاستمرارية البصرية، ويوضح جدول (2) و (3) المفردات الرئيسة مع مفرداتها الثانوية وقيمها الممكنة.

3. المحور الثالث: الإجراءات التطبيقية

يناقش هذا المحور الإجراءات والخطوات المتبعة وصولاً إلى تحقيق هدف البحث، بدءاً بوصف المنهج المعتمد والعينة البحثية وبيان حدودها، وأداة المسح وقياس المتغيرات، وانتقاء الوحدة التحليلية، والأوجه المسحية، وأخيرا تحليل النتائج.

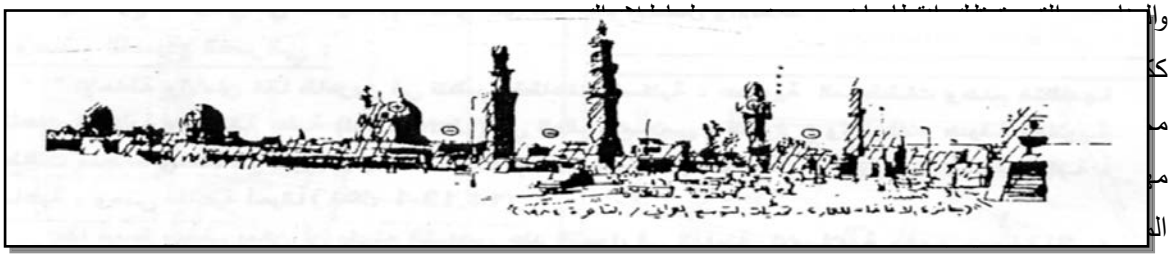

شكل (1): سيطرة المئذنة والقبة على خط السماء في تكوين النسيج الحضري للمدينة الإسلامية./ المصدر:(المظفر،2005،ص72)

جدول (2): الاطار النظري للاستمرارية البصرية/ المصدر: الباحثتان

	المفردات الرئيســـة	المفردات الثانويـــــــة	
للاستمرارية البصرية	أهداف الاستمرارية	الوحدة	الترتيب أو النسق
		التجانس	التماثل
		المحاكاة	
	عناصر الاستمرارية	سطوح	
		أشكال	
		استخدامات	
	أدوات الاستمرارية	تعددية العناصر	
		تناغم العلاقات الشكلية	
		التكرار الإيقاعي لفواصل التشكيل	
	العوامل المؤثرة في الاستمرارية البصرية	عدد الأجزاء	
		خصائص الأجزاء	
		اتجاه الأجزاء	
		موقع الأجزاء (الفواصل بين الأجزاء)،	
		الخبرة السابقة للمتلقي	

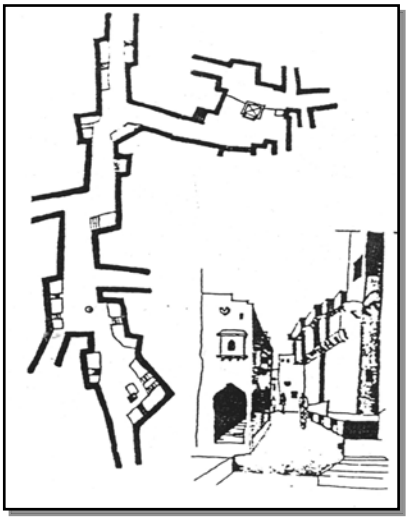

شكل (2): المفاجأة البصرية في ضيق الفضاء واتساعه من فضاء ديناميكي اتجاهي الى فضاء مستقر ضمن ايقاع طبيعي تلقائي./المصدر: (ابراهيم، 1982، ص47)

جدول (3): المفردات الخاصة – مستويات تحقق الاستمرارية البصرية / المصدر: الباحثتان

	المفردات الرئيســـة	المفردات الثانويـــــــة	
المفردات الخاصة للاستمرارية البصرية (مستويات التحقق)	مستوى (1) استمرارية التكوين الكتلي	الحجم	
		الشكل	
		الاتجاه	
		الحدود	
		الصلادة والفراغ	الفراغ بين الكتل
			الفراغ في الكتل
	مستوى (2) استمرارية تنظيم السطوح	خط السماء	
		ارتداد المباني	
		الخصائص البصرية	الالوان،
			مواد البناء والانهاء
		معالجة الواجهات	الخطوط الافقية والعمودية
			التفاصيل
	مستوى (3) استمرارية العلاقات الشكلية	المقياس	
		التناسب	
		الايقاع	التكرار
	مستوى (4) استمرارية النمط المعماري–المحلي	شكلية	العناصر الشكلية
			ومواد البناء
		وظيفية	

1.3. منهج البحث

اعتمد البحث أسلوب الدراسة التحليلية الوصفية في تحقيق هدف البحث شبه التجريبي.

2.3. العينة البحثية

استند مجتمع البحث على المشاريع التصميمية المقترحة لتطوير المنطقة المحيطة بمرقد الامامين الكاظمين الشريفين والمقدمة من قبل المكاتب الاستشارية لتوفير العينة ذات العلاقة بموضوع البحث، باعتبارها مدينة مقدسة عند المسلمين (مركز الكاظمية التقليدي) استطاعت المحافظة على طابعها الروحي والاجتماعي والثقافي وديمومة وحيوية متجددة مستمدة من وجود مرقد الامامين الكاظمين، كما استطاعت المدينة من المحاقظة على هويتها الاسلامية المحلية واحتفاظها بسكانها الاصليين. وحظيت المدينة بالعديد من دراسات التطوير المقترحة والتي ركزت على الحفاظ على طابع المدينه من حيث الشكل، المقياس، الانماط، خط الافق والاشكال المعماريه.

استند البحث إلى انتقاء عينة قصدية بوصفها المشاريع المقترحة لتطوير المنطقة المحيطة بمرقد الامامين الكاظمين والمقدمة الى أمانة بغداد (عام 2009) في مسابقة لتطوير المنطقة، كون تلك النتاجات قد وظفت المفردات التراثية لتعبر عن هويتها الاجتماعية المستدامة، وفي ضوء الأسس أعلاه تحدد المشروعين الفائزين بالجائزتين الاولى والثانية:

1. مقترح مكتب الديوان. 2. مقترح مكتب الشهرستاني،

وبواقع محورين لكل مشروع لتصبح اربع حالات دراسية. يقدم كل من الملحق (1) و(2) شرحا عن المشاريع، كما جاء في في دراسات التطوير، وبما يرتبط بالموضوع قيد البحث، فضلا عن المخططات الأفقية والعمودية والصور التوضيحية لتلك المشاريع.

3.3. أداة المسح

استند البحث إلى استمارة الملاحظة (Observation List) كونها وسيلة للاختبار (يُلاحظ الملحق 3).

كما اعتمدت الطريقة الوصفية التحليلية المستندة إلى تقنية الملاحظة في ضوء النصوص والصور المعتمدة بشأنها أساسا لقياس المتغيرات، بواسطة الاستمارة التي أعدت خصيصا لذلك.

4.3. الوحدة التحليلية

تم اعتماد المشهد الحضري كوحدة تحليلية، وقد جرى تفضيل الواجهات الثلاثية البعد بسبب سهولة عملية تحديد وتقييم مستويات تحقق الاستمرارية (فيما يخص بعض المتغيرات) مقارنة في حالة كون الوحدة التحليلية اللقطات الثنائية البعد، اضافة كون هدف البحث الضمني هو عملية الوصول إلى طبيعة التنظيم الشكلي للمفردات التراثية وفق مستويات الاستمرارية، لذا فان اختيار المخططات الثلاثية البعد لها الأفضلية في جعل التصميم مقروءاً من خلال ما يعرض من تمثيلات بصرية واضحة المعالم. كما تم تحديد مستويين للمشهد الحضري للمشاريع الممثلة للعينة البحثية، المشهد الحضري لمحاور الرئيسة المؤدية للمرقد والمشهد الحضري من فضاء الساحة الرئيسة المحيطة بالمرقد، لما له أهمية فاعلة في تحقيق أهداف المشروع من جهة وأهداف البحث من جهة أخرى وبما يتواءم مع مفردات الأطار النظري المستخلص.

5.3. الأوجه المسحية

تضمنت العملية المسحية ثلاثة أوجه إجرائية، الوجه الأول وهدفه تعريف العينة البحثية قيد الإجراءات التطبيقية والتحليل الوصفي لها بغية التعرف على مستويات استمرارية المفردات التراثية المستدامة التي اعتمدت في تصميمها. أما الوجه الثاني فهدفه التحقق من مصداقية مؤشرات مستويات تحقق الاستمرارية وإمكانية تقليص عدد المتغيرات، فقد أجرت الباحثتان تجربة استطلاعية أولية (Pilot Study) هدفها التحقق من مفاهيم المتغيرات وتشخيص الفاعلة منها، شملت التجربة مشروع واحد من المشاريع المنتخبة، ونتج عنها تقليص أو دمج أو فصل بعض المتغيرات اعتماداً على مبدأ تكرار فاعلية المتغير. اما الوجه الثالث فهدفه إجراء الاختبار للعينة المنتخبة، إذ جرى الاختبار الرئيس وفقاً لاستمارة الملاحظة وللمشاريع كافة ، يُلاحظ جدول (4،5،6،7).

جدول (4): مستويات تحقق الاستمرارية (مشروع (1): مقترح مكتب الديوان). المصدر: الباحثتان

	المفردات الرئيسة	المفردات الثانوية		الوصف (المشهد الحضري من فضاء الساحة الرئيسة المحيطة بالمرقد)		
المفردات الخاصة للاستمرارية البصرية (مستويات التحقق)	مستوى (1) استمرارية التكوين الكتلي	الحجم		استمرارية التنوع البسيط بحجوم الكتل البنائية وارتفاعاتها بشكل متزن.		1
		الشكل		استمرارية التنوع في شكل كتل المباني (وحسب طبيعتها الوظيفية) بشكل متجانس.		
		الاتجاه		تغير اتجاه وحدود الكتل البنائية واستمراريتها في بعض الاجزاء وحسب معالجة التكوينات المعماريه المستحدثة وبزوايا محدده مطله على الساحة مما يمنحها الخصوصية.		2
		الحدود				
		التشكيل الكتلي الفضائي	الفضاء الحضري الخارجي	ويختلف حسب تصميم ومعالجة الكتل البنائية	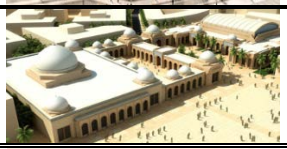	3
			الاروقة	استمرارية الفراغات وبنسب متناسبة وحسب نمط العناصر المستخدمة في الاروقة المحيطة بالساحة والاجزاء الاخرى.		4
	مستوى (2) استمرارية تنظيم السطوح	خط السماء		استمرارية خط السماء وبارتفاع 2-3 طابق، رغم التداخل الفضائي بين الكتل والسماء والذي يظهر جلياً بصورة متوازنة ومتجانسة.	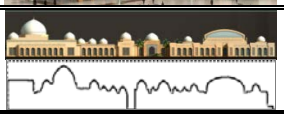	5
		ارتداد المباني		يعتمد التصميم المقترح على تأهيل المباني التاريخية المميزه مع إعادة اعمار المساحات الخالية أو المهدمه بين المباني التراثية.	ملحق (1)	
		الخصائص البصرية	الالوان	استمرارية استخدام الالوان المتناغمة ومواد البناء والانهاء.	 	6
			مواد البناء والانهاء			
		معالجة الواجهات	الخطوط الافقية والعمودية	استمرارية الاروقة المحيطة بالساحة كعناصر عمودية اضافة الى بعض الاجزاء، واستمرارية الخطوط الافقية الناتجة من تحديد عدد الطوابق والاستخدام المتكرر للتفاصيل المتنوعة.		
			التفاصيل	استمرارية استخدام التفاصيل المتنوعة والمتناسبة وضمن وحدة كلية.	انظر الصور السابقة.	
	مستوى (3) استمرارية العلاقات الشكلية	المقياس		تناسب ابعاد الابنية والعناصر مع مقياس الانسان على مستوى جميع الابنية المحيطة بالساحة.	انظر الصور (2،6)	
		التناسب		استمرارية علاقات تناسب ابعاد الابنية مع بعضها، اضافة الى تناسب العناصر والتفاصيل.	انظر صورة (1،6)	
		الايقاع	التكرار	استمرارية علاقات التكرار التام والمتغير للعناصر والتفاصيل.	انظر صورة (6،7)	
	مستوى (4) استمرارية النمط المعماري-المحلي	شكلي	العناصر الشكلية	استمرارية استخدام العناصر التي تتوافق مع المباني التراثيه للاحياء التقليدية القديمة في الكاظميه. من شناشيل، أروقة، أقواس، قباب، ... الخ.	 	7
			ومواد البناء	استخدام مواد البناء المحلية (الخشب) في بعض التفاصيل، شناشيل، الشبابيك.		
		وظيفي		نفس الاستخدام للفعاليات الدينيه والاجتماعية و الثقافية والتجارية لمركز الكاظمية الديني.		

جدول (5): مستويات تحقق الاستمرارية (مشروع (1): مقترح مكتب الديوان). المصدر: الباحثتان

	المفردات الرئيسـة	المفردات الثانويـة		الوصف (المشهد الحضري للمحور الرئيسي المؤدي للمرقد – شارع القبلة)		
المفردات الخاصة للاستمرارية البصرية (مستويات التحقق)	مستوى (1) استمرارية التكوين الكتلي	الحجم		استمرارية التنوع البسيط بحجوم الكتل البنائية وارتفاعاتها بشكل متزن.	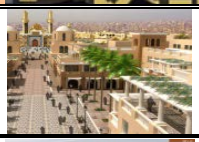	1
		الشكل		استمرارية التنوع في شكل كتل المباني والتدرج الملحوظ (وحسب طبيعتها الوظيفية) وبشكل متجانس.		
		الاتجاه		تغير اتجاه وحدود الكتل البنائية واستمراريتها في بعض الاجزاء وحسب توسع الفضاءات العامة المستحدثة (البلازا، مداخل المحور) .	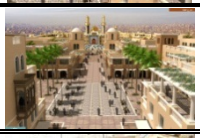	2
		الحدود				
		التشكيل الكتلي الفضائي	الفضاء الحضري الخارجي	وجود الفواصل–الفراغ المتكررة بين الكتل بسبب وجود المحاور الثانوية. (انظر صورة 5)		3
			الاروقة	استمرارية الفراغات وبنسب متناسبة وحسب نمط العناصر المستخدمة (الاروقة المستمرة، الباكونات، الشناشيل، ووحدائق المرتفعة) على طول واجهة المباني.(انظر صورة 5)		4
	مستوى (2) استمرارية تنظيم السطوح	خط السماء		استمرارية خط السماء وبارتفاع 3–4 طابق، وبتدرج قليل، رغم التداخل الفضائي البسيط المتوازن بين الكتل والسماء.		5
		ارتداد المباني		تغير في ارتداد المباني على المستوى الافقي (توسع الفضاءات العامة المستحدثة –البلازا، والمداخل) وعلى المستوى العمودي (تدرج المباني)		6
		الخصائص البصرية	الالوان	استمرارية استخدام الالوان المتناغمة ومواد البناء والانهاء.	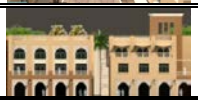	7
			مواد البناء والانهاء			
		معالجة الواجهات	الخطوط الافقية والعمودية	استمرارية الاروقة كعناصر عمودية اضافة الى بعض الاجزاء(مداخل المحور)، واستمرارية الخطوط الافقية الناتجة من تحديد عدد الطوابق والاستخدام المتكرر للتفاصيل المتنوعة.		8
			التفاصيل	استمرارية استخدام التفاصيل المتنوعة والمتناسبة وضمن وحدة كلية.	انظر الصور السابقة.	
	مستوى (3) استمرارية العلاقات الشكلية	المقياس		تناسب ابعاد الابنية والعناصر مع مقياس الانسان على مستوى جميع الابنية.	انظر الصورة (4)	
		التناسب		استمرارية علاقات تناسب ابعاد الابنية مع بعضها، اضافة الى تناسب العناصر والتفاصيل.	انظر صورة (7،8)	
		الايقاع	التكرار	استمرارية علاقات التكرار التام والمتغير للعناصر والتفاصيل.	انظر صورة (6،7،8)	
	مستوى (4) استمرارية النمط المعماري–المحلي	شكلي	العناصر الشكلية	استمرارية استخدام العناصر التي تتوافق مع المباني التراثيه للاحياء التقليدية القديمة في الكاظميه. من أروقة، شناشيل، أقواس، قباب، ... الخ.	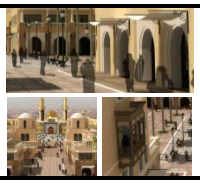	9
			ومواد البناء	استخدام مواد البناء المحلية (الخشب) في بعض التفاصيل، شناشيل، الشبابيك.		
		وظيفي		تنفتح على المحور المحلات التجارية والاسواق المتخصصه والمطاعم والمعارض والفنادق التي تخدم الزوار والسكان مع مشاغل حرفيه تتخللها استراحات.		

جدول (6): مستويات تحقق الاستمرارية (مشروع (2): مقترح مكتب الشهرستاني). المصدر: الباحثتان

	المفردات الرئيسة	المفردات الثانوية		الوصف (المشهد الحضري من فضاء الساحة الرئيسة المحيطة بالمرقد)		
المفردات الخاصة للاستمرارية البصرية (مستويات التحقق)	مستوى (1) استمرارية التكوين الكتلي	الحجم		التغير في استمرارية حجم وشكل الكتل المحيطة بالساحة العامة المحيطة بالمرقد. إذ تتغير الاستمرارية الشكلية والحجمية للرواق الدائري المحيط بالساحة والمسقفات في العناصر العمودية التي تعرف المداخل الاربعة الرئيسية للساحة.		1
		الشكل				
		الاتجاه		ايحاءات الحركة الديناميكية المستمرة للرواق المحيط بالساحة (بسبب الشكل الدائري) عدا في مناطق مداخل الساحة.		2
		الحدود		التواصل التام في الحدود حول الفضاء (الرواق الدائري) بينما تظهر الفواصل في المداخل المؤدية الى الساحة المحيطة بالمرقد.		3
		التشكيل الكتلي الفضائي	الفضاء الحضري الخارجي	تظهر الفراغات بين عناصر المداخل الاربعة المؤدية الى الساحة المحيطة بالمرقد.	انظر الصورة (3)	
			الاروقة	استمرارية الفراغات وبنسب مختلفة وحسب نمط العناصر المستخدمة في الاروقة المحيطة بالساحة والعناصر المعرفة لمداخل الساحة.		4
	مستوى (2) استمرارية تنظيم السطوح	خط السماء		يظهر التداخل الفضائي بين الكتلة والسماء جليا في مناطق دون اخرى ويتركز في اربعة مواقع والمتمثلة بمحاور الوصول الرئيسية الى المرقد في حين ان بقية اجزاء الساحة محاطة بهياكل من الاروقة المقباة المستمرة الارتفاع.		5
		ارتداد المباني		تغير في ارتداد الكتل البنائية في مناطق المداخل المؤدية الى الساحة المحيطة بالمرقد.	انظر الصورة (1،4)	
		الخصائص البصرية	الالوان	استمرارية استخدام الالوان المتناغمة ومواد البناء والانهاء.	انظر الصور السابقة.	
			مواد البناء والانهاء			
		معالجة الواجهات	الخطوط الافقية والعمودية	استمرارية الرواق المحيط بالساحة كعناصر عمودية اضافة الى بعض الاجزاء العمودية.		6
			التفاصيل	استمراريةاستخدام التفاصيل المتنوعةوضمن وحدةكلية.	انظر الصور السابقة.	
	مستوى (3) استمرارية العلاقات الشكلية	المقياس		تغير في استمرارية المقياس بسبب النسب الكبيرة لاحجام الاقواس التي تعرف المداخل الاربعة الرئيسة للساحة والتي غيرت من المقياس الانساني المستمر للرواق الدائري بشكل كبير.	انظر صورة (1،6)	
		التناسب		تغير في علاقات التناسب بسبب هيمنة العناصر النصبية التي تعرف المداخل الاربعة الرئيسة للساحة.	انظر صورة (4،6)	
		الايقاع	التكرار	استمراريةعلاقات التكرارالتام والمتغيرللعناصروالتفاصيل	انظر صورة (4،6،7)	
	مستوى (4) استمرارية النمط المعماري-المحلي	شكلي	العناصر الشكلية	استمرارية استخدام العناصر التي تتوافق مع المباني التراثيه للاحياء التقليدية القديمة في الكاظميه. من أروقة، أقواس، قباب ...		7
			ومواد البناء	----		
		وظيفي		----		

جدول (7): مستويات تحقق الاستمرارية البصرية (مشروع (2): مقترح مكتب الشهرستاني) المصدر: الباحثتان

	المفردات الرئيســـة	المفردات الثانويـــــــة		الوصف (المشهد الحضري للمحور الرئيسي المؤدي للمرقد – المحور الشمالي المقابل لشارع القبلة)		
المفردات الخاصة للاستمرارية البصرية (مستويات التحقق)	مستوى (1) استمرارية التكوين الكتلي	الحجم		التنوع بشكل وحجوم الكتل البنائية وارتفاعاتها وبشكل منسجم.	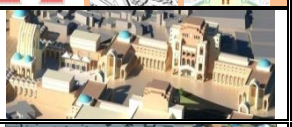	1
		الشكل				
		الاتجاه		تغير اتجاه وحدود الكتل البنائية واستمراريتها وحسب توسع الفضاءات العامة المصممة (البلازا ومدخل المحور).		2
		الحدود				
		التشكيل الكتلي الفضائي	الفضاء الحضري الخارجي	استمرارية اتصال الكتل البنائية عدا في بعض الاجزاء وبشكل جزئي.		3
			الاروقة	استمرارية الفراغات وبنسب متناسبة وحسب نمط العناصر المستخدمة (الاروقة المستمرة، مداخل الابنية والساحة).(انظر صورة 2)		
	مستوى (2) استمرارية تنظيم السطوح	خط السماء		يظهر التداخل الفضائي بين الكتلة والسماء بصورة واضحة وبارتفاع (2–4) وبصورة متوازنة.	انظر الصورة (1)	
		ارتداد المباني		تغير في ارتداد المباني على المستوى الافقي (توسع الفضاءات العامة المستحدثة –البلازا، ومدخل) وعلى المستوى العمودي (تدرج المباني).	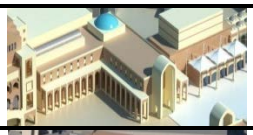	4
		الخصائص البصرية	الالوان	استمرارية استخدام الالوان المتناغمة ومواد البناء والانهاء.		5
			مواد البناء والانهاء			
		معالجة الواجهات	الخطوط الافقية والعمودية	استمرارية الاروقة كعناصر عمودية اضافة الى بعض الاجزاء (كمداخل المحور، ...)، واستمرارية الخطوط الافقية الناتجة من تحديد عدد الطوابق والاستخدام المتكرر للتفاصيل المتنوعة. انظر الصورة (3)		6
			التفاصيل	استمرارية استخدام التفاصيل المتنوعة والمتناسبة وضمن وحدة كلية.	انظر الصور السابقة.	
	مستوى (3) استمرارية العلاقات الشكلية	المقياس		استمرارية تناسب ابعاد الابنية والعناصر مع مقياس الانسان.	انظر الصورة (3،4،6)	
		التناسب		استمرارية علاقات تناسب ابعاد الابنية مع بعضها، اضافة الى تناسب العناصر والتفاصيل.	انظر صورة (2،5)	
		الايقاع	التكرار	استمرارية علاقات التكرار التام والمتغير للعناصر والتفاصيل.	انظر الصور السابقة.	
	مستوى (4) استمرارية النمط المعماري–المحلي	شكلي	العناصر الشكلية	استمرارية استخدام العناصر التي تتوافق مع المباني التراثيه للاحياء التقليدية القديمة في الكاظميه. من أروقة، أقواس، قباب، ...	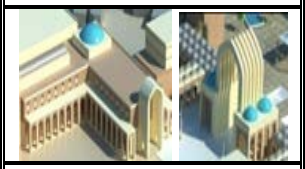	7
			ومواد البناء	----		
		مظلة		يعتبر مركز ثقافي تجاري الذي يخدم زوار المنطقة		

4. المحور الرابع: النتائج والاستنتاجات

يتناول هذا المحور طرح اهم نتائج الدراسة العملية واستنتاجات البحث.

1.4. نتائج الدراسة العملية

اظهر تحليل نائج الدراسة العملية ان تحقيق الاستمرارية البصرية للمفردات التراثية يتحقق بنسبة اعلى في المشاريع المنتخبة في: لاحظ الملحق رقم (4)

- استمرارية تنظيم السطوح من حيث: الخصائص البصرية ومعالجة الواجهات، واستمرارية العلاقات الشكلية.
- استمرارية العلاقات الشكلية: من حيث تكرار العناصر، الايقاع، ثم المقياس والتناسب.
- اما استمرارية النمط المعماري المحلي فتظهر في استخدام العناصر الشكلية التراثية.
- فيما يخص استمرارية التكوين الكتلي فتتحقق الاستمرارية البصرية بصورة اوضح في التشكيل الكتلي والفضائي وخاصة على مستوى الفضاءات الانتقالية كالاروقة، حيث تظهر هيمنتها على التكوين الكتلي كتنظيم فضائي وشكلي باستخدام الاقواس وتكرارها بايقاعات مختلفة.

2.4. الاستنتاجات

- أفرزت الطروحات جملة من الابعاد الخاصة بمفهوم الاستدامة الاجتماعية والتي اهتمت في رسم ملامح المفهوم التي يمكن اعتمادها لتحقيق العمارة المستدامة، من اهمها استدامة الانسان والمجتمع، تاكيد الاستدامة الحضارية والهوية الاجتماعية– الثقافية.
- في حين اكدت الطروحات المعمارية والحضرية توظيف المفردات التراثية من خلال استخدام الانماط والعناصر المعمارية المحلية واستخدام مواد وتقنيات البناء المحلية.
- ممكن اعتبار الاستمرارية البصرية للمفردات التراثية في المشهد الحضري احد صيغ تحقيق الاستدامة الاجتماعية في مشاريع التطوير الحضري المعاصر.
- اشرت الدراسات اهمية استخدام العناصر المعمارية المحلية والمواصفات التي تصمم عموما بوصفها استجابة للبيئة والمناخ الإقليمي، اضافة الى استخدام العناصر المعمارية التي تبقي الثقافة والهوية المحلية وتخلق الإحساس بالمكان؛ اختيار مواد البناء التي تستعمل في الهيكل الإنشائي.
- يمكن تحقيق الاستمرارية البصرية للمفردات التراثية بعدة مستويات، تتباين من المستوى الشكلي، مستوى تنظيم السطوح، ومستوى العلاقات الشكلية ، ومستوى النمط المعماري المحلي.
- يتباين مستوى تحققها في المشاريع حسب خصوصية المشروع، ومستوى الاستدامة الاجتماعية المحدد.

المصادر والمراجع العربية

- إبراهيم، د.عبد الباقي، "**تأصيل القيم الحضارية في بناء المدن الإسلامية المعاصرة**"، مركز الدراسات التخطيطية والمعمارية، القاهرة، 1982.
- التوني، سيد، "**مطارحات عن الثقافة والعمارة**"، مجلة قسم الهندسة المعمارية، كلية الهندسة ، جامعة القاهرة، 1988.
- الأحبابي، شيماء حميد حسين، "**الاستدامة الجتماعية في العمارة المحلية**"، اطروحة دكتوراه غير منشورة مقدمة إلى قسم الهندسة المعمارية في كلية الهندسة بجامعة بغداد، بغداد، 2010.
- الزبيدي، مها صباح سلمان، "**الاستدامة البيئية في تشكيل التجمعات الاسكانية في العراق**"، اطروحة دكتوراه غير منشورة مقدمة إلى قسم الهندسة المعمارية في كلية الهندسة بجامعة بغداد، بغداد، 2006.
- الطالب، طالب حميد، "**الماضي والمستقبل ونظرتنا للعمارة المعاصرة**"، مجلة المدينة العربية، العدد 43، منظمة المدن العربية، السنة الثانية، 1990.
- العنبكي، هادي عبد المحسن، "**المغزى الاجتماعي للإطار العمراني**"، بيت الحكمة، سلسلة المائدة الحرة، مطبعة اليرموك، بغداد، 1999.

- القره غولي، أنوار صبحي، "**الوحدة الشكلية في العمارة كنظام**"، رسالة ماجستير غير منشورة مقدمة الى الجامعة التكنولوجية، بغداد، 1999.

- الكناني، كامل، "**تخطيط المدينة العربية الاسلامية- الخصوصية والحداثة**"، مجلة المخطط والتنمية، العدد 15، المعهد العالي للتخطيط الحضري والاقليمي، بغداد، 2006.

- المظفر، رياض منير محمد رضا، "**فهم المدينة العربية الإسلامية بكونها نظاماً في ضوء المتغيرات الإجتماعية والإقتصادية والتكنولوجية**"، رسالة ماجستير غير منشورة، المعهد العالي للتخطيط الحضري والإقليمي، جامعة بغداد، 2005.

- النعيم، مشاري عبد الله، "تحدي العمارة والاستدامة"، مجلة البناء العدد148 ، رمضان1423هـ ، ديسمبر2002م، دار العلم، جدة، المملكة العربية السعودية، 2002.

- أمين، امير صالح، "**نحو رؤية لعمليات الحفاظ على التراث لتدعيم هوية المجتمعات الاسلامية في عصر العولمة**"، مؤتمر الأزهر الهندسي الدولي التاسع، 12-14 ابريل، القاهرة، 2007.

- بابان، سامال عثمان، "**العمارة المستدامة: دور مناهج محاكاة الطبيعة على استراتيجيات البناء الشكلي المستدام**"، رسالة ماجستير غير منشورة مقدمة إلى قسم الهندسة المعمارية في الجامعة التكنولوجية، بغداد، 2004.

- بثيون، رنا ممتاز، "**الاستدامة المعمارية: إستراتيجية محاكاة الطبيعة والشكل المعماري في العمارة المستدامة**"، رسالة ماجستير مقدمة إلى قسم الهندسة المعمارية في الجامعة التكنولوجية، بغداد، 2005.

- تقرير التنمية البشرية لعام 1993، نيويورك، برنامج الامم المتحدة الانمائي، 1993.

- تقرير التنمية البشرية لعام 2004، نيويورك، برنامج الامم المتحدة الانمائي، 2004.

- علي الحيدري، "**شواهد من المشهد الحضري وتفاصيل الفضاء العمراني**"، المجلة العراقي للهندسة المعمارية، الاعداد: التاسع عشر والعشرون والحادي والعشرون، تشرين الثاني 2010.

- علي، عمر حسين، "**الخصائص الشكلية للفضاءات المفتوحة في المدن التاريخية- دراسة تحليلية للمشاريع المقترحة لتطوير الفضاءات المفتوحة في مدينة الكاظمية**"، رسالة ماجستير غير منشورة مقدمة إلى قسم الهندسة المعمارية في الجامعة التكنولوجية، بغداد، 2012.

- قنطقجي، د.سامر مظهر، "**النظرية التنموية في فكر ابن خلدون ومالك بن نبي**"،2009 ، www.kantakji.com.

- مكتب الديوان، مسابقة تصميم المنطقة المحيطة بمرقد الكاظمين الشريفين، دراسة مقدمة لأمانة بغداد كجزء من متطلبات تصميم المنطقة المجيطة بمرقد الكاظمين الشريفين،2009.

- مكتب الشهرستاني، مسابقة تصميم المنطقة المحيطة بمرقد الكاظمين الشريفين، دراسة مقدمة لأمانة بغداد كجزء من متطلبات تصميم المنطقة المجيطة بمرقد الكاظمين الشريفين،2009.

-نعمة، صبا جبار و الأحبابي، شيماء حميد حسين، "**آليات تحقيق الاستدامة الاجتماعية في البنية الحضرية التقليدية (حالة دراسية في مركز مدينة الكاظمية التقليدية)**، بحث منشور في مجلة الهندسة، العدد3، مجلد17، حزيران 2011.

- يوسف، محسن صلاح الدين، "**الصورة الذهنية للمدينة**"، 1983.

المصادر والمراجع الأجنبية

- Able, Chris, “Architecture & Identity: Towards a Global Eco Culture”, Architectural press an imprint of Butterworth Heinemann, London, 1997.

- Al-Katib, Ahmed, **"A New Dictionary of Scientific and Technical Term"**, Librairi De Liban, Beirut, 1989.
- Amin, M., **"Architecture of Careen Islamic Complexes-Features & Positional of reuse"**, PhD, Cairo University, 1988.
- Correa, Charles, **"Quest for Identity"**, Cambridge, 1990.
- David A. Lauer & Stephen Pentak, **"DESIGN BASICS"**, Thomson Wadsworth, Canada, Seventh Edition, 2008.
- Esther Hiu Kwan Yung, Edwin Hon Wan Chan & Ying Xu, **"Sustainable Development and the Rehabilitation of a Historic Urban District – Social Sustainability in the Case of Tianzifang in Shanghai",** wileyonlinelibrary.com),2011, **Iraq Virtual Science Library.(** Greenwood , Tom, "**Sustainable Design Guide"**, ESP Design,(2004). -
Inc, USA, 1996 - Hall, S. and Du Gay, P. (Eds.) , **"Questions of Cultural Identity"**, Sage
- Human Development Report 1990, New York, UNDP, 1990.
- Human Development Report 1994, New York, UNDP, 1994.
- Issac,Arc,**"Approach to Architectural Design"** Butterworth & Co. (publishers), London, 1971.
- Meggs, Philip ., **"Type and Image: The Language of Graphic Design"**, Van Nostrand Reinhold, New York, 1989.
- Park, Niels L., **"The Visual Perception of the Built Environment"**, Delft University press, 1977.
- Stenberg,1999, http://www.hallbarasverige.gov/se.html.
- Wheatly, p., **"Levels of Space Awareness in the Tradition Islamic City"**, in Ekistics, No.253, 1976.
- Webster, Merriam, Encyclopedia Britannica/ 2010 Ultimate DVD.
- Webster, A Merriam, **"Webster's New Collgiate Dictionary.**

ملحق (1): مقترح مكتب الديوان (مكتب الديوان، 2009)

• الفكرة الأساسية، هي كون المرقد الشريف هو قلب المدينة ونواتها، تحيط به من الخارج حلقات مختلفة ومتعاقبة من نسيج حضري عمراني يفصل منطقة الحرم عن الخارج لتشكل جميعها مع المرقد الشريف وحدة متكاملة. ان محور الخطة المقترحة هو تلبية متطلبات الاعداد الكبيرة لزائري مرقد الكاظمين الشريف خلال المناسبات الدينيه والحفاظ على النسيج الحضري التاريخي للمنطقة المحيطة بالمرقد، مع اعادة تأهيل المناطق الحضرية فيها. تحيط بالساحه ثلاث حلقات تتدرج ارتفاعاتها كلما ابتعدنا الى الخارج. اربعة محاور رئيسية تخترق الاطواق الثلاث المحيطة بالمركز الديني للكاظميه وتربط الكاظمية وما حولها مع بقية اجزاء مدينة بغداد، صممت كطرق واسعه للمشاة تنفتح عليها المحلات التجارية والاسواق المتخصصه والمطاعم والمعارض والفنادق التي تخدم زوار المنطقة وساكنيها. مع مشاغل حرفيه تتخللها استراحات للزوار.

الحلقة (1):وتتكون من ما تبقى من النسيج التاريخي الحضري، وتأهيل المباني التاريخية المميزه من الدور والخانات وصيانتها مع إعادة استخدامها للفعاليات الدينيه والاجتماعية و الثقافية والتجارية. ان اعادة اعمار المساحات الخالية أو المهدمه بين المباني التراثية القائمه سيتم بنمط متوافق مع المباني التراثيه ويشكل معها نموذجا" للاحياء التقليدية القديمة في الكاظميه ذات الفناء الداخلي..

الحلقة (2):وتضم المنطقة السكنية وتتميز بتجانس معماري محدود، بنمط مبانيها الذي يحاكي بعض عناصر المنطقة التاريخية المتاخمة لها دون تكرار حرفي لعناصر العماره التقليدية فيها مع عدد من الأنشطة الحرفية والصناعية البسيطه تتخللها حركة مرور المركبات مع مواقف للسيارات. ارتفاع المباني فيها منخفض لايزيد عن ثلاثة طوابق

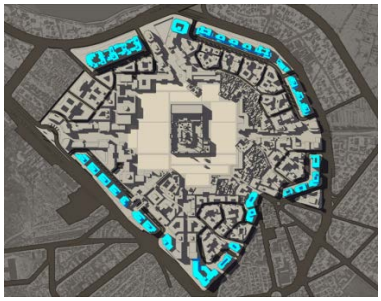

الحلقة (3): وتتكون من مجموعة من المباني السكنية وابنية الفنادق الحديثة بمحاذاة الطرق الرئيسية حول المركز التاريخي للكاظمية لتشكل طوقا" حولها و بارتفاع خمسة الى ستة طوابق

الابنية التكميلية:

المكتبة

قاعة متعددة الاغراض

قاعة متعددة الاغراض

ملحـــق (2): مقتـــرح مكتـــب الشهرســـتاني (مكتـــب الشهرستاني،2009،ص ص57-11)

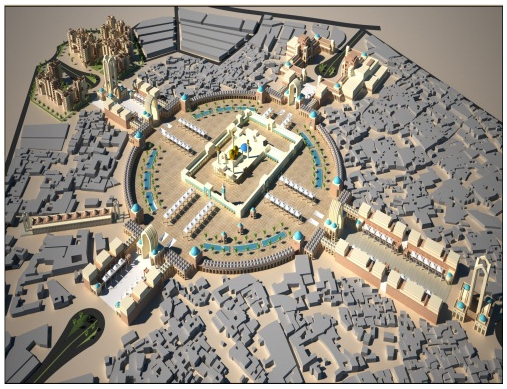

• السياسة التخطيطية المتبعة في التصميم المقترح: الحفاظ قدر الإمكان على النسيج الحضري، توفير صحن كبير لتجمع اكبر عدد ممكن من الزائرين، زيادة المحاور الحركية والبصرية المؤدية للمرقد، توفير اكبر عدد ممكن من ساحات وقوف السيارات وعدم السماح بدخول السيارات إلى المنطقة القديمة، توفير شاخصين مميزين لإبراز منطقة الكاظمية من بعيد واربعة شواخص أخرى لإبراز المنطقة المحيطة بالمرقد، توفير عدد كاف من المباني العامة، وتوفير مباني سكنية بعدد يكفي لإيواء النازحين من منطقة التطوير.

• وأخذت النقاط التالية بنظر الاعتبار في إعداد التصاميم: أن وجود السكان في المنطقة وضمن محلاتهم وفعالياتهم التجارية، هو جزء متكامل مع فعالية الزيارة، تحويل وإعادة تأهيل بعض الأبنية التراثية إلى مساكن فندقية ودور استراحة تتمتع بخدمات معاصرة مع الحفاظ على طرازها العمراني الأصيل، ومن الضروري عند دراسة الكتل البنائية والفضاءات المحيطة بالمشهد ألكاظمي الشريف أن يتم ألالتزام بمبدأ الارتفاعات التي تضمن هيمنة المرقد الشريف من جميع المحاور الحركية والبصرية المحيطة به ، وعلى أن يؤخذ بالتزايد في الأرتفاع تدريجياً صعوداً مبدأ من مقياس جدار الصحن المحيط بالمشهد الشريف.

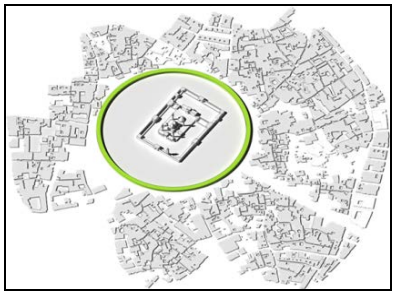

ساحة دائرية للزوار

تحسين محاور الوصول

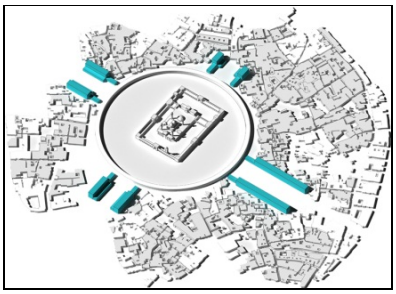

الأبنية الخدمية على طول محاور الحركة

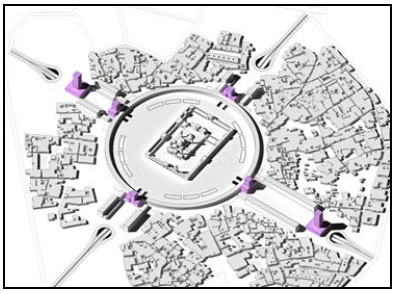

شواخص إبراز المدينة القديمة

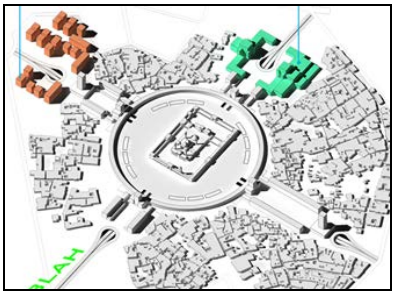

ساحة د الابنية العامة والسكنية الجديدة

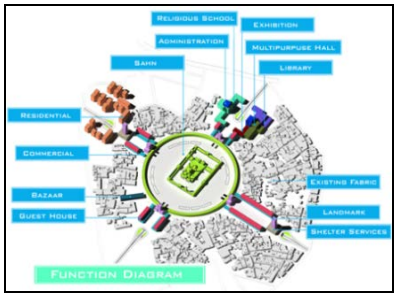

المخطط الوظيفي النهائي

المعالم كمداخل أساسية

الابنية العامة

الأبنية الخدمية على طول محاور الحركة

Optimal Dimensions of Small Hydraulic Structure Cutoffs Using Coupled Genetic Algorithm and ANN Model

Dr.Prof.Rafa Hashim Al-Suhaili
Prof., Civil Eng. Dept., College of Eng.,
University of Baghdad, Iraq
Email:rafaalsuhili@yahoo.com

Rizgar Ahmed Karim
Asst. Lec., Dam and W. R. Eng. Dept.,
Faculty of Eng., University of Sulaimani, Iraq
Rizgar_Karim@yahoo.com

ABSTRACT

A genetic algorithm model coupled with artificial neural network model was developed to find the optimal values of upstream, downstream cutoff lengths, length of floor and length of downstream protection required for a hydraulic structure. These were obtained for a given maximum difference head, depth of impervious layer and degree of anisotropy. The objective function to be minimized was the cost function with relative cost coefficients for the different dimensions obtained. Constraints used were those that satisfy a factor of safety of *2* against uplift pressure failure and *3* against piping failure.

Different cases reaching 1200 were modeled and analyzed using geo-studio modeling, with different values of input variables. The soil was considered homogeneous anisotropic. For each case, the length of protection (L) and the volume of the superstructure (V) required to satisfy the factors of safety mentioned above were calculated. These data were used to obtain an artificial neural network model for estimating (L) and (V) for a given length of upstream cutoff (S1), length of downstream cutoff (S2), head difference (H), length of floor (B), depth of impervious layer (D) and degree of anisotropy (kx/ky).

A MatLAB code was written to perform a genetic algorithm optimization modeling using the obtained ANN model .The obtained optimum solution for some selected cases were compared with the Geo-studio modeling to find the length of protection required in the downstream side and volume required for superstructure. Values estimated were found comparable to the obtained values from the Genetic Algorithm model.

Key words: optimization, genetic algorithm, artificial neural networks, geo-Studio, uplift pressure, exit gradient, factor of safety.

الأبعاد المثالية لحواجب منشأ هيدروليكي صغير بأستخدام مدمج خوارزميةً وراثيةً ونموذجَ شبكة عصبية اصطناعية

الأستاذ الدكتور رافع هاشم السهيلي
استاذ، قسم الهندسة المدنية، كلية الهندسة
جامعة بغداد، العراق

رزكار أحمد كريم
مدرس مساعد، قسم هندسة السدود و الموارد المائية
كلية الهندسة، جامعة السليمانية، العراق

الخلاصة

تم في هذا البحث بناء نموذج الأمثلية باستخدام تقنية جينات الوراثية و تقنية الشبكات العصبية الصناعية لايجاد الأبعاد المثلى للقواطع الاساس في كل من المقدم و المؤخر و كذلك طول الارضية الاساس و طول الحماية المطلوبة في المؤخر في المنشات الهيدروليكية. تم ايجاد هذه الابعاد لقيم معطات لكل من اعلى فرق للشحنة بين مقدم و مؤخر المنشاء، و لعمق طبقة صماء

و درجة التباين في قيم خواص التربة مع الاتجاه. دالة الهدف التي تم ايجاد القيم الصغرى لها هي دالة الكلفة بمعاملات كلفة نسبية. اما المحددات المستخدمة في النموذج فهي معاملات الامان ضد ضغط الاصعاد و غليان التربة بقيم 2، 3 على التوالي.

تم نمذجة عدة حالات وصل الى 1200حالة باستخدام برنامج Geo-studio. في هذه النمذجة تم اعتبار التربة متجانسة و ذات تباين مع الاتجاه. لكل حالة تم حساب طول الحماية L و حجم المنشاء V المطلوبة لتحقيق معاملات الامان المشار اليها أعلاه. تم استخدام البيانات الخاصة بالحالات اعلاه لبناء نموذج شبكات العصبية لحساب L و V لقيم معطات من عمق القاطع في المقدم (S1)، عمق القاطع في المؤخر(S2) و فرق الشحنة بين المقدم و المؤخر(H)، طول الارضية(B) ، عمق طبقة الصماء (D) و درجة التباين(kx/ky) مع الاتجاه في خواص التربة.
تم كتابة برنامج Matlab لنموذج الجينات الوراثية يستخدم نموذج شبكات العصبية المشار اليه اعلاه. باستخدام هذا النموذج تم ايجاد الحل الامثل لبعض الحالات المختارة و تم مقارنتها بالنتائج المناظرة التي تم الحصول عليها باستخدام برنامج Geo-studio كانت نتائج النموذجين متقاربة.

الكلمات الرئيسية: الأمثلية، الخوارزمية الجينية، الشبكات العصبية الاصطناعية، جيو-ستوديو، الضغط الاصعاد، غليان التربة، معامل الأمان.

1. INTRODUCTION

The most critical aspects that the designer of hydraulic structures should take into account are the failures due to uplift pressure and / or piping phenomenon at the toe of the structure. Proper factors of safety should be adopted for both aspects.

In order to provide the required factors of safety against both uplift pressure and piping due to exit gradient, the designers usually provide cutoffs at the upstream and the downstream sides of the foundation of the hydraulic structures. The upstream cutoffs in general decreases the uplift pressure and exit gradient. However, they reduce the uplift pressure in a rate more than that for the exit gradient. In order to control the exit gradient, a downstream cutoff should be provided, which has direct effect on the exit gradient. The designer should decide the depth of both cutoffs so as to achieve the required factors of safety.

In order to have an additional control of piping downstream of the structure, designers provide a downstream protection just after the toe of the foundation with a suitable length decided to provide the factor of safety against exit gradient piping. This protection is usually provided as an apron or a carefully designed filter, **Al-Suhaili, 2009.**

The designer faces the difficulty of deciding the optimum depths required to control both uplift pressure and piping failure. The decision variables are the minimum depth required of both upstream and downstream cutoffs, weight of the superstructure required and length of the downstream filter required.

Many researchers, **Al-Suhaili et al.,1988,Al-Suhaili,2009, Al-Fatlawy,2007, Khassaf et al.,2009, Al Dury,1986, Ismail and Aziz,2005, Ghobadian and Khodaei,2009, Shadravan et al.,2004 , Griffiths and Fenton,1993 and1998, and Haszpra et al.,2000,** had studied the effect of upstream or downstream cutoffs either on uplift pressure on the foundation of the structure or on the variation of exit gradient downstream of the structure. The results were usually provided in a form of dimensionless curves that can help in the design process.

Recently with the availability of a new era of models that have been developed such as Artificial Neural Network models and Genetic Algorithm models, these techniques provide models for designing hydraulic structures instead of the dimensionless curves used before.

The objective of this research is to develop a model to help designers in finding the optimum dimensions of a hydraulic structure foundation using a coupled Artificial Neural Network (ANN) model and Genetic Algorithm (GA) techniques.

Al- Duri, 1986, had investigated the protection at the downstream of hydraulic structures. **Al-Suhaili et al. 1988,** had investigated exit gradient variation downstream of hydraulic structures, using the solution of Laplace equation by Schwrz-Christoffel conformal mapping. **Ilyinsky and Kacimov, 1992,** had investigated an analytical estimation of ground-water flow around cutoff walls and into interceptor trenches, developing analytical solutions for different cases using Schwarz-Christoffel transformation. **Griffiths and Fenton, 1993,** had investigated the seepage beneath water retaining structures found on spatially random soil. **Griffiths and Fenton, 1998,** had investigated a probabilistic analysis of exit gradients due to steady seepage. **Haszpra et al. 2000,** had investigated seepage around structures built into flood levees. **Manna et al., 2003,** had investigated the groundwater flow beneath a sheet pile analyzed using six-node triangular finite element method. **Shadravan et al., 2004,** had investigated the cutoff wall analysis and design of Karkheh storage dam. **Ismail and Aziz, 2005,** had investigated the seepage analysis of Tushka spillway barrages with stability analysis. **Al-Fatlawy, 2007,** had investigated the seepage analysis through soil foundation under dams. **Mukhopadhyay, 2008,** had investigated the seepage analysis through foundation using a finite element model and flownet Seepage analysis. **Moellmann, et al., 2008,** had investigated a probabilistic finite element analysis of embankment stability under transient seepage conditions. **Khassaf et al. 2009,** had investigated seepage analysis underneath Diyala weir foundation. **Al-Suhaili, 2009,** had investigated an analytical solution for exit gradient variation downstream of inclined sheet pile. **Ghobadian and Khodaeik, 2009,** had investigated the effects of cutoff walls and drains on the uplift pressure and exit gradient under hydraulic structures to prevent piping phenomena. **Goel and Pillai, 2010,** had investigated the variation of exit gradient downstream of weirs on permeable foundations. None of the above researches had used a coupled model of Genetic Algorithm with ANN model; hence in this research such model was used.

2. THE OPTIMIZATION MODEL FORMULATION

As previously mentioned, the most critical design of a hydraulic structure is the foundation design. The required for the design are the length of floor (B), depth of upstream cutoff (S1), depth of downstream cutoff (S2), length of protection at the downstream side against exit gradient (L) and

the uplift pressure or due to erosion of the downstream side, when the hydraulic gradient exceeds the critical exit gradient. The designer can control these failures by providing the recommended factors of safety against both uplift pressure and exit gradient failures. The controlling process was done by selecting the dimensions of S1, S2, B, and L for a given (H), (D) and (kx/ky). It is better to select optimum dimensions; the following objective function of such a problem could be introduced.

the volume of superstructure (V) for a given head difference (H), depth of impervious layer (D) and given soil properties underneath the structure, horizontal permeability kx, and vertical permeability ky. **Fig. 1** shows these dimensions.

The values of (S1, S2, L, and V) are affected by the maximum expected difference in head between the upstream and downstream sides of the hydraulic structure (H) and the soil strata properties (kx and ky). The most critical failures that may occur for such structures are either due to

$$\text{Min.} \quad f(x) = C1S1+C2S2+C3V+C4L+C5B \tag{1}$$

Where: f(x) is the cost function that should be minimized.

C1, C2, C3, C4 and C5 are the relative cost of each dimension.

This function is subjected to:

$$\text{F.o.s}_{\text{uplift}} = \frac{\gamma c V}{uplift\ force} \geq 2 \tag{2}$$

Where: $\text{F.o.s}_{\text{uplift}}$ is the factor of safety against uplift pressure,

V: volume of concrete of the superstructure, (L^3)

γc: Concrete weight density, (F/L^3)

and the uplift force is estimated by integrating the uplift pressure curve along the base of the structure.

The other constraint is:

$$\frac{icr}{i} \geq 3 \tag{3}$$

Where: *icr* is the critical exit gradient and $\cong 1$,

i is the computed exit gradient at the downstream side of the structure.

Further constraints could be imposed on the selected dimensions such as:

$$\left\{ \begin{array}{l} S1_{min.} \leq S1 \leq S1_{max.} \\ S2_{min.} \leq S2 \leq S2_{max.} \\ B_{min.} \leq B \leq B_{max.} \end{array} \right\} \tag{4}$$

3. GEO-STUDIO MODEL

The problem under-study explained in the previous section, is represented in the Geo-studio program (GEOSTUDIO.2004.V6.02-LND). This program was applied for 1200 case. For each case the program solves the seepage equation of the steady-state flow and anisotropic homogeneous soil using the finite element technique. From the results of the head distribution in the nodes, the required volume of concrete (V) and the required length of the downstream protection (L) are estimated such that the constraints of **Eqs. (2) and (3)** were achieved respectively.

Fig. 2 shows the structure for one of the cases with the discretization process. The elements used are square and rectangular as shown, with four nodes at the corners. This figure shows also the system of both element and node numbering.

Fig. 3 shows the distribution of the exit gradient along the downstream side of the structure. The required length of protection can be estimated using this curve and **Eq. (3).**

Table 1 shows the results of some cases analyzed using the Geo-studio models.

4.ARTIFICIAL NEURAL NETWORK (ANN) MODEL.

The results of L and V for the 1200 cases were used for building an ANN model capable of estimating L and V as output variables using S1, S2, H, B, D and kx/ky as input variables.

In order to obtain this model, the SPSS software (Statistical Procedure for Social Science, version 19.0) was used. For application of this software, six nodes were selected for the input layer which represents the input variables (S1, S2, H, B, D and kx/ky). Two nodes were selected for the output layer which represents the output variables (L and V). One hidden layer was selected for simplicity. To build the ANN model, many running trials were performed, in each one the software parameters were changed as follows:

- Selection the division of the data into training, testing, and validation sets.
- Also the selection of the division method either blocked, stripped, or random.
- Testing the proper number of nodes in the hidden layer.
- Changing the learning rate and momentum factor.

The selection of the best ANN model was achieved according to the smallest error and the highest correlation coefficient of the predicted and observed outputs.

The applied data to the software were the 1200 cases used in the Geo-Studio program. **Table 2** represents the best data division and **Fig. 4** shows the architecture of the ANN network.

Table 3 shows the bias and weight matrices for the input and hidden layers.

Figs. 7- a and 7-b show the comparison between predicted and observed values of L and V respectively.

The results of the ANN model indicated high correlation coefficients between the observed and predicted values of L and V as r_L= 98.3% and r_V= 99.4% respectively. **Table 6** shows the comparison of the values of L and V estimated

using both Geo-studio and ANN models, which indicates the capability of the ANN model to produce acceptable results.

5- OPTIMIZATION USING GENETIC ALGORITHM (GA) MODEL

The steps are used in the Genetic Algorithm models are shown in the appendix:

A MatLAB code was written for the Genetic Algorithm model using the Algorithm shown above. In order to apply this model values for the Genetic Algorithm, parameters were selected as np = 100, pc = 0.8, pm = 0.2, ML = 0.1, S1min = 0.5m, S1max = 4m, S2min = 0.5m, S2max = 4m, Bmin = H, Bmax = 2.5H.

Sensitivity analysis was also done for each parameter in order to find the effect of each one on the results obtained by the model. It was found that pc, pm and ML had little effect on the solution, and the above selected values give stable solution. Different values of np = 10, 20, 30, 40, 60, 80, 100 were tested and np = 100 gave the stable solution, and upon increasing this value above 100, the same solution was obtained. With these selected values, the number of iteration where the software reached the stable solution was found to be 2.

It is also worth to mention that the algorithm of genetic model solution is robust, i.e., in each run the results exhibit some changes among the output results for the same input values. This is true because the solution starts with random generation of S1, S2 and B, moreover the crossing-over and mutation selection is also randomly selected, and in each run different random matrices of those variables was generated. However, for each case the values of S1, S2 and B that give the least value of f(x) should be selected, however, the difference between f(x) values is small.

In order to compare the values of the obtained optimum solution using the Genetic Algorithm model, with the values obtained using Geo-studio model three cases were used as shown **in Tables 7, 8 and 9.**

Table 7 shows the results of using the Genetic Algorithm model for case (A). The second run solution was selected, since it gives the minimum f(x) value. The obtained value of S1=3.97m, S2=0.86m and B=5.02m were then approximated by S1=4.0m, S2=0.90m and B=5.0m respectively to be used in a simulation of this case in Geo-studio analysis for checking. This approximation was done to make the discretization process in the Geo-Studio modeling easy.

Table 8 shows the results of the use of Genetic Algorithm model for case (B) where H was increased to 10m and kx/ky to 4. The fifth run was selected, since it gives the minimum f(x) value. The obtained value of S1=3.58m, S2=0.61m and B=10.13m were then approximated to S1=3.60m, S2=0.60m and B=10.0m respectively to be used in a simulation in Geo-studio analysis for checking.

Table 9 shows the results of the use of Genetic Algorithm model for case (C) increasing kx/ky to 8. The third run solution was selected, since it gives the minimum f(x) value. The obtained value of S1=2.5687m, S2=0.82m and B=10.1396m were then approximated by S1=2.50m, S2=0.80m and B=10.0m respectively to be used in a simulation in Geo-studio analysis for checking.

These cases were re-analyzed using the Geo-studio model to find whether the obtained values of L and V by the Genetic Algorithm is compared with these obtained by the Geo-studio solution for the same approximated values of S1, S2 and B, and for the selected H, D and kx/ky values. The comparison is shown in **Table 10** which shows good agreement.

6. CONCLUSIONS

From the present work, the following conclusions could be obtained:

1) The obtained artificial neural network model, using depth of upstream cutoff (S1), depth of downstream cutoff (S2), head differences (H), length of floor required (B), depth of impervious layer (D) and degree of anisotropy(kr = kx/ky) to obtain values of the length of protection in the downstream side (L) and volume required for superstructure (V), that satisfies the related constraints of safety factors, is efficient with correlation coefficients 98.3% and 99.4% respectively. The required number of hidden nodes was 13 with one hidden layer.

2) The genetic algorithm model indicates that the values of probability of crossing-over, probability of mutation and mutation level have little effect on the obtained optimal solutions for the problem studied. Moreover, the generated population size that gave the stable solution is not less than 100 and the required number of iterations to reach this stable solution is 2.

3) The optimum solution obtained using the genetic algorithm model is robust, i.e, each run gave different solutions, and however, a slight difference was obtained for the decision variables for most of the solutions. Hence, the designer should select the solution that gives the minimum objective function {f(x)}.

4) The optimum solution obtained using the genetic algorithm model for upstream cutoff length (S1), downstream cutoff length (S2) and length of floor required for hydraulic structure (B) with the corresponding L and V values were compared with the L and V values obtained using geo-studio models and found to be comparable.

REFERENCES

Al-Duri, R. M. S. A., Feb., 1986,"*Protection of Hydraulic Structures Downstream*", M.Sc. Thesis, department of Water Resources Engineering, University of Technology, Baghdad.

Al-Fatlawy, R. A. K., May, 2007,"*Effect of Degree of Anisotropy on Exit Gradient under Dams using the Finite Element Method"*, M.Sc. Thesis, Department of Civil Engineering, University of Kufa, Iraq.

Al-Suhaili, R. H. S., Kharrufa, N. S and Al-Oubaidy A. S, 1988,"*Exit Gradient Variation Downstream of Hydraulic Structures"*, Scientific Journal Published by the University of Technology, Vol.5, No. 3.

Al-Suhaili, R. H. S., 2009, "*Analytical Solution for Exit Gradient Variation Downstream of Inclined Sheet Pile"*, The 6th Engineering Conference of Engineering College, College of Engineering, University of Baghdad, Iraq.

Ghobadian R. and Khodaei K., 2009, " *Effect of Cutoff Wall and Drain on Uplift Pressure and Exit Gradient under Hydraulic Structure by Numerical Solution of General Equation of Fluid Flow in Soil using Finite Volume Method"*, Journal of Water and soil, Volume 23, No.4, Winter 2009, p. 148-160.

Gole A. and Pillai N. N., 2010, "*Variation of Exit Gradient Downstream of Weirs on Permeable Foundations"*, The pacific Journal of Science and Technology, Volume 11, No. 1, p. 28-36.

Griffiths D. V. and Fenton G. A.,1993, "*Seepage Beneath Water Retaining Structures Founded on Spatially random Soil*", Geotechnique Volume 43, Issue 4, p. 577-587, Department of Engineering Mathematics, University of Dalhousie, Canada.

Griffiths D. V. and Fenton G. A.,1998, "*Probabilistic Analysis of Exit Gradients Due to Steady Seepage"*, Journal of Geotechnical and Geo-Environmental Engineering, Volume 124, No. 9, p. 789-797, Department of Engineering Mathematics, University of Dalhousie, Canada.

Haszpra O., Kalina E. and Hamvas F., 2000, "*Seepage Around Structures Built Into Flood Levees"*, Periodical Polytechnics Search Civil Engineer, Volume 45, No. 1, p. 141-149, Budapest University of Technology and Economics, Budapest, Hungary.

Ilyinsky N. B. and Kacimov A. R., 1992, "*Analytical Estimation of Ground-Water Flow Around Cutoff Walls and Into Interceptor Trenches"*, Journal of Ground Water, University of Kazan, Institute of Mathematics and Mechanics, volume 30, No. 6, p. 901-907.

Ismail Sh. S. and Aziz M., 2005,"*Toshka Spillway Barrages Stability Analysis*", Ninth International Water Technology Conference, (IWTC 9 2005), Sharm El-Sheikh, Egypt, p. 527-540.

Khassaf S. I., Al-Adili A. Sh. and Rasheed R. S., 2009, *"Seepage Analysis Underneath Diyala Foundation"*, Thirteenth International Water Technology conference, IWTC 13 2009, Hurghada, Egypt.

Manna M. C., Bhattacharya A. K. and Choudhury S., 2003, *"GroundWater Flow Beneath a Sheetpile Analyzed Using Six-Noded Traiangular Finite Elements"* IE (I) Journal – CV, Volume 84, August 2003, p. 121-129.

Moellmann A., Vermeer P. A. and Huber M., 2008, *"A Probabilistic Finite Element Analysis of Embankment Stability Under Transient Seepage Conditions*", Sixth International Probabilistic Workshop, Darmstadt 2008, Institute of Geotechnical Engineering, University of Stuttgart, German, p. 551-562.

Mukhopadhyay S., 2008, *"Seepage Analysis Through Foundation Using Finite Element Method and Flow Net*", The 12th International Conference of International Association for computer Methods and Advances in Geo-mechanics (IACMAG), 1-6 October,2008,Goa, India.

Shadravan B., Mirghasemi A. A. and Pakzad M, 2004, *"Karkheh Storage Dam Cutoff Wall Analysis and Design*", Proceedings of Fifth International Conference on Case Histories in Geotechnical Engineering, New York, NY, April 13-17, 2004, p. 133-141.

APPENDIX: GENETIC PROGRAM STEPS

1) Structure data input:
   - Enter the maximum expected difference in head between upstream and downstream sides (H in meters),
   - Enter limits of floor length (B maximum in meters),
   - Enter limits of floor length (B minimum in meters),
   - Enter limits of maximum upstream cutoff length (S1max. in meter) < depth of impervious layer (D),
   - Enter limits of minimum upstream cutoff length (S1min.in meter),
   - Enter limits of maximum downstream cutoff length (S2max. in meter),
   - Enter limits of minimum downstream cutoff length (S2min. in meter), and
   - Enter value of impervious layer depth (D in meter)
   - Enter kr = kx / ky ratio of horizontal to vertical permeability.

2) Genetic Algorithm / population, cross-over, mutation parameters:
   - Enter number of population solutions to be generated (np),
   - Enter cross-over probability (pc),
   - Enter mutation probability (pm),
   - Enter mutation level (ML), and

- Enter number of iterations to be performing (ni).

3) Genetic Algorithm objective function parameter input:
   - Minimize $f(x) = C1S1+C2S2+C3V+C4L+C5B,$ (5)
   - Enter (C1) as the percent cost for S1,
   - Enter (C2) as the percent cost for S2,
   - Enter (C3) as the percent cost for V,
   - Enter (C4) as the percent cost for L, and
   - Enter (C5) as the percent cost for B.

4) Generate (np) random S1 values between $S1_{max}$ and $S1_{min}$

$$S1_{min} \leq S1 \leq S1_{max}$$

5) Generate (np) random S2 values between $S2_{max}$ and $S2_{min}$

$$S2_{min} \leq S2 \leq S2_{max}$$

6) Generate (np) random B values between B_{max} and B_{min}

$$B_{min} \leq B \leq B_{max}$$

7) Find number of couples to be cross-over (NOCC)

$$NOCC = \left| \frac{np*pc}{2} \right| \quad (6)$$

8) Generate a matrix (randomly) between (1 and np) with (8*NOCC) elements.

9) Make cross-over, odd element with the near even element.

10) Make new populations,

$$\text{New Population} = (np + 8*NOCC) \quad (7)$$

11) Find S1, S2 and B for a mentioned new population, find the values of (Land V) from the ANN program and then calculate the value of f(x) from equation (4.1).

12) Sort values in ascending order and kill (remove) the last (8*NOCC) cases.

13) Find number of persons to be muted (NOPM),

$$NOPM = pm * np \quad (8)$$

14) Generate a matrix randomly (number of 1 to np) with elements (NOPM * number of input variables)

15) Make mutation accordingly; find NOPM persons using (± ML).

16) Add to population in step (11) or

[np +NOPM(+ML) + NOPM(-ML)]

17) Find f(x) for them, sort in ascending order, and kill (remove) last (2*NOPM) cases.

18) Go to make another iteration, go back to step (8).

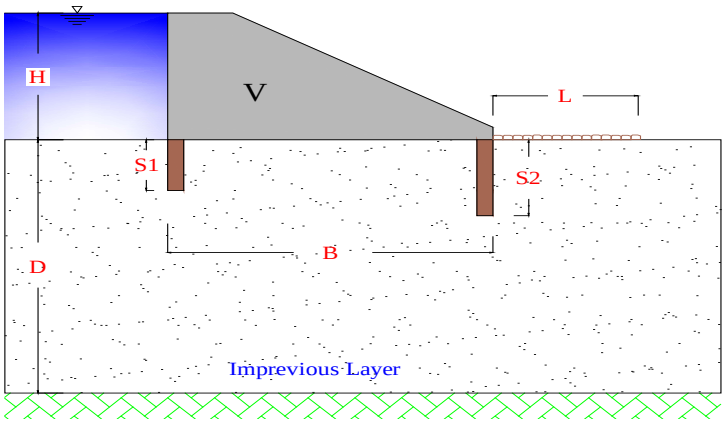

Figure 1. Schematic representation of the problem under study.

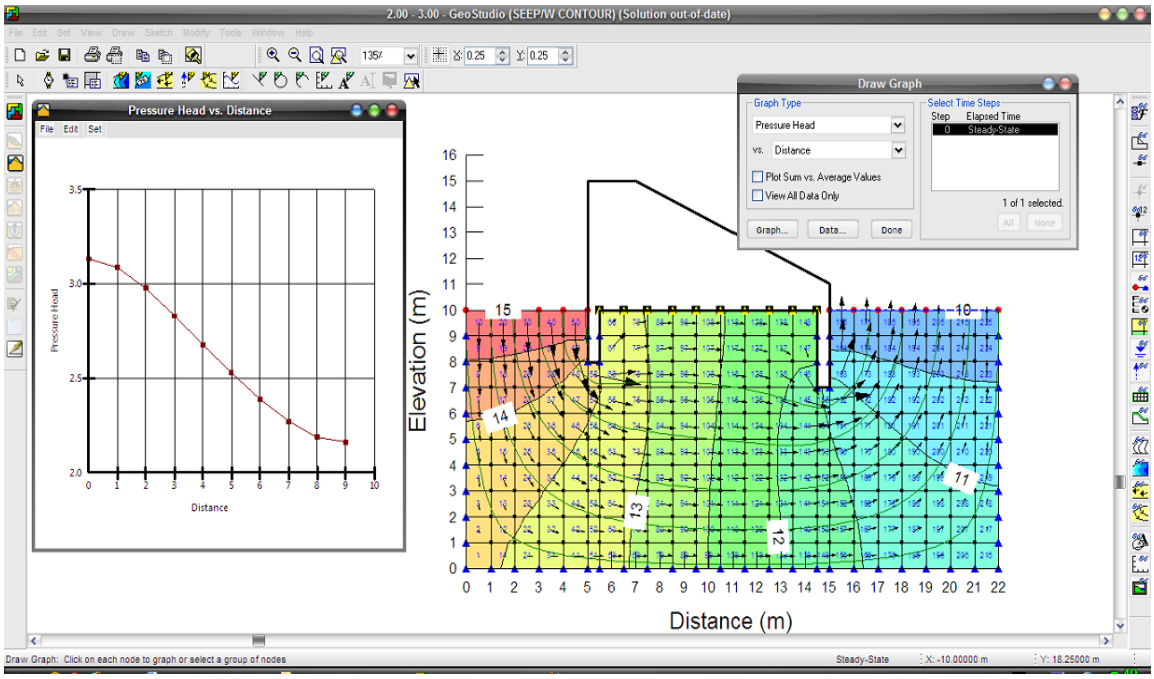

Figure 2. Uplift pressure distribution beneath the Structure, flow lines and equipotential lines.

(Note: on the left figure, x=0 refers to the upstream point of the structure foundation on the right figure**)**

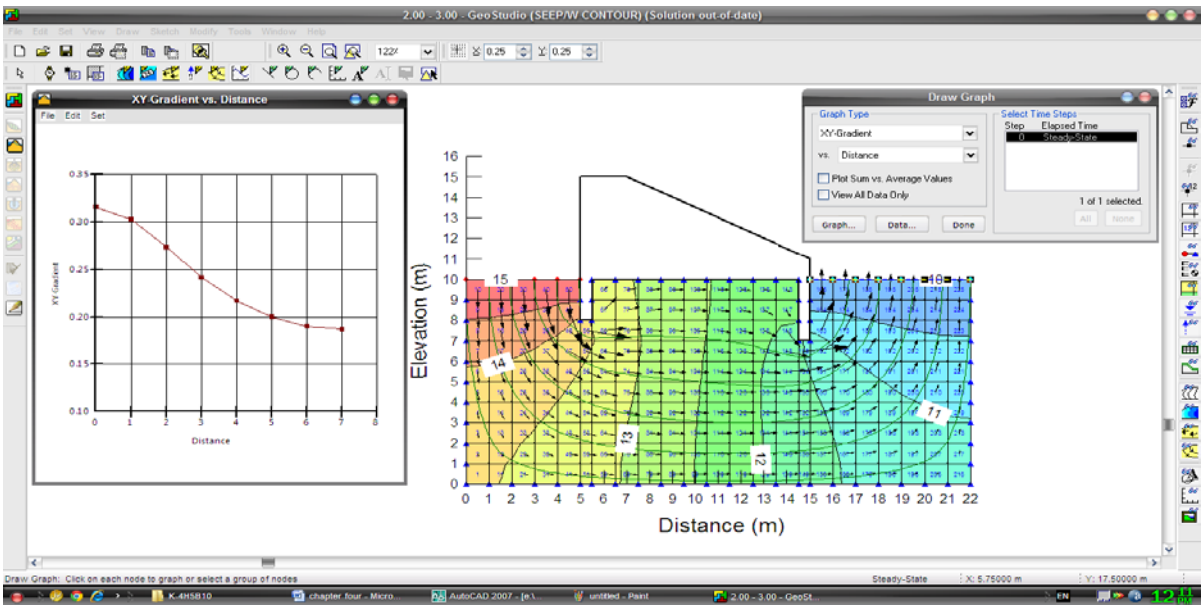

Figure 3. Distribution of the exit gradient along the downstream side.

(Note: on the left figure, x=0 refers to the downstream point of the structure foundation on the right figure)

Table 1. Results obtained for L and V using the Geo-studio models.

S1 (m)	S2 (m)	L (m)	V (m^3)
1	1	2.65	105.701
1	1.5	2.72	116.696
1	2	2.66	125.408
1	2.5	2.46	134.658
1	3	2.11	142.067
1	3.5	1.23	149.912
1	4	0.00	156.281
1.5	1	2.40	97.891
1.5	1.5	2.48	108.809
1.5	2	2.41	117.593
1.5	3	1.76	134.736
1.5	3.5	0.39	142.972
1.5	4	0.00	149.701
2	0.5	1.98	82.774
2	1	2.18	92.711
2	1.5	2.26	103.441
2	2	2.18	112.177
2	2.5	1.92	121.698
2	3	1.42	129.495
2	3.5	0.00	137.967
2	4	0.00	144.931

Table 2. Data division selected for the ANN model.

Item		N	%Total output
Sample	Training	960	80%
	Testing	180	15.0%
	Holdout	60	5.0%
Valid		1200	100%
Excluded		0	
Total		1200	

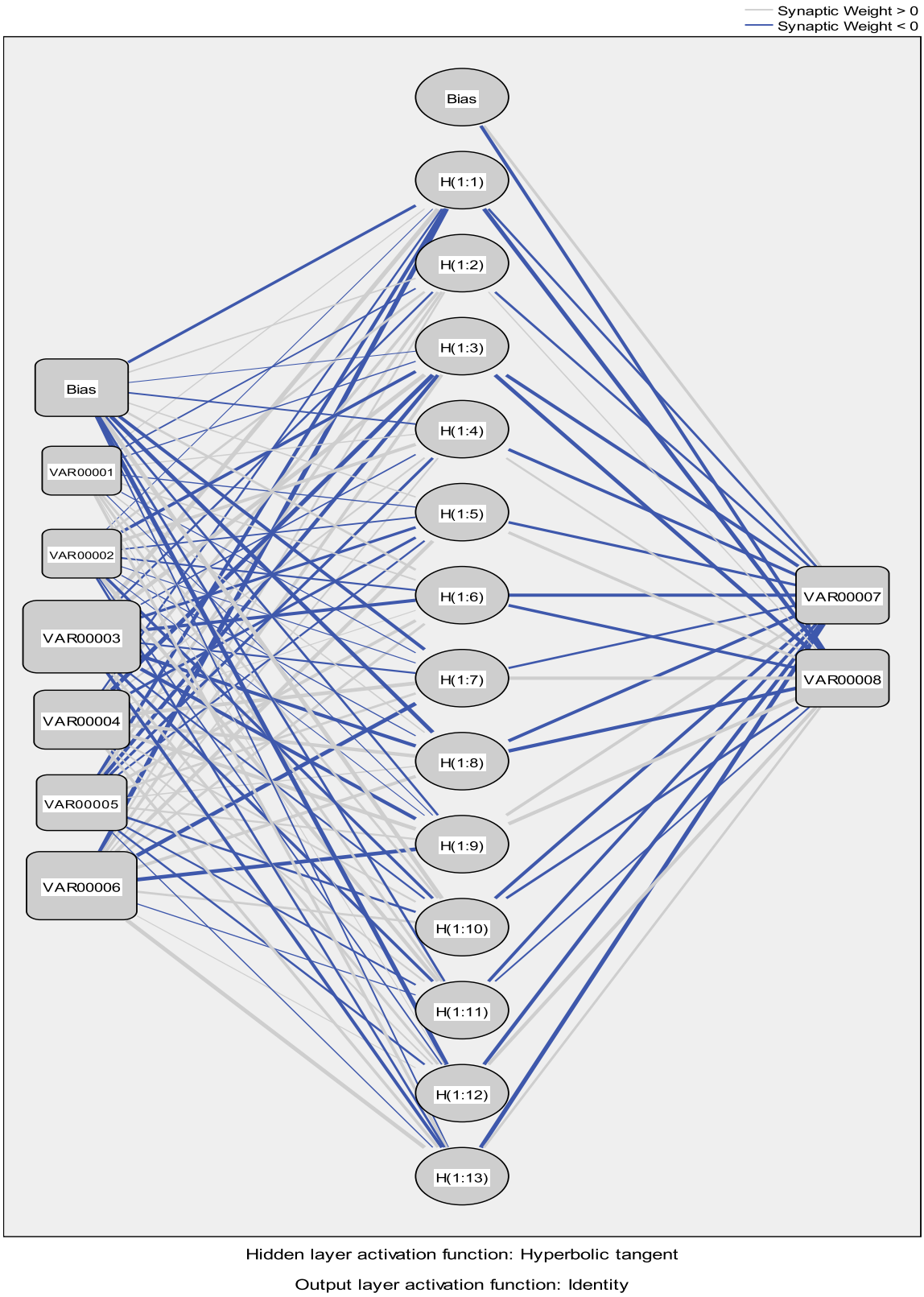

Figure 4. Architecture of the artificial neural network model.

Table 3. Bias and weight matrices for the ANN model.

Predictor		Predicted														
		Hidden Layer 1													Output Layer	
		H (1:1)	H (1:2)	H (1:3)	H (1:4)	H (1:5)	H (1:6)	H (1:7)	H (1:8)	H (1:9)	H (10:1)	H (1:11)	H (1:12)	H (13:1)	VAR007	VAR008
Input Layer	(Bias)	-0.556	0.098	-0.009	0.127	0.084	0.295	-0.945	-1.794	-0.196	1.984	-0.216	-2.078	-0.067		
	VAR0001	0.033	-0.101	-0.052	0.064	-0.044	0.112	-0.029	0.062	-0.017	0.219	0.317	0.004	0.414		
	VAR0002	-0.005	0.256	-0.914	1.134	-0.102	-0.158	-0.028	-0.038	-0.006	-0.511	1.103	-0.066	-0.179		
	VAR0003	3.265	-0.157	2.824	-0.072	-0.577	-1.310	-0.160	-1.571	-1.462	-0.135	-0.542	0.373	-0.613		
	VAR0004	-0.132	0.442	-4.170	0.122	-0.474	0.028	2.961	1.930	2.154	0.155	0.126	0.093	0.437		
	VAR0005	-0.815	0.399	-1.271	-0.409	-0.150	0.756	0.365	0.065	0.180	-0.279	-0.156	-0.176	-0.034		
	VAR0006	-5.794	0.131	0.537	0.089	1.297	0.373	-2.889	1.057	-3.650	0.342	-0.038	0.024	2.018		
Hidden Layer	(Bias)														0.406	-0.711
	H (1:1)														-0.227	-1.699
	H (1:2)														-0.241	0.039
	H (1:3)														-1.063	-1.614
	H (1:4)														-0.799	0.166
	H (1:5)														-0.513	0.619
	H (1:6)														-1.211	-0.742
	H (1:7)														-0.271	1.447
	H (1:8)														-0.949	-1.621
	H (1:9)														0.636	1.576
	H (1:10)														-0.882	-0.389
	H (1:11)														-0.604	-0.102
	H (1:12)														-1.103	0.916
	H (1:13)														-2.068	0.238

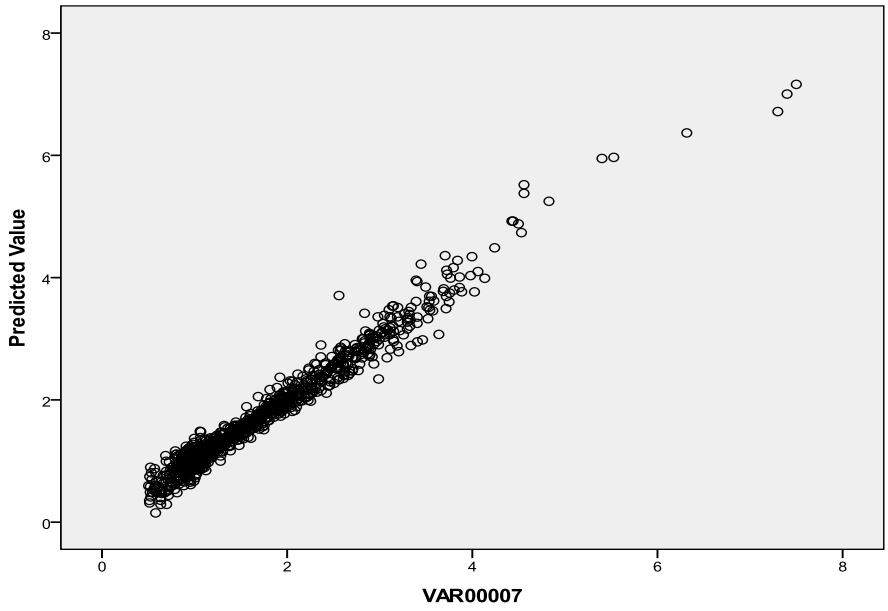

Figure 7- a. Comparison between predicted and observed values of (l).

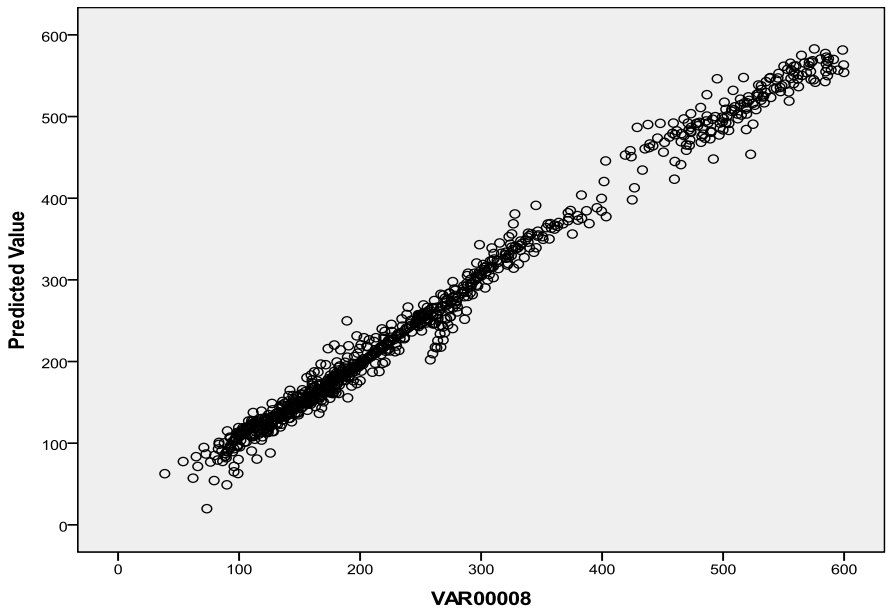

Figure 7- b. Comparison between predicted and observed values of (v) using the ANN model.

Table 6. Comparison of (L and V) values using Geo-studio and ANN Model.

S1	S2	H	B	D	kx/ky	Calculated L value using Geo-studio	Calculated V value using Geo-studio	Estimated L value using ANN model	Estimated V value using ANN model	% difference for L value	% difference for V value
1.50	2.50	5	5	10	1	2.867	133.238	2.836	138.876	1.08	-4.23
3.00	3.00	6.25	5	10	2	1.498	152.259	1.57	158.722	-4.79	-4.24
3.00	1.50	8	5	10	4	2.953	509.584	2.976	510.245	-0.78	-0.12
3.50	2.50	8	5	10	4	3.044	551.282	3.160	537.973	-3.82	2.41
2.50	2.50	12.5	5	10	8	1.19	145.94	1.175	146.53	1.28	-0.41
2.00	1.50	5	7.5	10	1	1.997	157.43	2.08	160.836	-4.28	-2.16
4.00	1.00	10	7.5	10	2	2.4	247.939	2.379	256.261	0.87	-3.35
1.50	2.50	10	7.5	10	2	3.755	332.517	3.706	340.982	1.32	-2.54
1.50	2.00	10	7.5	10	4	1.895	325.049	1.903	329.873	-0.42	-1.48
1.50	2.00	12.5	7.5	10	8	1.17	266.24	1.12	264.57	4.15	0.63
2.75	1.50	5	10	10	1	1.41	188.15	1.36	181.91	3.37	3.32
2.00	0.50	5.00	10.0	10	1	1.36	175.79	1.368	174.367	-0.59	0.81
4.00	2.00	15	10	10	4	2.46	471.00	2.476	490.375	-0.65	-4.11
2.50	1.50	15	10	10	4	2.58	493.52	2.66	498.24	-3.07	-0.96
2.00	3.00	30	10	10	8	1.413	141.755	1.350	136.985	4.44	3.36
4.00	2.50	30	10	10	8	1.22	117.834	1.253	124.391	-2.72	-5.56
3.00	2.00	7.5	12.5	10	1	2.48	373.93	2.509	383.94	-1.17	-2.68
3.00	1.00	10	12.5	10	2	1.826	465.25	1.886	468.02	-3.29	-0.60
1.00	2.00	10	12.5	10	4	1.12	547.143	1.19	533.47	-6.23	2.5
2.00	2.50	20	12.5	10	8	1.14	292.8	1.08	293.81	5.07	-0.34

Table 7. Optimum solution obtained using Genetic Algorithm model for case (A).

H = 5 m, D = 10 m, kx/ky = 1

Optimum solution obtained using Genetic Algorithm model						
Run No.	S1 (m)	S2 (m)	B (m)	L (m)	V (m^3)	F(x)
1	3.5	0.908	5.57	1.88	106.93	23.79
2	3.97	0.8601	5.0267	1.8128	81.6163	18.7174
3	3.645	1.47	5.0	2.087	100.28	22.54
4	3.56	0.598	5.344	1.78	94.48	21.182
5	3.5	0.71	5.7	1.78	102.88	22.95

Table 8. Optimum Solution obtained using Genetic Algorithm model for case (B).

H = 10 m, D = 10 m, kx/ky = 4:

Optimum solution obtained using Genetic Algorithm model						
Run No.	S1 (m)	S2 (m)	B (m)	L (m)	V (m^3)	F(x)
1	3.77	1.52	10.6	0.83	359.12	75.35
2	3.71	0.53	10.18	0.77	338.4	70.87
3	3.55	1.58	11.22	0.78	379.35	79.47
4	3.65	1.44	10.50	0.85	356.44	74.77
5	3.58	0.61	10.13	0.79	338.42	70.84

Table 9. Optimum solution obtained using Genetic Algorithm model for case (C).

H = 10 m, D = 10 m, kx/ky = 8:

Optimum solution obtained using Genetic Algorithm model						
Run No.	S1 (m)	S2 (m)	B (m)	L (m)	V (m^3)	F(x)
1	1.6492	0.7161	10.7606	1.00	476.8957	98.2226
2	1.2946	0.6998	10.0684	0.694	476.9712	97.9759
3	2.5687	0.8212	10.1396	0.6626	474.7486	97.8914
4	1.6708	0.5426	10.9744	0.6508	477.16.83	98.2470
5	3.40	0.8176	10.4655	0.6290	473.7681	97.9640

Table 10. Comparison of estimated (L and V) values for the three cases selected.

Case No.	Given Values			Estimated Values							% difference for L value	% difference for V value
				Genetic Algorithm Optimization					Geo-Studio Model			
	H (m)	D (m)	Kx/ky	S1 (m)	S2 (m)	B (m)	L (m)	V (m^3)	L (m)	V (m^3)		
A	5	10	1	4	0.9	5	1.81	81.616	1.79	82.233	-1.11	0.75
B	10	10	4	3.6	0.60	10	0.89	338.42	0.91	357.08	2.19	-5.23
C	10	10	8	2.6	0.80	10	0.66	474.74	0.70	469.86	-5.83	1.04

Assessment Efficiency Evaluation of Al-Diwaniya Sewage Treatment Plant in Iraq

Dr. Awatif Soaded Alsaqqar
alsaqqar@yahoo.com
Assistant professor
Baghdad University-Engineering College/Civil Department

Dr. Basim Hussein Khudair
basim22003@yahoo.com
Lecturer
Baghdad University-Engineering College/Civil Department

M.Sc. Ahmid Mekki
abd_almokhtar59@yahoo.com
Lecturer
Al-Qadesiha University-Engineering College/Civil Department

ABSTRACT

This study aims to evaluate the performance of the sewage treatment plant in Al-Diwaniya, one of cities in the southern part in Iraq. This evaluation could be used to facilitate effluent quality assessment or optimal process control of the plant. The influent reaching the plant is considered a medium to strong in strength with BOD_5/COD ratio in the range 0.23 and 0.69 which can be considered an easily degradable sewage by the biological processes performed by the activated sludge unit. The quality of the effluent was found to be higher than the Iraqi standards for disposal to water bodies. The BOD_5/COD ratios of the treated sewage varied over a wide range as low of 0.13 to 1.48 indicating operational problems in the plant. Regression analysis was performed to estimate the removal percentages of BOD_5, COD, TSS and NO_3 that the plant should perform by to reach the disposal limitations.

Key words: sewage treatment plants, performance evaluation, wastewater characteristics, BOD_5, COD, TSS, NO_3, BOD_5/COD ratio.

تقييم كفاءة الاداء لمحطة معالجة مياه الصرف الصحي في الديوانية، العراق

د. عواطف سؤدد عبدالحميد
استاذ مساعد
جامعة بغداد-كلية الهندسة/القسم المدني

د. باسم حسين خضير
مدرس
جامعة بغداد-كلية الهندسة/القسم المدني

احمد مكي جبار
مدرس
جامعة القادسية/كلية الهندسة-القسم المدني

الخلاصة:

تهدف هذه الدراسة الى تقييم كفاءة الاداء لمحطة معالجة مياه الصرف الصحي في مدينة الديوانية احدى المدن في جنوب العراق . ويمكن من خلال هذه الدراسة تقييم وتخمين صفات المياه المطروحة او السيطرة المثلى في تشغيل المحطة . و تتغاير مياه الفضلات الداخلة الى المحطة من متوسطة الى عالية القوة وبنسبة طلب الاوكسجين الحيوي الى طلب الاوكسجين الكيمياوي 0,23 و 0,69 والتي تصنف هذه المياه بسهولة التحلل بواسطة الطرق البايولوجية (طريقة الحماة النشطة) . اما االمياه المعالجة من هذه المحطة فقد وجدت بانها لا

تتطابق مع معايير المياه التي يمكن رميها الى المسطحات المائية، وان نسبة طلب الاوكسجين الحيوي الى طلب الاوكسجين الكيمياوي للمياه المطروحة من هذه المحطة تراوحت من 0,13 الى 1,48 والتي تؤشر الى وجود مشاكل تشغيلية في المحطة. وقد اجريت تحاليل احصائية لتخمين نسب الازالة للطلب الاوكسجين الحيوي، والاوكسجين الكيميائي و المواد العالقة والنترات بحيث يتم تشغيل المحطة بموجبها للوصول الى المعايير اللازمة لرمي المياه المعالجة الى المصادر المائية.

الكلمات الرئيسية: محطة معالجة المجاري، تقييم الاداء، خواص مياه الصرف الصحي، المتطلب الحيوي للاوكسجين، المتطلب الحيوي الكيميائي، كمية المواد الصلبة العالقة، نترات، نسبة طلب الاوكسجين الحيوي الى طلب الاوكسجين الكيمياوي.

1.INTRODUCTION

Sewage is created from different sources as residential, institutional, commercial and industrial activities. It is collected and transported via a network of pipes to a sewage treatment plant (STP). The main aim of this plant is the removal of pollutants from the wastewater and consequently the reduction of solids, organic matter and nutrients so it will be possible to discharge the treated effluent to natural water bodies, **Erbe et al., 2002.**

The proper operation and control of STPs is receiving increasing attention because of the rising concern about environmental issues. Improper operation of STPs may bring serious environmental problems, as its effluent is discharged to a water body. Sewage treatment plants are designed and operated in order to mimic the natural treatment processes to reduce pollutant loads to a level that nature can handle. In this regard, special attention is necessary to assess the environmental impacts of existing sewage treatment facilities **Jamrah, 1999**.

Performance evaluation of existing treatment plant is required (1) to assess the Existing effluent quality and/or to meet higher treatment requirements and, (2) to know about the treatment plant whether it is possible to handle higher hydraulic and organic loadings. The general yardstick of evaluating the performance of a sewage treatment plant is the degree of BOD_5 or

COD and suspended solids reduction, which constitute organic pollution. The performance efficiency of the treatment plant depends not only on proper design and construction but also on good operation and maintenance, **Sundara et al., 2010.**

Silvia et al., 2011, evaluated the operational conditions to verify the existence of a relationship between design and operational parameters and the performance of the sewage treatment plants under study. The hydraulic retention time (HRT) was included in the evaluation, because this variable could be calculated for all units and it reflects in a simplified way loading conditions. The plants were classified as under loaded (actual BOD load less than the minimum recommended range), normally or usually loaded (BOD load within the range) and overloaded (BOD load higher than the maximum range). Additionally, in order to analyze whether there was a difference in the performance of smaller and larger plants, all systems were ranked by flow, and split into two groups: low flows (0 to 50 % of mean flows) and high flows (50 to 100 % of mean flows). Also a monitoring index (MI–average number of samples collected per year in each plant) was

investigated as a possible indicator of the operational level in the plant (higher MI values could be associated with more operator's involvement and, therefore, possibly a better operation).

2.OBJECTIVE OF THIS STUDY

The main objective of this study is to evaluate the performance of the Al-Diwaniya sewage treatment plant, one of the southern cities in Iraq. This evaluation could be used to facilitate effluent quality assessment or optimal process control of the plant. A detailed characterization of the incoming sewage and a performance evaluation was carried out for this plant through the removal of BOD_5, COD, TSS and nutrients.

3.AL-DIWANIYASEWAGE TREATMENT PLANT (STP)

This plant is located on road 8 in the southern part of Al-Diwaniya city on Shut Al-Diwaniya, a branch of the Euphrates River **Fig.1**. The design capacity of this plant is 4DWF (dry weather flow) which is 80000 m^3/d. The plant consists of two identical stream lines that treat the sewage in two stages, Primary and Secondary treatment processes. The primary stage consists of a rack screen and the detritus for the sedimentation of inorganic suspended solids. The secondary treatment is an activated sludge process for the biological degradation of the organic content. The effluent from the primary treatment enters a distribution chamber that receives the return sludge from the secondary sedimentation tank. The mixture from this chamber is distributed to the aeration tanks of the two streams.

The final effluent from the secondary sedimentation tanks flows into the chlorine tank for disinfection before it is discharged to the river. The wasted sludge from the secondary sedimentation tanks is collected in a holding tank where the supernatant is pumped back to the distribution chamber and the settled sludge is pumped to the drying beds. The plant is designed to yield an effluent of 20 mg/L BOD_5 and 30mg/L suspended solids.

4.DATA COLLECTION AND ANALYSIS

The data used in this paper was provided from Al-Diwaniya STP for the period January 2007 to September 2008, which represented the average monthly values of the mainly parameters of the influent and effluent.

5.RESULTS AND DISCUSSION

1- Characteristics of the influent sewage

Fig. 2 shows the average monthly BOD_5, COD, TSS, NO_3 and PO_4 of the untreated sewage flowing into the plant. From these data, the influent reaching the plant is considered of a medium to strong strength according to the classification in **Table 1** given by Metcalf and Eddy, 2003. The BOD_5 ranged from 149 to 344.93 mg/L with an average of 199.11 mg/L, where COD ranged from 329.63 to 814.38 mg/L

and 468.42 mg/L average. The concentrations of total suspended solids (TSS) were between 277.05 to 919.25 mg/L and an average of 455.81 mg/L. The detained BOD_5/COD ratio shown in **Fig. 3** for the influent wastewater in is study was in the range 0.23 and 0.69 and this ratio for untreated sewage could be considered as a normal case (0.3-0.8) according to **Table 2**. Hence this waste is considered to be easily degradable by the biological processes performed by the activated sludge process, **Metcalf and Eddy, 2003.** As for the nutrients, the recorded values were for 2008 only. PO_4 ranged from 31.25 to 72.0 mg/L with an average of 44.98 mg/L where NO3 ranged from 4.9 to 6.53 mg/L with an average of 5.56 mg/L as shown in **Table 3**.

2- Characteristics of the effluent

The quality of the effluent from the plant has been found to be higher than expected from the Iraqi effluent standards for disposal to water bodies. The BOD_5 exceeded 20 mg/L limit for disposal limitations over the whole period as shown in **Table 4**. The values of COD were in less than the limitation 100 mg/L in year 2008. These values of BOD_5 and COD could constitute potential pollution problems to the water bodies since it contains organic compounds that require large amounts of oxygen for degradation. As for the effluent (treated sewage) the BOD_5/COD ratio varied over a wide range 0.17 to 0.95, reaching 1.09 and 1.48 in 2008 as shown in **Fig. 3**, these values are very large than those shown in **Table 2** for the treated sewage. This may indicate problems in the treatment process which affects the performance and removal efficiency of different pollutants from the sewage being treated in this plant. As for the suspended solids most of the values exceeded 30 mg/L. High concentrations of nutrients in the form of PO_4 and NO_3 were observed in the effluent, with an average of 5 mg/L for PO_4 and 22mg/L for NO_3. These pollutants are the major parameters causing eutrophication in water bodies.

3- Overall efficiency of Al-Diwaniya STP

The average monthly overall removal of BOD_5, COD, TSS and NO_3 during the period 2007–2008 in Al-Diwaniya STP was 70.09, 73.15, 82.21 and 38.74% respectively as shown in **Table 5**. Low removal of organic matter (BOD_5, COD) may be due to the recycling of old sludge that contains fewer microorganisms, which may cause insufficient MLSS for aerobic decomposition of organic matter. Also the DO during aeration could be absorbed by the microorganisms due to less availability of fresh organic matter (Ravi et al., 2010).Also over loading due to increase in population, increase in water use and discharge of trade effluents reaching the plant may cause poor performance in WWTPs. The treatment efficiency may be badly affected if the system is hydraulically under loaded, **Sundara et al., 2010.**

4- Performance of Al-Diwaniya STP

From the previous analysis of the effluent from Al-Diwaniya STP, it is clear that the plant is not functioning in the proper design specifications, which maybe the result of operational problems in the working units. These problems affect the performance of the plant to remove different pollutants like BOD_5, COD, TSS and nutrients to the desired disposal limitations. All of the disposal limitations were exceeded, which will cause pollution threads in the receiving river. It is hard to specify which unit or units not working within the proper design criteria to yield the disposal limitations, as no water quality measurements are taken from each unit in the plant (before and after each unit). A major tool required for proper process control is frequent and accurate sampling and laboratory analysis ,**Sundara et al., 2010.**

The following is a brief discussion on how the working conditions of different units in the plant can affect the effluent quality.

1-High organic concentrations (BOD_5 and COD) maybe caused by:

a- Improper aeration in the aeration basin, where not enough dissolved oxygen (DO) is existed for aerobic decomposition. Continuous measurement for DO concentrations (which is not recorded) in the basin will provide a clear observation on the amount of DO supplied and consumed for aerobic decomposition of organic matter. The concentration of DO in the aeration basin depends on many factors; temperature, basin geometry, degree of mixing and wastewater characteristics. Where the main factor is the aeration method used, mechanical aeration or air diffusors, **Eckenfelder et al., 2002.**

b- Large masses of organisms grow in the aeration basin are to be settled in the secondary sedimentation tank (clarifier) and are returned to the aeration basin as Qr or wasted from the system as Qw, play the main operating factor in this system. If there is a problem in the settling procedure of the clarifier then high concentration of microbial mass is measured as BOD_5 or COD in the effluent, **Santo et al., 2005.**

2- High concentration of suspended solids (SS) are recorded in the effluent may be due to:

a- Insufficient removal of TSS in the primary treatment as in grit chambers and in primary sedimentation tanks. The removal of SS depends on size of the settled particles and their specific gravity. The main issue in this stage of treatment is the separation of organic from inorganic particles.

b- Improper settling in the secondary sedimentation tank for the removal of the microbial mass. This may be due to some problems in the aeration basin: excessive turbulence, anaerobic conditions and toxic shock loading ,**Qasim, 1999**. The ability of biological solids to flocculate due to the natural presence of exocellular enzymes and polymers creates flocs that settle

rapidly enough allowing an economically sized clarifier to produce acceptable effluent quality. Smaller flocs that remain isolated and do not become incorporated into a larger floc mass report to the effluent instead of reporting to the underflow. These solids comprise a high percentage of the effluent suspended solids (TSS) and thus effluent particulate pollutant concentration, **Parker, 1983.**

3- High concentration of nutrient in the form of PO_4 and NO_3

The existing activated sludge system is not designed for nutrient removal. To improve the effluent quality, new units should be added or the development of the existing units for nutrient removal. The most common process for biological nitrogen removal consists of an anoxic tank (for denitrification) followed by the aeration tank (for nitrification), **Metcalf and Eddy, 2003**.

Al-Diwaniya STP has to specify the operation problems of the working units by taking more water quality measurements for each unit. The performance and stability of the activated sludge process is affected by many parameters that should be considered in evaluating the plant. The effective parameters are: solid retention time SRT, specific biomass growth rate μ, specific substrate utilization rate U and the biomass yield coefficient (Y) (Metcalf and Eddy, 2003).

4- Regression analysis for removal efficiency

A regression study was performed for each parameter to estimate the removal efficiency with respect to the disposal limitations with high correlations (R^2). The equations estimating the removal percentage were as follows:

BOD_5: $y = 0.0004x + 0.816$, R^2:0.93, Fig.4

COD: $y = 0.0004x + 0.5993$,R^2:0.95, Fig.5

TSS: $y = 0.0001x + 0.8745$, R^2:0.88, Fig.6

NO_3: $y = 0.0004x + 0.9568$, R^2:0.92, Fig.7

These equations could help to upgrade the units so the performance of the plant will give better effluents for disposal.

6.CONCLUSIONS

1-The influent to Al-Diwaniya STP is considered medium to high in strength. The BOD_5/COD ratio of this wastewater ranged 0.23 to 0.67 which is normal and the wastewater is easily degradable by biological processes.

2- The quality of the effluent was found to be higher than the Iraqi standards for disposal to water bodies. The BOD_5/COD ratios of the treated sewage varied over a wide range as low of 0.13 to 1.48 indicating poor performance in the plant.

3-The average removal percentages for BOD_5, COD, TSS and NO_3 were 70.09, 73.13, 82.21 and 48.74% respectively, which were not enough to treat the sewage to disposal limitations of 20, 100, 30 and less of 1 mg/L respectively .

4-Regression analysis was performed to estimate the removal percentages of BOD_5, COD, TSS and NO_3 that the plant should perform by to reach the disposal limitations.

REFERENCES

- Eckenfelder W. W., Malina, J. F. and Patterson J. W., 2002 "*Aeration: Principles and Practice"* Vol. 11, CRC Press LLC.
- Erbe, V., Risholt, L. P., Schilling, W. and Londong, J., 2003 "*Integrated Modeling for Analysis and Optimization of Wastewater Systems"* the Odenthal case. Urban Water, Vol. 4, No. 1. pp 63-71.
- Jamrah A. I.,1999. *"Assessment of characteristics and biological treatment technologies of Jordanian wastewater"*. Bioprocess engineering, Vol. 21, pp 331-340.
- Metcalf and Eddy, 2003, "*Wastewater engineering –Treatment and Reuse"* 4th edition, McGraw Hill Publishing Co. Inc.
- Parker, D.S., 1983, *"Assessment of Secondary Clarifier Design Concepts."* *Journal Water Pollution Control Federation*, 44, 349 – 359.
- Qasim Syde R., 1999, *"Wastewater treatment plants – Planning, Design and Operation"* CBR College publishing.
- Ravi Kumar, P., Liza Britta Pinto, Somashekar, R.K, 2010, "*Assessment of the efficiency of sewage treatment plants: a comparative study between Nagasandra and Mailasandra sewage treatment plants*" Kathmandu University, Journal of Science, Engineering and Technology Vol. 6, No. II, November, pp 115-125.
- Santo I., Fernandes E., Araujo M. and Ferreira E., 2005 "*Biological Process Optimal Design in Wastewater Treatment Plants"* 6th World Congress of Structural and Multidisciplinary Optimization, Rio de Janeiro, Barazil.
- Sílvia C. Oliveira and Marcos von Sperling, 2011, "*Performance evaluation of different wastewater treatment technologies operating in a developing country"* Journal of Water, Sanitation and Hygiene. for Development. 01. 1
- Sundara K. Kumar, P. Sundara Kumar and Dr. M. J. Ratnakanth Babu, 2010, "*Performance evaluation of waste water treatment plant*" International Journal of Engineering Science and Technology ,Vol. 2(12), 7785-7796.

Table 1. Strength classification of untreated sewage, **Metcalf and Eddy, 2003.**

Parameter (mg/L)	Weak	Medium	Strong
Total dissolved solids	270	500	860
Total suspended solids	120	210	400
BOD5	110	190	350
COD	250	430	800
TOC	80	140	260
Total N	20	40	70
Total P	4	7	12
Chloride	30	50	90
Sulfate	20	30	50

Table 2. Ratios of various parameters used to characterize wastewater,**Metcalf and Eddy, 2003.**

Type of wastewater	BOD_5/COD	BOD_5/TOC
Untreated	0.3 – 0.8	1.2 -2.0
After primary settling	0.4 – 0.6	0.8 – 1.2
Final effluent	0.1 – 0.3	0.1 – 0.5

Table 3. Influent wastewater characteristic of Al-Diwaniya STP (2007-2008).

Month	BOD_5 mg/L	COD mg/L	TSS mg/L	Temp.	pH	NO_3 mg/L	PO_4 mg/L
Jan.07	150.00	380.00	400.00	15.70			
Feb.07	344.93	706.00	919.25	21.10			
Mar.07	190.87	814.38	749.00	22.66			
Apr.07	150.00	430.00	573.50	26.40			
May.07	158.75	409.70	311.64	30.73	7.26		
Jun.07	149.00	407.17	368.71	30.98			
Jul.07	175.71	404.67	392.15	31.20			
Aug.07	174.00	403.50	361.00	31.40			
Sep.07	173.33	407.13	488.88	21.36	7.09		
Oct.07	149.00	380.00	311.64	15.70	7.09		
Nov.07	344.93	814.38	919.25	31.40	7.26		
Jan.08	234.25	561.53	481.61	13.11	7.16	46.75	
Feb.08	234.14	585.63	495.25	15.63	7.05	72.00	
Mar.08	218.78	552.11	451.44	20.36	7.07	52.50	
Apr.08	169.25	375.06	338.50	24.71	7.18	46.60	
May.08	185.33	359.00	367.35	28.06	7.12	39.60	
Jun.08	201.67	352.05	321.29	29.80	7.16	31.25	4.90
Jul.08	166.25	329.63	279.63	30.13	7.07	33.14	6.53
Aug.08	225.80	337.05	277.05	31.10	7.14	45.00	5.48
Sept.08	186.25	359.50	309.11	31.43	7.18	38.00	5.33
Min	149.00	329.63	277.05	13.11	7.05	31.25	4.90
Max	344.93	814.38	919.25	31.43	7.26	72.00	6.53
Mean	199.11	468.42	455.81	25.15	7.14	44.98	5.56
Typical concentration (mg/L)	250	700	250	6.5	6.5	<1	10

Table 4. Effluent (treated) wastewater characteristic of Al-Diwaniya STP (2007-2008).

Month	BOD_5 mg/L	COD mg/L	TSS mg/L	NO_3 mg/L	PO_4 mg/L
Jan.07	62.20	300.00	217.00		
Feb.07	48.00	374.67	152.67		
Mar.07	50.00	140.13	71.11		
Apr.07	96.25	142.00	108.50		
May.07	89.00	101.20	70.71		
Jun.07	78.57	125.85	90.56		
Jul.07	54.00	117.83	104.00		
Aug.07	25.00	91.75	72.25		
Sep.07	25.00	68.89	54.11		
Oct.07	96.25	68.89	54.11		
Nov.07	62.88	374.67	217.00		
Jan.08	40.88	114.47	92.06	18.25	
Feb.08	37.71	84.75	59.00	24.30	
Mar.08	30.22	74.83	40.22	28.50	
Apr.08	34.83	74.13	37.38	30.00	
May.08	38.33	67.41	33.94	28.00	
Jun.08	50.33	107.76	64.33	15.50	5.55
Jul.08	40.13	67.95	37.74	16.00	5.23
Aug.08	52.80	46.74	21.26	29.00	4.63
Sept.08	75.00	50.75	28.44	14.00	4.63
Min	25.00	46.74	21.26	14.00	4.63
Max	96.25	374.67	217.00	30.00	5.55
Disposal limits	20	100	30	<1	<1

Table 5. Average monthly overall removal of BOD_5, COD, TSS and NO_3 in Al-Diwaniya STP

Month	%BOD	%COD	%TSS	%NO_3
Jan. 7	58.53	21.05	45.75	
Feb.07	86.08	46.93	83.39	
Mar.07	73.80	82.79	90.51	
Apr.07	35.83	66.98	81.08	
May.07	43.94	75.30	77.31	
Jun.07	47.27	69.09	75.44	
Jul.07	69.27	70.88	73.48	
Aug.07	85.63	77.26	79.99	
Sept.07	85.58	83.08	88.93	
Oct.07	35.40	81.87	82.64	
Nov.07	81.77	53.99	76.39	
Jan.08	82.55	79.62	80.89	60.96
Feb.08	83.89	85.53	88.09	66.25

Mar.08	86.19	86.45	91.09	45.71
Apr.08	79.42	80.24	88.96	35.62
May.08	79.32	81.22	90.76	29.29
Jun.08	75.04	69.39	79.98	50.40
Jul.08	75.86	79.39	86.50	51.72
Aug.08	76.62	86.13	92.33	35.56
Sept.08	59.73	85.88	90.80	63.16
Min	35.40	21.05	45.75	29.29
Max	86.19	86.45	92.33	66.25
Mean	70.09	73.15	82.21	48.74

Figure 1. Google earth photo for Al-Diwaniya STP, Diwaniya project, Iraq.

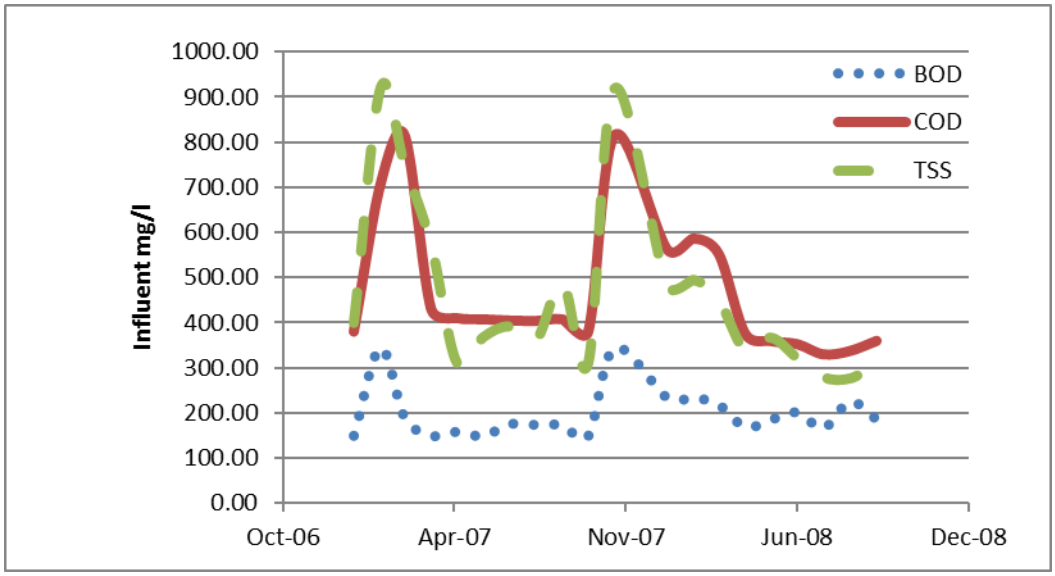

Figure 2. Influent variation for BOD_5, COD and TSS.

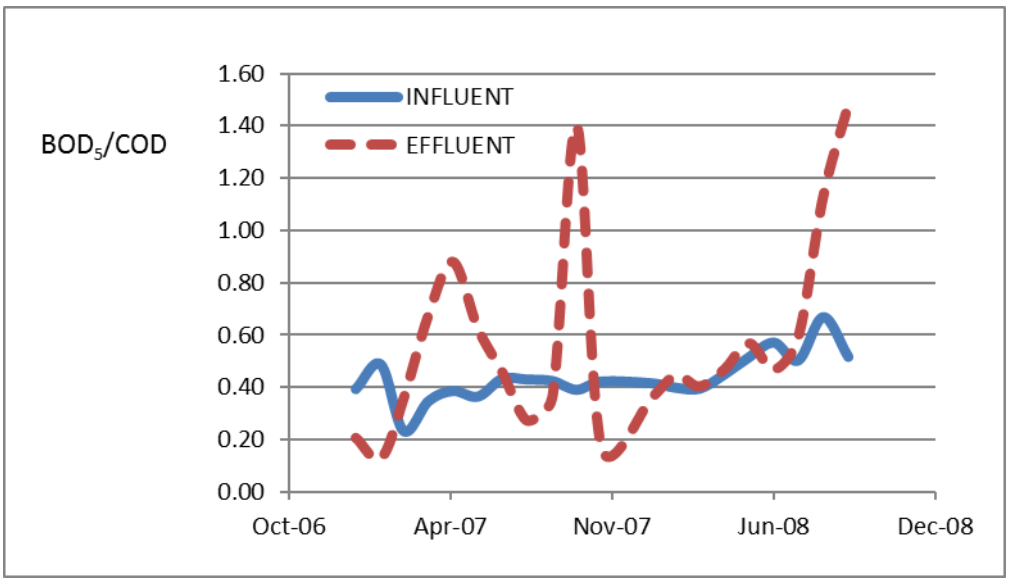

Figure 3. Variation of BOD_5/COD ratios for the influent and effluent.

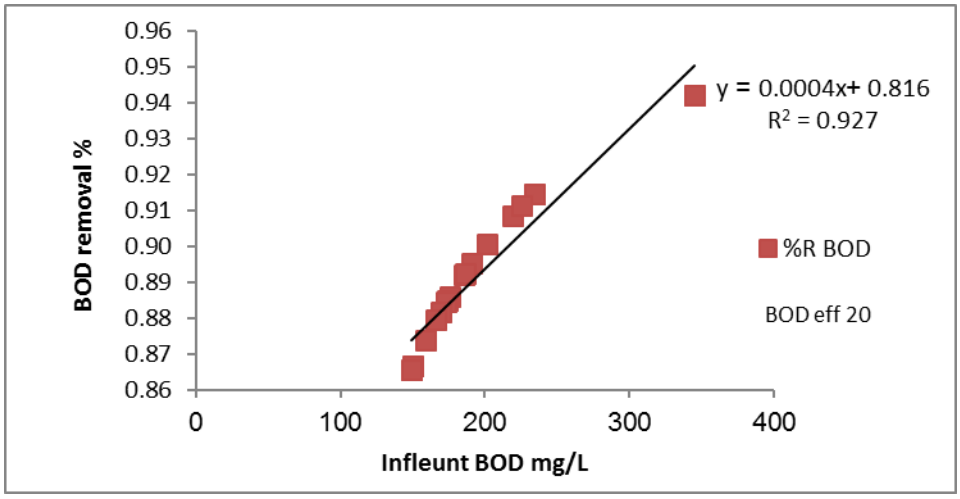

Figure 4. Regression equation for BOD_5 removal.

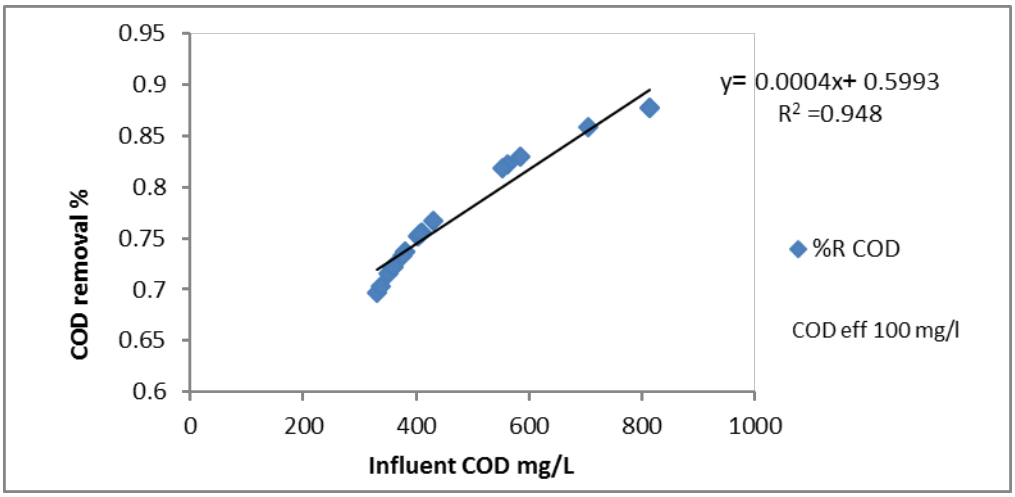

Figure 5. Regression equation for COD removal.

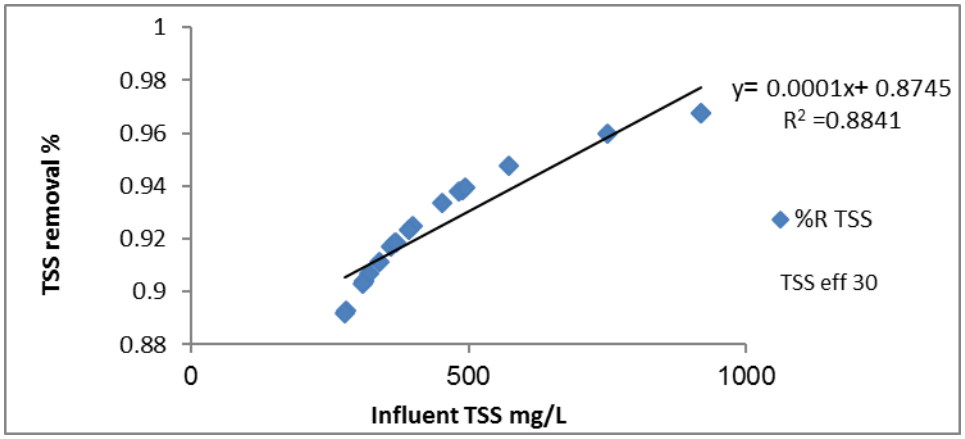

Figure 6. Regression equation for TSS removal**.**

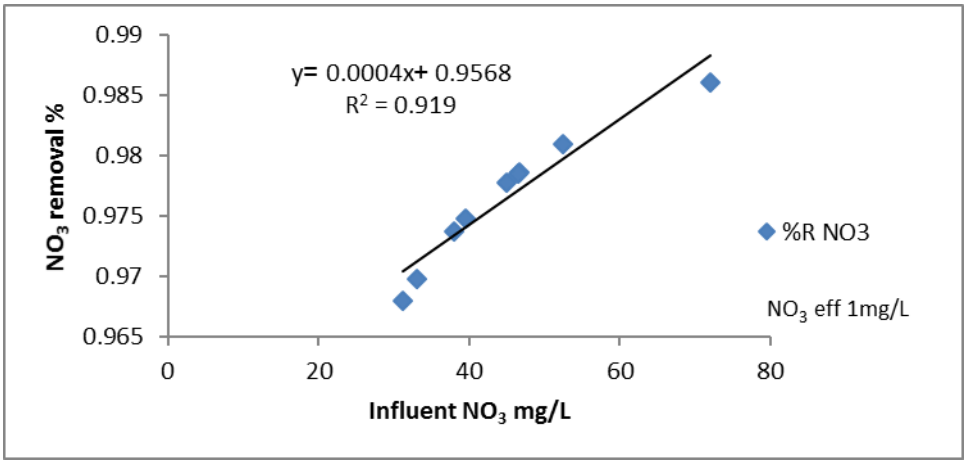

Figure7. Regression equation for NO_3 removal.

Prediction of Coefficient of Permeability of Unsaturated Soil

Prof. Dr.Mohammed Y.Fattah
Building and Construction Engineering Dept., University of Technology, Baghdad, Iraq.
myf_1968@yahoo.com.

Dr. Mahmood D. Ahmed
Civil Engineering Dept., College of Engineering, University of Baghdad, Iraq.
mahmoud_baghdad@yahoo.com.

Nawar A. Ali
Civil Engineering Dept., College of Engineering, University of Baghdad, Iraq.
nawarakil_87@yahoo.com

ABSTRACT

A simple technique is proposed in this paper for estimating the coefficient of permeability of an unsaturated soil based on physical properties of soils that include grain size analysis, degree of saturation or water content, and porosity of the soil. The proposed method requires the soil-water characteristic curve for the prediction of the coefficient of permeability as most of the conventional methods. A procedure is proposed to define the hydraulic conductivity function from the soil water characteristic curve which is measured by the filter paper method. Fitting methods are applied through the program (SoilVision), after indentifying the basic properties of the soil such as Attereberg limits, specific gravity, void ratio, porosity, degree of saturation and wet and dry unit weights.

Keywords: permeability, unsaturated soil, soil water characteristic curve, filter paper.

ايجاد معامل النفاذية للترب غير المشبعة

ا.د. محمد يوسف فتاح
قسم البناء والانشاءات
الجامعة التكنولوجيا

د. محمود ذياب احمد
قسم الهندسة المدنية
كلية الهندسة / جامعة بغداد

نوار عقيل علي
قسم الهندسة المدنية
كلية الهندسة / جامعة بغداد

الخلاصة

تم توظيف طريقة بسيطة لتقدير معامل النفاذية للترب غير المشبعة بالاعتماد على الخصائص الفيزيائية للترب والتي تتضمن التدرج الحبيبي ودرجة التشبع او المحتوى المائي والمسامية للتربة. هذه الطريقة تحتاج الى ايجاد منحني خصائص الرطوبة للتربة لايجاد معامل النفاذية حيث تعتبر خطوة ضرورية لايجاد معامل النفاذية. في هذا البحث تم استخدام طريقة بسيطة واقتصادية لايجاد منحني الرطوبة وذلك باستخدام طريقة ورقة الترشيح. بعد ان تم ايجاد منحني خصائص الرطوبة، استخدم برنامج (Soil Vision) بعد تعريف الخصائص الاساسية مثل حدود اتربرك والوزن النوعي و درجة التشبع والكثافة الرطبة والجاف.

الكلمات المفتاحية: النفاذية، الترب غير المشبعة، منحني خصائص التربة، ورقة الترشيح.

1.INTRODUCTION

In seepage analysis of unsaturated soil, the coefficient of permeability is an important parameter because many field problems are analyzed on the basis of soil permeability. Various measuring techniques have been developed in the laboratory and in the field to evaluate the unsaturated coefficient of permeability, **Fredlund and Rahardjo, 1993.** The direct measurement of coefficient of permeability of unsaturated soil can be tedious, time-consuming, and expensive. Furthermore, the accuracy of some testing results is often relatively poor, and the number of measurements required to adequately characterize an area can rapidly become prohibitive, as soil properties often show large in situ variability **Mbonimpa, 2006.** For these reasons, it is more convenient to have a practical method for estimating the expected hydraulic properties and to assess how these values may be influenced by changing conditions. The coefficient of permeability of unsaturated soil is not a constant like one of saturated soil. It can vary widely with the variation of the moisture content of soil. The relationship between water content and matric suction is called soil–water characteristic curve. Therefore, the coefficient of permeability is often represented by the function of matric suction. Commonly, the coefficient of permeability of unsaturated soil is predicted using the soil-water characteristic curve. Numerous experimental researches have been made on soil- water characteristic curve by many researchers such as **Fredlund and Xing, 1994**.

2. SOIL WATER CHARACTERISTIC CURVE

The soil-water characteristic curve for a soil is defined as the relationship between water content and suction for the soil. The

water content defines the amount of water contained within the pores of the soil. In soil science, volumetric water content, θ, is most commonly used. In geotechnical engineering practice, gravimetric water content, *w*, which is the ratio of the mass of water to the mass of solids, is most commonly used. The degree of saturation, *S*, is another term commonly used to indicate the percentage of the voids that are filled with water. The above variables have also been used in a normalized form where the water contents are referenced to residual water content (or to zero water content) ,**Fredlund and Xing, 1994**.

There are two defining breaks along most soil water characteristic curve SWCC and these are referred to as the “air entry value” of the soil and the “residual value” of the soil. These points are illustrated in **Fig.1**, the air entry value is the point at which the difference between the air and water pressure becomes sufficiently large such that water can be displaced by air from the largest pore space in the soil. The residual degree of saturation is the point at which a further increase in suction fails to displace a significant amount of water, **Brooks and Corey, 1964.**

In this paper the soil-water characteristic curve relationship has been used to estimate the hydraulic conductivity.

3. COEFFICIENT OF PERMEABILITY FOR UNSATURATED SOIL

The coefficient of permeability *k* of an unsaturated soil is not a constant. The coefficient of permeability depends on the volumetric water content θ, which, in turn, depends upon the soil suction, ψ. When the coefficient of permeability at any soil suction, $k(\psi)$, is referenced to the saturated coefficient of permeability *ks*, the relative coefficient of permeability, $k_r(\psi)$, can be written as follows

k_s, the relative coefficient of permeability, $k_r(\psi)$, can be written as follows:

$$k_r(\psi) = \frac{k(\psi)}{k_s} \qquad (1)$$

The relative coefficient of permeability as a function of volumetric water content, $k_r(\theta)$, can be defined similarly. The relative coefficient of permeability, ($k_r(\psi)$ or $k_r(\theta)$), is a scalar function. The volumetric water content, θ, can be used in its normalized form, which is also referred to as the relative degree of saturation:

$$\Theta = \frac{\theta - \theta_r}{\theta_s - \theta_r} \qquad (2)$$

where:

Θ = the normalized volumetric water content or relative degree of saturation,

θ_s= the saturated volumetric water content, and

θ_r= the residual volumetric water content.

Degree of saturation, *S*, which indicates the percentage of the voids filled with water, is often used in place of the normalized water content, Θ, **Frendlund and Xing, 1994.**

4. MODELS FOR PREDICTION THE COEFFICIENT OF PERMEABILITY OF UNSATURATED SOIL

The coefficient of permeability for an unsaturated soil is primarily predicted from the soil-water characteristic curve. There are two approaches to obtain the permeability function of an unsaturated soil: (i) empirical equations, and (ii) statistical models. Several measured permeability data are required to use an empirical equation. A statistical model can be used to predict the permeability function when the saturated coefficient of permeability, k_S, and the soil-water characteristic curve are available. Several empirical equations for the permeability function of unsaturated soils are listed in **Table 1**. These equations can be used in engineering practice when measured data are available for the relationship between the coefficient of permeability and suction, $k(\psi)$, or for the relationship between the coefficient of permeability and the water content, $k(\theta)$, **Frendlund and Xing et al., 1994**.

Two hydraulic conductivity models built upon statistical pore size distributions that have received considerable attention in geotechnical engineering practice are the van **Genuchten, 1980 and Fredlund, et al., 1994** models**.** Both allow concurrent modeling of the soil-water characteristic curve and the hydraulic conductivity function.

Van Genuchten, 1980, proposed a flexible closed-form analytical equation for the relative hydraulic conductivity function $k_r(\psi)$ by substituting equation of Gardner (1958) into the statistical conductivity models proposed by **Burdine, 1953 and Mualem, 1976** as follows:

$$k_r(\psi) = \frac{\left\{1 - (a_{vg}\psi)^{n_{vg}-1} \cdot \left[1 + (a_{vg}\psi)^{n_{vg}}\right]^{-m_{vg}}\right\}^2}{\left[1 + (a_{vg}\psi)^{n_{vg}}\right]^{m_{vg}/2}} \qquad (3)$$

where

ψ = soil suction (kPa);

a =model parameter related to air-entry value (suction value at which air starts to enter largest pores in the soil);

n = model parameter related to pore size distribution of the soil;

m = model parameter related to the asymmetry of the SWCC model curve.

Fredlund et al.و 1994, combined **Fredlund and Xing,1994**, equations with the statistical pore size distribution model of **Childs, and Collis-George 1950** to obtain a model for the relative hydraulic conductivity function as:

$$k_r(\psi) = \frac{\int_{\ln(\psi)}^{b} \frac{\theta(e^y) - \theta(\psi)}{e^y}\, \theta'(e^y)\, dy}{\int_{\ln(\psi_{av})}^{b} \frac{\theta(e^y) - \theta_s}{e^y}\, \theta'(e^y)\, dy} \quad (4)$$

Where:

y: is a dummy variable of integration representing ln(θ),

$b = \ln(10^6)$kPa,

ψ= soil suction (kPa);

ψ_{aev} : is the air-entry pressure,

θ': is the derivative with respect to ψ.

5. PREVIOUS WORKS ON UNSATURATED HYDRAULIC CONDUCTIVITY

Chiu and Shackelford 1998, studied the hydraulic conductivity of compacted sand-kaolin mixture. The measured unsaturated hydraulic conductivity ($k_{measured}$) values are compared with predicted unsaturated hydraulic conductivity ($k_{prediction}$) values using the Brooks-Corey-Burdine and van Genuchten-Mualem relative hydraulic conductivity functions. In general, the accuracy of ($k_{prediction}$) decreases with an increase in kaolin content or an increase in ψ_m. In addition, $k_{measured}$ tends to be under predicted for kaolin contents of 10 and 30% at relatively high suctions (1.0 m $<\psi_m<$6.0 m) and overpredicted for kaolin contents of 0 and 5% at relatively low suctions (0.1m $<\psi_m<$1.0 m). For a given kaolin content and ψ_m, $k_{\mathbf{prediction}}$ based on the Brooks-Corey-Burdine function tends to be more accurate than $k_{\mathbf{prediction}}$ based on the van Genuchten-Mualem function. Finally, for 1.0 m $<\psi_m<$6.0 m, $k_{\mathbf{prediction}}$ based on analysis using the maximum volumetric water content (θ_m) attained under steady-state flow conditions typically is more accurate than $k_{\mathbf{prediction}}$ based on analysis using the saturated volumetric water content, θ_s, where θ range between (84-90)% of θ_m.

Vanapalli et al., 2005, proposed a simple expression to estimate the unsaturated hydraulic conductivity of coarse-grained soils. A technique was proposed using a relationship between the relative conductivity k_r and the normalized degree of saturation, which is referred as the adjusted degree of saturation, Sγ. To estimate the unsaturated hydraulic conductivity the grain size distribution, the porosity, the degree of saturation (or water content), the saturated permeability of the soil, are required. The mathematical relationship is expressed as a normalized function:

$$K_r = s^{7.9\gamma} = \Theta^{7.9\gamma} \quad (5)$$

A relationship between the fitting parameter, γ and the index soil properties such as the porosity, and the fine content is proposed. The expression is:

$$\gamma = 0.012(1/n\,[\text{clay\%}]^2 + [\text{silt\%}]) + 0.38 \quad (6)$$

Gao et al. 2008, studied permeability of unsaturated remolded clay under different compaction conditions. Five specimens were compacted under different water contents with standard Proctor compaction effort to examine the influence of compacted water content on the permeability of unsaturated clay. The first specimen was compacted at optimum water content, which is 18.4%; the second and third samples were compacted wet of optimum water content, their compaction water content were 20.4% and 22.4%, respectively. The fourth and fifth specimens were compacted dry of optimum water content, 16.4% and 14.4% were their compaction water respectively. Three specimens were compacted using reduced, standard, and modified Proctor compaction efforts in order to analyze effects of compaction effort on permeability of remolded clayey soil. The results indicated that the permeability coefficient decreases with the increase of compaction water content, and the difference reduces with the increase of suction, and permeability coefficient can be assumed identical when the suction reach to 1000 kPa. The permeability coefficient of samples compacted with standard Proctor compaction effort and reduced Proctor compaction effort are very similar. The value of k_w (modified) k_w (standard) is about 1/100 in saturated state, and which increases as the suction increases.

When the suction reaches 1000kPa, the value decreases to 1/10 gradually.

Lamara et al.,2008, studied the reliability of indirect methods for predicting the hydraulic conductivity of dune sand widely present in the Algerian Sahara. The results obtained were promising and test clearly of the major contribution that may bring along the hydraulic property prediction models to the unsaturated soil mechanics practice. **Zapata's et al. model,2000,** was used to evaluate the soil water characteristic curve depending on the grain size distribution information. The unsaturated hydraulic conductivity has been predicted, using two statically based models **Mualem-van Genuchten,1980 and Fredlund et al.,1994,** beside **Vanapalli et al.,2005,** empirical model. The results obtained were promising and attested clearly that some models can yield good predictions.

6. EXPERIMENTAL WORK

In this paper, the aim of experimental work is to define the soil water characteristic curve (SWCC) by measurement of the soil suction.

A soil sample was collected from a site east of Baghdad. The physical properties of this soil was studied by conducting a series of tests in the laboratory, these include: specific gravity, Atterberg limits, grain size distribution by sieve analysis and hydrometer, compaction test and permeability test (falling head). The total and matric suction are measured by the filter paper method at different degrees of saturation.

A brown clayey soil was brought from a site east of Baghdad. Standard tests are performed to determine the physical properties of the soil. Details are given in **Table 2**. Grain size distribution of the soil used revealed 6 % sand, 24% silt and 70% clay as shown in **Fig. 2**. According to the Unified Soil Classification System USCS the soil is classified as CL.

7. TOTAL AND MATRIC SUCTION OF SOIL MEASUREMENT BY FILTER PAPER METHOD

The filter paper method has long been used in soil science and engineering practice and it has recently been accepted as an adaptable test method for soil suction measurements because of its advantages over other suction measurement devices. Basically, the filter paper comes to equilibrium with the soil either through vapor (total suction measurement) or liquid (matric suction measurement) flow. At equilibrium, the suction value of the filter paper and the soil will be equal. After equilibrium is established between the filter paper and the soil, the water content of the filter paper disc is measured. Then, by using filter paper water content versus suction calibration curve, the corresponding suction value is found from the curve. This is the basic approach suggested by ASTM Standard Test Method for Measurement of Soil Potential (Suction) Using Filter Paper **ASTM D 5298**. In other words, **ASTM D 5298** employs a single calibration curve that has been used to infer both total and matric suction measurements. The **ASTM D 5298** calibration curve is a combination of both wetting and drying curves, as shown in **Fig.3**.

8. MEASUREMENT OF SOIL SUCTION

Glass jars that are between 250 to 500 ml volume sizes are readily available and can be easily adopted for suction measurements. Glass jars, especially, with 3.5 to 4 inch (88.9 to 101.6 mm) diameter can contain the 3 inch (76.2 mm) diameter Shelby tube samples very nicely. A testing procedure for total suction measurements using filter papers can be outlined as will be described in the following sections **,Bulut et al., 2001.**

9. EXPERIMENTAL PROCEDURE

1. Use a container that a Shelby-tube soil sample can be fit into easily without the disturbance of the soil sample.
2. Cut the soil sample into two halves for matric suction measurements.
3. Make sure that the surfaces of the soil samples are smooth and flat for establishing an intimate contact between the soil sample and the filter paper for matric suction measurements.
4. For matric suction measurements, insert a single Whatman No. 42 filter paper in between two larger in diameter protective filter papers. Put the other half of the soil sample on top, keeping the sandwiched filter papers in between and in intimate contact with the soil samples. Tape the two pieces of the soil sample together.
5. Insert a clean PVC O-ring, with the sharp edge facing up, on top of the soil sample for total suction measurements. Place two of Whatman No. 42 filter paper on top of the ring.
6. Put the lid on and tape it tight to prevent any moisture exchange between the air inside and air outside of the jar, insert the glass jar into a well-insulated container for suction equilibrium.
7. Soil suction measurement set up, as described in the previous steps, will be kept in a temperature-controlled environment for at least one week.
8. Previous steps are repeated for every soil sample.
9. After at least one week of equilibrium period, record all the weights with their corresponding tin numbers.
10. Remove a glass jar from the temperature controlled container. Time is critical at this stage and thus it is suggested that two people share the work, the time that the filter papers are exposed to the lab environment should be minimal, preferably less than a few seconds.
11. Open the glass jar and quickly carry the filter paper to the moisture tin using tweezers, in less than a few seconds, immediately close the lid of the moisture tin with the wet filter paper inside.
12. After closing the lid of the moisture tin, immediately weigh the tin with the wet filter paper inside. This is a total suction measurement.
13. Continue with the matric suction measurement by removing the tape that was holding the soil samples together. Remove the filter paper that was sandwiched between the two protective filter papers. Immediately carry the filter paper to the moisture tin, close the lid of the moisture tin and weigh the tin with the wet filter paper inside. This is a matric suction measurement.
14. After opening all the glass jars and recording the weight of the moisture tins with the wet filter papers inside, carry them to a hot oven with the lids half open. Leave them in the oven for at least 10 hours. Before taking them out from the oven, close their lids for equilibrium and leave them in the oven for about 5 minutes.
15. Weigh the hot tin with the dry filter paper inside.
16. Calculate the moisture content of each filter paper for both total and matric suction measurements.
17. Obtain the suction value from an appropriate calibration curves or by these relations. These steps are documented in **plates 1 to 6.**

10. INPUT DATA IN SOIL VISION

Total and matric suction of the soil samples are measured by remolding the samples at different degrees of saturation (40%, 50%, 60%, 70%, 80%,

and 90%) using the filter paper method. A sample of the data documented during the measurement of soil suction is shown in **Table 3**. **Figs.4 and 5** show the relationship between the total and matric suction and the degree of saturation, respectively.

From Fig.4, it can be shown that the sl 0.001 0.01 0.1 il decreases with increase of degree of saturation and the rate of decreasing in matric suction is not equal to the rate of increase of the degree of saturation.

From the program (Soil Vision), and after inputting all the required properties of the soils used in this analysis, (i.e., total unit weight, dry unit weight, liquid limit, plasticity index, void ratio, porosity, matric suction value, degree of saturation, and grain size distribution), the soil water characteristic curve is predicted (relation between the gravitation water content and the matric suction) through applying fitting methods, such as the method proposed by **Fredlund and Xing,1994 and van Genuchten, 1980,** for fitting the soil water characteristic curve **Fig.6**.

11. ESTIMATED UNSATURATED HYDRAULIC CONDUCTIVITY (K)

In this paper, Soil Vision program has been used in order to find the properties of soil such as volumetric water content and unsaturated hydraulic conductivity. After determination of the relation between the volumetric water content and matric suction using fitting of the Fredlund and Xing model at every degree of saturation, a relationship between the hydraulic conductivity and matric suction can be estimated from Soil Vision program.

The Fredlund and Xing model (1994) in Soil Vision program is used to calculate unsaturated hydraulic conductivity as the following equation:

$$k = k_{sat} \frac{\int_{\psi}^{\psi_r} \frac{\theta(y) - \theta(\psi)}{y^2} \theta` y dy}{\int_{\psi}^{\psi_r} \frac{\theta(y) - \theta_s}{y^2} \theta` y dy} \qquad (7)$$

y: is a dummy variable of integration representing ln(ψ),

ψ = soil suction (kPa),

ψ_r is the suction corresponding to the residual water content θ_r,

θs = the saturated volumetric water content,

θ`: is the derivative with respect to ψ.

The most variable parameter in the Soil Vision program is saturated hydraulic conductivity and Fredlund and Xing fit of soil-water characteristic carve by fitting in each degree of saturation from 100% to 40%. Finally, the unsaturated hydraulic conductivity carve is predicted in **Fig.7** for different degrees of saturated.

A steep permeability function indicates a rapid reduction in the water coefficient of permeability for a small increase in matric suction. In this case, the quantity of water flow in to the unsaturated zone is considerably reduced.

12. CONCLUSIONS

- From the soil water characteristic curve (SWCC) which was determined by experimental method (i.e. filter paper method) for the study soil, the matric suction values were found to increase by about (15-63)% with decrease of the degree of saturation from 90% to 40%, and the rate of increase is not equal to rate of decrease in degree of saturation.
- From the soil water characteristic curve (SWCC), the unsaturated hydraulic conductivity value was calculated, and was found to decrease by about (38-99) % with increase of the matric suction for each degree of saturation.

13. REFERENCES

Al-Khafaf, S. and Hanks, R. J.,1974, "*Evaluation of the Filter Paper Method for Estimating Soil Water Potential,"* Soil Science, Vol. 117, No. 4, pp. 194-199.

ASTM-D-422-00, "*Standard Test Method for Particle – Size Analysis of Soils*", Annual Book of ASTM Standards, Vol. 04.08, Soil and Rock, pp. 1 – 8.

ASTM-D-698-00, "*Standard Test Methods for Laboratory Compaction Characteristics of Soil Using Standard Effort (12,400 ft-lbs/ft^3 (600 kN-m/m^3)"* Annual Book of ASTM Standards, Vol. 04.08, Soil and Rock, pp. 1 – 11.

ASTM-D854-00, "*Standard Test Method for Specific Gravity of Soil Solids by Pycnometer,"* Annual Book of ASTM Standards, Vol. 04.08, Soil and Rock, pp. 1 – 7.

ASTM-D-1557-02, *"Standard Test Methods for Laboratory Compaction Characteristics of Soil Using Modified Effort (56,000 ft-lbf/ft^3 (2,700 kN-m/m^3))"*, Annual Book of ASTM Standards, Vol. 04.08, Soil and Rock, PP. 1 – 10.

ASTM-D-4318-00, "*Standard Test Methods for Liquid Limit, Plastic Limit, and Plasticity Index of Soils"*, Annual Book of ASTM Standards, Vol. 04.08, Soil and Rock, pp. 1 – 16.

ASTM-D-5298-03, "*Standard Test Method for Measurement of Soil Potential (Suction) Using Filter Paper*", Annual Book of ASTM Standards, Vol. 04.08, Soil and Rock, pp. 1 – 6.

Bulut, R., Lytton, R. L., and Wray, W. K., 2001, *"Soil Suction Measurements by Filter Paper"*, Geotechnical Special Publication Number 115, Proceedings of Geo-Institute Shallow Foundation and Soil Properties Committee Sessions at the

ASCE, 2001, *"Civil Engineering Conference"*, pp. 243-261.

Bulut, R., Leong, E. C., 2008, "*Indirect Measurement of Suction*", Geotechnical and Geological Engineering, Vol. 26, pp. 633-644.

Brooks, R.H., and Corey, A.T., 1964, "*Hydraulic Properties of Porous Media*", Colorado State University, Hydrology paper No.3, March, Vol. 27, March.

Burdine, N. T., 1953, "Relative Permeability Calculations from Pore Size Distribution Data", Trans. AIME, 198, pp. 71–77.

Chandler, R. J. and Gutierrz, C. I., 1986, "*The Filter Paper Method of SuctionMeasurements*", Geotechnique, Vol. 36, No. 2 pp. 265-268.

Childs, E. C., and Collis-George, N., 1950. *"The Permeability of Porous Materials"*, Proc. R. Soc. London, Ser. A, 201, pp392–405.

Chiu, T., and Shackelford, C. D., 1998, *"Unsaturated Hydraulic Conductivity of Compacted Sand-Kaolin Mixtures"*, Journal of Geotechnical Geoenvironmental Engineering, ASCE, 124(2), pp. 160–170.

Fredlund , D.G., and Rahardjo, H., 1993, "*Soil Mechanics for Unsaturated Soils*" John Wiley & Sone Inc. New York, United States of America.

Fredlund, D.G., Xing, A., and Huang, S.Y. ,1994, "*Predicting the Permeability Function for Unsaturated Soils Using the Soil-Water Characteristic Curve*", Canadian Geotechnical Journal, 31(4), pp. 533-546.

Fredlund, D.G., Xing, A., 1994, "*Equation for the Soil Water Characteristic Curve"*, Canadian Geotechnical Journal Vol. 31, No. 3, pp. 521 – 532.

Fredlund, D. G., Sheng, D., Zhao, J., 2001, "*Estimation of Soil Suction from the Soil-Water Characteristic Curve*", Canadian Geotechnical Journal, Vol.4, pp. 168-198.

Fredlund, D. G., 2006, "*Unsaturated Soil Mechanics in Engineering Practice*", Journal of Geotechnical and Geoenvironmental Engineering, ASCE, Vol. 132, No. 3, pp. 286 – 321.

Fredlund, M.D., Fredlund, D.G, and Wilson, G.W., 1997, "*Prediction of the Soil-Water Characteristic Curve from Grain-Size Distribution and Volume-mass Properties",* Proceedings, Third Brazilian Symposium on Unsaturated Soils, NSAT'97, Rio de Janeiro, Brazil, April 22–25, Vol. 1, pp. 13–23.

Fredlund, M.D., Wilson, G.W., and Fredlund, D.G.,1997, "*Indirect Procedures to Determine Unsaturated Soil Property Functions",* In Proceedings of the 50th Canadian Geotechnical Conference, Golden Jubilee, Ottawa, Ont., 20–22 October 1997. BiTech Publishe Ltd., Richmond, B.C. Vol. 1, pp. 407–414.

Gao, L.X., Luan, M.T., and Yang,Q., 2008, "*Experimental Study on Permeability of Unsaturated Remolded Clay"* , Electronic Journal of Geotechnical Engineering (EJGE), Vol. 13, Bund. D, pp. 1 – 15.

Gardner, W.R.,1958, "*Some Steady State Solutions of the Unsaturated Moisture Flow Equation with Application to Evaporation from a Water Table*", Soil Science., 85(4), pp. 228-232.

Ho, P.G., 1979, "*The Prediction of Hydraulic Conductivity from Soil Moisture Suction Relationship"*, B.Sc. Thesis, University of Saskatchewan, Saskatoon, Canada.

Lamara, M., and Derriche, Z.,2008, "*Prediction of Unsaturated Hydraulic Properties of Dune Sand on Drying and Wetting Paths",* Electronic Journal of Geotechnical Engineering (EJGE), Vol. 13, Bund. B, pp. 1 – 19.

Mbonimpa M., Aubertin M., and Bussiere B., 2006, "*Predicting the Unsaturated Hydraulic Conductivity of Granuar Soil from Basic Geotechnical Properties using the Modified Kowacs Model and Statistical Models*". Canaidan Geotechnical Journal.43, pp. 773-787.

Mualem, Y., 1976, "*A New Model for Predicting the Hydraulic Conductivity of Unsaturated Porous Media*", Water Resource. Res., 12, pp. 513-522.

Richards, L.A. 1931, "*Capillary conduction of liquids through porous medium"*. Physics. 1: 318-333. (As seen in Fredlund and Xing, 1994).

Rijtema, P.E., 1965, "*An Analysis of Actual Evapotranspiration",* Agricultural Research Reports (Wageningen), No. 659. (As seen in Fredlund and Xing, 1994).

Usre's Guide Manual of Soil Vision, 2001, "*SoilVision Systems Ltd*". Saskatoon, Saskatchewan, Canada.

User's Guide Manual of SEEP/W, 2002, "*GEO-SLOPE International Lt*d". Calgary, Alberta, Canada.

Vanapalli, K. S., Catana, C. M., and Lobbezoo, J. P., 2005, "*A Simple Technique to Estimate the Coefficient of Permeability of Unsaturated Coarse-Grained Soils Using Conventional Soil Properties",* In: Proceeding of

International Conference on Problematic Soils, Famagusta. N. Cyprus, pp.103-114.

Van Genuchten, M. T., 1980, "*A Closed Form Equation for Prediction of the Hydraulic Conductivity of Unsaturated Soils*", Soil Science Society America Journal, 44, pp. 892 – 898.

Wind, G.P., 1955, "*Field Experiment Concerning Capillary Rise of Moisture in Heavy Clay Soil"*. Netherlands Journal of Agricultural Science, 3: 60-69. (As seen in Fredlund and Xing, 1994).

Table 1. Empirical equations for the unsaturated coefficient of permeability $k(\theta)$),**Frendlund et al.,1994.**

Function	Reference
$k_r = \psi^n$, where $\Theta = (\theta - \theta_r)/(\theta_s - \theta_r)$	Averjanov (1950)
$k = k_s \left(\frac{\theta}{\theta_s}\right)^n$	Campbell (1973)
$k = k_s \exp[\alpha(\theta - \theta_s)]$	Davidson et al. (1969)
$k = k_s$, for $\psi \le \psi_{aev}$ $k_r = \left(\psi/\psi_{aev}\right)^{-n}$ for $\psi \ge \psi_{aev}$	Brooks and Corey(1964)
$k_r = \exp(-\alpha\psi)$ $k = k_s/(\alpha\psi^n + 1)$	Gardner (1958)
$k = a\psi + b$	Richards (1931)
$k = k_s$ for $\psi \ge \psi_{aev}$ $k_r = \exp[-\alpha(\psi - \psi_{ave})]$ for $\psi_{aev} \le \psi \le \psi_1$ $k = k_1\left(\frac{\psi}{\psi_1}\right)$ for $\psi > \psi_1$	Rijtema (1965)
$k = \alpha\psi^{-n}$	Wind (1955)

Table 2. Index properties of the soils**.**

Index property	Index value
Liquid limit % (LL)	49.8
Plasticity index % (PI)	25
Specific gravity (Gs)	2.79
Sand %	6
Silt %	24
Clay%	70
Classification (USCS)	CL
Optimum moisture content	20.32%
Dry unit weight (kN/m^3)	17.13

Table 3. Measurement of soil suction using filter paper method.

MEASUREMENT OF SOIL TOTAL SUCTION USING FILTER PAPER							
Degree of Saturation %		**40**	**50**	**60**	**70**	**80**	**90**
Water Content of Filter Paper %	**Wf**	**10.3**	**11.6**	**14.7**	**15.3**	**16.5**	**18**
Total Suction, log kPa	**h_t**	**4.5246**	**4.4233**	**4.1819**	**4.1351**	**4.0413**	**3.9248**
MEASUREMENT OF SOIL MATRIC SUCTION USING FILTER PAPER							
Degree of Saturation %		**40**	**50**	**60**	**70**	**80**	**90**
Water Content of Filter Paper	**Wf**	**25.3**	**32**	**46**	**55.3**	**71.4**	**86**
Matric Suction, log kPa	**h_t**	**3.3561**	**2.8342**	**2.3985**	**1.7935**	**1.4481**	**1.251**

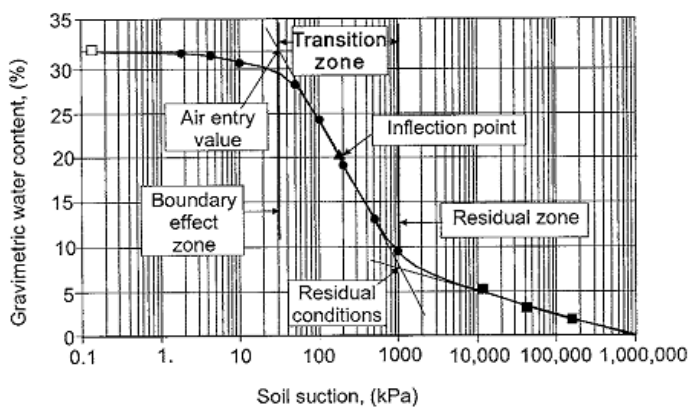

Figure 1. Illustration of the in situ zones of desaturation defined by a soil – water characteristic curve, **after Fredlund, 2006.**

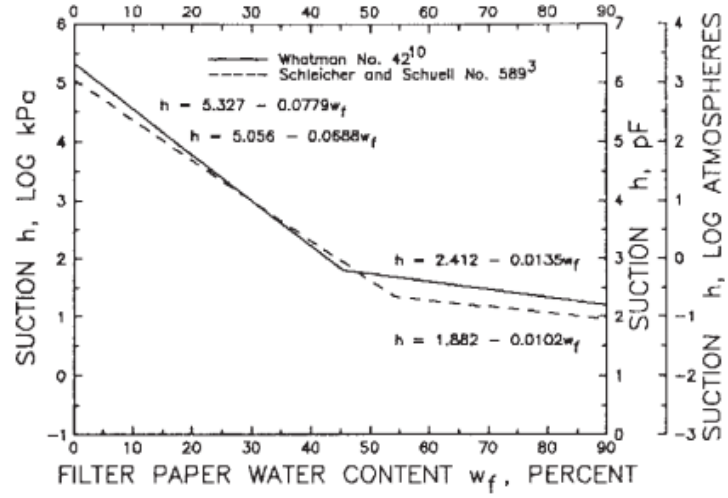

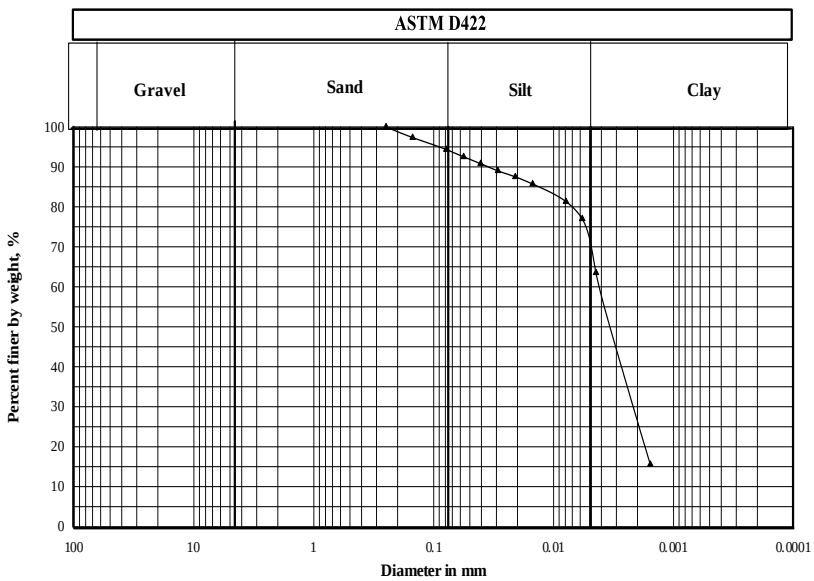

Figure 2. Grain size distribution of the soil. used.

plates (1)

plates (2)

plates (3)

plates (4)

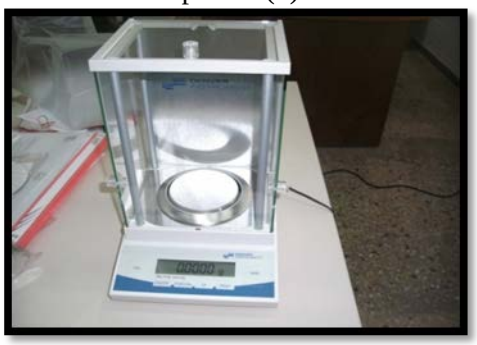

plates (5)

plates (6)

Figure 3. Calibration suction-water content curves for wetting of filter paper (from **ASTM-5298-03).**

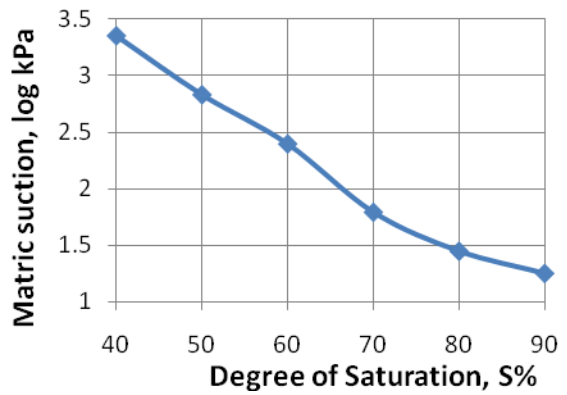

Figure 4. Relationship between the matric suction and degree of saturation.

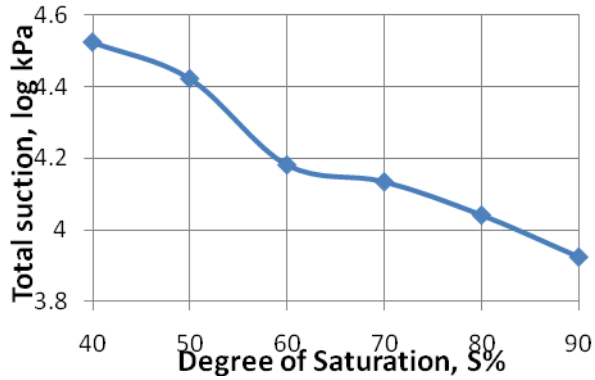

Figure 5. Relationship between the total suction and degree of saturation.

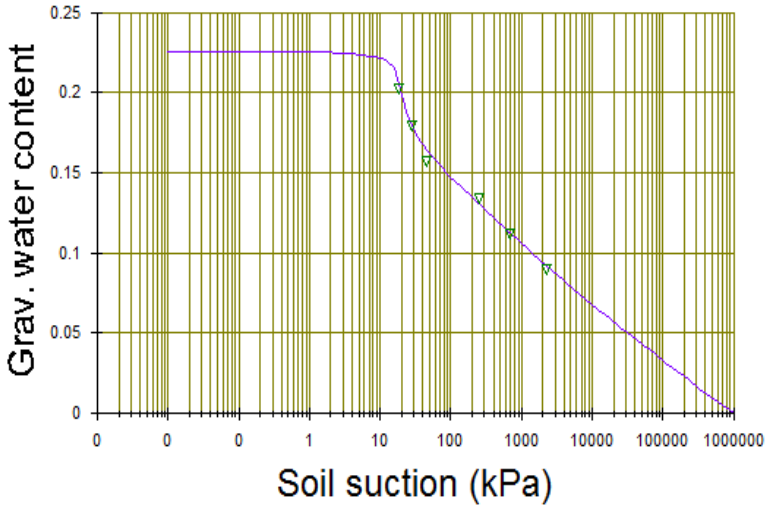

Figure 6. Relationships between the gravitational water content and the matric suction obtained by the program Soil Vision by using Fredlund and Xing (1994) fitting.

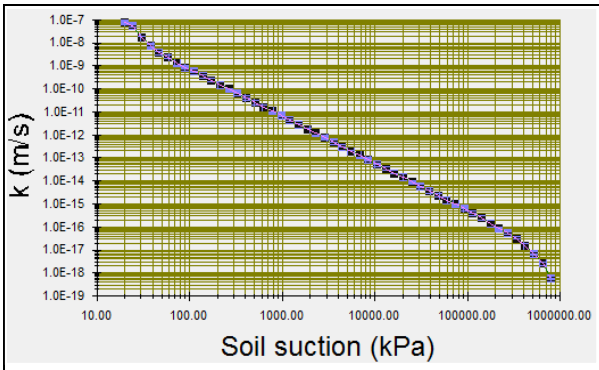

a-Hydraulic conductivity at S = 100%.

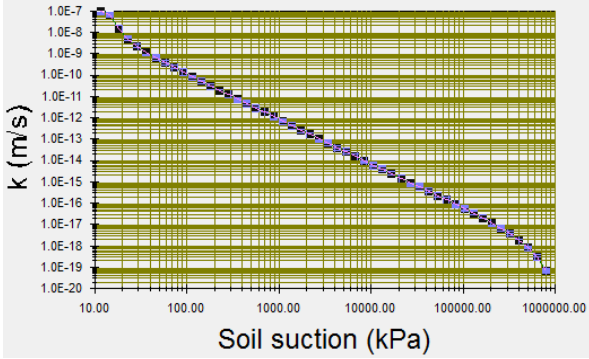

b-Hydraulic conductivity at S = 90%.

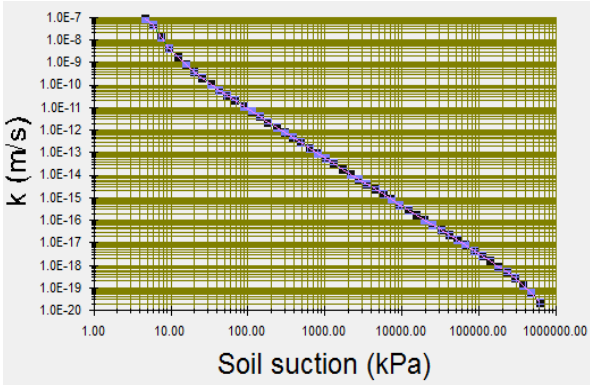

c- Hydraulic conductivity at S =80% .

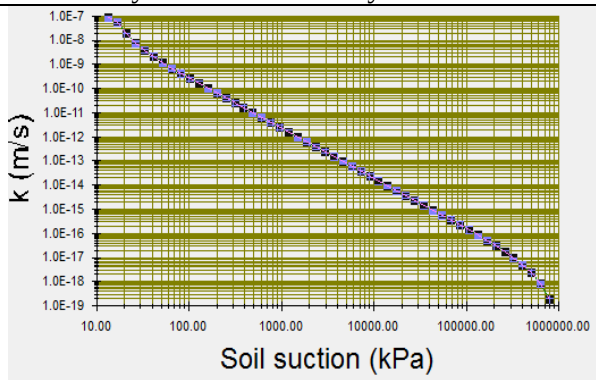

d- Hydraulic conductivity at S =70%.

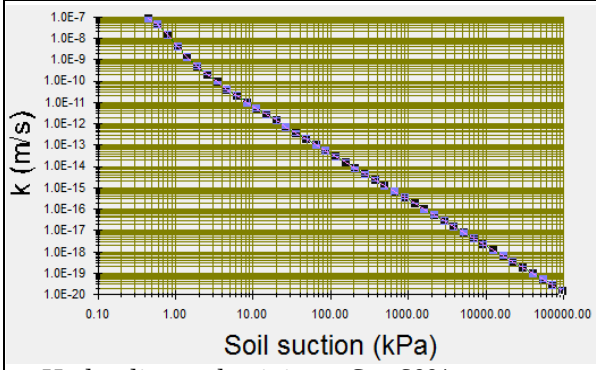

g-Hydraulic conductivity at S = 60%.

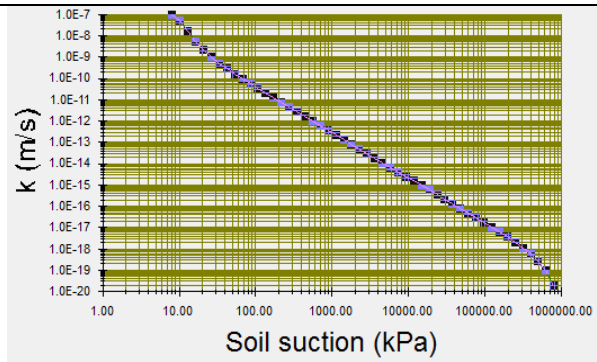

h-Hydraulic conductivity at S =50%

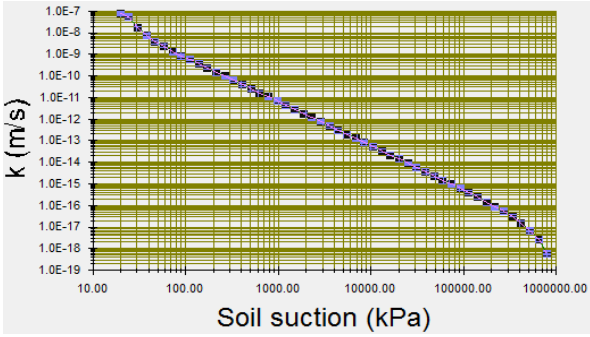

j- Hydraulic conductivity at S =40% .

Figure 7. Relationships between the hydraulic conductivity and the matric suction for different degrees of saturation obtained by the program soil vision.

A Comparative Study of Single-Constraint Routing in Wireless Mesh Networks Using Different Dynamic Programming Algorithms

Sabreen Mahmood Shukr
(Master of Science)
Department of Computer Engineering
College of Engineering
University of Baghdad
Email: msh2008msha@yahoo.com

Nuha Abdul Sahib Alwan
Assistant Professor
Department of Computer Engineering
College of Engineering
University of Baghdad
Email: n.alwan@ieee.org

Ibraheem Kassim Ibraheem
Assistant Professor, Ph.D.
Department of Electrical Engineering
College of Engineering
University of Baghdad
Email: ibraheem151@gmail.com

ABSTRACT:

Finding the shortest route in wireless mesh networks is an important aspect. Many techniques are used to solve this problem like dynamic programming, evolutionary algorithms, weighted-sum techniques, and others. In this paper, we use dynamic programming techniques to find the shortest path in wireless mesh networks due to their generality, reduction of complexity and facilitation of numerical computation, simplicity in incorporating constraints, and their conformity to the stochastic nature of some problems. The routing problem is a multi-objective optimization problem with some constraints such as path capacity and end-to-end delay. Single-constraint routing problems and solutions using Dijkstra, Bellman-Ford, and Floyd-Warshall algorithms are proposed in this work with a discussion on the difference between them. These algorithms find the shortest route through finding the optimal rate between two nodes in the wireless networks but with bounded end-to-end delay. The Dijkstra-based algorithm is especially favorable in terms of processing time. We also present a comparison between our proposed single-constraint Dijkstra-based routing algorithm and the mesh routing algorithm (MRA) existing in the literature to clarify the merits of the former.

Key words: wireless mesh networks; dynamic programming; single-constraint optimization; Dijkstra algorithm; Bellman-Ford algorithm; floyd-warshall algorithm; MRA.

مقارنة دراسية لتحديد المسار بمحدد واحد في الشبكات اللاسلكية المعشقة باستخدام مختلف خوارزميات البرمجة الديناميكية

صابرين محمود شكر
قسم هندسة الحاسبات
كلية الهندسة – جامعة بغداد

أ.م. نهى عبد الصاحب العلوان
قسم هندسة الحاسبات
كلية الهندسة – جامعة بغداد

أ.م.د. ابراهيم قاسم ابراهيم
قسم الهندسة الكهربائية
كلية الهندسة – جامعة بغداد

الخلاصة:

العثور على الطريق الاقصر في الشبكات اللاسلكية المعشقة هو امر هام. العديد من التقنيات قد استخدمت على حل هذه المشكلة مثل البرمجة الديناميكية، الخوارزميات التطورية، وتقنية المجموع الموزون للمحددات، وغيرها. في هذا البحث، استخدمنا تقنية البرمجة الديناميكية لإيجاد الطريق الاقصر الشبكات اللاسلكية المعشقة بسبب عموميته، والحد من التعقيد وتيسير الحساب العددي، بساطة في دمج المحددات، ومطابقته للطبيعة العشوائية لبعض المشاكل. مشكلة التوجيه هي مشكلة تحسين اهداف متعددة مع بعض المحددات مثل سعة المسار و الوقت من بداية المسار إلى نهايته. مشكلة التوجيه بمحدد واحد في خوارزميات Dijkstra، Bellman-Ford، و Floyd-

Warshall والفرق فيما بينهم قد عرض في هذا العمل. هذه الخوارزميات تجد الطريق الاقصر من خلال ايجاد السعة المثلى بين عقدتين في الشبكات اللاسلكية ولكن مع تحديد الوقت الذي تحتاجه من بداية المسار الى نهايته. يتميز خوارزمي Dijkstra بقصر وقت المعالجة. وقد تناولنا أيضا المقارنة بين خوارزمياتنا وخوارزمية MRA المستحدثة سابقا وبيان فضل الأولى.

الكلمات الرئيسية: الشبكات اللاسلكية المعشقة، البرمجة الديناميكية، محدد واحد، خوارزمي Dijkstra، خوارزمي Bellman-Ford، خوارزمي Floyd-Warshall، خوارزمي MRA.

1. INTRODUCTION

Wireless mesh network (WMNs) are an attractive technology because they extend the network coverage, deliver community broadband Internet access services and increase the capacity of wireless access networks, **Cheng, H. et al., 2012, Capone A. et al., 2010, and Mountassir T. et al., 2012.** WMNs also reduce the need for costly wired network infrastructures, **Capone A. et al., 2010, and Marina M. K. et al., 2010.** Nodes in these networks establish and maintain connectivity amongst them automatically, **Raja N. K. et al., 2012.** The coverage of the network depends on the number of nodes, their location in relation to one another and the radio technology used because each node exchanges routing information only with its neighbors, **Kowalik K. et al., 2006.** To speed up the operation of finding the optimal path between two nodes in the WMNs, the dynamic programming technique is employed.

Dynamic programming (DP) is a powerful algorithmic paradigm which is used to solve large classes of optimization problems, **Lew A. et al., 2007.** The key attribute that a problem must have in order for dynamic programming to be applicable is optimal substructure, **Camen T. et al., 2001.** Optimal substructure means that the solution to a given optimization problem can be obtained by a combination of optimal solutions to its sub-problems. DP has many applications such as integer knapsack problem, optimal linear search problem, optimal binary search tree problem, integer linear programming, finding the shortest path problem and others, **Lew A. et al., 2007**. In this work, DP is used to find shortest paths problem in wireless networks in the context of quality of service (QoS) routing. The importance of focusing on DP techniques for routing stems from the fact that DP has been proven to be effective for many unconstrained and multi-objective optimization problems. For some problems, it is even the most efficient approach known for the solution. Wireless networks can be unidirectional or bidirectional mesh wireless networks. Each type of wireless network can make use of routing algorithms under the framework of dynamic programming techniques to determine the shortest paths between the nodes.

In unidirectional wireless networks, networks can be represented as a multi-stage directed acyclic graph (DAG). There are two fundamental processes to solve the shortest path problems in multi-stage directed graphs, **Moon T. K. and Stirling W. C., 2000.** The first one is known as forward dynamic programming algorithm and the other is known as backward dynamic programming algorithm. For wireless mesh networks, there are other applicable unconstrained DP algorithms such as the Dijkstra, Bellman-Ford and Floyd-Warshall techniques, **Stallings W., 2011, Glisic S. and Lorenzo B., 2009.** The processing time and the amount of information that must be collected from other nodes, **Stallings W., 2011** are the important aspects in which these algorithms differ from each other. Unconstrained shortest path problems and single-constraint optimization for path selection have been proved to be NP-complete, because they are all solved in polynomial time, **Dasgupta S. et al, 2007, and Allard G. et al., 2004.** A problem is NP-complete if all decisions for the problem can be verified in polynomial time, **Dasgupta S. et al., 2007.**

The routing problem is a multi-objective optimization problem with metrics such as path rate or capacity, end-to-end delay, hop count, and probability of errors. These QoS requirements need to be bounded or optimized.

In general, the QoS metrics need to be optimized by making meaningful trade-offs due to their inter-conflicting nature.

In this paper, we address the single-constraint routing problem in Dijkstra-based, Bellman Ford-based and Floyd Warshall-based DP framework. These algorithms find the shortest path from the source node to the destination node in the wireless network through maximizing path rate and limiting end-to-end delay. Also, we show that our Dijkstra-based algorithm is preferable over the mesh routing algorithm (MRA) in finding the shortest path in wireless mesh networks. MRA, **Crichigno J. et al., 2008, and Helonde, J. B. et al., 2011,** is also a dynamic programming algorithm to compute high-capacity end-to-end delay bounded paths. There are numerous other optimization methods each with advantages and disadvantages. The most prominent is dynamic programming due to its generality, reduction of complexity and facilitation of numerical computation, simplicity in incorporating constraints, and its conformity to the stochastic nature of some problems, **Lew A. and Mauch H., 2007, Doerr B. et al, 2009, and Ilaboya R. et al., 2011.** Evolutionary algorithms such as the genetic algorithm (GA) are most appropriate for complex non-linear models where the location of a global minimum is a difficult task. Due to global search, GAs are computationally expensive and need more time to be computed as compared with DP, **Doerr B. et al., 2009.** The remainder of the paper is organized as follows: Section 2 presents the DP algorithms (MRA, Dijkstra, Bellman-Ford, and Floyd-Warshall) that deal with single constraints to find the shortest path in wireless mesh networks. Section 3 summarizes the simulation results and discussion. Finally, Section 5 concludes the paper.

2. SINGLE-CONSTRAINT DP ALGORITHMS

In this section, four single-constraint DP algorithms (MRA, Dijkstra, Bellamn-Ford, and Floyd-Warshall) are explained. All these algorithms follow the same method to find the shortest path in wireless networks. The method optimizes the path capacity and bounds the end-to-end delay. This method is designed to dispense with combined metrics. Combined metrics (weighted sum techniques) are optimized when the end-to-end delay metric is minimized and the path capacity is maximized simultaneously. The weighted sum technique does not guarantee any optimal trade-off solution between the metrics. Hence, with the weighted sum technique, solutions that best satisfy QoS requirements are not guaranteed, **Crichigno J. et al, 2008.**

In what follows, we explain the difference between the MRA algorithm and our single-constraint Dijkstra-based algorithm, **Shukr S. et al, 2012** and also explain the single-constraint Bellman-Ford and Floyd-Warshall algorithms.

2.1 The MRA Algorithm

The mesh routing algorithm (MRA), **Crichigno J. et al, 2008 and Helonde, J. B. et al., 2011** is a dynamic programming approach to compute high-capacity end-to-end delay bounded paths.

Fig. 1 is used to show how the algorithm operates, where rate r(*l*) is shown over each link in Mbps, and the delay of each link t(*l*) equal to 2ms.

Now, we want to find the path from u to y with maximum capacity R and with delay exactly equal to 6ms (τ= 3 hops time). This path is denoted by $P_6^*(u,y)$. Only through w or x, we reach y. The path rate from u to y is:

$$R(P_6^*(u,y))=\max\begin{Bmatrix} \min\{R(P_{6-2}^*(u,w)),6\} \\ \min\{R(P_{6-2}^*(u,x)),3\} \end{Bmatrix} \quad (1)$$

The two paths ($P_{6-2}^*(u,w)$ and $P_{6-2}^*(u,x)$) can be similarly found. **Fig.2** explains how to solve the shortest path problem in **Fig.1** using the MRA algorithm. After we search all possible paths and discard some of them like *P3* and *P6* because their end-to-end delays greater than 6ms, we choose *P5* as the maximum path rate (5Mbps) with end-to-end delay equal to 6ms among all remaining paths.

The following pseudo-code shows how the MRA algorithm operates to find the maximum capacity path with end-to-end delay bounded by τ.

The MRA algorithm

1. **INPUT:** *G(V,E)*, source node vs, destination node vd, delay bound τ.
2. **OUTPUT:** P_{vd}^{vs}

3. /*Initialization*/
4. **IF** pair u, w ϵ V and $d < \tau$ **THEN**
5. $P_d^*(u,w)$ =NIL
6. **IF** ∃ l = (u,w) ϵ E | $t(l)=d$ **THEN**
7. $P_d^*(u,w)=l$
8. **END IF**
9. **END IF**
10. /*main loop*/
11. **IF** $d < \tau$ **THEN**
12. **IF** pair u, w ϵ V **THEN**
13. **FOR ALL** l=(u,v) ϵ E | $d > t(l)$ **DO**
14. **IF** $P^*_{d-t(l)}(v,w) \neq$ NIL **THEN**
15. **IF** [$P_d^*(u,w)$ = NIL] or [$R(P_d^*(u,w)) <$ $R(l \oplus P^*_{d-t(l)}(v,w))$] **THEN**
16. $P_d^*(u,w) = l \oplus P^*_{d-t(l)}(v,w)$
17. **END IF**
18. **END IF**
19. **END FOR**
20. **END IF**
21. **ENF IF**
22. **RETERN** P^{vs}_{vd} .

2.2 Dijkstra-Based Algorithm

We propose a Dijkstra DP technique that computes high-capacity paths while simultaneously bounding the end-to-end delay to an upper limit. **Fig.3** explains how the algorithm works.

Beginning with the source node (*vs*), the algorithm finds node (*u*) whose *R(P(vs,u))* is the maximum capacity among all nodes. After that the algorithm finds the links (l_{uv}) that connect *u* and *v* for all *v* provided that the delay from *vs* to *v* does not exceed τ. So the path from *vs* to *v* is either $P(vs,v)$ or $P(vs,u) \oplus l_{uv}$ depending on which has the maximum capacity, and at the same time, does not violate the delay bound. The path from *vs* to *v* throught *u* has a rate equal to *min*{*R(P(vs,u))*, *r*(l_{uv})}. The paths *P(vs,u)* and *P(vs,v)* are not necessarily disjoint. If *R(P(vs,u)*$\oplus l_{uv}$*)*> *R(P(vs,v))* then $P(vs,v)$ is *P(vs,u)*$\oplus l_{uv}$.

By the same way we can expand the path to reach the destination node (*vd*) and find P^*_τ(*vs*,*vd*) and R(P^*_τ(*vs*,*vd*)) denoting the shortest path (greatest capacity) and its rate respectively.

In short, our proposed algorithm adopts unconstrained (capacity or rate) Dijkstra optimization but prunes off the paths that violate the delay bound resulting in a single-constraint optimization effect. This is achieved by comparing rates to decide between paths, and then comparing delays. The latter comparison may change the decisions resulting from the former.

To show the difference between this algorithm and MRA algorithm, **Fig.4** shows the spanning tree of the same network in **Fig.1** using Dijkstra-based algorithm. It is clear that the optimum path *P1* is rapidly discovered. From this example, it is clear that our proposed algorithm is better than MRA because MRA employs flooding in its search, but with optimization.

Moreover, our algorithm is different from the MRA in that it is Dijkstra-based and, therefore, retains all the corresponding advantages such as fast shortest-path determination, and having an order of N^2 (N is the number of the nodes) rendering it efficient to use with relatively large networks. The algorithm in the following pseudo-code is used to return a maximum-capacity path such that the end-to-end delay is bounded by τ, and its rate.

The single-constraint Dijkstra-based algorithm

1. **INPUT**: no. of nodes n, source node vs, destination node vd, delay bound τ, t(l) for all l, r(l) for all l.
2. **OUTPUT**: P^*_τ(vs,,vd) , R(P^*_τ(vs,,vd)).
3. /*Initialization*/
4. **FOR** ALL nodes
5. Visited nodes = NIL
6. R(P(vs,node))=0
7. D(P(vs,node))=∞
8. Parent(node)= NIL
9. **END**
10. R(P(vs,vs))=∞
11. D(P(vs,vs))=0
12. **FOR** i=1: (n-1)
13. **FOR** ALL visited nodes
14. Rate(node) = R(P(vs,node))

```
    END
    r_max = max[rate(node)]
    u=node corresponding to r_max.
    /* u is the visited node */
    FOR ALL nodes v
        IF (t(l_uv) + D(P(vs,u))) < τ THEN
            IF r(l_uv) < R(P(vs,u)) THEN
                cap=r(l_uv)
            ELSE cap= R(P(vs,u))
            END IF
            IF cap> R(P(vs,v)) OR
                D(P(vs,v)) > τ THEN
                R(P(vs,v)) = cap
                parent(v) = u
                /* P(vs,v) = P(vs,u) ⊕ l_uv
                */
                D(P(vs,v)) = D(P(vs,u)) +
                t(l_uv)
            ENDIF
        ELSE IF D(P(vs,v))> τ THEN
                R(P(vs,v)) = 0
                D(P(vs,v)) = ∞
        END IF
    END FOR
END FOR
    IF parent(vd) ≠ NIL THEN
        P(vs,v) = [vd]
        t = vd
        WHILE t ≠ vs
            p = parent(t)
            P(vs,vd) = [p P(vs,vd)]
            t = p
        END
    END IF

P*_τ(vs,,vd) = P(vs,vd)
RETURN P*_τ(vs,,vd) , R(P*_τ(vs,,vd))
```

2.3 Bellman-Ford Algorithm

In the following pseudo-code, Bellman-ford algorithm finds the optimal path from source node (s) to all other nodes in the network. It uses output information from rates matrix, introduced earlier in the previous sub-section. First, we have only the s node in the path. For all links in the network, and from s node, we will find all rates and the corresponding nodes and compare between them to find the maximum rate ($r1_{max}$) and its corresponding node (m). Then, in the same manner but from node m, we will find $r2_{max}$ and its corresponding node. Then $r1_{max}$ will compare with $r2_{max}$ and the smallest be the maximum rate from the s node to the third node in the path. We do all these steps with delay bounded by τ. All above processes will be repeated until all nodes in the network are examined.

The single-constraint Bellman-Ford based algorithm

```
INPUT: no. of nodes n, no. of links L,
source node vs, destination node vd,
delay bound τ, t(l) for all l, r(l) for all l,
links between all nodes.
OUTPUT: P*_τ vs,,vd) , R(P*_τ (vs,,vd)).
/*Initialization*/
FOR ALL nodes
    Visited nodes = NIL
    R(P(vs,node))=0
    D(P(vs,node))=∞
    Parent(node)= NIL
END
R(P(vs,vs))=∞
D(P(vs,vs))=0
FOR i=1: (n-1)
    FOR ALL visited nodes
        Rate(node) = R(P(vs,node))
    END FOR
    r_max = max[rate(node)]
    u=node corresponding to r_max.
    /* u is the visited node */
    FOR ALL links j
        /*find the node v which is
        connected to node u through
        link j */
        FOR ALL nodes v
            IF (t(luv) + D(P(vs,u))) < τ
            THEN
                IF r(luv) < R(P(vs,u))
                THEN
                    cap=r(luv)
                ELSE cap= R(P(vs,u))
                END IF
                IF cap> R(P(vs,v)) OR
                    D(P(vs,v)) > τ THEN
                    R(P(vs,v)) = cap
                    parent(v) = u
```

```
                    /* P(vs,v) = P(vs,u) ⊕ luv */
                    D(P(vs,v)) = D(P(vs,u)) + t(luv)
                ELSE IF D(P(vs,v))> τ THEN
                    R(P(vs,v)) = 0
                    D(P(vs,v)) = ∞
                END IF
            END IF
        END FOR
    END FOR
    IF parent(vd) ≠ NIL THEN
        P(vs,v) = [vd]
        t = vd
        WHILE t ≠ vs
            p = parent(t)
            P(vs,vd) = [p P(vs,vd)]
            t = p
        END
    END IF
END FOR
P*τ(vs,,vd) = P(vs,vd)
RETURN P*τ(vs,,vd) , R(P*τ (vs,,vd)).
```

2.4 Floyd-Warshall Algorithm

Floyd-Warshall algorithm in the following pseudo-code determines the shortest path between all pairs of nodes in the network. Floyd-Warshall algorithm uses a set of nodes as intermediate nodes to find the routes between the nodes in the network. Suppose we wish to find the route from *vs* node to *vd* node in the network. First, there is only node 1 as intermediate node between node *vs* and node *vd*. r_{s1} represent the rate between node *vs* and node 1 and r_{1d} represent the rate between node 1 and node *vd*. The smallest between node r_{s1} and r_{1d} will be the maximum rate ($r1_{max}$) between node *vs* and node *vd* under there is only node 1 as intermediate node. Then, the above process will be repeated but with node 2 as intermediate node and with $r2_{max}$ as the maximum rate between node *vs* and node *vd* under node 2 as intermediate node. The rate $r1_{max}$ will be compared with $r2_{max}$ and the largest will be the maximum rate between node *vs* and node *vd* and so on. We do all these steps with delay bounded by τ. All these processes will be repeated until the all optimum routes between all pairs in the network are found.

The single-constraint Floyd-Warshall based algorithm

```
INPUT: no. of nodes n, no. of links L, source node vs, destination node vd, delay bound τ, t(l) for all l, r(l) for all l, links between all nodes.
OUTPUT: P*τ(vs,,vd) , R(P*τ (vs,,vd)).
/*Initialization*/
FOR ALL nodes
    Visited nodes = NIL
    Parent(node)= NIL
END
FOR k=1: n
    FOR i=1: n
        FOR j=1: n
            IF node (i) = node (j) THEN
                /* rate and delay between node i and j stay the same*/
            ELSE
                IF R(i,k) ==0 THEN
                    /*there is no change*/
                END IF
                IF R(k,j) ==0 THEN
                    /*there is no change*/
                END IF
                IF D(i,k) + D(k,j) < τ THEN
                    Cap= min(R(i,k) , R(k,j))
                    IF (cap > R(i,j)) OR (D(i,j) > τ) THEN
                        IF parent(i,k) == NIL
                            parent(i,j) =k
                        ELSE
                            parent(i,j) = parent(i,k)
                        END IF
                        R(i,j) = cap
                        /* P(i,j) = P(i,k) ⊕ P(k,j) */
                        D(i,j) = D(i,k) + D(k,j)
                    END IF
```

```
                    ELSE
                      IF D(i,j) > τ THEN
                            R(i,j) = 0
                            D(i,j) = ∞
                            Parent(I,j) = NIL
                      END IF
                    END IF
                  END IF
            END FOR
      END FOR
END FOR
IF (R(vs,vd) !=0) AND (D(vs,vd) !=∞)
THEN
    P(vs,vd) = [vd]
    t = vd
    WHILE P(t,vs) != 0
                p = parent(t,vs)
                P(vs,vd) = [p P(vs,vd)]
                t = p
    END
    P(vs,vd) = [vs P(vs,vd)]
END IF
P*τ(vs,,vd) = P(vs,vd)
RETURN P*τ(vs,,vd) , R(P*τ (vs,,vd)).
```

3. RESULTS AND DISCUSSION

The simulation program to implement the comparison between the single-constraint DP algorithms (MRA, Dijkstra, Bellman-Ford, and Floyd-Warshall) was coded in Matlab 8.0. The resultant shortest route depends on link rate and end-to-end delay. The simulation model parameters are chosen as follows: Number of nodes in the simulated network= 50. Topology area: Nodes are distributed randomly on 1000*1000 m^2. This network topology ensures that the node coverage area is 200 *m*. Thus, some nodes may be in the coverage area of others.

Figs. 5, **6**, and **7** show the topology of the network and the shortest route in terms of maximum capacity in Dijkstra, Bellman-Ford, and Floyd-Warshall with a single constraint from node 1 to node 15, node 23 to node 24, and node 49 to node 50 respectively. All the routes in the three figures are bounded by a 50 *ms* delay. The route in **Fig.5** has a capacity of 7.8151 *Mbps* while the route in **Fig.6** has a capacity of 8.1306 *Mbps* and the route in **Fig. 7** has a capacity of 8.1634 *Mbps*.

As shown from **Figs. 5**, **6**, and **7**, there is no difference among the results of the three algorithms (Dijkstra, Bellman-Ford, and Floyd-Warshall) because all of them find the shortest route between two nodes in the network. However, these approaches differ in the amount of information that must be collected from other nodes in the network. In Bellman-Ford algorithm, the node must collect only the information from its neighbors and knowledge of its link costs, to update its costs and paths. While in the Dijkstra algorithm, the node must know the link costs of all links in the network. The information must be exchanged with all other nodes. Thus, Bellman-Ford is better than Dijkstra from this point of view.

As for the processing time of the algorithms, the processing time in the Dijkstra algorithm is $O(N^2)$, where N is the number of nodes in the network, whereas in Bellman-Ford, the processing time is O(NL), where L is the number of links in the network. The processing time in the Floyd-Warshall is $O(N^3)$. The Dijkstra algorithm is better than other two algorithms in the processing time feature.

4. CONCLUSION

Wireless mesh networks are likely to be the essence of future communication. Finding shortest paths in WMNs by optimizing some QoS metrics is very challenging. Because it is difficult to provide optimization for all the metrics used to solve the routing problem simultaneously, we use a technique that optimizes one QoS measure and bounds or constrains the other. This paper presents single-constraint shortest path problem in Dijkstra, Bellman-Ford, and Floyd-Warshall dynamic programming algorithms that optimize the path capacity and bound the end-to-end delay. Despite the fact that the simulation results of the three algorithms are the same but they are different in the processing time of the algorithms and the amount of information that must be collected from other nodes in the wireless network. From the perspective of processing time, the Dijkstra algorithm is the best because the processing time is $O(N^2)$, while in Bellman-Ford algorithm is O(NL) and in Floyd-Warshall is $O(N^3)$. Bellman-Ford is better than the other algorithms in the amount of

information must be collected from the nodes because the node only collects the information from its neighbors. Another comparison was implemented between the MRA and single-constraint Dijkstra-based algorithms to show the difference between them. The result of this comparison explains that our proposed algorithm is better than the MRA algorithm in the search of the shortest path due to its comparatively reduced computational complexity, whereas MRA is more time-consuming due to its flooding-like search method.

5. REFERENCES

Allard G. and Jacquent, P.H.,2004,"*Heuristic for Bandwidth Reservation in Multihop Wireless Networks,"* INRIA Rocquencourt, No. 5075, January.

Camen T. H., Leiserson C. E., Rivest R. L. and Stein C., 2001, "*Introduction to Algorithms*", 2nd Edition.

Capone A., Carello G., Filippini I., Gualandi S. and Malucelli F., 2010, "***Routing, Scheduling*** *and Channel Assignment in Wireless Mesh Networks: Optimization Models and Algorithms***",** Ad Hoc Networks, vol. 8, no. 6, August, pp. 545-563.

Cheng H., Xiong N., Vasilakos, A. V., Yang L. T., Chen G. and Zhuang, X., 2012, "*Nodes Organization for Channel Assignment with Topology Preservation in Multi-Radio Wireless Mesh Networks"*, Ad Hoc Networks, vol. 10, no. 5, pp. 760-773.

Crichigno J., Khoury J., Wu M. Y. and Shu W., 2008, "*A Dynamic Programming Approach for Routing in Wireless Mesh Networks*," IEEE Global Telecommunications Conference, pp. 1-5.

Dasgupta, S., Papadimitriou, C. and Vazirani, U., 2007 "*Algorithms*", McGraw-Hill.

Doerr B., Eremeev A., Horoba C., Neumann F. and Theili M., 2009, "*Evolutionary Algorithms and Dynamic Programming"*, GECCO'09: Proceedings of the 11th Annual Conference on Genetic and Evolutionary Computation, ACM, New York, NY, USA, 8-12 July, pp. 771-778.

Glisic, S. and Lorenzo, B., 2009,"*Advanced Wireless Networks"*, 2nd edition, Wiley, July.

Helonde, J. B., Wavhai, V., Deshpande, V. S. and Bhagwat, L. B.,2011,"*Performance Analysis of Mesh Routing Algorithm for Routing Metrics Link Capacity and Delay Against Inter-Arrival Time Dependencies"*, WOCN: Proceedings in 8th International Conference on Wireless and Optical Communications Networks.

Ilaboya, R., Atikpo, E., Ekoh, G. O., Ezugwu, M. O. and Umokoro, L., 2011, "*Application of Dynamic Programming to Solving Reservoir Operational Problems"*, Journal of Applied Technology in Environmental Sanitation, vol. 1, no. 3, October, pp. 251-262.

Kowalik K. and Davis M., 2006, "*Why Are There So Many Routing Rrotocols for Wireless Mesh Networks"*, Irish Signal and Systems Conference, Dublin, 28-30 June.

Lew A. and Mauch H.,2007, *"Dynamic Programming: A Computational Tool"*, New York: Springer-Verlag, Berlin Heidelberg,.

Marina, M. K., Das, S. R. and Subramanian, A. P., 2010, "*A Topology Control Approach for Utilizing Multiple Channels in Multi-Radio Wireless Mesh Networks***",** International Journal of Computer and Telecommunications Networking, vol. 54, no. 2, February, pp. 241-256.

Moon, T. K. and Stirling, W. C.,2000 ,"*Mathematical Methods and Algorithms for Signal Processing*", Upper Saddle River, New Jersey: Prentice-Hall,.

Mountassir, T., Nassereddine, B., Haqiq, A. and Bennani, S., 2012, "*Wireless Mesh Networks Topology Auto Planning*", International Journal of Computer Applications (0975 – 8887), vol. 52, no. 2, August, pp. 27-33.

Raja N. K., Saritha, R., Senthamaraiselvan, A. and Arulanandam, K.,2012,"*QSWMCA -*

Quality of Service in Wireless Mesh Networks by Configuration Arguments", International Journal of Computer Network and Information Security, vol. 4, no. 6, June, pp. 1-9.

Shukr, S. M., Alwan, N. A. S. and Ibraheem, I. K.,2012, "*The Multi-Constrained Dynamic Programming Problem in View of Routing Strategies in Wireless Mesh Networks*", International Journal of Information and Communication Technology Research, vol. 2, no. 6, June, pp. 471-476.

Stallings, W., 2011, "*Data and Computer Communications*", Ninth Edition, Prentice Hall,.

6. SYMBOLS AND ACRONYMS

$\sum$	Summation Operator
$\oplus$	Concatenation
$\exists$	There Exist
|	OR
∞	Infinity
τ	End-to-End Delay Bound
d, vd	Destination Nodes in the Wireless Network
d	Delay of the Path So Far
D(P)	End-to-End Delay of Path P
E	Number of Edges in the Graph
G(V,E)	Graph with V Vertices and E Edges
l	Link in the Path P
l_{uv}	Link Connecting Node u and Node v
L	Number of Links in the Wireless Network
m, u, v, w, x, y	Nodes in the Wireless Network
N	Number of Nodes in the Wireless Network
NIL	Nothing
P	Path
P_{vd}^{vs}	Path Between *vs* and *vd*
$P_{\tau}^{*}(vs,,vd)$	Maximum-Capacity Path Between *vs* and *vd* with End- to-End Delay Less Than τ
r_{max}	Maximum Rate
r(l)	Rate of Link l
R(P)	Rate of Path P
s, *vs*	Source Node in the wireless Network
t(l)	Expected Delay of Link l

DAG	Directed Acyclic Graph
DP	Dynamic Programming
GA	Genetic Algorithm
MRA	Mesh Routing Algorithm
NP	Nondeterministic Polynomial Time
QoS	Quality of Service
WMN	Wireless Mesh Network

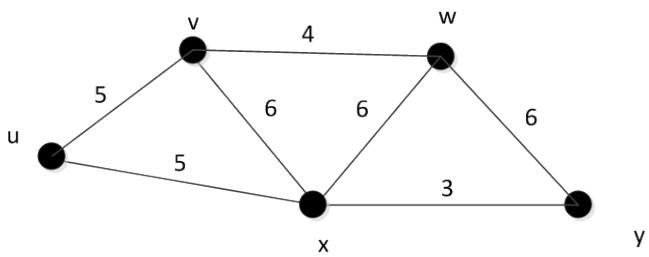

Figure 1. A network with rate r(l) over each link.

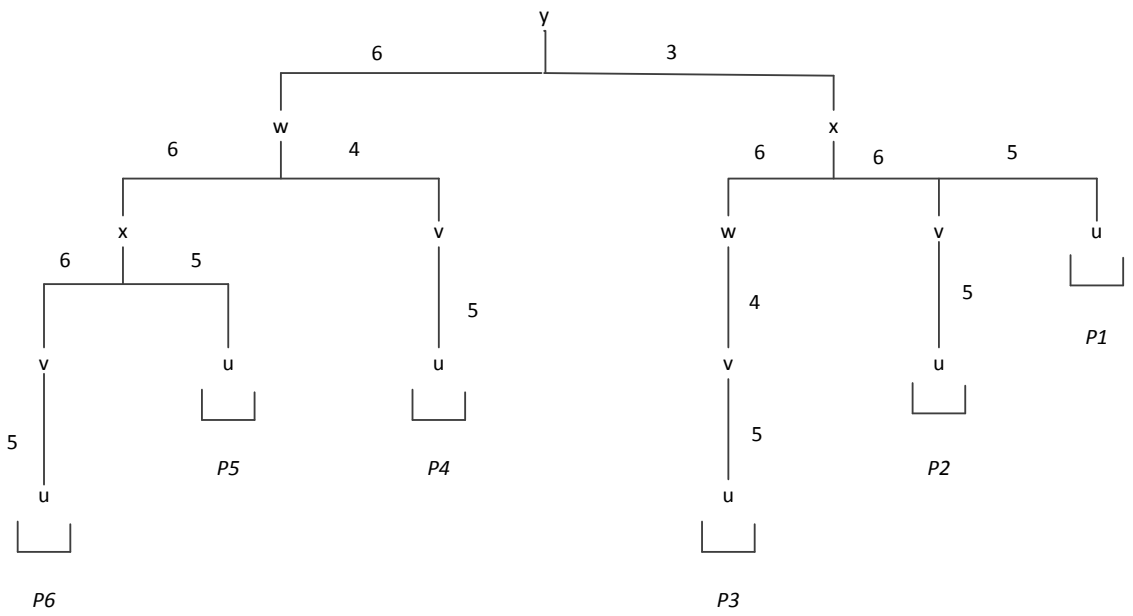

Figure 2. Spanning tree layout explains how to solve the shortest path problem of in Fig. 1 using MRA algorithm.

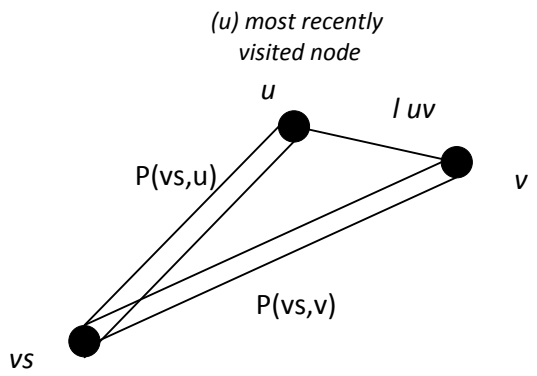

Figure. 3: The path from *vs* to *v*.

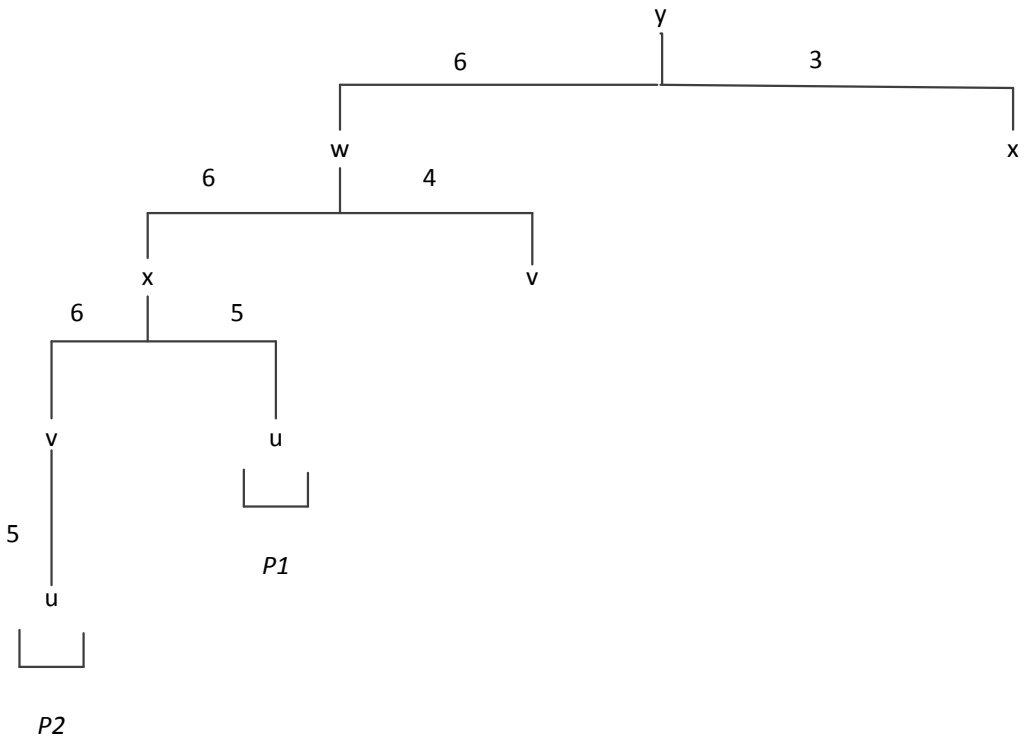

Figure 4. Spanning tree layout explains how to solve the shortest path problem of in Fig. 1 using Dijkstra-based algorithm.

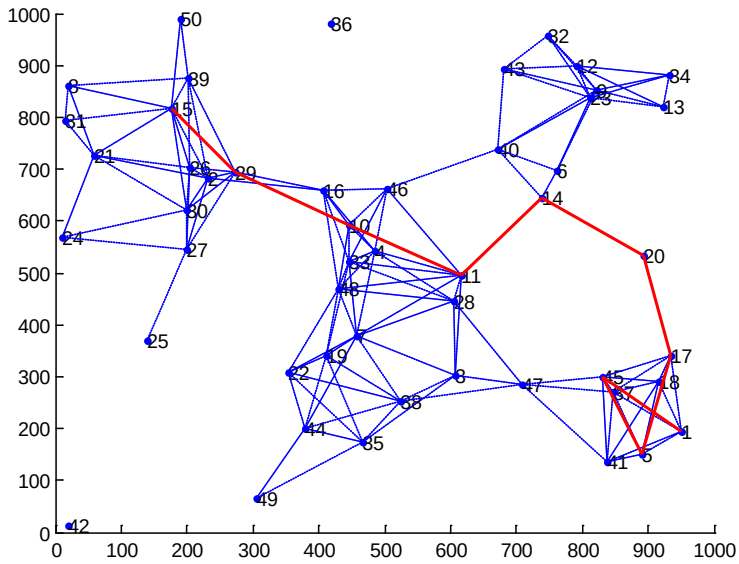

Figure 5. Network topology with source node (1) and destination node (15) showing shortest route under single- constraint DP algorithms with maximum capacity and a 50ms end-to-end delay bound.

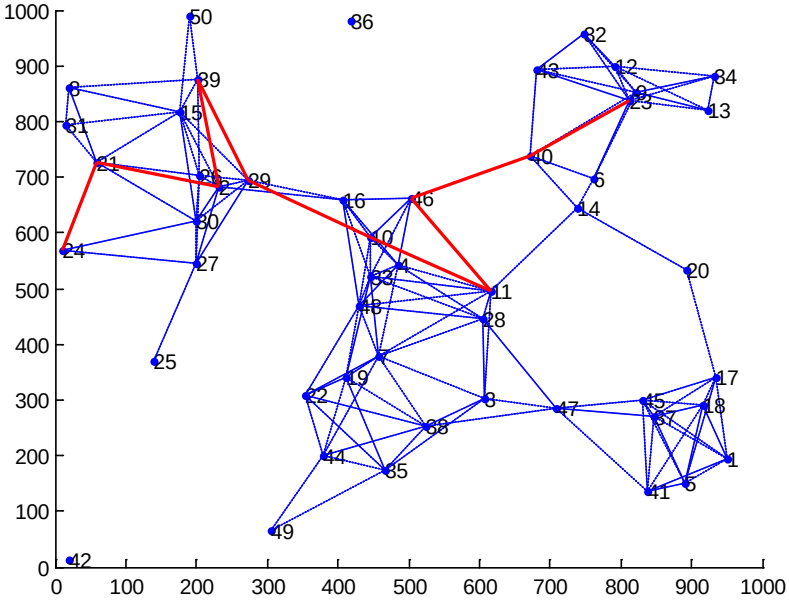

Figure 6. Network topology with source node (23) and destination node (24) showing shortest route under single- constraint DP algorithms with maximum capacity and a 50ms end-to-end delay bound.

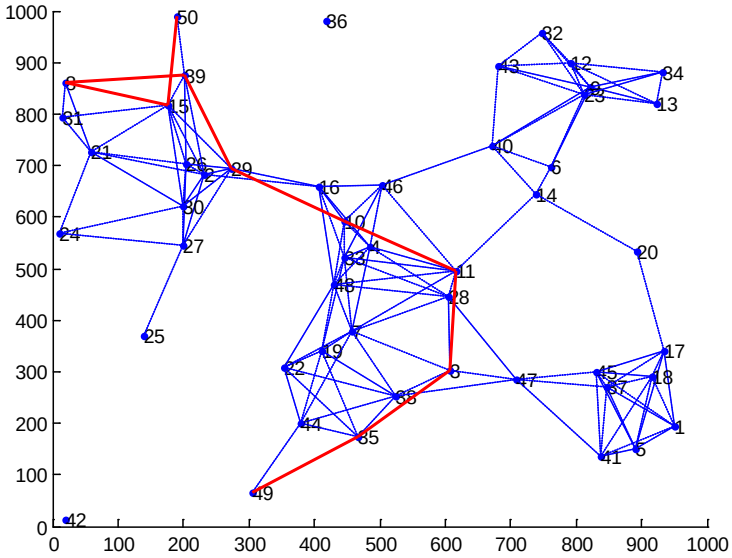

Figure 7. Network topology with source node (49) and destination node (50) showing shortest route under single- constraint DP algorithms with maximum capacity and a 50ms end-to-end delay bound.

Experimental Investigation for TiO2 nanoparticles as a Lubricant-Additive for a Compressor of Window Type Air-Conditioner System

Asst.Lect. Haider ali hussen
Department of Mechanical Engineering
College of Engineering- AL-Mustansiriyah University
E-mail: (haidereng25@yahoo.com)

ABSTRACT

The coefficient of performance of a window type Air-Conditioner system can be improved if a reduction in the work of compressor can be achieved by a suitable technique. The present study investigates the effect of dispersing a low concentration of TiO2 nanoparticles in the mineral oil based lubricant, as well as on the overall performance of a window type Air-Conditioner system using R22 as the working fluid. An enhancement in the COP of the refrigeration system has been observed and the existence of an optimum volume fraction noticed, with low concentrations of nanoparticles suspended in the mineral oil. Results showed that the average compressor work reduced by 13.3%, which ultimately resulted in an increase of 11.99% in the COP due to the addition of nanoparticles in the lubricating oil.

Key words: nanoparticle; nanofluid , lubricant , air-conditioner system, coefficient of performance

تحقيق تجريبي للدقائق النانوية لاوكسيد التيتانيوم المضاف لمزيّت ضاغط مكيّفِ هواء نوعِ شباكي

م.م حيدر علي حسين
قسم الهندسة الميكانيكيةِ، كلية الهندسة / جامعة المستنصرية

الخلاصة

معامل أداءِ نظامَ مكيّفِ هواء شباكي يُمْكِنُ أَنْ يُحَسّنَ إذا قل استهلاك عملِ الضاغطِ والذي يُمْكِنُ أَنْ يُنجَزَ مِن قِبل تقنية مناسبة. تَتحرّى الدراسةُ الحاليةُ تأثيرُ تركيز منخفض للدقائق النانوية لاوكسيد التيتانيوم في الزيت المعدني ، بالإضافة إلى الأداءِ العامّ بإستعمال نظامِ مكيّفِ هواء ذو مائع تبريد R22. لوحظَ تحسين في معامل اداء النظامِ التبريدَ و لوحظَ ان الكسر الحجمي المثالي

كان عند تراكيز واطئة من الدقائق النانوية في الزيت المعدني. . اظهرت نَتائِجَ الإختبارِ بأنّ معدل عملَ الضاغطِ خفّضَ الى 13.3 %، الذي أدّى إلى زيادةِ في النهاية 11.99 % في معامل اداء بسبب إضافةِ دقائق نانوية في الَزْيت.

1. INTRODUCTION

One recent report , **Omer, AM 2007**, proposed by the USA Department of Energy showed that the global energy consumption in 2020 would be more than twice of the present level according to the current tendency. Such an increasing energy requirement will aggravate energy shortage and environment pollution. Forty percent of the annual global energy demand is consumed by buildings, while more than half of the building energy demand is consumed for air-conditioning, and this proportion is larger in hot-weather areas. Therefore, improvement in energy efficiency of air-conditioning system can significantly reduce the global energy consumptions. Nanofluids, which are suspensions of nanoparticles in base fluids, have been introduced as new enhanced media , especially during the last decade. An experimental investigation has been carried out on nanofluid effects on the coefficient of performance of a window type Air-Conditioner system. Many researches were accomplished in this field**. Ruixiang, W., 2010,** studied the application of nano-fluids in refrigerating systems is considered to be a potential way to improve the energy efficiency and reliability of HVAC&R facilities and to make economic the use of environmentfriendly refrigerants. The reliability and performance of RAC with nanoparticles in the working fluid have been investigated experimentally. A new mineral-based nano-refrigeration oil (MNRO), formed by blending some nanoparticles (NiFe2O4) into naphthene based oil B32, was employed in the RAC using R410a as refrigerant. The results indicate that the mixture of R410a/MNRO works normally in the RAC. The cooling/heating EER of the RAC increased about 6% by replacing the Polyol-Easter oil VG 32 lubricant with MNRO. **Venkataramana, M., 2012,** studied the ir-reversibility at the process of a vapour-compression refrigeration system (VCRS) with nanoparticles in the working fluid was investigated experimentally. Mineral oil (MO) with 0.1 gL^{-1}TiO2 nanoparticles mixture were used as the lubricant instead of Polyol-ester (POE) oil in the R134a, R436A (R290/R600a56/44wt.%) and R436B (R290/R600a-52/48-wt.%) VCRSs.The VCRS ir-reversibility at the process with the nanoparticles was investigated using second law of thermodynamics. The results indicate that R134a, R436A and R436B and MO with TiO2 nanoparticles work normally and safely in the VCRS. The VCRSs total ir-reversibility (529, 588 and 570 W) at different process was better than the R134a,R436A and R436B and POE oil

system (777, 697 and 683 W). The same tests with Al2O3 nanoparticles showed that the different nanoparticles properties have little effect on the VCRS ir-reversibility. Thus, TiO2 nanoparticles can be used in VCRS with reciprocating compressor to considerably reduce irreversibility at the process. **R. Krishna Sabareesh, 2012,** studied the coefficient of performance of a refrigeration system can be improved if a reduction in the work of compression can be achieved by a suitable technique, for a specified heat removal rate. The present study investigates the effect of dispersing a low concentration of TiO2 nanoparticles in the mineral oil based lubricant, on its viscosity and lubrication characteristics, as well as on the overall performance of a Vapor Compression Refrigeration System using R12 (Dichlorodifluoromethane) as the working fluid. An enhancement in the COP of the refrigeration system has been observed and the existence of an optimum volume fraction noticed, with low concentrations of nanoparticles suspended in the mineral oil. The physics involved in the interaction of nanoparticles with the base fluid has been further elucidated by estimating the Optical Roughness Index using a Speckle Interferometer, by performing measurements on the pin surface following tests with a Pin-on-Disk tester. Is to compare the work of compressor when lubricated with nanolubricant (nanoparticles of Tio_2 dispersed in mineral oil) with its work when lubricated with mineral oil only, to evaluate the enhancement in the coefficient of performance of the air conditioner system.

2. THEORETICAL ANALYSIS

A window type Air-Conditioner system consists of a compressor, condenser, expansion valve and evaporator that are connected in a closed loop through piping that has heat Transfer with the surroundings, as shown in **Fig. 1**. Therefore, the rate of heat transfer to the cycle at the low temperature, in the evaporator, can be written as, **ASHRAE, 2009.**

$$Q_e = \dot{m}((h_3 - h_2) \quad (1)$$

where: Q_e = Cooling duty gained in evaporator (kW).

Similarly, the rate of heat transfer between the refrigerant and the sink in the condenser is

$$Q_c = \dot{m}((h_4 - h_1) \quad (2)$$

By applying the first law of thermodynamics,the work input to the compressor can also be expressed as

$$\text{Wc} = \dot{m}((h_4 - h_3) \quad (3)$$

where h_4 is the enthalpy of refrigerant at the outlet of compressor (kJ/kg).

The Compressor input power (Wc, kJ/s) is given as

$$\text{Wc} = \text{I V COS } \Theta \quad (4)$$

where COS Θ = power factor=0.7 ,**Ministry of Electricity in Iraq**, I is the current in Amper, and v is the voltage in Volt.

Defining the COP as the refrigeration effect over the compressor work, we get

$$COP = Qe/Wc \qquad (5)$$

3. EXPERIMENTAL APPARATUS

3.1. General Description

The used experimental rig is comprised of a window type air condition which was built for the objective of the present work. A Mitsubishi trade mark of 2-ton window type Air-Conditioner cooling unit (model WRC-1801K3SA) is selected to be as a test rig. The overall physical external dimensions of the evaporator are (42.8×42.4×8.2) cm, and condenser are (60×42.4×8.2) cm. **Fig.2** shows photographs of the unit, and manifests the instrumentation and measurement tools. The unit is powered by a reciprocating compressor (Mitsubishi co., model JAH5522E-RE68295A). As designed, the SAC is utilized R22 as a circulating refrigerant and a 3 GS Mineral lubricating oil. All components of the unit are connected by copper tubing with brazed connection.

3.2. Measuring Instruments

A Bourdon gauge type "AIMINDER" shown in **Fig.3** was used to measure the refrigerant side pressure at different locations, including pressure drop across the evaporator and condenser as shown in **Fig.2**. Two pressure gauges were installed on the high pressure side having a range of (0 to 500psi), the division (5 psi), and two pressure gauges installed on the low pressure side having range (-30 to 220psi), the division (2 psi).The temperature of the refrigerant is measured by three temperature gauges were installed on the refrigerant to measure the temperature of the refrigerant at different position. The technique used is by installing the thermometer immersed through the flow as shown in **Fig.2**. This method provides a direct contact between the bulb and the refrigerant to give more accurate measured values for temperature measurements. **Fig.4** shows temperature gauge were installed on the high pressure side and low pressure side. These where manufactured by HEIZUNGWILDMANN with a temperature range of (0 to 120 ºC) at a division of (2º). The current was measured by digital clamp meter, type (266 Digital clamp meters).Voltage is measured by using Multimeter type (PRO'SKIT 345) where the measuring is obtained continuously. All temperature and pressure gauges used for experiments were calibrated in the Central Institution for Standardization and Specify Control with error ± 0.4 % for

temperature gauge and error ±0.3 % for pressure gauge .

4. PREPARATION OF NANOFLUID

In this study two-**step** has been used to prepare of nanofluid. This method require produce nanoparticle firstly and then mixing with the base fluid. The first step Titanium Oxide TiO_2 is used as nanoparticle with specification(20 nm mean diameter, 3900 kg/m³ density, 8.9 w/m.℃ Thermal conductivity and 886.2 J/kg.℃ Specific heat. The second step The ultrasonic mixer is shown in **Fig.5** have its specifications are given (Model JP-120ST, Ultrasonic Frequency 40 kHz , Ultrasonic Power 720 Watt , Capacity 38 liter and Heating Power 800 Watt. Twelve transducers are used at the bottom of the bath, drain valve and basket; the transducers convert the electrical signal with low frequency (50 Hz) to high frequency (40 kHz) mechanical vibrations. The valve for emptying the tank and basket used to put the flask on it.

5. NANOPARTICLES VISCOSITY

The viscosity of the mineral oil relates indirectly to the load carrying capacity and power consumption rate of the compressor used in refrigeration system. The addition of foreign particles in the mineral oil alters the viscosity of the oil. **Lee et al., 2009**, found that addition of fullerene nanoparticles increased the viscosity of oil, and the enhancement was proportionate to the volume fraction. From the tribological characteristics of bearings, it is known that in a boundary lubrication system, an optimum level in the viscosity enhancement can result in a notable reduction in the power consumption**,** Bi, **Sheng Shan, 2008,[Jwo, Ching Song, 2009,and Sajith, V 201***0* **.**Considering these observations, the addition of nanoparticles must be low enough to make the process viable and effective; in reducing the power consumption. An optimal percentage of nanoparticles in the mineral oil is 0.01% volume fractions of TiO2 nanoparticles, **R. Krishna Sabareesh, 2012**. **Fig.6** shows optimal percentage of TiO2 nanoparticles in mineral oil 200 h after preparation .

6. RESULTS AND DISCUSSIONS

The results of performance comparison of the investigated refrigerants R22 without nanoparticles and with nanoparticles in the window type air-conditioning system are shown in **Figs. 7 to 10**. The result of the system compression ratio obtained at different ambient air temperatures for refrigerant R22 without nanoparticles and with nanoparticles is shown in **Fig. 7**. From the figure it was observed that the pressure ratios for the investigated refrigerants increased with the increase of ambient air temperature. Increase ambient air temperature will increase the temperature gradient between ambient air and conditioned room, which will increase the work of compressor and the compressor pressure ratio. **Fig. 8** shows the variation of the compressor power with ambient air temperature of R22 without nanoparticles

and with nanoparticles. From the figure, it can be deduced that compressor power increases as the ambient air temperature increases. This is as a result of the dependence of compressor power on the outside temperature. Increase in the outside temperature increased the load on the system which increased the compressor power. The average compressor input power for R22 with nanoparticles was (2.1 to 13.3) % lower than that of R22 without nanoparticles. The variation of the compressor discharge temperature with ambient air temperature for R22 without nanoparticles and with nanoparticles is shown in **Fig. 9**. As depicted in the figure, the compressor discharge temperature increases as the ambient air temperature increases for R22 without nanoparticles and with nanoparticles. Increase in discharge temperature is as a result of increase in the work of compressor due to increase in the ambient air temperature. The average compressor discharge temperature for R22 with nanoparticles was (3.33 to 8.95) % lower than that of R22 without nanoparticles. **Fig. 10** shows the variation of COP with varying ambient air temperature for the investigated. This figure indicates that when ambient air temperature increases the COP reduces for both R22 without nanoparticles and with nanoparticles. COP is inversely proportional to the power input through the compressor, therefore, increase in compressor power due to increase in ambient air temperature reduces the COP of the system. The average COP for R22 with nanoparticles was (7.93 to 11.99) % higher than that of R22 without nanoparticles.

7. CONCLUSION

In this paper the performances of refrigerant R22 without nanoparticles and with nanoparticles in the window type air-conditioning system were investigated experimentally and compared. Based on the investigation results, the following conclusions are drawn:

- The COP of R22 with nanoparticles is 7.93 to 11.99 % higher than that of R22 without nanoparticles.
- The compressor discharge temperature of R22 with nanoparticles lower than that of R22 without nanoparticles.
- The average compressor input power for R22 with nanoparticles was (2.1 to 13.3) % lower than that of R22 without nanoparticles.

REFERENCE

- ASHRAE. "*ASHRAE Handbook—Fundamentals (SI) ,2009*" ,Chapter 2
- Bi, Sheng shan, Shi, Lin, Zhang, Li, 2008."*Application of Nanoparticles in Domestic Refrigerators*''. Appl. Thermal Eng. 28, P 1834-1843.
- Lee, Kwangho, Hwang, Yujin, Cheong, Seongir, Kwon, Laeun,

Kim,Sungchoon,Lee, Jaekeun, 2009. "*Performance Evaluation of Nano-Lubricants of Fullerene Nanoparticles in Refrigeration Mineral Oil"*. Current Applied Physics 9, p 128-131.

- Jwo, Ching Song, Jeng, Lung Yue, Teng, Tun Ping, Chang, Ho, 2009. *''Effects of Nanolubricant on Performance of Hydrocarbon Refrigerant System''*. Am. Vacuum Soc., P 1473-1477.
- R. Krishna Sabareesh , N. Gobinath (2012) '' *Application of TiO2 Nanoparticles as a Lubricant-Additive for Vapor Compression Refrigeration Systems an Experimental Investigation* '' international journal of refrigeration v35 ,p 1989-1996
- Ruixiang Wang, Qingping Wua, Yezheng Wu, 2010) '*Use of Nanoparticles to Make Mineral oil Lubricants Feasible for Use in Aresidential Air Conditioner Employing Hydro-Fluorocarbons Refrigerants*" ' Energy and Buildings V42 ,p 2111-2117
- Omer AM. "*Energy Environment and Sustainable Development"*.Renew Sustain Energy Rev 2007.V1,p 50-57
- Sajith, V., Sobhan, C.B., Peterson, G.P., 2010.'' *Experimental Investigations on the Effects of Cerium Oxide Nanoparticle Fuel Additives on Biodiesel* ''. Adv. Mech. Eng., Article ID 581407
- Venkataramana Murthy , Senthilkumar ,2012, "*The use of TiO2 nanoparticles to reduce refrigerator irreversibility* " Energy Conversion and Management V59,p122-132

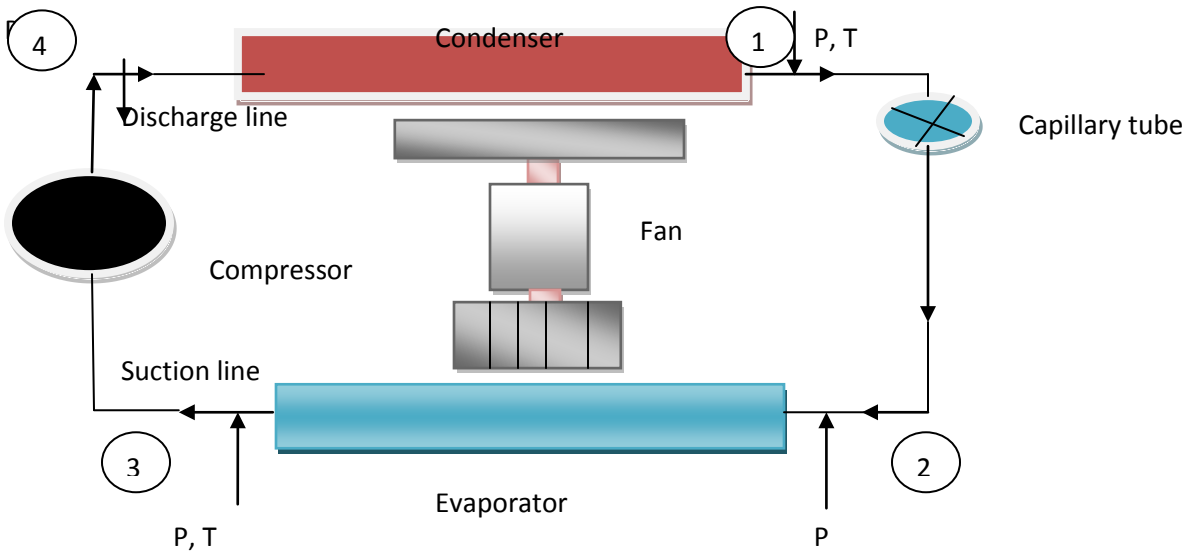

Figure 1. Schematic of a window type air-conditioner cycle.

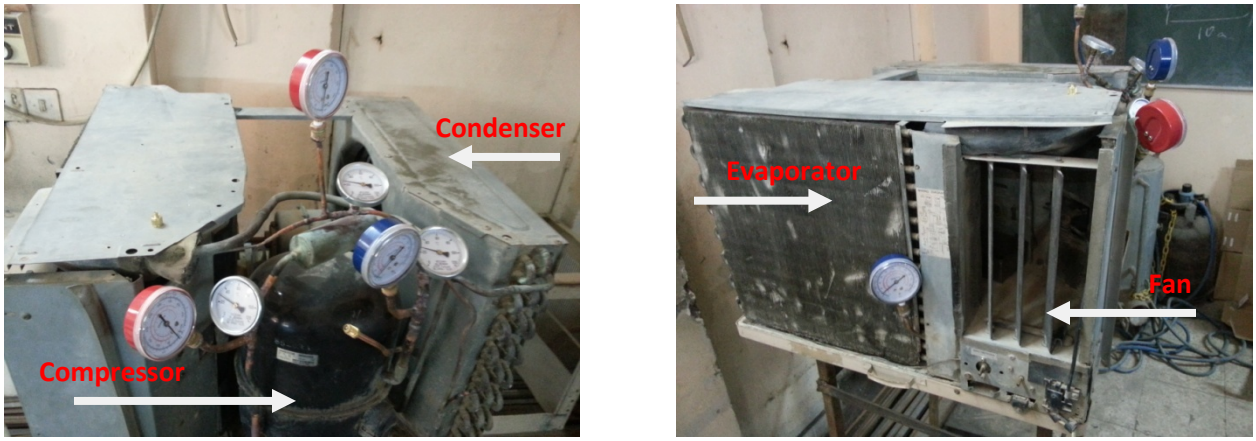

Figure 2. Photograph of test apparatus.

Figure 3. Pressure gauges.

.

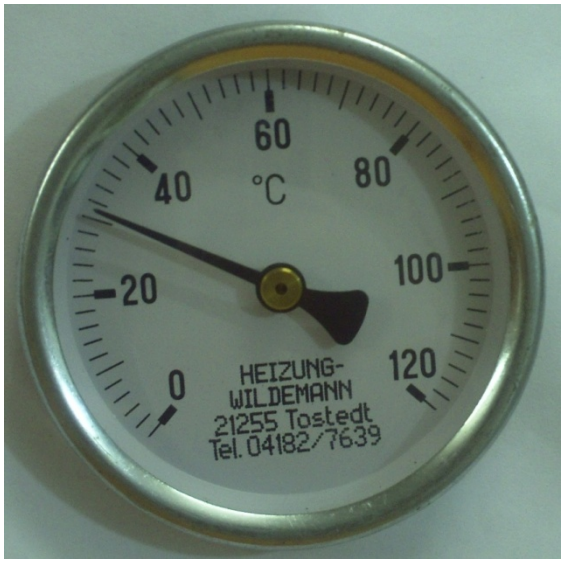

Figure 4. Temperature gauge.

Figure 5. Ultrasonic mixer with electric motor.

Figure 6. 0.01% Volume fractions of TiO2 nanoparticles in mineral oil 200 h after preparation.

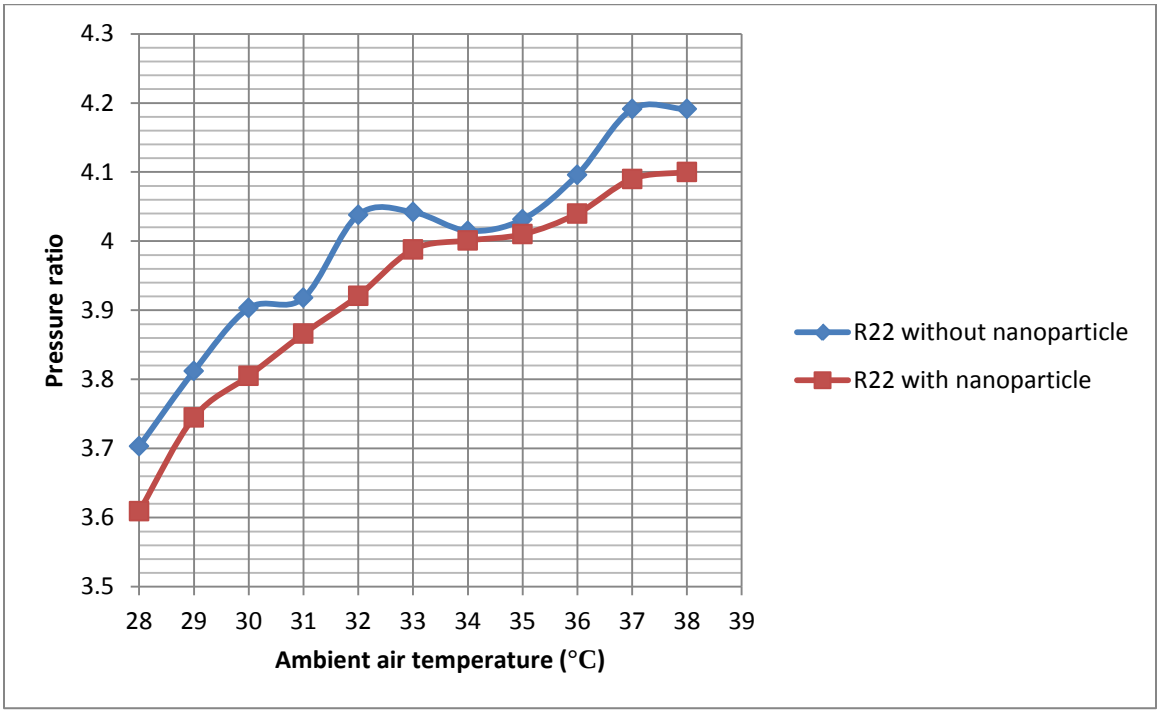

Figure 7. Variation of pressure ratio with ambient air temperature.

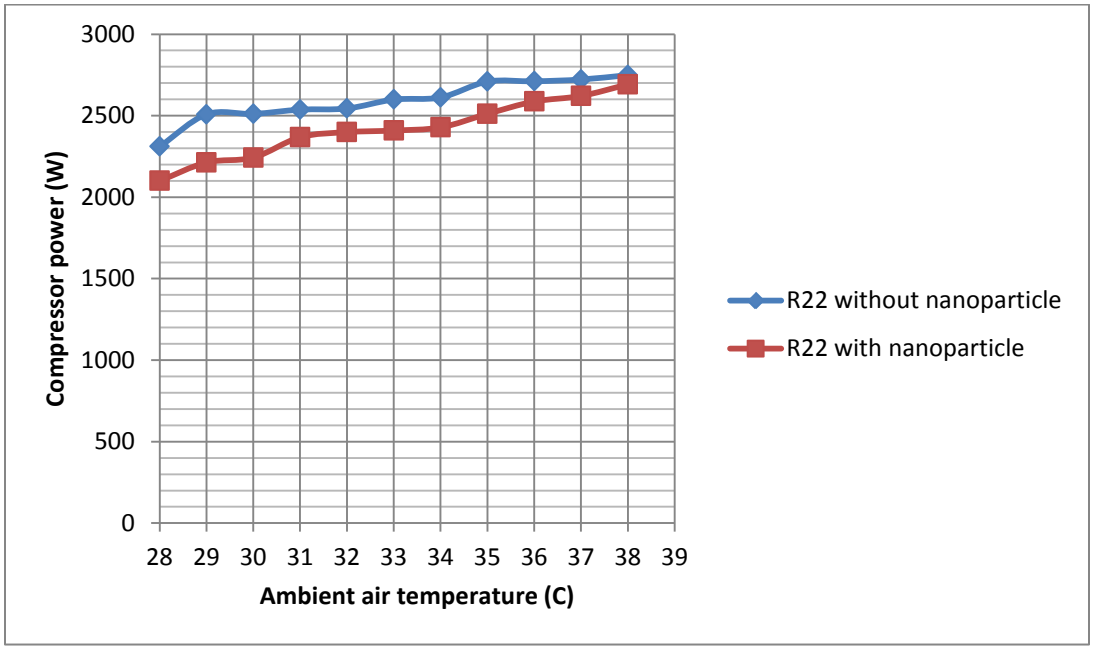

Figure 8. Variation of compressor power with ambient air temperature.

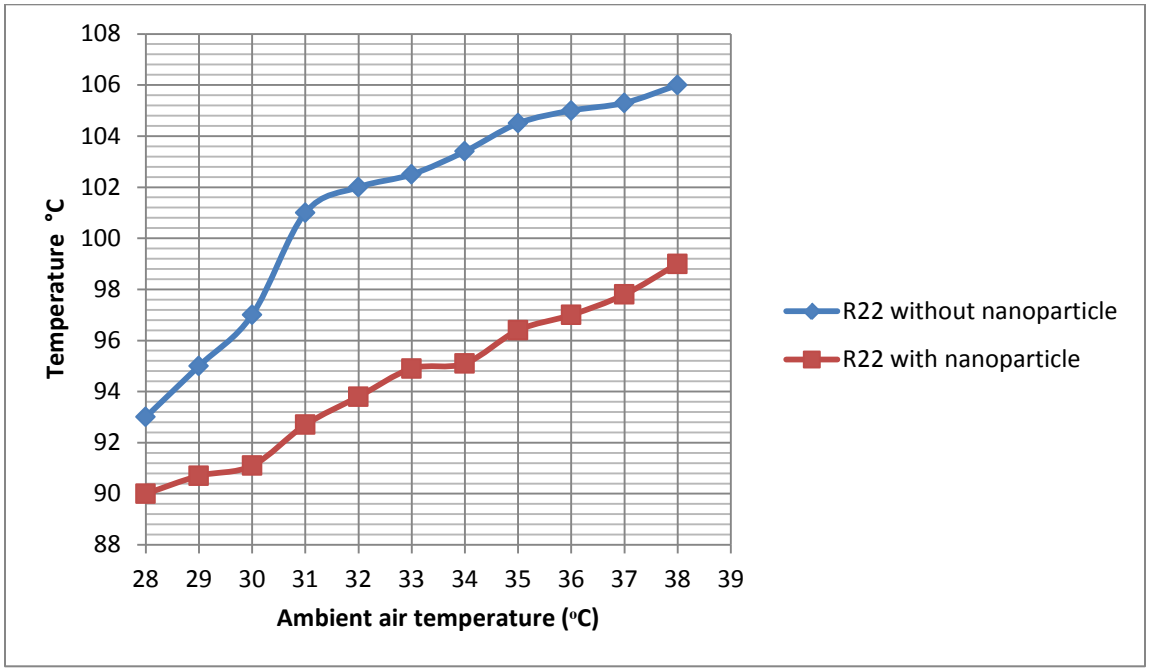

Figure 9. Variation of compressor outlet temperature with ambient air temperature.

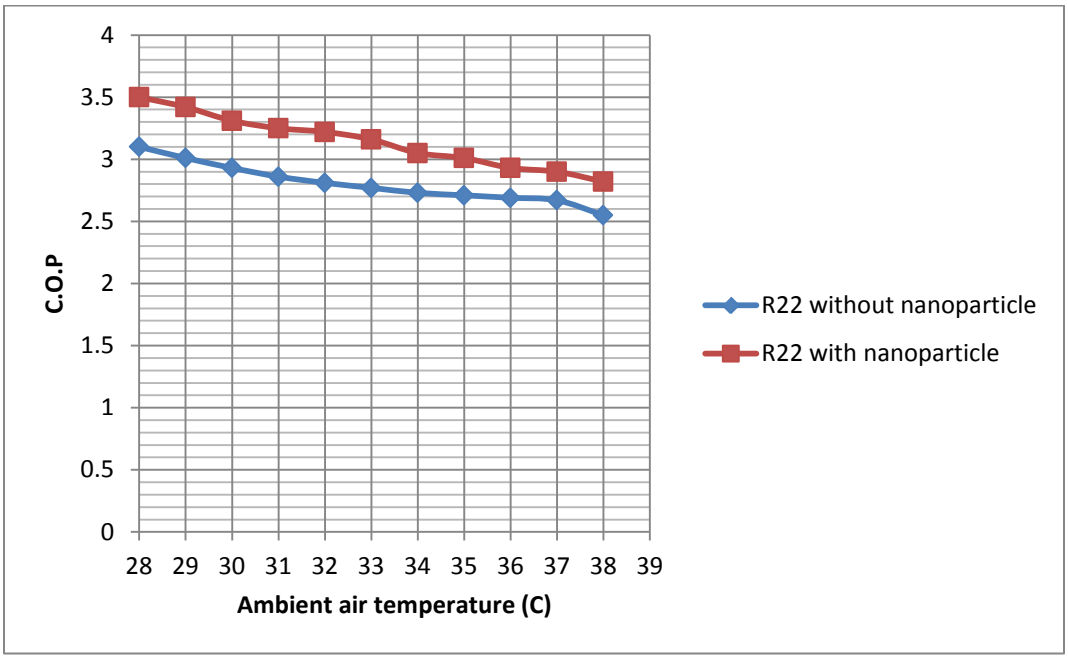

Figure 10. Variation of coefficient of performance (COP) with ambient air temperature.

Experimental and Numerical Study on Cavitation Effects in Centrifugal Pumps

Ass. Prof. Dr. Ali Abdul Mohsin Hassan
Department of Mechanical Engineering
College of Engineering \ Baghdad University
dralicit@yahoo.com

Nabeel Ahmed Kamal
Department of Mechanical Engineering
College of Engineering \ Baghdad University
nabeelahmed1976@yahoo.com

ABSTRACT

Experimental and numerical investigations of the centrifugal pump performance at non-cavitating and cavitating flow conditions were carried out in the present study. Experiments were performed by applying a vacuum to a closed-loop system to investigate the effects of the net positive suction head available (NPSHa), flow rate, water temperature and pump speed on the centrifugal pump performance. Accordingly, many of the important parameters concerning cavitation phenomenon were calculated. Also, the noise which is accompanied by cavitation was measured. Numerical analysis was implemented for two phase flow (the water and its vapor) using a 2-D simulation by ANSYS FLUENT software to investigate the internal flow of centrifugal pump under cavitating conditions. It was observed that with decreasing NPSHa, the values of the pump head, flow rate and efficiency initially remain constant, but with further reduction in NPSHa these parameters will decrease. Also, it was found that at 3% head drop the percentage drop of the flow rate is less than 2% whereas the percentage drop of the efficiency is greater than 3%. Numerically, it was noticed that the cavitation regions appear at the leading edge of suction side of the impeller blades which represents the lowest pressure area inside the computational domain of the centrifugal pump.

Key words: centrifugal pump, cavitation, NPSH, FLUENT, experiments

دراسـة عملية و عددية حـول تـأثيـر ظاهرة التكهف فـي المضخات النابذة

أ.م.د. علي عبد المحسن حسن
قسم الهندسة الميكانيكية / كلية الهندسة / جامعة بغداد

نبيل أحمد كمال
قسم الهندسة الميكانيكية / كلية الهندسة / جامعة بغداد

الخُلاصة

يتناول هذا البحث دراسة عملية وعددية لإداء مضخة نابذة عند ظروف الجريان غير المتكهف والمتكهف. التجارب العملية أجريت بطريقة تقليل الضغط الداخل الى المضخة بواسطة منظومة تفريغ الهواء، حيث تم دراسة تأثير تغيير قيم رفع السحب الصافي الموجب المتوفر (NPSHa) و معدل الجريان الحجمي و درجة حرارة الماء وسرعة المضخة على اداء المضخة النابذة وعليه عدة متغيرات مهمة تخص ظاهرة التكهف تم أحتسابها، وكذلك تم قياس مستوى الضوضاء المصاحبة لظاهرة التكهف. التحليل العددي لهذه الدراسة تضمن إجراء محاكاة ثنائية الأبعاد للجريان ثنائي الطور (للماء وبخاره) باستخدام حقيبة (ANSYS FLUENT) لتحري ظروف الجريان المتكهف داخل المضخة النابذة. النتائج العملية أظهرت أنه عند تقليل قيمة (NPSHa) فإن قيم رفع المضخة ومعدل الجريان والكفاءة تبقى ثابتة بشكل أولي، ولكن مع أستمرار تقليل قيمة (NPSHa) فإن هذه القيم سوف تنخفض. كذلك لوحظ أنه عند هبوط رفع المضخة بنسبة 3% فأن نسبة هبوط معدل الجريان تكون أقل من 2% في حين أن نسبة هبوط الكفاءة تكون أكثر من 3%. المحاكاة العددية أظهرت أن مناطق التكهف تظهر عند الحافات الأمامية لريش البشارة من جهة السحب حيث أنها تتشكل في المساحة الأقل ضغطا داخل المضخة.

الكلمات الرئيسية: مضخة نابذة، تكهف، رفع السحب الصافي الموجب المتوفر، فلونت، تجارب

1. INTRODUCTION

In many engineering applications, cavitation represents the subject of extensive experimental and numerical researches because it is one of the most serious problems encountered in the operation of pumps. Cavitation refers to the formation of vapor bubbles in regions within the flow field of a liquid, when the liquid absolute pressure drops to reach the vapor pressure corresponding to the operating temperature of this liquid. In some respects, it is similar to boiling except that the latter is generally considered to occur as a result of an increase of temperature rather than a decrease of pressure, **Brennen, 1994**. Cavitation occurs in any situation where fluid is moving relatively to a solid surface (particularly impeller and casing). As the vapor bubbles are transported through the impeller, they reach a zone of higher pressure where they collapse abruptly. If the collapse occurs on the surface of a solid, the liquid rushing in to fill the vacuous space left by the bubbles impacts tiny areas with tremendous localized pressures and thereby pits and erodes the surface. Cavitation reduces pump head, capacity and efficiency because a large number of vapor bubbles will block the impeller channels, which leads to a sudden drop in the pump performance at the cavitation critical point. In addition to the pitting and erosion, cavitation can also cause noise and vibration, **Sanks, et al. 1998.** Cavitating flows in centrifugal pumps were studied by experimental and numerical methods. **Guelich, in 1989** introduced an experimental study dealt with the erosion rate in an impeller of a centrifugal pump based on cavity length and he correlated damaged impellers by deducing the cavity length ,**Sloteman 2007,and . Harihara, and Parlos, 2006,** presented an experimental study of the sensor less approach to detect variable levels of cavitation in centrifugal pumps. The onset of pump cavitation was detected using only the line voltages and phase currents of the electric motor driving the pump. **Cernetic, et al., 2008** introduced experimentally the detection and monitoring of cavitation in centrifugal pumps by using noise and vibration signals. It was found that the noise and vibration levels increase with decreasing NPSHa value. **Houlin, et al., 2010,** presented a numerical simulation and experimental verification dealt with the effects of blade number on characteristics of a centrifugal pump in non-cavitation and cavitation conditions. It was noticed that with the increase of blade number, the area of low pressure region grows continuously, where the clog phenomenon becomes obvious in flow passage of impeller with the more blade number.

2. EXPERIMENTAL WORK

An experimental work was carried out to investigate and study the cavitation phenomenon and its effect on the centrifugal pump performance at different operation conditions. The experimental rig was designed and installed in this work, which allows to carry out the experiments by applying a vacuum to a closed-loop system where this method is usually used to attain cavitation phenomenon in the pumps. **Fig. 1** shows schematically the experimental rig, and this rig is shown photographically in **Fig. 2**. The test pump is a horizontal single-stage volute casing centrifugal pump with an open radial impeller which has three blades. As shown in **Fig.1**, the test pump is connected to the cylindrical vacuum tank which in turn is connected to the single stage dry vacuum pump which used to achieve the required vacuum inside the system. An electrical heater (with thermostat) was attached to the tank to change the temperature of water (the working fluid) for different operation conditions. A transparent Perspex pipe was installed in the suction pipe to observe the water that coming from the vacuum tank to assure that there are no bubbles present in the flow. In order to change the speed of the centrifugal pump, a motor speed controller was attached to the test rig to vary the pump speed to the desired value. The flow rate was adjusted by using the discharge gate valve.

Numerous measuring devices were used in this work, which are as follows: flow meter (rotameter) to measure the water flow rate, pressure gauges to measure the pump suction and discharge pressures and also the vacuum tank pressure, thermometer to measure the water temperature, digital photo tachometer to measure the pump speed, digital sound level meter (decibel meter) to measure the

pump noise and digital clamp meter to measure the voltage and current of the pump motor.

Different experiments were carried out on the experimental rig which involve changing the flow rate with values (10.95, 11.95, 12.95, 13.95 and 14.95 m^3/h), water temperature with values (25.5, 35.5 and 45.5 ˚C) and pump speed with values (2560 and 2660 rpm), as well as the effect of decreasing NPSHa with range (10 to 1 m) which occurs as a result of vacuum process to investigate the effect of these parameters on the centrifugal pump performance at non-cavitating and cavitating flow conditions. Cavitation condition was adjusted by decreasing NPSHa (i.e., pump suction pressure) at the pump suction port as a result of vacuum process.

After accomplishing all of the experiments and the experimental readings were recorded, the calculations were performed to predict the centrifugal pump performance and the equations that used to analyze the experimental readings and to calculate the parameters are illustrated below:

The total pump head (H) of the centrifugal pump is calculated as follows **Kubota, 1972**:

$$H = \frac{P_d - P_s}{\rho g} + \text{Height difference between measuring points} \quad (1)$$

The net positive suction head available (NPSHa) can be computed by the following equation (White 1998):

$$NPSHa = \frac{P_s}{\rho g} + \frac{v_s^2}{2g} - \frac{P_V}{\rho g} \quad (2)$$

There are two important parameters are usually used in the cavitating flow field, which are Thoma cavitation number (σ_{TH}) and cavitation number (σ), and these two dimensionless numbers are defined as follows, **Schiavello and Visser, 2008:**

$$\sigma_{TH} = \frac{NPSHa}{H} \quad (3)$$

$$\sigma = \frac{P_s - P_V}{\frac{1}{2}\rho U^2} \quad (4)$$

where U is the inlet-blade tip speed = ΩR_{1T} , and R_{1T} represents the inlet-blade tip radius.

Another parameter called suction specific speed (N_{SS}) which is a dimensionless quantity that describes the suction characteristics of a pumping system. This parameter can be computed by the following equation, **Schiavello and Visser, 2008:**

$$N_{SS} = \frac{\Omega Q^{\frac{1}{2}}}{(g\,NPSHa)^{\frac{3}{4}}} \quad (5)$$

The pump efficiency (η_p) which represents the hydraulic efficiency is calculated as follows, **Girdha and Moniz, 2005:**

$$\eta_P = \frac{P_H}{P_M} = \frac{\rho g Q H}{V I \cos\theta\, \eta_e} \quad (6)$$

Where, P_H is the pump hydraulic power (water horsepower) and P_M is the motor power (brake horsepower).

Because the inlet and outlet boundaries of the computational domain in the numerical simulation were considered to be at the suction and discharge ports of the centrifugal pump and for comparison between the experimental and numerical results, the pressure measuring points in the experimental work also were considered to be at these boundaries, where the head loss due to friction in the suction and discharge pipes between pressure gauges and the suction and discharge ports of the pump was taken in consideration.

Among the mentioned parameters, the most common parameters that are widely utilized to describe the cavitation progress stages are NPSHa, (σ_{TH}) and (σ). Therefore, in the present study the values of NPSHa and (σ_{TH}) were utilized for comparison with the other parameters, where some parameters were plotted versus the NPSHa and the remaining were plotted versus the (σ_{TH}) especially with the dimensionless parameters. It is important

to note that all curves were plotted to terminate at the critical point that corresponding to the 3% drop in pump head (i.e., at NPSHr value), where this point can be determined experimentally by reducing the pump suction pressure below the critical pressure and then determining the critical point for each curve after calculating the value of 3% head drop.

3. NUMERICAL SIMULATION

The numerical work of the present study aims to analyze the cavitating behavior inside the centrifugal pump by using a numerical simulation which represents an important tool to disclose the mechanism of cavitation characteristic in pumps. To do this, ANSYS FLUENT software release 13.0 was used to simulate the two phase flow (the water and its vapor) inside the centrifugal pump. The cavitation model implemented in FLUENT is based on the so-called "full cavitation model" which developed by **Singhal, et al. in 2001** ,**Stuparu, et al. 2011** and it accounts for all first-order effects like phase change, bubble dynamics, turbulent pressure fluctuations and non-condensable gases. Cavitation was modeled in this work with the help of homogeneous mixture multiphase model. The standard $(k\text{-}\varepsilon)$ turbulence model and SIMPLEC algorithm were chosen in FLUENT.

In the present work, a 2-D model of the centrifugal pump including a spiral volute casing and curved blades impeller was implemented. The geometry of the pump was created by using professional software "SolidWorks", version 2011. The meshes required for the calculations were generated by using the CFD pre-processing package, "GAMBIT", version 2.4.6. An unstructured 2-D triangular-pave mesh was used for the generation on the computational domain surface as well as a boundary layer mesh was created around the blades. The created computational domain of the centrifugal pump has three zones: inlet zone (pump inlet port), blades zone (pump impeller) and outlet zone (volute casing and pump outlet port), and the total number of nodes in the domain are 24927. The geometrical parameters of the used impeller are shown in **Table 1**.

Table 1. Geometrical parameters for the used impeller**.**

Parameter	Value
Blade shape	Circular arc (non-twisted)
Impeller inlet diameter (mm)	46
Impeller outlet diameter (mm)	120
Blade thickness (mm)	3
Blade inlet width (mm)	11.5
Blade outlet width (mm)	11.5
Number of blades	3

In this work, the study by FLUENT was implemented with two boundary conditions. The first boundary condition is (pressure inlet-pressure outlet) which was employed to plot many contours to illustrate the cavitation regions inside the computational domain under different conditions. The second boundary condition is (velocity inlet-pressure outlet) which was employed to make FLUENT software predicts the inlet pressure of the pump and hence important parameters can be predicted numerically. Both boundary conditions are based on the experimental results.

4. RESULTS AND DISCUSSION

4.1 Experimental Results

Fig. 3 indicates the influence of NPSHa on the pump head for different flow rates, which shows that when the NPSHa decreases, the head values initially remain approximately constant (no cavitation is present at this stage). A further reduction in the NPSHa will decrease the head, where this process continues until the 3% drop in head has been reached. Reducing NPSHa means that decreasing the inlet pressure (suction pressure) of the pump according to **Eq.2,** and this will result in creating and growing the regions of vapor bubbles inside the pump. A large number of vapor bubbles will block the impeller channels, which leads to a sudden drop in the pump head. This figure also illustrates that when the flow rate increases, the NPSHa decreases because the pump inlet pressure will decrease with increasing the flow

rate (due to increasing the velocity of flow). Although the pump inlet velocity increases with increasing the flow rate, but this increasing in inlet velocity will be smaller than the decrease that occurs in the inlet pressure, so NPSHa will decrease as the flow rate increases according to **Eq.(2)**. In addition, it is found that the value of NPSHr (which indicated by black dot) increases with increasing the flow rate where the inlet critical pressure increases with increasing the flow rate. Accordingly, it is concluded that NPSHa is inversely proportional to flow rate, whereas NPSHr is directly proportional to flow rate. According to the numerical results, the inception of cavitation occurs at NPSHa (which called NPSHi) is approximately equal to (3.22 m) for flow rate (12.95 m^3/h), where the flow with NPSHa less than (3.22 m) represents a cavitating flow for all flow rates as indicated in this figure.

Fig. 4 indicates the influence of NPSHa on the pump head for different temperatures, which illustrates that the values of both NPSHa and NPSHr decrease with increasing the temperature because the vapor pressure will increase with increasing the temperature, where vapor pressure is a direct function of temperature. This figure also shows that there are no significant changes in the head values with increasing the temperature at the studied values.

Fig. 5 indicates the influence of NPSHa on the pump head for different pump speeds, which shows that decreasing the speed leads to increase the NPSHa and decrease the NPSHr; where the decrease in speed leads to increase the pump inlet pressure and decrease the inlet critical pressure. Also, it is seen that decreasing the speed leads to decrease the head because the pump outlet pressure (discharge pressure) will decrease with decreasing the speed, where the decrease in outlet pressure will be greater than the increase in inlet pressure which occurs as a result of decreasing the speed.

Fig.6 indicates the influence of NPSHa on the pump flow rate for different flow rates, which illustrates that the flow rate curves have the same behavior of the head curves concerning the effect of decreasing NPSHa which leads to a sudden drop in the pump flow rate due to blocking the impeller channels with vapor bubbles.

Through comparative study of **Figs.3** and **6** concerning the influence of decreasing NPSHa on the head and flow rate curves, it has been attributed to the fact that when the 3% drop in head has been achieved, the percentage of flow rate drop is less than 2% at the same critical point. As an example, in **Fig.7** which shows the influence of decreasing NPSHa on the head and flow rate curves for the case of flow rate (12.95 m^3/h), this figure clearly shows that the percentage of drop for flow rate is less than that in the head which is equal to 1.16% for this case. This can be explained that the pump head has higher sensitivity to cavitation than flow rate.

Fig. 8 indicates the influence of NPSHa on the pump efficiency for different flow rates, which shows that the efficiency curves have the same behavior of the head and flow rate curves concerning the effect of decreasing NPSHa, where the percentage of efficiency drop at 3% head drop is more than 3% because the drop in both the head and flow rate has been considered in calculating the efficiency according to **Eq. (6).** As an example, the percentage of efficiency drop for the curve with flow rate (12.95 m^3/h) is equal to 4.08%. This figure also shows that the curves with flow rates (11.95 and 12.95 m^3/h) have the highest efficiency values, and the curves with flow rates (10.95 and 13.95 m^3/h) come below them, while the curve with flow rate (14.95 m^3/h) has the lowest efficiency value. The reason for this is that the two highest efficiency curves have flow rates that are too close to the best efficiency point (BEP) flow rate; whereas the other three curves have flow rates relatively far from the BEP flow rate. It is quite apparent that the BEP flow rate is located between the flow rates (11.95 and 12.95 m^3/h).

Fig.9 indicates the influence of NPSHa on the Thoma cavitation number for different flow rates, which illustrates that the Thoma cavitation number decreases linearly as NPSHa decreases because it is directly proportional to NPSHa according to

Eq.(3). Also, it is shown that when the flow rate increases the Thoma cavitation number increases too because the increase in flow rate causes a reduction in the head which leads to increase Thoma cavitation number. Although the increase in flow rate will result in decreasing the NPSHa as discussed previously, but the decrease in head will be greater than that in NPSHa as a result of increasing the flow rate. Also, this figure illustrates that the critical point of the Thoma cavitation number (at 3% head drop) increases with increasing the flow rate because this critical point has been calculated according to NPSHr which is directly proportional to flow rate.

Fig. 10 indicates the influence of NPSHa on the pump noise level for different flow rates, which shows that when the NPSHa decreases the noise level increases, where the noise level starts to increase rapidly at NPSHa is approximately (9 m), and this behavior continues with decreasing NPSHa until it reaches approximately (6 m), then noise level increases slowly until NPSHa reaches approximately (3 m), after that the noise level starts again to increase rapidly with decreasing NPSHa due to a large number of vapor bubbles will collapse as they enter the region of higher pressure. This figure also shows that the difference in the pump noise level between non-cavitating and cavitating flow (at 3% head drop) is about 8 dB. Also, it is seen in this figure that the noise level decreases slightly with increasing the flow rate.

Fig.11 indicates the influence of Thoma cavitation number on the cavitation number for different flow rates, which illustrates that the cavitation number decreases linearly as Thoma cavitation number decreases that is because cavitation number depends on the pump inlet pressure according to **Eq. (4),** and Thoma cavitation number is directly proportional to NPSHa which in turn depends on the inlet pressure. Also, it is shown that the cavitation number decreases with increasing the flow rate because the pump inlet pressure decreases with increasing the flow rate (due to increasing the velocity of flow). On the other hand, the critical point of the cavitation number (at 3% head drop) has been calculated according to the pump inlet pressure that corresponding to the NPSHr, hence it increases with increasing the flow rate as shown in this figure because NPSHr is directly proportional to flow rate.

Fig.12 indicates the influence of Thoma cavitation number on the suction specific speed for different flow rates, which shows that the suction specific speed increases nonlinearly as Thoma cavitation number decreases. Decreasing Thoma cavitation number means that decreasing NPSHa as discussed previously, and according to **Eq.(5)** the suction specific speed is inversely proportional to NPSHa, hence decreasing any of these two parameters (Thoma cavitation number or NPSHa) leads to increase the suction specific speed. Also, it is shown that the suction specific speed increases with increasing the flow rate because it is directly proportional to flow rate. On the other hand, the critical point of the suction specific speed (at 3% head drop) has been calculated according to NPSHr, hence this critical point decreases with increasing the flow rate, where the effect of NPSHr will be slightly greater than the flow rate in **Eq.(5).**

4.2 Numerical Results and Comparison

Figs. 13 to **15** indicate the influence of decreasing NPSHa on the inception and growth of cavitation regions (vapor regions) inside the computational domain of the centrifugal pump according to the first boundary condition. **Figs. 13**, **14** and **15** illustrate the computational domain at NPSHa values (3.22 m), (2.27 m) and (1.45 m) respectively. In these figures, it is shown that the cavitation regions appear at the leading edge of suction side of the impeller blades which represents the lowest pressure area inside the domain and the area of these regions expands as a result of decreasing NPSHa, where the value of NPSHa (1.45 m) is equal to NPSHr according to the experimental results of this test. On the other hand, it was found that these cavitation regions expand with increasing the temperature whereas they reduce with decreasing the speed because the NPSHa decreases with increasing the temperature and it increases with decreasing the speed as it is concluded in the experimental results.

Fig. 16 indicates the influence of decreasing NPSHa on the head numerically according to the second boundary condition. In this figure, it is

shown that the head remains approximately constant with decreasing NPSHa, but with further reduction in the NPSHa the head will decrease, where this process continues until the 3% drop in head has been reached. After the critical point, the drop in the head will be more rapidly with decreasing NPSHa.

Fig. 17 shows the comparison between the experimental and numerical result of the (Head-NPSHa) curve, which illustrates that the numerical head curve follows the same behavior of the experimental head curve but with some differences between them, where the numerical curve falls below the experimental curve with an average difference of (9%), and its critical point exceeds the critical point of the experimental curve with a difference of (16.6%). The difference between the numerical and experimental result in this figure is may be due to simplifying the solution of this simulation from three-dimensional to two-dimensional approach.

5. CONCLUSIONS

The main study conclusions can be summarized as follows:

(1) With decreasing NPSHa, the pump head, flow rate and efficiency will decrease where it was found that at 3% head drop, the percentage drop of flow rate is less than 2% whereas the percentage drop of efficiency is greater than 3%.

(2) NPSHa decreases with increasing the flow rate and temperature and it increases with decreasing the speed, whereas NPSHr increases with increasing the flow rate and it decreases with increasing the temperature and decreasing the speed.

(3) Pump noise level increases with decreasing NPSHa and flow rate.

(4) Cavitation regions appear at the leading edge of suction side of the impeller blades which represents the lowest pressure area inside the computational domain of the centrifugal pump, where these cavitation regions expand with decreasing the NPSHa and increasing the temperature whereas they reduce with decreasing the speed.

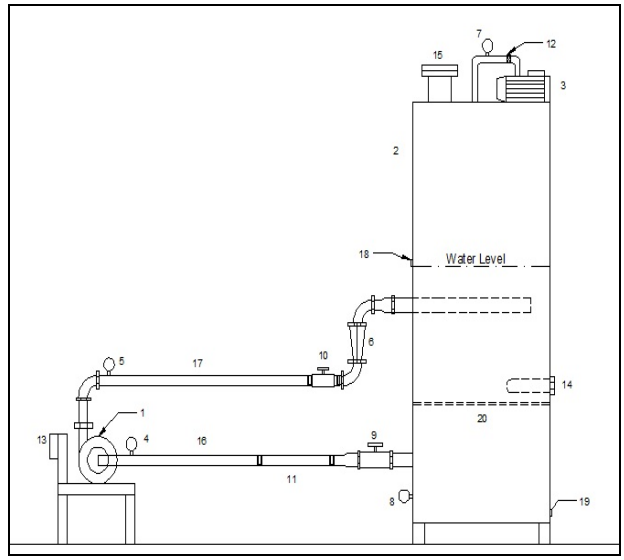

1	Centrifugal Pump (Test Pump)	11	Transparent Perspex Pipe
2	Vacuum Tank	12	Pneumatic Valve (0.5 in)
3	Vacuum Pump	13	Motor Speed Controller
4	Suction Pressure Gauge	14	Electrical Heater & Thermostat
5	Discharge Pressure Gauge	15	Filling & Ventilation Opening (4 in)
6	Flow Meter (Rotameter)	16	Suction Pipe (1.5 in)
7	Tank Pressure Gauge	17	Discharge Pipe (1.5 in)
8	Thermometer	18	Water Level Indicating Hole
9	Suction Gate Valve (2 in)	19	Drain Hole
10	Discharge Gate Valve (1.5 in)	20	Stainless Steel Strainer

Figure 1. Schematic representation of the experimental rig.

Figure 2. Photograph of the experimental rig.

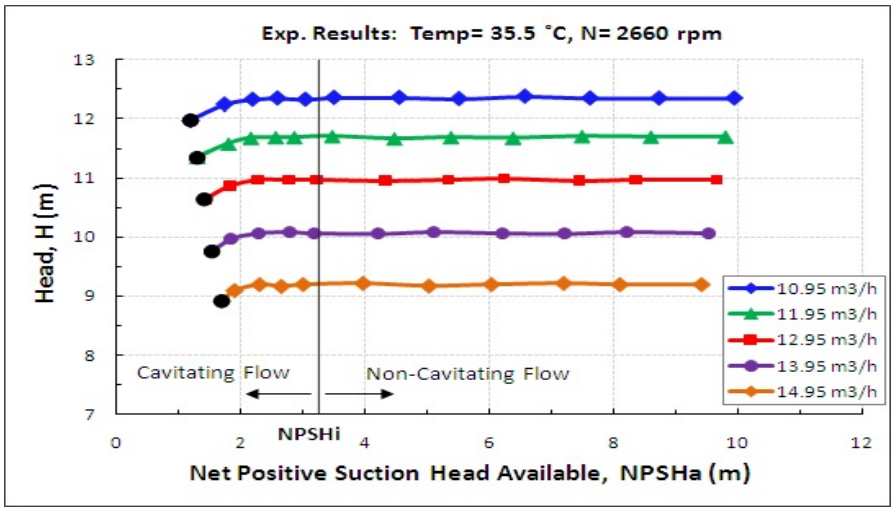

Figure 3. Influence of NPSHa on the head for different flow rates.

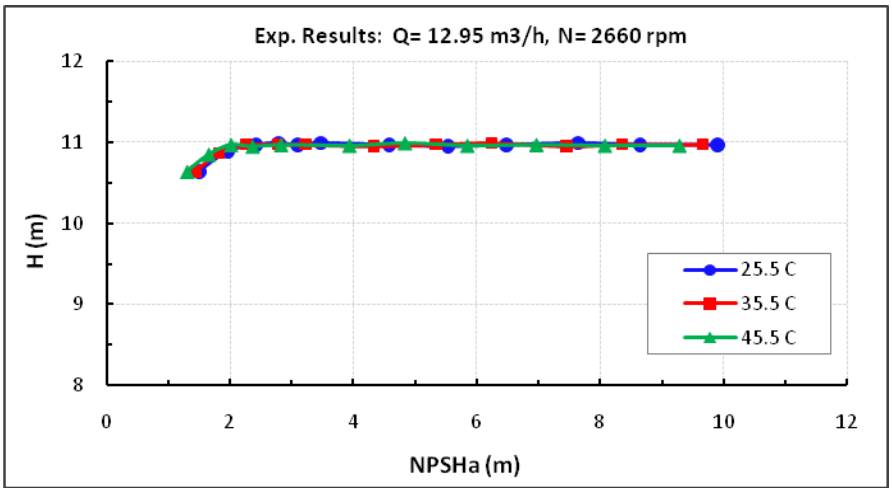

Figure 4. Influence of NPSHa on the head for different temperatures.

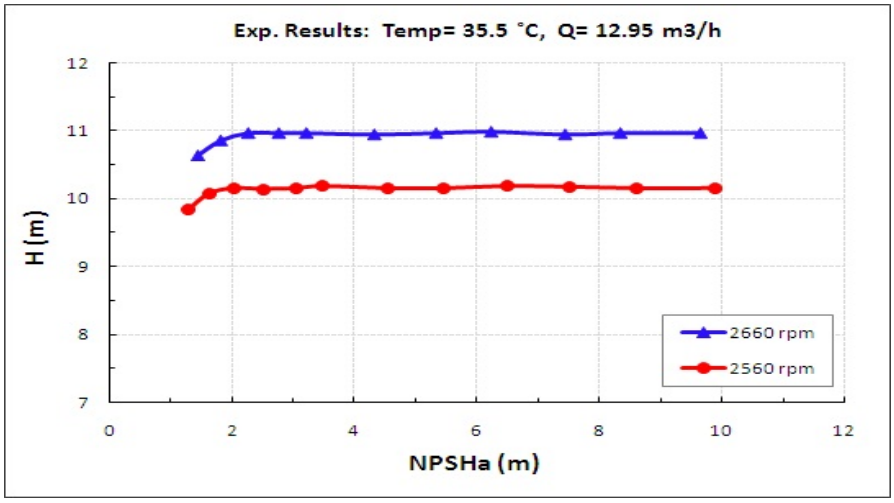

Figure 5. Influence of NPSHa on the head for different speeds.

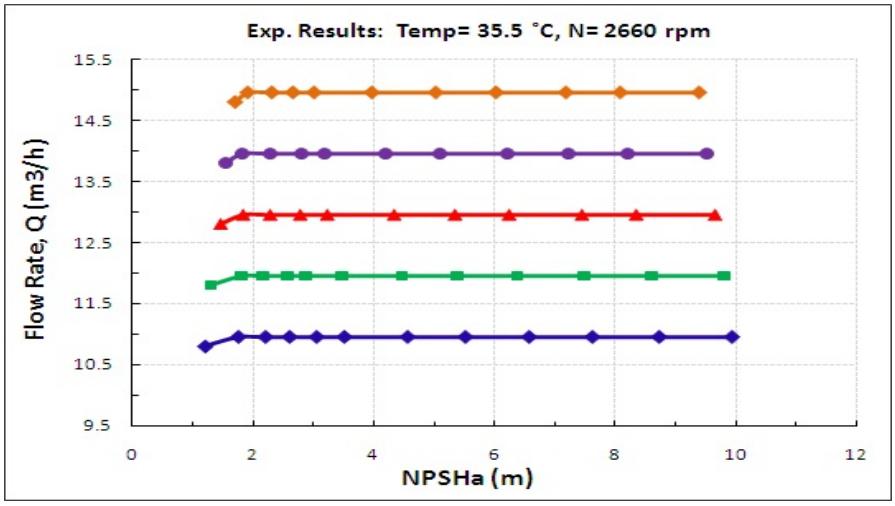

Figure 6. Influence of NPSHa on the flow rate for different flow rates.

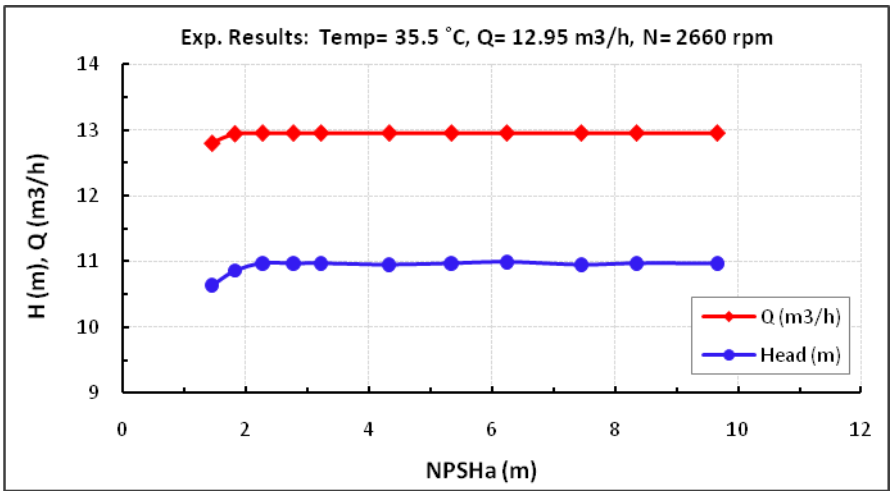

Figure 7. Influence of NPSHa on the head and flow rate.

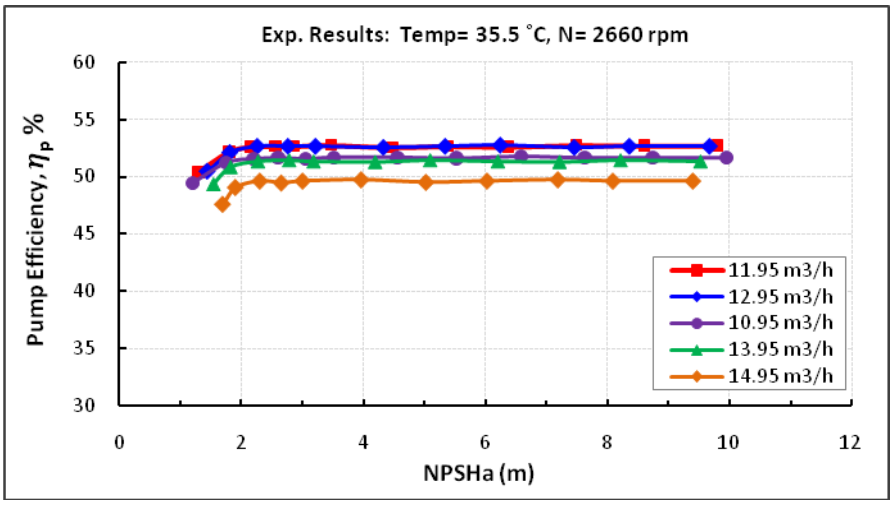

Figure 8. Influence of NPSHa on the efficiency for different flow rates.

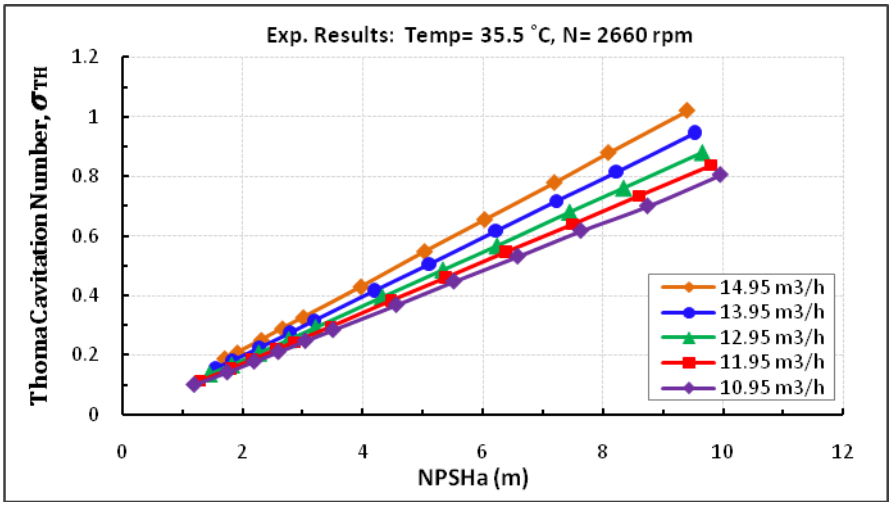

Figure 9. Influence of NPSHa on the Thoma cavitation number for different flow rates.

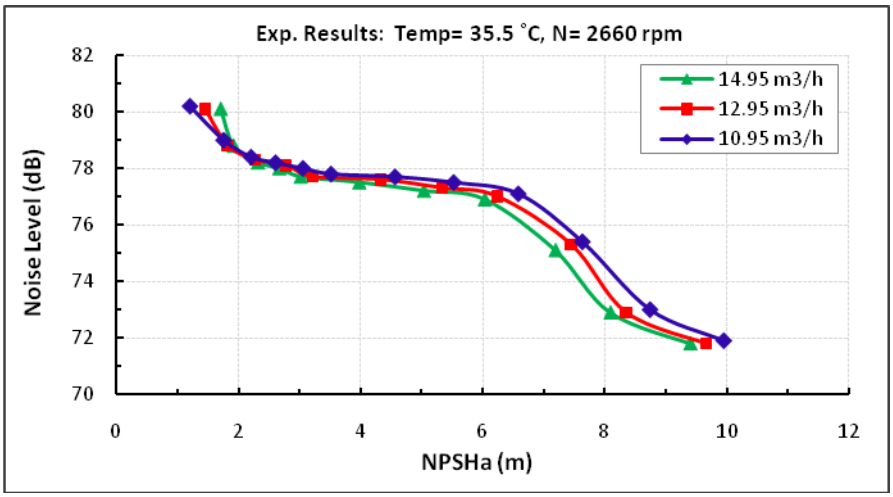

Figure 10. Influence of NPSHa on the pump noise level for different flow rates.

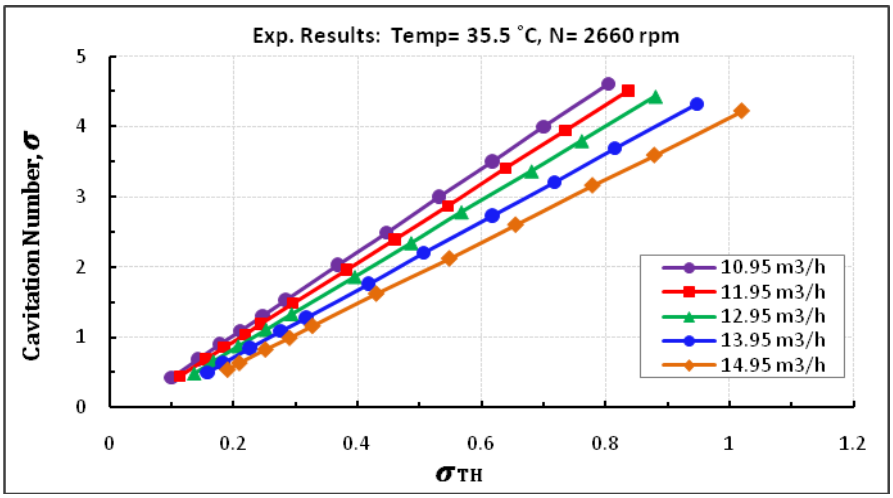

Figure 11. Influence of Thoma cavitation number on the cavitation number for different flow rates.

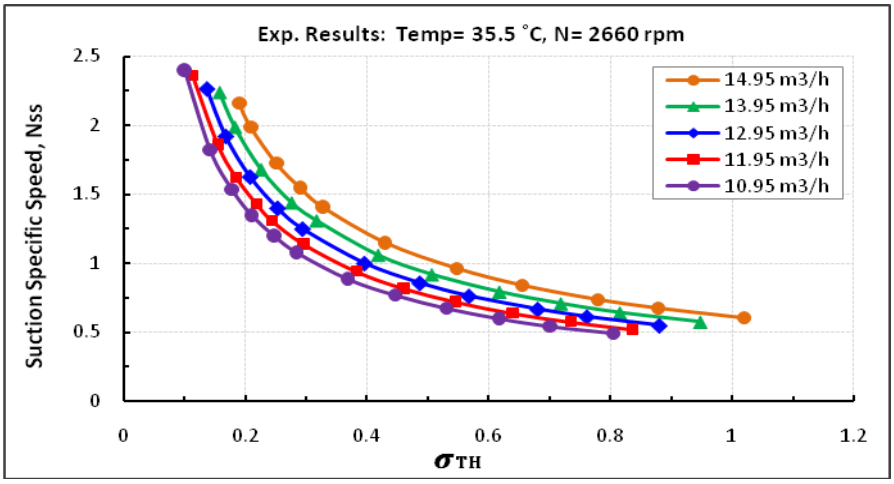

Figure 12. Influence of Thoma cavitation number on the suction specific speed for different flow rates.

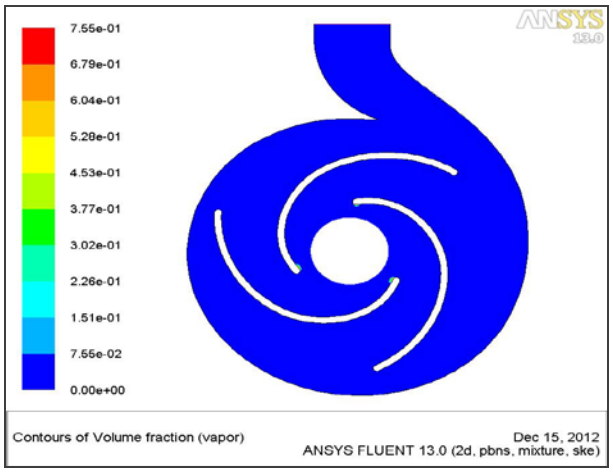

Figure 13. Cavitation regions (NPSHa = 3.22 m, 35.5 ˚C and 2660 rpm).

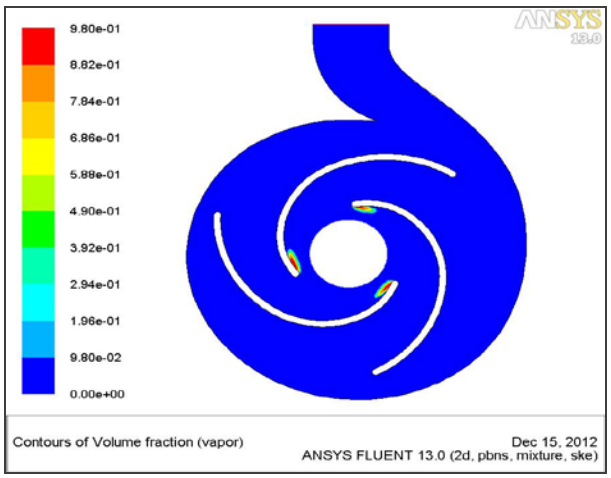

Figure 14. Cavitation regions (NPSHa = 2.27 m, 35.5 ˚C and 2660 rpm).

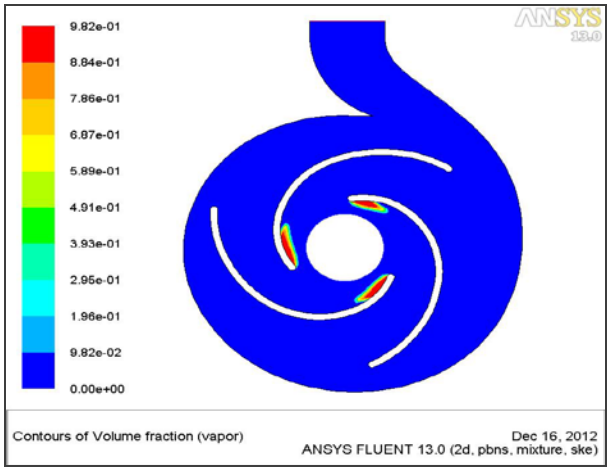

Figure 15. Cavitation regions (NPSHa = 1.45 m, 35.5 ˚C and 2660 rpm).

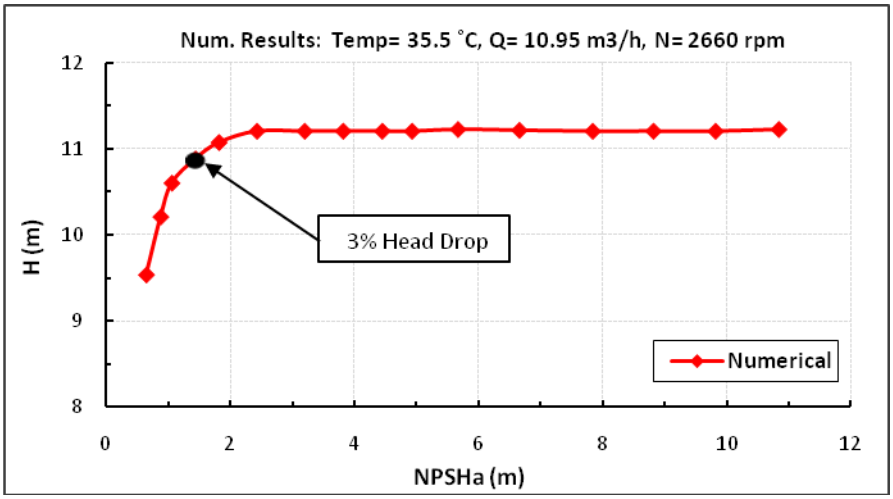

Figure 16. Influence of NPSHa on the head.

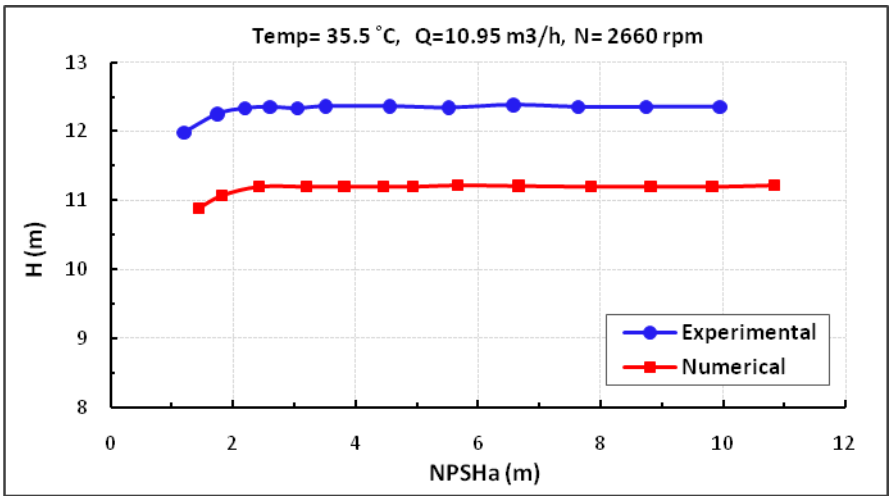

Figure 17. Comparison between experimental and numerical (Head-NPSHa) curve.

REFERENCES

Brennen, C.E., 1994, "*Hydrodynamics of Pumps*", Concepts NREC and Oxford University Press.

Cernetic, J., Prezelj, J., and Cudina, M., 2008, "*Use of Noise and Vibration Signal for Detection and Monitoring of Cavitation in Kinetic Pumps*", University of Ljubljana, Faculty of Mechanical Engineering, Slovenia, pp. 2199-2204, June 29-July 4.

Girdhar, P., and Moniz, O., 2005, First Edition, "*Practical Centrifugal Pumps*", IDC Technologies, Netherlands.

Harihara, P.P., and Parlos, A.G., 2006, "*Sensorless Detection of Cavitation in Centrifugal Pumps*", ASME International Mechanical Engineering Congress and Exposition, November 5-10, Chicago, USA.

Houlin, L., Yong, W., Shouqi, Y., Minggao, T., and Kai, W., 2010, "*Effects of Blade Number on Characteristics of Centrifugal Pumps*", Chinese Journal of Mechanical Engineering, Vol. 23, pp. 1-6.

"*Kubota Pump Hand Book*", 1972, First Edition, Volume 1, Kubota Ltd. Pump Export Department.

Sanks, R.L., Tchobanoglous, G., Bosserman, B.E., and Jones, G.M., 1998, Second Edition, "*Pumping Station Design"*, Butterworth-Heinemann, USA.

Schiavello, B., and Visser, F.C., 2008, "*Pump Cavitation-Various NPSHR Criteria, NPSHA Margins and Impeller Life Expectancy*", Twenty Fourth International Pump Users Symposium.

Sloteman, D.P., 2007, "*Cavitation in High Energy Pumps-Detection and Assessment of Damage Potential*", Twenty-Third International Pump Users Symposium, pp. 29-38.

Stuparu, A., Susan-Resiga, R., Anton, L.E., and Muntean, S., 2011, "*A New Approach in Numerical Assessment of the Cavitation Behavior of Centrifugal Pumps",* International Journal of Fluid Machinery and Systems, Vol. 4, No.1, pp. 104-113, January-March.

White, F.M., 1998, Fourth Edition, "Fluid Mechanics", McGraw-Hill Series.

NOMENCLATURES

g = Acceleration due to gravity (m/s^2)
H = Pump head (m)
I = Current (amp)
k = Turbulent kinetic energy (J/kg)
N = Rotational speed (rpm)
NPSHa = Net positive suction head available (m)
NPSHi = Incipient net positive suction head (m)
NPSHr = Net positive suction head required (m)
N_{SS} = Suction specific speed
P = Static pressure (Pa)
P_H = Pump hydraulic power (watt)
P_M = Motor power (watt)
Q = Volumetric flow rate (m^3/s)
R_{1T} = Inlet-blade tip radius (m)
Temp = Temperature (˚C)
U = Inlet-blade tip speed (m/s)
V = Voltage (volts)
v = Average velocity of flow (m/s)

Greek Symbols

ε = Turbulent dissipation rate (J/kg)
η_e = Motor efficiency
η_p = Pump efficiency
$\cos\theta$ = Power factor
ρ = Density (kg/ m^3)
σ = Cavitation number
σ_{TH} = Thoma cavitation number
Ω = Angular speed = πN/30 (rad/s)

Subscript Symbols

d = Discharge
s = Suction
V = Vapor

Abbreviations

BEP = Best Efficiency Point
CFD = Computational Fluid Dynamics

Experimental and Theoretical Investigation of Noise Effect in Centrifugal Fan Impeller

Asst. Prof. Dr. Manal Hadi Saleh
University of Baghdad/College of Eng.
Manalhadi2005@yahoo.com

Asst. Prof. Dr. Muna Sabah Kassim
University of Al – Mustansirya/College of Eng.
munahdr@yahoo.com

Amina Hmoud Hnaef
Mechanical Engineering
Sahmali46@yahoo.com

ABSRACT

In this work a study was made in centrifugal fan blower to investigate the effect of impeller blade design on sound pressure level (SPL). Shroud and unshroud impeller of nine blades are used. The sound generation from flow inside the test rig at different positions was displayed by using spectral analyzer. The experiments were carried out in anechoic chamber with small holes in its walls, under ambient condition about (25-27) C ° to avoid the effect of temperature on the sound pressure level. The results showed that (SPL) decreased with the increase of distance from the source about (3-4)dB when distance varied about (0.8-1.06)m, and the (SPL) decreased with the decrease of velocity about (8-12)dB when velocity varied between (13000-2600) r.p.m., and when the velocity remain constant (SPL) increased with the increased of pressure about (7-15)dB when the pressure varied between (36-8)mbar. For the purpose of comparison, two types of impellers were tested under same conditions, the results showed that (SPL) increased when shroud used on the impeller. The mathematical results show good agreement with the experimental results. The study also concluded a spectral analysis of the noise generated using 1/3 octave band filter. The analysis showed that (SPL) increased with frequency range of (0.8-400) Hz. The maximum sound pressure level was appeared clearly in the frequency range between 200 – 400 Hz .

Key words: centrifugal blower; noise; frequency; rotational speed; static pressure; flow rate

دراسة عملية ونظرية لدراسة ظاهرة الضوضاء في منفاخ الطرد المركزي

أ.م.د. منال هادي صالح
قسم هندسةالميكانيك
كلية الهندسة / جامعة بغداد

أ.م.د. منى صباح قاسم
قسم هندسةالميكانيك
كلية الهندسة / الجامعة المستنصرية

آمنة حمود ضايف
قسم هندسةالميكانيك
كلية الهندسة / جامعة بغداد

الخلاصة

في هذا البحث تمت الدراسة على مروحة ذات الطرد المركزي لدراسة تاثير تغيير تصميم ريش بشارة المروحة على مستوى ضغط الصوت الصادر منها. حيث تمت الدراسة على نوعين من البشارات مغطاة وغير مغطاة ذات 9 ريش. تم قياس الصوت المتولد من الجريان داخل غرفة العزل باستخدام محلل طيفي. التجارب اجريت في غرفة عزل صوتي تحوي على ثمان ثقوب مخروطية على جدرانها الخارجية، الغرفة تعمل تحت تاثير الضروف الجوية بدرجة حرارة تتراوح ما بين 25–27 م، تم العمل بهذه الضروف لتجنب تاثير درجة الحرارة على مستوى ضغط الصوت(م. ض. ص.). النتائج اثبتت ان مستوى ضغط الصوت يقل مع زيادة المسافة عن المصدر الصوتي بنسب تتراوح م بين(3–4) ديس بيل ولابعاد تختلف ما بي 0.8م – 1.06م عن مصدر الصوت، ويقل م.ض.ص مع نقصان السرعة بنسب تتراوح ما بين(8–12) ديس بيل عند تغير السرعة ما بين(13000–2600) دورة لكل دقيقة، وعند بقاء السرعة والعوامل الاخرى ثابتة فان مستوى ضغط الصوت يزداد مع زيادة الضغط الاستاتيكي وهذه الزيادة ما بين(7–15)

dB عند تغير الضغط من 8ملي بار الى 36 ملي بار. لغرض المقارنة نوعين مختلفة من البشارات تم استخدامها تعمل عند نفس الضروف، النتائج اثبتت ان مستوى ضغط الصوت يزداد عند استخدام البشارة المغطاة. النتائج النظرية اعطت توافق جيد مع النتائج العملية ، الدراسة ايضا اعطت التحليل الطيفي للضوضاء المتولدة باستخدام مرشح(octave3/1). التحليل بين ان زيادة م.ض.ص مع التردد للقيم مابين 0.8 –400هيرتز . القيمة العظمى لمستوى ضغط الصوت تتحقق عند الترددات ما بين 200–400 هيرتز.

1. INTRODUCTION

In industrial ventilation applications, noise can be a significant concern. High acoustic levels promote worker fatigue. The noise generated by a fan depends on fan type, airflow rate, and pressure. Inefficient fan operation is often indicated by a comparatively high noise level for a particular fan type. If high fan noise levels are unavoidable, then ways to attenuate the acoustic energy should be considered. Centrifugal turbo machines are common devices used in many flow control applications due to their ability to achieve relatively high-pressure ratios in a short axial distance compared with axial fans. They are often found in gas turbine engines, heating ventilation and air-conditioning systems and pumps. Because of their widespread use, the noise generated by these machines causes one of the serious problems. The noise is often dominated by tones at the blade passage frequency and its higher harmonics. This is a consequence of the strong interactions between the flow discharged from the impeller and the cut-off in the casing. In addition to the discrete tones, the broad band noise is generated from the trailing edge due to the fluctuations of the turbulent boundary layers or separated flows on the impeller blade, **Jeona and Leeb, 2002.**

Acoust, J., 1978, studied the Sources of broadband noise in FC (forward curved blades) centrifugal fans experimentally using a 0.28m diameter fan. Strong tangential and axial gradients of mean velocity and static pressure were found in the housing. Very large variations in velocity and velocity fluctuations occurred across the blade passages. Both the inlet and discharge rotor noise showed a continuous reduction in level with flow from maximum flow to the stall region. A miniature microphone mounted at various points on the blade surfaces showed a large increase in pressure fluctuations from the leading to the trailing edge of the blades. The fluctuations on the suction surface were much stronger than those on the pressure surface. **Choi, 1993,** Identify which aspects of the fluid dynamics were associated with noise generation in centrifugal turbo machinery. Research emphasis was placed on the generation of noise at frequencies other than the blade passage tones. In order to avoid noise generated by the interaction of the discharged flow and stationary objects outside of the impeller, experiments were performed on a centrifugal impeller without diffuser and casing. With this discharge configuration, the radiated noise spectra were show to be dominated by harmonically related broad humps at low frequency. These were proven to be generated by the interaction of a coherent unsteady flow structure rotating around the impeller discharge and the trailing edges of the impeller blades. **Xiaoliang, et al., 2008,** reduce the noise of the T9_19No.4A centrifugal fan, whose impeller had equidistant forward swept blades, two new impellers with different blade spacing were designed and an experimental study was conducted both the fans aerodynamic performances and noise were measured when the two redesigned impellers were compared with the original ones. The test results were discussed in detail and the effect of the noise reduction method for a centrifugal fan using impellers with no isometric forward swept blades was analyzed which could serve as a reference for researches on reduction of fan noise. **Wolfram, et al., 2011,** studied a typical acoustic spectrum of a fan consists of both broadband and tonal components; the overall acoustic level was dominated by the tonal part, especially the tone at blade passing frequency (BPF) and higher harmonics. **Hsien, et al., 2011,** presented a new robust multi—criteria optimization method that employs the Taguchi method to design and analyze an ultra-thin centrifugal fan. The objective of this study was to obtain the maximum volume flow rate, static pressure, and minimum noise of a fan. The proposed approach utilizes a combined

orthogonal array and computational fluid dynamics method to simulate the internal flow field of the ultra-thin centrifugal fan. This study employs signal-to-noise ratio and analysis of variance to determine the Pareto-optimal robust design solution. This research also identifies the optimal design parameters that affect the cooling performance of the centrifugal fan. The experimental results confirm the effectiveness of this approach The Taguchi method is a highly practical tool for process design, wherein mathematical models for system performance do not exist. The method provides a simple, efficient, and systematic approach to optimize designs for performance, quality, and cost. The Taguchi parameter design can optimize performance characteristics by setting design parameters, and reduces the sensitivity of system performance to the source of variation. **Sasaki, 2012,** presented a preliminary attempt towards the prediction of the broadband noise from the flow features, compatible with industrial constraints. In the case of low-solidity impeller, the wake rapidly expands in a wide outer part of the blades under the influence of the separation forced by the tip vortex. The broadband noise level in the low-frequency domain became large because the wake vortices with large scale in the low frequency domain were shed from the blade. Since the relative flow of the high-solidity impeller at the maximum efficiency point remains attached over the blades, the strength of vortex-shedding in the wake was reduced. Therefore the broadband noise at the maximum efficiency point was substantially decreased. At the off-design point in low flow rate, the number of blades had limited influence on the flow regime in the wake because separation likely occurs from the leading edge.

2. EXPERIMENTAL DEVICE

In this work, an experimental study about the tonal noise sources in a centrifugal fan with backward curved blades had been carried out. Acoustic pressure measurements at the blower exit duct and pressure fluctuation measurements on the volute surface had been made for different flow rates. A correlation study of both pressure signals has been made in order to explain some of the features of the aerodynamic tonal noise generation. A strong source of noise caused by the interaction between the fluctuating flow leaving the impeller and the volute tongue is appreciated. The unsteady forces exerted on the fan blades constitute another noise generation mechanism, which affects the whole extension of the impeller, thus transmitting pressure fluctuations to the entire volute casing. The relative importance of this mechanism compared to the impeller–tongue interaction depends on the flow rate. The fan used in this study is a single-stage machine with shrouded and unshrouded impeller and external volute.

2.1 Test Rig Equipment

The Rig consists of the following main parts as shown in **Fig. 1**.

2.1.1 Anechoic Chamber

Anechoic chamber is a room that has been prepared to minimize sound reflections from walls. The Anechoic Room is used to prevent the undesirable outside noise to effect the test. However, a free-field microphone can be used, **Barlow, et al., 1999, and Holman and Gajda, 1984**.

The anechoic chamber is shown in **Fig. 2** with the size of 1.5m long by 1.0m wide and 0.9m high. It consists of four parts:

1- Wooden structure of 3.5 cm thickness.
2- External wooden cover has a thickness of 8mm.
3- Sheets of cork material inside the wooden structure have a thick of 3.5 cm.
4- Triangular sponge was used to distribute on all sides, ceiling and floor of the room made from wood. Each sponge has base (10cm x10cm) and height 10 cm as shown in **Figs. 3 and 4**.

There are 8 holes. Each hole is in the form of cone have a length of 5cm and two diameters the first diameter is 2.5cm and the second diameter is 1.4cm, was used to put the device of (**SPL**) for measuring purposes.

2.1.2 Pipes

There are two types of pipes used in this work:

1- Rigid pipe: it is a pipe of 6.25 cm of diameter and 2.5m length as shown in **Figs. 5 and 6**. An orifice meter was fixed on the

entering pipe with manometers in each side of the orifice meter to measure the determined pressure across the orifice meter for all the cases studied. A gate valve was fixed in the existing pipe to get a specified mass flow rate inside the system.

2- Flexible pipe: it is a pipe of 6.25cm of diameter, and 25cm length as shown in **Fig. 7**. this pipe was used because of its flexibility to insulate and absorb the blower vibration.

2.1.3 Blower

The blower model ct 6007of unshrouded rotor type shown in **Fig. 8** was used in this work; of (a centrifugal type) which has different speed, and the specification of the blower is shown in **Table 1**.

2.1.4 The Impeller

Two type of impellers used for the test shrouded and unshrouded. It is fitted on the rotating shaft which is directly connected to the motor shaft. The blades of this impeller are of backward shape having a thickness of (3mm).

2.2 Measuring Instruments:

2.2.1 Sound level meter

Sound pressure level is the measurement of sound strength on a logarithmic scale (base ten). The sound level meter is shown in **Fig. 9** and has an auto range Rs-232 type K/J.

2.2.2 Sound and vibration analyzer

The **SVAN 957** is digital, Type 1 sound and vibration level meter along with analyzer. The instrument is intended to general acoustic and vibration measurements, environmental monitoring, occupational health and safety monitoring as shown in **Fig. 10**.

2.2.3 Digital manometer:

A p200 UL model of a digital device, used to measure the pressure inside the inlet pipes before, and after orifice plate, as shown in **Fig. 11**, its range are: Low pressure 0_19.99 mbar and High pressure 0_100 m bar.

2.2.4 Interface temperature

The thermocouples used in this experiment were type K and insolated. These average values of the temperature were taken for each flow and pressure measurement as shown in **Fig. 12**.

2.2.5 Digital photo tachometer

This digital photo tachometer was used to measuring the velocity of the blower impeller for each flow and each pressure measurement as shown in **Fig. 13** with the applied target.

EXPERIMENTAL STEPS:

1. Operate the blower at a specified speed
2. Open the gate valve (full open)
3. Record the thermometer reading
4. Use the manometer to measure the maximum pressure at that blower speed.
5. By controlling the gate valve, take four readings of different pressures where the last reading is for the maximum pressure.
6. Record the spectrum sound analysis using the (Svantek pc++) device in the eight openings of the anechoic chamber for each pressure.

Repeat steps (1- 6) for five blower speeds.

3. MATHEMATICAL MODEL

The backward inclined blower wheel design has blades that are slanted away from the direction of wheel rotation**, Kunjur and Krishnamurty, 1997**. The term applied to this type of balding is BI or backward inclined. Centrifugal fans are widely used and the noise generated by these machines causes one of the serious problems, **Beranek, 1960**.

In order to calculate the radiated acoustic field of a centrifugal fan, the modification of the generated noise by the casing should be considered. The unsteady flow is generated due to the rotation of the impeller at a rotation velocity N near a wedge. For the centrifugal fan, the rotation of the impeller results in an inflow across the inlet section. Let Q denote the volume flow rate, represented by a source located at the center of the impeller. Assuming the fluid is incompressible and inviscid, the main feature of the flow considered is the non-zero circulation around every impeller blade. The impeller was assumed to rotate with a variable angular velocity and the flow field of the impeller is incompressible and inviscid. The impeller has (b) number of blades. The inlet flow is modeled by a point source located at the center of the impeller. A major component of fan noise for the large commercial fan currently in service is

the tone noise generated by the rotating blades of the fan, as they interact with the stator blades and the struts**, Faulkner, 1976 and Bartlett, 1934.**

Sound pressure level, SPL, is defined by the relation**, Faulkner, 1976.**

$$SPL = 10\log\,[p/p_{ref}]^2 \qquad (1)$$

Where:

P_{ref}= 2 × 10^{-5} r.m.s sound pressure (Pa)

Or

$$SPL = 20\log\left[\frac{p}{p_{ref}}\right] \qquad (2)$$

Since the wave fronts generated with each pulsation are always in phase, the resultant wave motion diverges uniformly in a spherical manner. Now, as seen previously for uniform spherical divergence, the sound intensity I at a distance r is given by:

$$I= w/4\pi r^2 \qquad (3)$$

Where:

w= acoustical power of the radiating source (W)

$4\pi r^2$ = surface area of a sphere of radius r (m^2)

In addition, it can be shown that for freely propagation plane waves, the intensity are related to the rms sound pressure as follows:

$$I=p^2/\rho c \qquad (4)$$

Combining the equations, to get finally, the relationship between sound pressure and sound power:

$$p^2/\rho c=w/4\pi r^2 \qquad (5)$$

With a little algebra, the more useful relationship between sound pressure level (SPL) and sound power level L_w is obtained:

$$SPL=L_w-20\log_{10}(r)-11 \qquad (6)$$

Where

L_w = sound power level of the point source (re10^{-12} W)

r = radial distance from source (m)

The frequency of the discrete tones is given by:

$$F_n=N*b/60 \qquad (7)$$

The origin of the discrete tones results from two sources. The first, for each time a blade passes appoint in space, a pressure fluctuation is created due the displacement of air and/or aerodynamic lift if the blade is in airfoil configuration. The broad band aerodynamic noise originates from vortices created at the leading and/or trailing edge of the blades and turbulence imparted to the fluid, usually in the form of eddy like flow. Here again the accurate prediction of noise levels for these fans is at best very difficult, but an empirical approximation which provides good first-order results for the average sound power level in the range of 500 to 400 Hz is:

$$L_w=10 \log Q +20 \log P_t +K \qquad (8)$$

Where:

K=constant depending on fan type, 35 for forward -or backward-curved blades and 43 for radial types.

4. RESULTS AND DISCUSSION

4.1 Experimental Results

In this work the spectral analysis of noise emitted from centrifugal blower was studied for different distance from the sound source in the anechoic chamber and the effect of changing the centrifugal blower velocity, types and pressures on the sound pressure level (SPL) was studied.

4.1.1 Spectral analysis of noise at different distances from the source :

Fig. 14 Shows the variation of the sound pressure level versus the frequency in different distances around the anechoic chamber (eight holes), for blower have unshroud impeller with 9 blades, angular velocity of 13000 r.p.m and a pressure of 32 mbar. It is clear that the maximum value of the SPL is in the first position 1(The closest distance from the source)

and the minimum value of the SPL is in the position of the hole at position 6 the farther position from the source) The peak amplitude of SPL at position 1and 6 can varied between (3–4) dB, for different types of impellers.

4.1.2 Spectral analysis of noise emitted for variable velocities:

Different types of impeller and different distances from the source was used to explain the effect of the variation of blower velocity on the maximum value of SPL in all cases, the results show that the increase of velocity caused increase of SPL in the range of (8– 12) dB depending on the value of velocity as shown in **Figs. 15 and16**.

4.1.3 Spectral analysis of noise for different pressures:

Spectral analysis of noise at different pressures was studied when other parameters were taken as constant. In all cases the only parameter changed was the pressure. , increasing pressure cause increase of the peak value of SPL at the range of (8-15) dB that depends on the value of specified pressure as shown in **Fig. 17**.

4.1.4 The Effect of the mass flow rate on SPL, and Reynolds number

Five values of velocity were taken and for each velocity the gate valve used to get four values of the mass flow rate. **Figs. 18 and 19,** show that the SPL decrease with the decrease of the mass flow rate.

4.2 Theoretical Results

A computer program was built to solve the sound pressure equation by using mat lab program. The data that controls program is volume flow rate, static pressure and the rotation velocity of flow. The mat lab program was used to simulate the noise propagation **Fig. 20 and Fig. 21** shows the relation between the SPL and position from the source at different velocity in shroud and unshroud impeller.

5. CONCLUSION

In this work many parameters were studied that affected the sound intensity caused by a centrifugal blower in anechoic chamber. The following major conclusions for the experimental and theoretical study can be drawn as follow:

1- An increase in the sound pressure level (SPL) with the velocity of the blower.

2- The noise resulted in the test section was in the frequency range of o.8 – 20000 Hz.

3- The sound pressure level increase with frequency for the range mentioned above.

4- The maximum sound pressure level was appeared clearly in the frequency range of 200 – 315 Hz.

5- The results show that using cover on the blades causes increase in pressure Increase the sound pressure level.

6- For the same number of impeller blades the flow velocity and pressure decrease for a light impeller material

REFERENCES

Barlow, J., Rae, W. and Pope, A. 1999, "*Low Speed Wind Tunnel Testing*", John Wiley& Sons.

Bartlett, F. "*The Prpblem of Noise*", 1934, Cambridg University Press.

Beranek, L., 1960,"*Noise Reduction*", Massachusetts Institute of Technology,.

Daniel Wolfram, Thomas Carolus, Michael Sturm, 2011, "*Fan Tone Generation in an Isolated Rotor Due to Unstable Secondary Flow Structures"*, Pollrich Ventilatoren GmbH, 41065 Monchengladbach, University of Siegen, Departement of Fluid- and Thermodynamics, 57068 Siegen, Germany.

Faulkner, L.L., 1976,"*Handbook Of Industrial Noise Control"* industrial press. Inc,.

Holman, J.P., and Gajda, w.j., 1984, "*Experimental Methods for Enginers*", McGraw-Hill Book Company, Fourth Edition,.

Impeller Located Near A wedge, 2002, "*DA Research Lab, LG Electronics Inc"*, 327-23, Kasan- dong, Kumchon-gu, Seoul 153-802, South Korea.

J. A coust. Soc. Am., 1978, "*Noise Generation in FC Centrifugal Fans"*, Volume 64, Issue S1, pp. S48-S48 America.

Jong- Soo Choi, 1993,"*Aerodynamic Noise Generation in Centrifugal Turbo Machinery*", The Pennsylvania State University, Korea.

Kuang-Hung Hsien, Shyh-Chour Huang, Sciences and Kaohsiung, Taiwan, 2011, "*Taguchi Method to Robust Multi--Criteria Optimum Design for Ultra-Thin Centrifugal Fan*", National Kaohsiung University of Applied.

Kunjur, A., Krishnamurty, S., 1997, "*A Robust Multi-Criteria Optimization, Approach*", vol.32, pp. 797-810, Mech. Mach. Theory.

Liu Xiaoliang, Qi Datong and Mao Yijun, 2008, "*Noise Reduction for Centrifugal Fan with Non-Isometric Forward-Swept Blade Impeller*" Higher Education Press and Springer-Verlag.

Soichi Sasaki, S., 2012, "*An Experimental Study on Broadband Noise of a Propeller Fan* ", pp.1-7, Nagasaki University's Academic.

Wan-Ho Jeona and Duck-Joo Leeb, "A numerical Study on the Flow and Sound Fields of Centrifugal impeller located near a wedge, DA research Lab., LG Electronics Inc., 32 7-23, Kasan-dong, Kumchon-gu, Seoul 153-802, South Korea.

NOMENCLATUR

Letter	Description	Units
SPL	*Sound pressure level*	*dB*
Fn	*frequency*	*Hz*
p	*Static pressure*	N/m^2
I	*Sound intensity*	W/m^2
w	*Acoustical power of the radiating source*	*W*
ρc	*Mass flow rate per unit area*	$Kg/s.m^2$
Lw	*Sound power level of the point source (re10-12 W)*	*W*
r	*Radial distance from source*	*m*
N	*Fan rotational speed*	*r.p.m*
b	*Number of blades*	–
n	*Harmonic; i.e. ,n = 1(fundamental)*	–
Q	*Volume flow rate*	m^3/s
$\dot{m}$	*Mass flow rate*	*kg/s*

Table 1. Specification of the blower model ct 6007.

Radiated power input	600W
Outlet diameter	10 cm
Type of curved blade	Backward curved blades
Impeller exit diameter	104 mm
The inlet and outlet Pipes diameter	2.5cm
Impeller inlet diameter	15 mm
Number of impeller blades	9
Speed	13000 rpm
Inlet blade angle	β1= 54 from tangential direction
Outlet blade angle	β2=42°from tangential
Blade thickness	2mm
Impeller thickness	3 mm
Maximum thickness, discharge width	24 mm
Length of blade	520mm
pitch	30mm

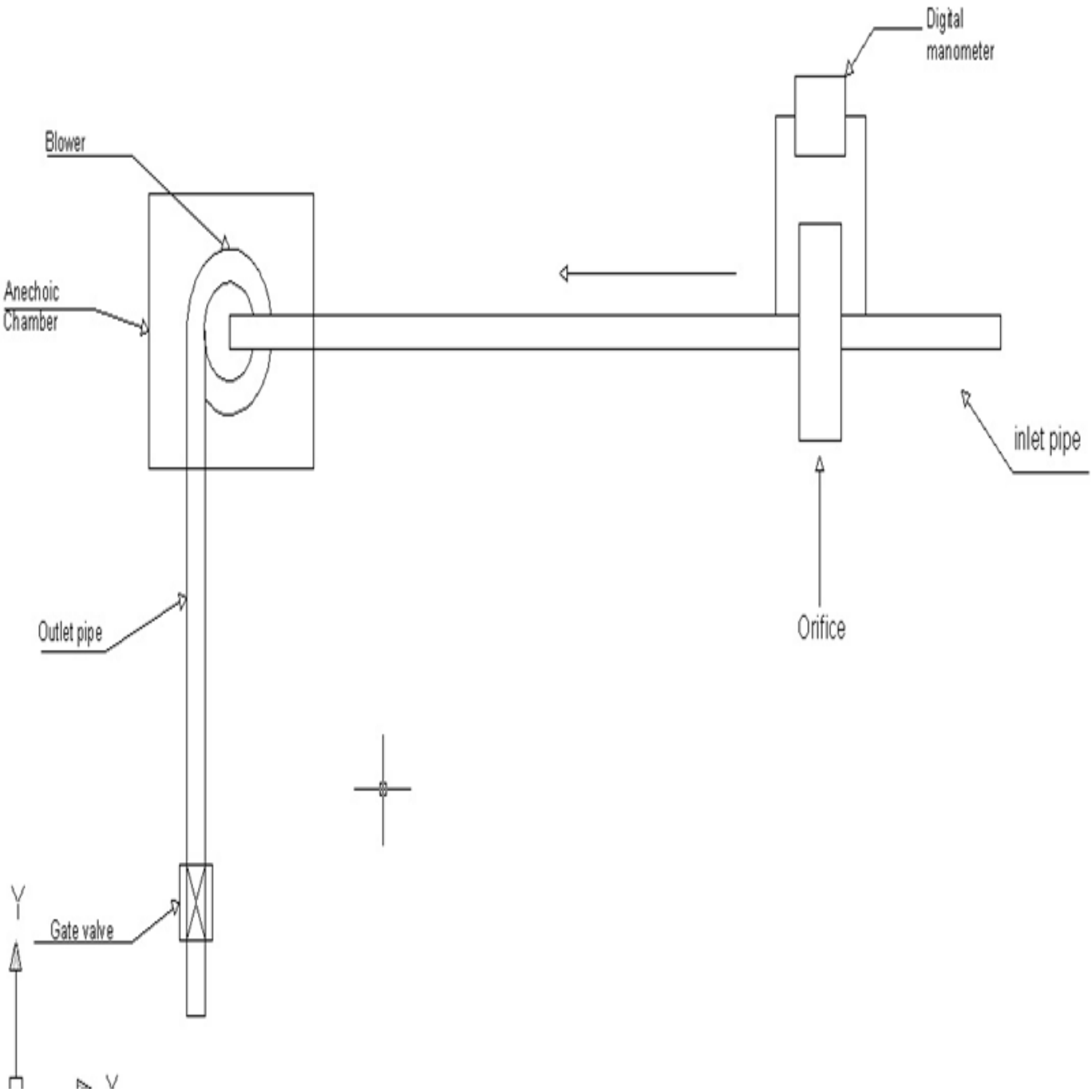

Figure 1. Schematic diagram of experimental apparatus.

Figure2. Outside of anechoic chamber.

Figure 3. Inside of anechoic chamber**.**

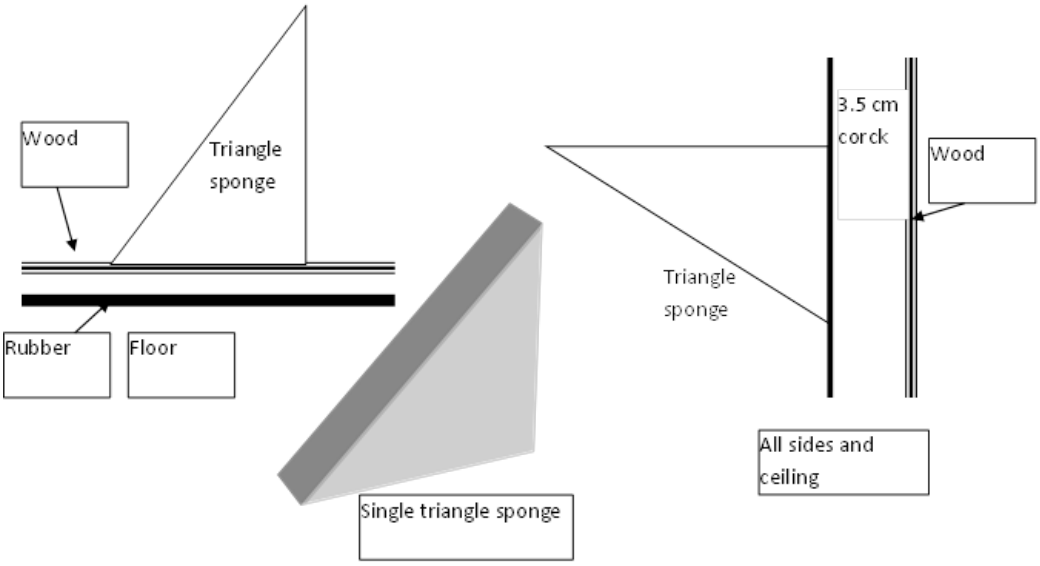

Figure4. Sponge distribution and dimensions.

Figure 5. Inlet pipes with orifice meter.

Figure 6. Outlet pipes with gate valve.

Figure7. Flexible pipes.

Figure 8. The centrifugal blower.

Fiure 9. Sound analyzer.

Figure10. Sound level meter.

Figure 11. Digital manometer.

Figure 12. Digital thermometer.

Figure 13. Digital tachometer.

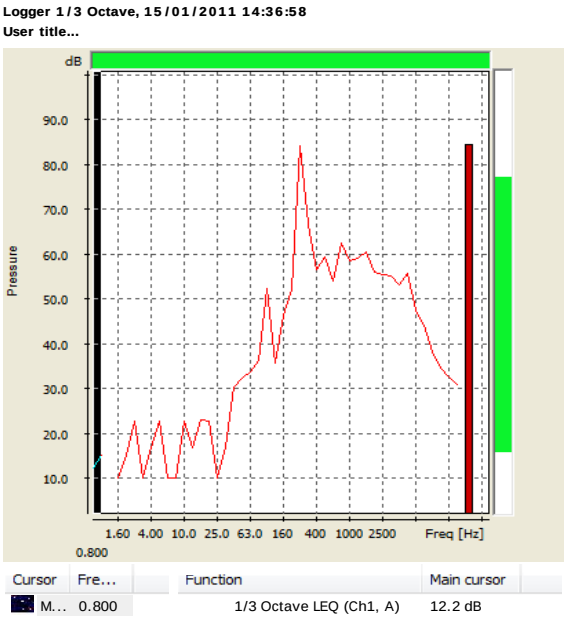

Position 2

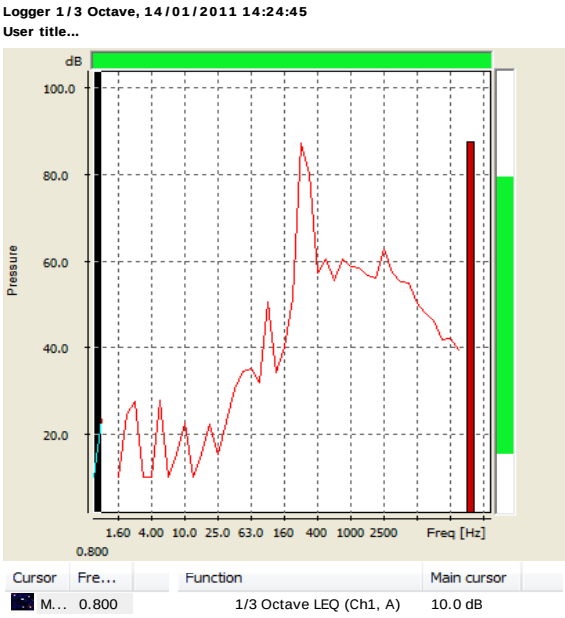

Position 1

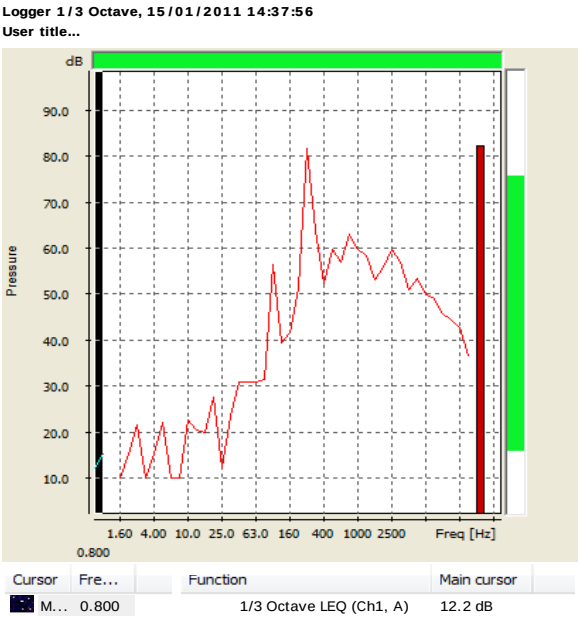

Position 4

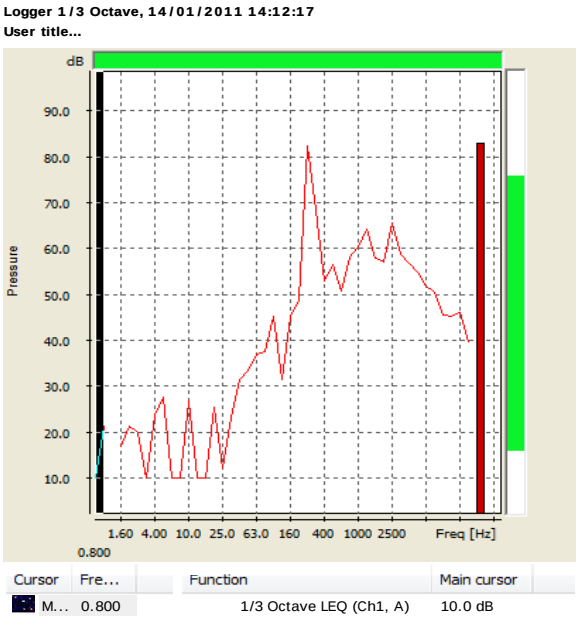

position 3

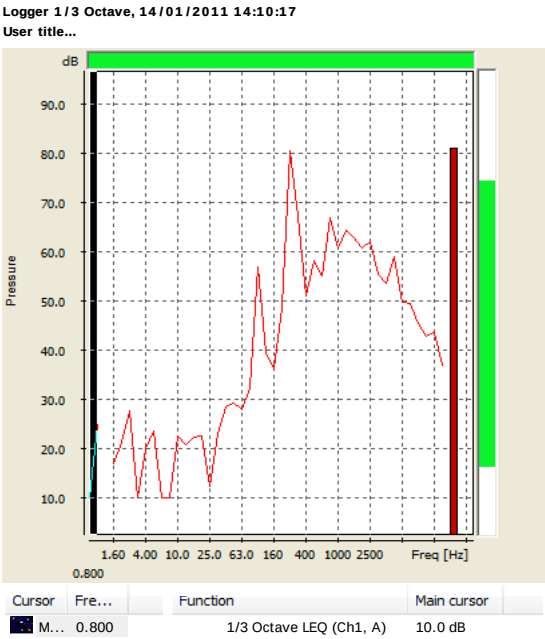

Position 6

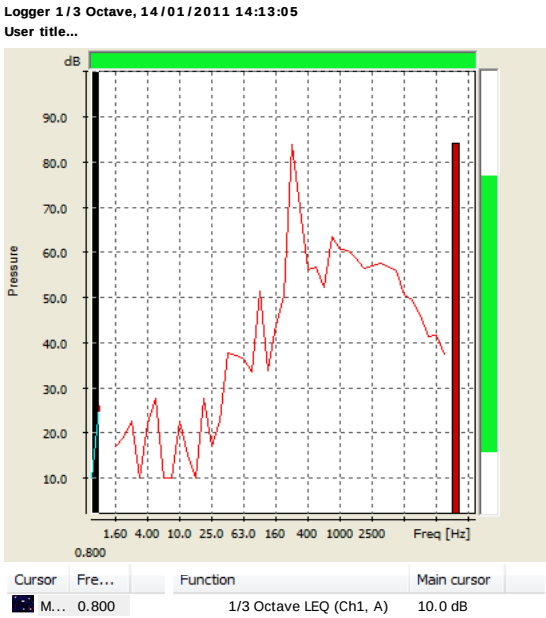

Position 5

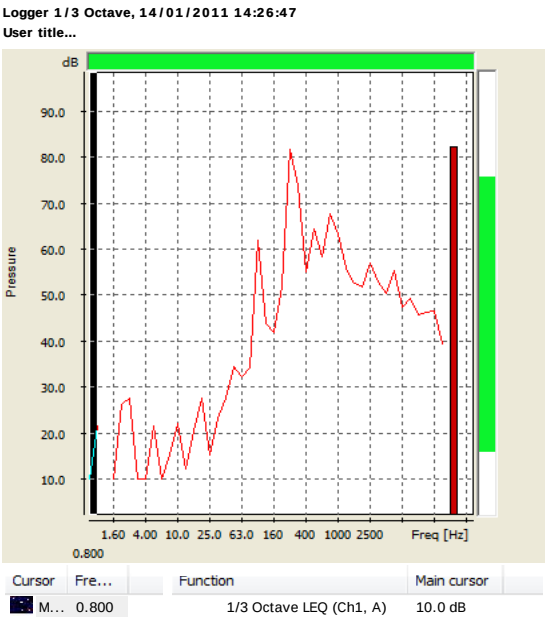

Position 8

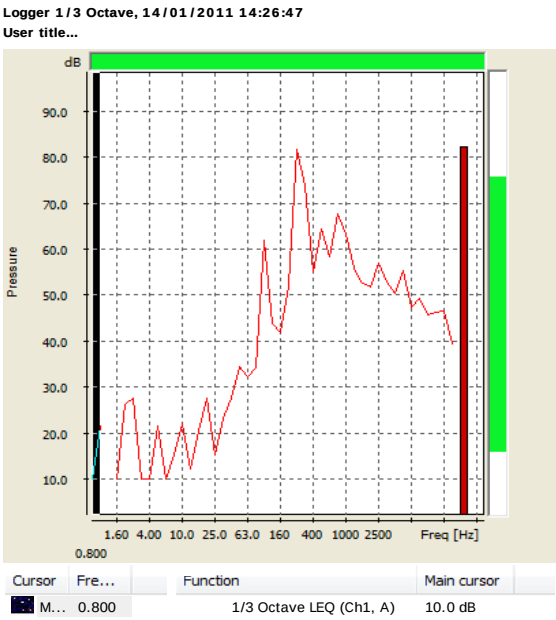

Position 7

Figure 14. Spectral analysis of noise at unshroud of 9 blades impeller at eight positions around the anechoic chamber, velocity=13000 r.p.m and pressure=32mbar.

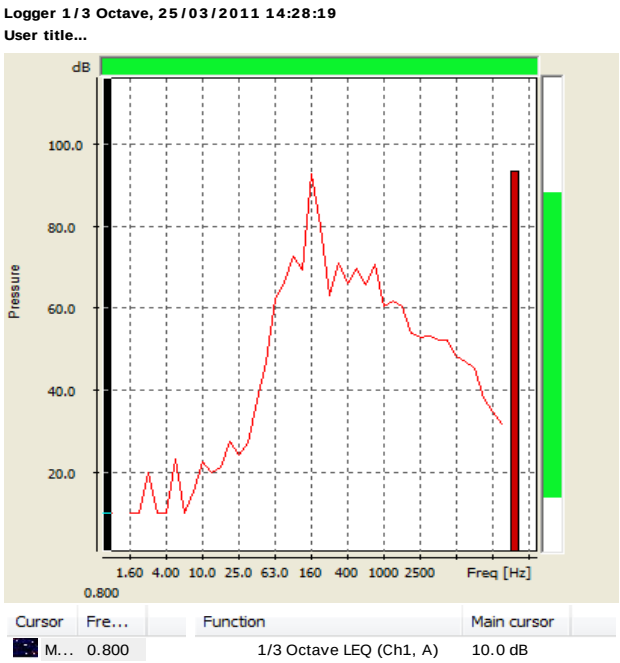

Velocity= 2600 r.p.m

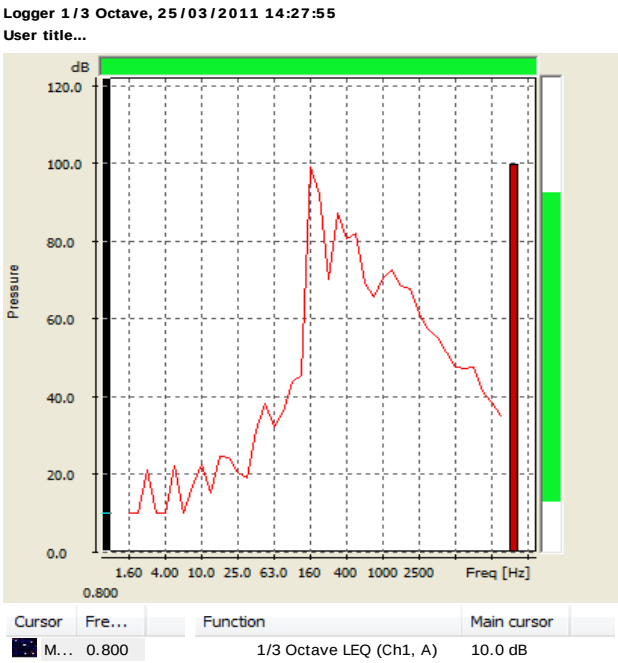

Velocity= 13000 r.p.m

Figure 15. Spectral analysis of noise in shroud of 9 blades impeller at different velocity.

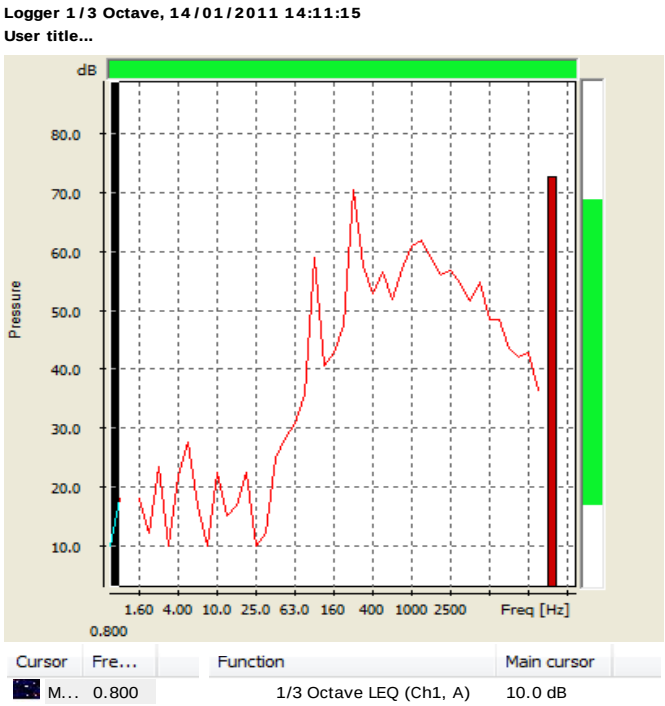

Velocity= 2600 r.p.m

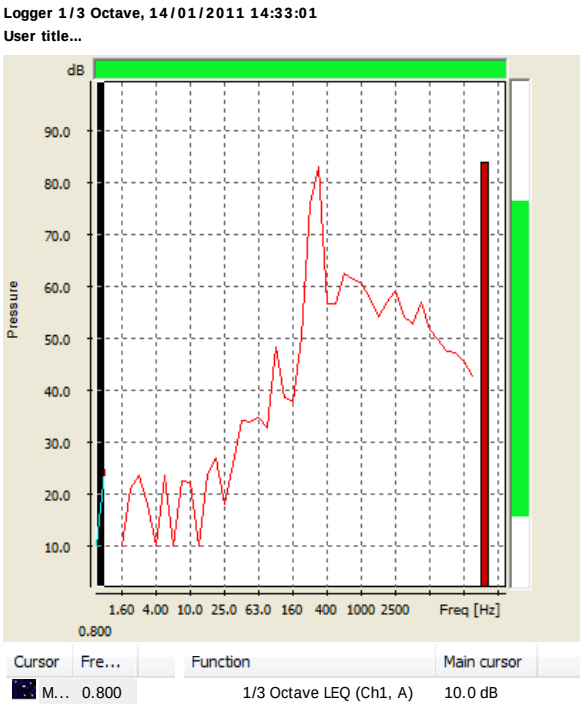

Velocity= 13000 r.p.m

Figure 16. Spectral analysis of noise at unshroud of 9 blades impeller at different velocities.

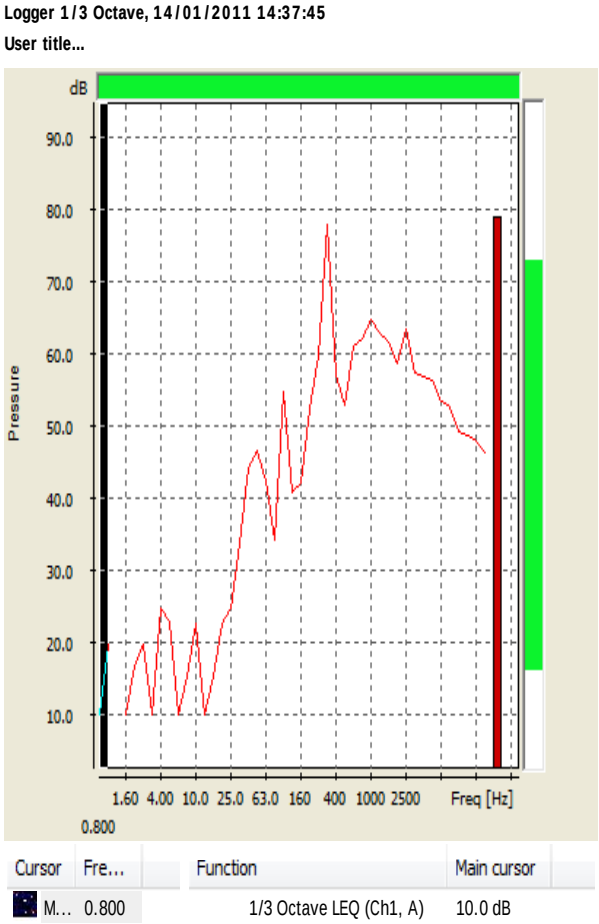

Shroud impeller
Velocity= 5200 r.p.m
Pressure= 24 mbar

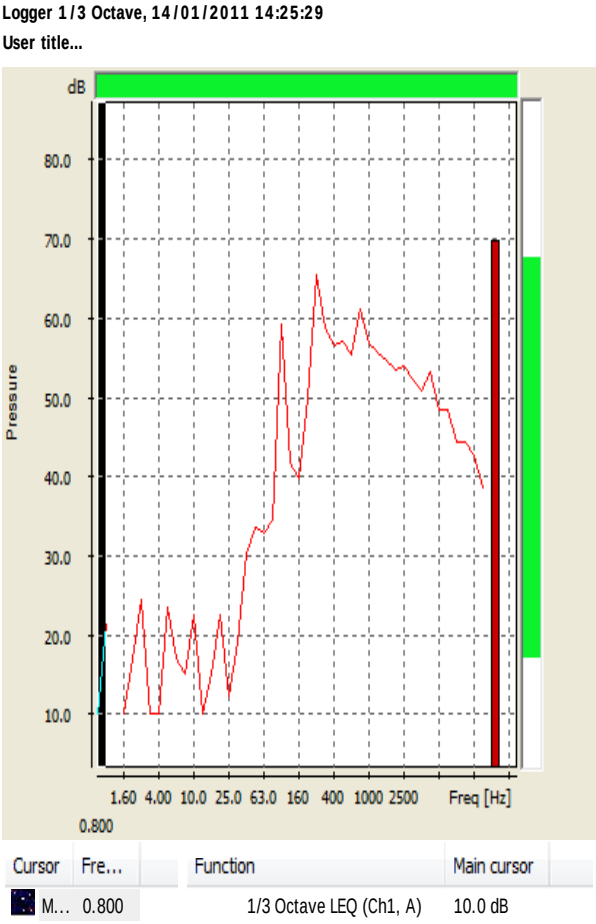

Unshroud impeller
Velocity= 5200 r.p.m
Pressure= 12 mbar

Figure 17. Spectral analysis of noise at different pressures

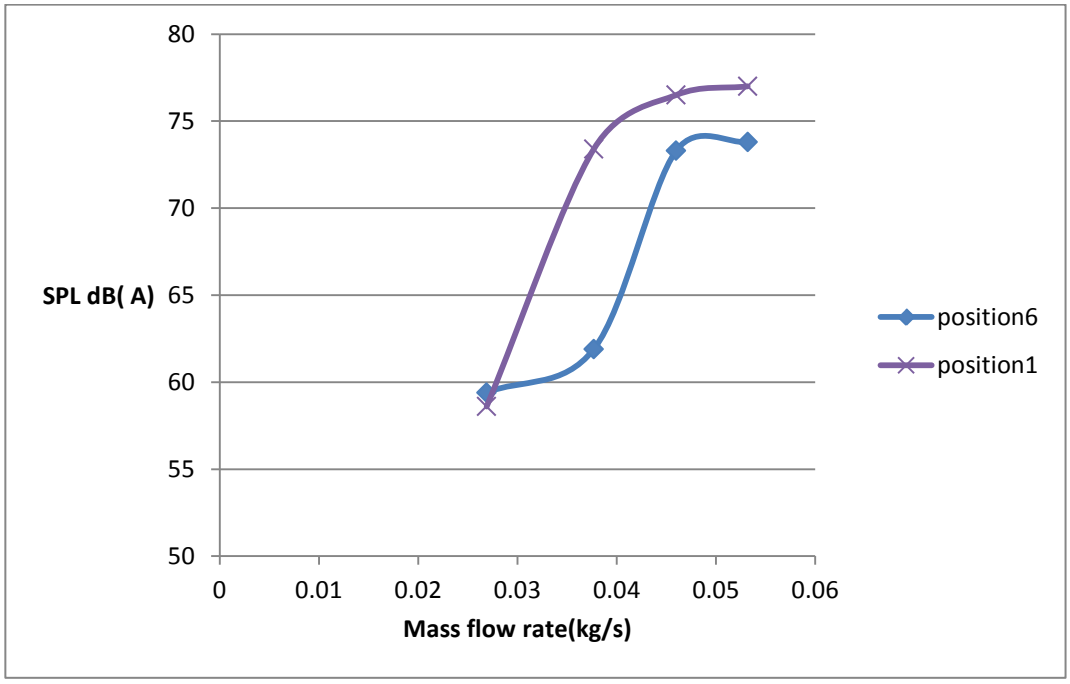

Figure 18. Variation of SPL with mass flow rate for unshroud impeller at velocity 5200 r.p.m.

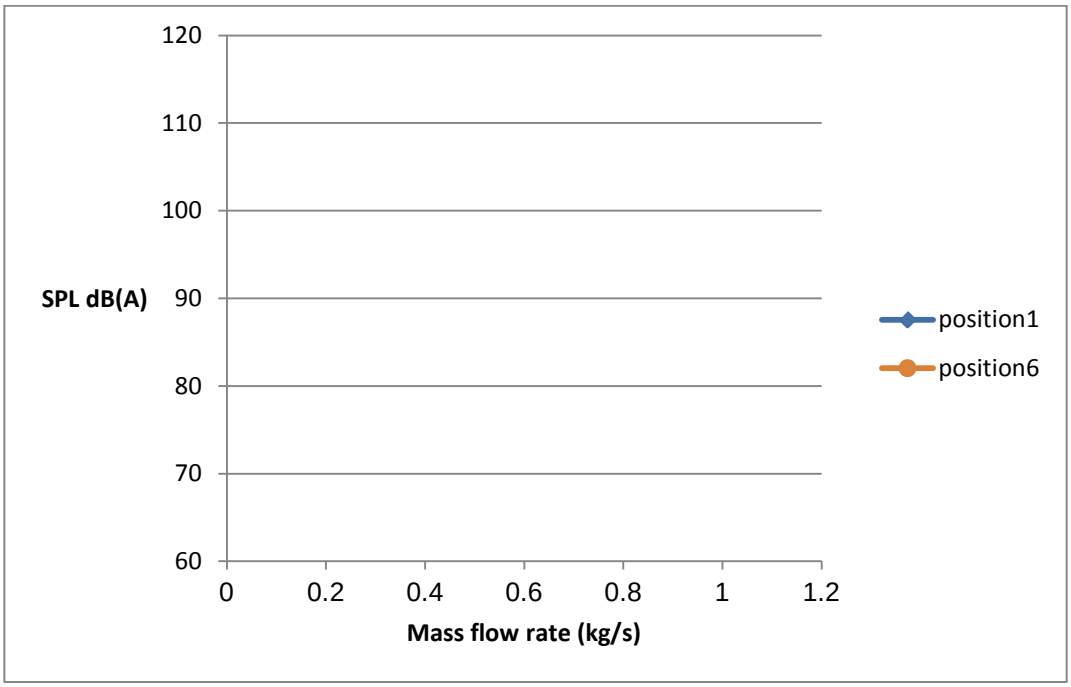

Figure 19. Variation of SPL with mass flow rate for shroud impeller at velocity 5200 r.p.m.

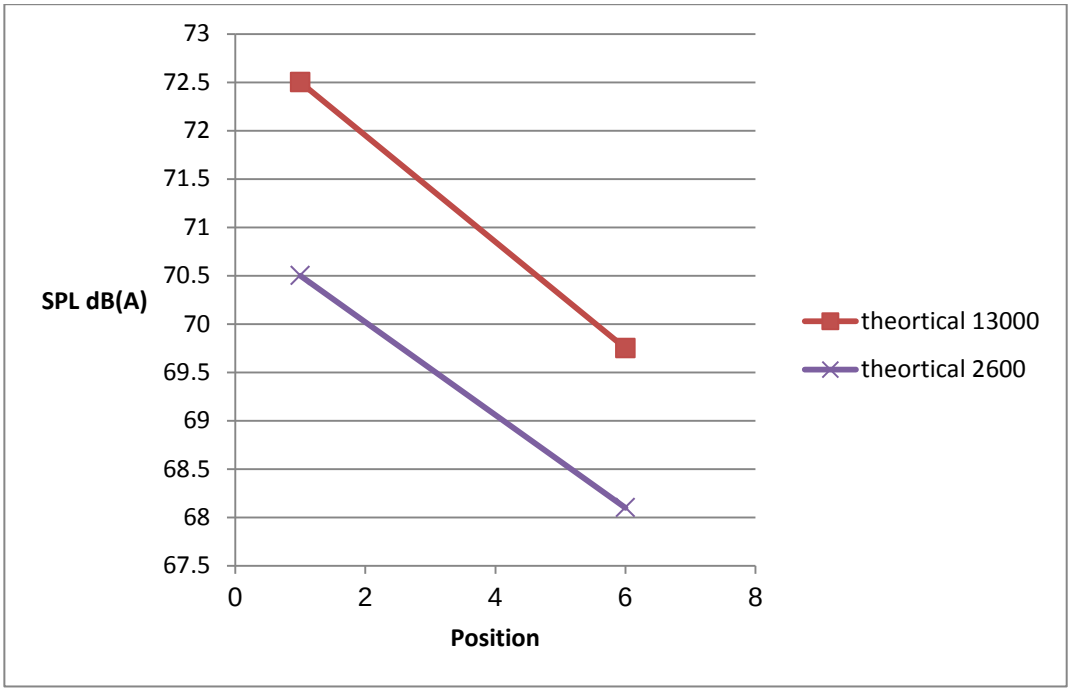

Figure 20. Variation of SPL with distance from the source in shroud impeller.

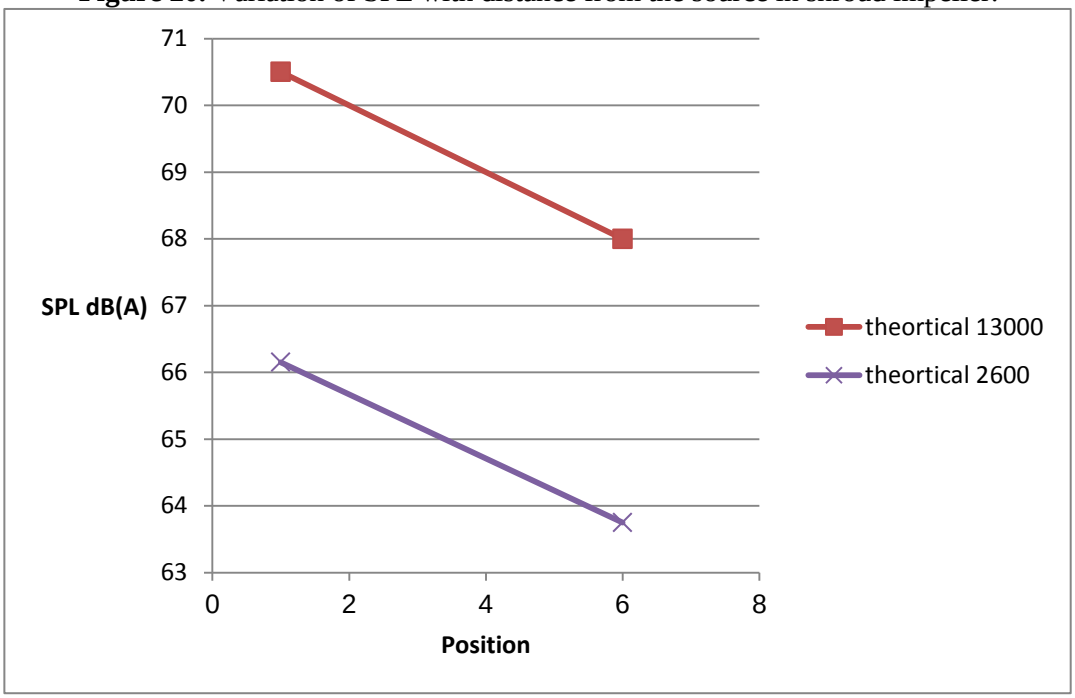

Figure 21. Variation of SPL with distance from the source in unshroud impeller.

Theoritical and Experimental Investigation of the Dynamical Behaviour of Complex Configuration Rotors

Prof. Mohsin Juber Jweeg
Dep. of Mechanical Eng.
College of Engineering
Alnhrain University

Lect.Mahmud Rasheed Ismail
Dep. of Mechanical Eng.
College of Engineering
Alnhrain University
Email: mahmech2001@yahoo.com

Zainab Mohammed Hwady
Dep. of Mechanical Eng.
College of Engineering
Alnhrain University

ABSTRACT:

The present work considers an alternative solution for a complex configuration of rotor discs by applying Galerkin Method. The theoretical model consists of elastic shaft carrying number of discs and supported on number of journal bearings. The equation of motion was discretized to finite degree of freedom in terms of the system generalized coordinates. The various effects of the dynamical forces and moments arising from the bearing, discs and shaft were included. Rayleigh beam model is used for analyzing the shaft while the discs are considered rigid . The validity and convergence of the present analysis was carefully checked by comparing with the Finite Element solution. An example of rotor consists of three different size discs and supported by two journal bearing was considered for the numerical solution .The results shows good agreements between the two methods ,where the maximum error not exceeds 5%. The convergence test showed that using few modes (not more than 6) are sufficient for the accurate analysis. The forward and backward whirl was investigated experimentally .The experimental results of a two discs rotor ,show a reasonable agreement where the maximum error not exceeds 11%. The unbalance response, Cambpell diagram, orbit response were plotted .The effects of geometry, disc sizes , location and arrangement on the unbalance response and natural frequencies of three discs rotor were further investigated .

Key words: Galerkin method, Cambpell diagram, whirl frequency, journal bearing , gyroscopic couple

مبحث نظري وتجريبي للتصرفات الديناميكية لدوارات معقدة الاشكال

أ.د. محسن جبر جويج
قسم الهندسة الميكانيكية
كلية الهندسة / جامعة النهرين

م.محمود رشيد اسماعيل
قسم الهندسة الميكانيكية
كلية الهندسة / جامعة النهرين

زينب محمد هويدي
قسم الهندسة الميكانيكية
كلية الهندسة / جامعة النهرين

الخلاصه:

تم في البحث الحالي اعتماد طريقه بديلة لتحليل الدوار المعقد ،وذلك باستخدام طريقة جالركين .يتألف النموذج النظري من عمود مرن يحمل عدد من الاقراص والمساند الزيتيه .تم نجزئة معادلة الحركه الى عدد محدد من درجات الحرية باستخدام الاحداثيات العامة .تم الاخذ بنظر الاعتبار التاثيرات الديناميكية للقوى والعزوم الناتجة من تأثيرات المساند الاقراص وعمود الدوران .تم اعتبار العمود كعمود رايلي اما الاقراص فاعتبرت كتل صلدة.اختبرت صحة وتقارب الحل بالمقارنة مع طريقة العناصر المحدده FEM.وكمثال عددي تم اختيار دوار مؤلف من عمود يحمل ثلاثة اقراص مختلفة الحجم ومسند على مسندين زيتين .بينت النتائج تطابق جيد بين الطريقتين حيث لم تتعدى نسبة الخطأ 5% بينما بينت تجربة اقتراب الحل بان استخدام عدد قليل من الاطوار (لايتعدى 6) يكفي للحصول على نتائج جيده .بعض الخصائص الديناميكيه مثل تردد التدويم الامامي والخلفي تم قياسها عمليا باستخدام نموذج لدوار مؤلف من قرصين ، فبينت النتائج تطابق مقبولا حيث لم تتعدى نسبة الخطأ 11%.تم رسم مخططات استجابة عدم الاتزان ومخطط كامبل وشكل المدارات لنماذج من الدوارات .بالاضافة الى ذلك، فقد تم دراسة تأثير حجم وترتيب وموقع الاقراص على الاستجابه والترددات الطبيعيه لدوار مؤلف من ثلاثة دسكات .

الكلمات الرئيسية : طريقة جالركين ،مخطط كامبل ،تردد التدويم ، مسند زيتي ،العزم الجايروسكوبي

1.INTRODUCTION

Rotors and rotary machines have a significant application in engineering and industries. Many catastrophic damages of machines are due to the undesired dynamical behavior of the rotors, such as; whirling and large deflection, resonance, imbalance shaking forces,…etc.

In 1869, the first attempt to formulate the dynamics of single disc rotor had been put forward by Rankin. However the first simplified acceptable model had been proposed by Jeffcott in 1919. From that time till now, enormous theoretical and experimental works had been achieved in this vast field, hence, rotor-dynamics bibliography is much extended. A comprehensive survey about this subject can be found in many references such as **Genta,2005**.

The main kinds of effects contribute the dynamical behavior of rotors; The elasticity ,inertia and gyroscopic effects of the shaft , the elasticity and damping of the oil film at bearings, and the gyroscopic ,inertial (lateral and rotational) and unbalance of the attached discs. Including all these effects, will complicate the analysis even for the simplest models و **Holmes,1978**. The dynamical analysis of multi disc and bearings rotors were normally achieved via numerical methods such as Finite Element, influence coefficients ,state space ,lumped analysis and transfer matrix method. For example, **Geradin,1984**, introduced a new Finite element model for evaluating the natural frequencies and dynamics response of multi disc rotos .**Rao ,1994**, used the Influence coefficient method to calculate the natural frequencies of multi disc rotor . **Das and Dutt,2012,** employed state space method to evaluate the vibration of multi disc rotors for controlling process .

The effect of the unbalancing of multi disc rotor on the dynamical behavior and stability was studied by **Ding ,1997 and Xie .et.al 2008** .They used the lumped mass method for the analysis. For all of the above mentioned methods ,the accurate analysis demand four degree of freedom for the individual station (two translations and two rotations).Hence large number of stations are needed for accurate numerical analysis. This lead to a huge global matrix for analyzing the Eigen value problem and frequency response. Analytical methods are seldom used except for simple or high approximated models, **Adams,2010**.Many experimental works was performed to justify the theoretical investigation of multi disc rotors .For example ,**Flack, et.al ,1981**, conducted experiment to investigate the effect of lubricant viscosity on the response of three mass rotor . **Ding, et al.,2005**, made experimental study to predict the nonlinear dynamic behaviors of a multi-bearing flexible rotor system.

In the present work, An alternative method for evaluating the dynamical behavior of multi discs and bearings rotor will be attempted . In this method , Galerkin procedure is employed, in which an appropriate shape functions are selected as basis functions for performing the analysis . Such functions take into account the elastic deformation of the shaft as well as the possibility of rigid body translation and rotation.

2.THEORY

For the multi discs and bearings model shown in **Fig.1**, the flexible shaft was considered to obey Rayleigh beam, and subjected to bending vibration at two orthogonal planes *x-z* and *x-y*. The various forces and moments due to the stiffness and damping of the bearing oil film, disc inertia, rotary inertia, gyroscopic and unbalancing for the rotor components, are shown in **Fig.2.**

The equations of motion of bending vibration can be written as, **Ding,2005**:

$$EI\frac{\partial^4 w}{\partial x^4}+\rho A\frac{\partial^2 w}{\partial^2 t}+C\frac{\partial w}{\partial t}-\rho I\frac{\partial^2}{\partial x^2}(\frac{\partial^2 w}{\partial t^2})-2\rho I\omega_{SP}\frac{\partial^2}{\partial x^2}(\frac{\partial v}{\partial t})=f_z(x,t) \quad (1)$$

$$EI\frac{\partial^4 v}{\partial x^4}+\rho A\frac{\partial^2 v}{\partial^2 t}+C\frac{\partial v}{\partial t}-\rho I\frac{\partial^2}{\partial x^2}(\frac{\partial^2 v}{\partial t^2})+2\rho I\omega_{SP}\frac{\partial^2}{\partial x^2}(\frac{\partial w}{\partial t})=f_y(x,t) \quad (2)$$

Dividing Eq. (1) and Eq. (2) by *EI* and arranging, giving:

$$\eta^{IV}+\ddot{\eta}+C^*\dot{\eta}-\beta\ddot{\eta}''-2\beta\Omega\dot{\mu}''=\alpha.f_z(\zeta,\tau)=Q_Z(\zeta,\tau)$$

$$\mu^{IV}+\ddot{\mu}+C^*\dot{\mu}-\beta\ddot{\mu}''+2\beta\Omega\dot{\eta}''=\alpha.f_y(\zeta,\tau)=Q_y(\zeta,\tau) \quad (3)$$

Where;

$$\eta=w/L\ ,\quad \mu=v/L\ ,\quad \zeta=x/L\ ,$$

$$\tau=(t/L^2)\sqrt{EI/\rho A}\ ,\ \Omega=\omega_{sp}L^2\sqrt{\rho A/EI}$$

$$\beta=I/L^2A\ ,\quad C^*=\frac{CL}{\sqrt{EI\rho A}}\ ,\alpha=L^3/EI \quad (4)$$

For simplicity the following notations were used;

$$\frac{\partial}{\partial \tau}(\ ) = (\ )^{\bullet} \quad \text{And} \quad \frac{\partial}{\partial \zeta}(\ ) = (\ )'$$

The R.H.S terms of Eq.(3) represents the dimensionless dynamical forces due to the bearing and discs at x-z and x-y planes. In case of, Q_z they are as follows;

1-bearing spring forces;

$$F_{SZ} = \frac{-\alpha}{L}\sum_{i=1}^{Nb} K_{iz} w(x,t) = -\sum_{i=1}^{Nb} K_{iz}^{*}\eta \tag{5}$$

2- bearing damping forces;

$$F_{DZ} = \frac{-\alpha}{L}\sum_{i=1}^{Nb} C_{iz}\frac{\partial w}{\partial t} = -\sum_{i=1}^{Nb} C_{iz}^{*}\dot{\eta} \tag{6}$$

2- Disc translation inertial forces:

$$F_{TZ} = \frac{-\alpha}{L}\sum_{j=1}^{Nd} m_j \frac{\partial^2 w}{\partial t^2} = -\sum_{j=1}^{Nd} m_j^{*}\ddot{\eta} \tag{7}$$

3- Disc imbalances forces;

$$F_{bz} = \frac{\alpha}{L}\sum_{j=1}^{Nd} mb_j e\omega_{sp}^2 \sin\omega_{sp} t = \sum_{j=1}^{Nd} mb_j^{*} e^{*}\Omega^2 \sin\Omega\tau \tag{8}$$

4-Disk gyroscopic moments;

$$M_{GZ} = -\frac{\alpha}{L}\sum_{j=1}^{Nd} J_j \omega_{sp}\frac{\partial}{\partial t}\left(\frac{\partial v}{\partial x}\right) = \sum_{j=1}^{Nd} J_j^{*}\Omega\dot{\mu}' \tag{9}$$

5-Disc rotational inertia moments;

$$M_{RZ} = \frac{-\alpha}{L}\sum_{j=1}^{Nd} J_j \frac{\partial^2}{\partial t^2}\left(\frac{\partial w}{\partial x}\right) = -\sum_{j=1}^{Nd} J_j^{*}\ddot{\eta}' \tag{10}$$

Where N_b and N_d are the number of bearings and discs, respectively .

For the plan x-y the same procedures can be used to obtain the components of the force Q_y as the follows:

$$F_{SY} = -\sum_{i=1}^{Nb} K_{iy}^{*}\mu \tag{11}$$

$$F_{DY} = -\sum_{i=1}^{Nb} C_{iy}^{*}\dot{\mu} \tag{12}$$

$$F_{TY} = -\sum_{j=1}^{Nd} m_j^{*}\ddot{\mu} \tag{13}$$

$$F_{bY} = \sum_{j=1}^{Nd} \overset{*}{mb}_j e^{*}\Omega^2 \sin\Omega\tau \tag{14}$$

$$M_{GY} = \sum_{j=1}^{Nd} J_j^{*}\Omega\dot{\eta}' \tag{15}$$

$$M_{RY} = -\sum_{j=1}^{Nd} J_j^{*}\ddot{\eta}' \tag{16}$$

In the above equations, the following dimensionless terms are considered;

$$K_{iz}^{*} = \frac{K_{iz}L^3}{EI}, \quad \overset{*}{K}_{iY} = \frac{K_{iY}L^3}{EI}, \quad C_{iY}^{*} = \frac{C_{iY}}{\sqrt{\rho AEI}}, \quad C_{iz}^{*} = \frac{C_{iz}}{\sqrt{\rho AEI}}, \quad J_j^{*} = \frac{J_j}{\rho AL^3}, \quad \overset{*}{mb}_j = \frac{mb_j}{\rho AL}, \quad m_j^{*} = \frac{m_j}{\rho AL}, \quad e^{*} = \frac{e}{L} \tag{17}$$

Substituting **Eqs.(5 to 10)** into the first of **Eq.(3)** giving the following equation of motion at (x-y) plane;

$$\eta^{IV} + \ddot{\eta} + \overset{*}{C}\dot{\eta} - \beta\ddot{\eta}'' - 2\beta\Omega\mu'' + \sum_{i=1}^{Nb}\overset{*}{K}_{iz}\eta + \sum_{i=1}^{Nb} C_{iz}^{*}\dot{\eta} + \sum_{j=1}^{Nd}\overset{*}{m}_j\ddot{\eta} - \sum \overset{*}{J}_J\Omega\dot{\mu}' + \sum_{j=1}^{Nd}\overset{*}{J}_j\ddot{\mu}'' = \sum_{j=1}^{Nd}\overset{*}{mb}_j e^{*}\Omega^2\sin\Omega\tau \tag{18}$$

Smilarly ,substituting Eqs.(11-16),into the second of Eqs.(3) giving the equation of motion at (x-z) plane;

$$\mu^{IV} + \ddot{\mu} + \overset{*}{C}\dot{\mu} - \beta\ddot{\mu}'' + 2\beta\Omega\dot{\eta}'' + \sum_{i=1}^{Nb}\overset{*}{K}_{iy}\mu + \sum_{i=1}^{Nb} C_{iY}^{*}\dot{\mu} + \sum_{j=1}^{Nd}\overset{*}{m}_j\ddot{\mu} - \sum_{j=1}^{Nd}\overset{*}{J}_j\Omega\dot{\eta}' + \sum_{j=1}^{Nd}\overset{*}{J}_j\ddot{\mu}'' = \sum_{j=1}^{Nd}\overset{*}{mb}_j e^{*}\Omega^2\sin\Omega\tau \tag{19}$$

To introduce Galerkin scheme ,a solution in term of the beam normal modes may be taken . Let such solutions of eqs(18) and (19) be;

$$\eta(\zeta,\tau)=\sum_{s=1}^{N}\phi_s(\zeta)q_s(\tau)+\phi_T(\zeta)q_T(\tau)+\phi_R(\zeta)q_R(\tau)$$

$$\mu(\zeta,\tau)=\sum_{s=1}^{N}\psi_s(\zeta)p_s(\tau)+\psi_T(\zeta)p_T(\tau)+\psi_R(\zeta)p_R(\tau) \tag{20}$$

In eqs.(20); $\phi_s(\zeta)$ and $\varphi_s(\zeta)$ stand for the normal modes of beam free vibration, ϕ_T and φ_T for translational modes and ϕ_R, φ_R for rotational modes in *z* and *y* directions, respectively.
In the absence of all the forces and moments the normalized mode shapes $\phi_s(\zeta)$ and $\varphi_s(\zeta)$ are those of free-free beam which take the following form, **Lund et al.,1978**:

$$\phi_s(\zeta)=\varphi_s(\zeta)=\sin\lambda_s\zeta+\sinh\lambda_s\zeta-\sigma_s(\cos\lambda_s\zeta+\cosh\lambda_s\zeta) \tag{21}$$

Where;

$$\sigma_s=\frac{\sinh\lambda_s-\sin\lambda_s}{\cosh\lambda_s-\cos\lambda_s}$$,and

λ_s are the Eigen values of the free-free beam.
The normalized modes of translational and rotational modes may be taken as;

$$\phi_T(\zeta)=\psi_T(\zeta)=1$$
$$\phi_R(\zeta)=\psi_R(\zeta)=\zeta$$

So that **Eq (20)** become;

$$\eta(\zeta,\tau)=\sum_{s=1}^{N}\phi_s(\zeta)q_s(\tau)+q_T(\tau)+\zeta q_R(\tau) \tag{22}$$

$$\mu(\zeta,\tau)=\sum_{s=1}^{N}\psi_s(\zeta)p_s(\tau)+p_T(\tau)+\zeta p_R(\tau) \tag{23}$$

Substitute **Eq. (22) into Eq. (18),** and following Galrkin procedure in which another series for the r modes is chosen as :

$$\phi_r(\zeta)=\sum_{r=1}^{N}\phi_r(\zeta)+1+\zeta$$

Now , multiply , integrate from 0 to 1 and make use of the orthogonally of the normal modes, the following matrix equation can be obtained as;

$$[A]\{q\}+[B]\{\ddot{q}\}+C^*[B]\{\dot{q}\}-\beta[S]\{\ddot{q}\}$$
$$-2\beta\Omega[s]\{\dot{p}\}+\sum_{i=1}^{Nb}\left(K_{iz}^*[H_i]\{q\}+C_{iz}^*[H_i]\{\dot{q}\}\right)$$
$$+\sum_{j=1}^{Nd}\left(m_j^*[T_j]\{\ddot{q}\}+J_j^*[V_j]\{\ddot{q}\}-J_j^*\Omega[V_j]\{\dot{p}\}\right)=\sum_{j=1}^{Nd}mb_j^*e^*\Omega^2\cos\Omega\tau[W_j] \tag{24}$$

By the similar procedures one can obtain from eq.(23) and (19) the following matrix equation;

$$[A]\{p\}+[B]\{\ddot{p}\}+C^*[B]\{\dot{p}\}-\beta[S]\{\ddot{p}\}$$
$$+2\beta\Omega[s]\{\dot{q}\}+\sum_{i=1}^{Nb}\left(K_{iy}^*[H_i]\{p\}+C_{iy}^*[H_i]\{\dot{p}\}\right)$$
$$+\sum_{j=1}^{Nd}\left(m_j^*[T_j]\{\ddot{p}\}+J_j^*[V_j]\{\ddot{p}\}+J_j^*\Omega[V_j]\{\dot{q}\}\right)=\sum_{j=1}^{Nd}mb_j^*e^*\Omega^2\sin\Omega\tau[W_j] \tag{25}$$

The elements of the matrices [*A*] ,[*B*] ,[*S*] ,[*H*i] ,[*T*j] ,[*Vj*] ,[*Wj*] are given in the appendix.

Finally, **Eqs. (24) and (25)** can be arranged in the following standard form;

$$[K_z]\{q\}+[C_z]\{\dot{q}\}-\Omega[G]\{\dot{p}\}+[M]\{\ddot{q}\}=\{W\}\cos\Omega\tau \tag{26}$$

$$[K_y]\{p\}+[C_y]\{\dot{p}\}+\Omega[G]\{\dot{q}\}+[M]\{\ddot{p}\}=\{W\}\sin\Omega\tau \tag{27}$$

Where;

$$[K_z]=[A]+\sum_{i=1}^{Nb}(K_{iz}^*[H_i],$$
$$[K_y]=[A]+\sum_{i=1}^{Nb}(K_{iy}^*[H_i],$$
$$[C_z]=C^*[B]+\sum_{i=1}^{Nb}(C_{iz}^*[H_i],$$
$$[C_Y]=C^*[B]+\sum_{i=1}^{Nb}(C_{iy}^*[H_i],$$
$$[G]=2\beta[S]+\sum_{j=1}^{Nd}J_j^*[V_j]$$,and
$$[M]=[B]-\beta[S]+\sum_{j=1}^{Nd}+m_j^*[T_i]+J_j^*[V_j]$$

$$\{W\} = \sum_{j=1}^{Nd} m b_j^* e^* \Omega^2 \left[W_j\right] \quad (28)$$

2.1 Unbalance response and critical speeds

Eqs.(26) and (27) can be arranged in a single equation by using the following complex vector;

$$\{u\}=\{q\}+i\{p\} \quad (29)$$

Now ,multiplying **Eq.(26)** by i ($i=\sqrt{-1}$), adding to **Eq.(25**) and applying **Eq.(29)** will give;

$$[K]\{u\}+[C]\{\dot{u}\}+i\Omega[G][I]\{\dot{u}\}+[M][I]\{\ddot{u}\}=\{W\}e^{i\Omega\tau} \quad (30)$$

Where;

$$[K]=\begin{bmatrix} K_z & 0 \\ 0 & K_y \end{bmatrix}, \quad [C]=\begin{bmatrix} C_z & 0 \\ 0 & C_y \end{bmatrix},$$

$$[I]=\begin{bmatrix} 1 & 0 \\ 0 & 1 \end{bmatrix} \quad (31)$$

Since the imbalanced force is harmonic, the steady state response of Eq.(30) can be written as;

$$\{u\}=\left[[K]+i\Omega[C]+i\Omega[G][I]-\Omega^2[M][I]\right]^{-1}\{W\}e^{i\Omega\tau} \quad (32)$$

Eq.(32) as well as **Eqs.(22) and (23)** can be used for calculating and plotting the response due to unbalancing at a given range of spin speeds .The speeds which give the maximum amplitude are the critical speeds. The effect of any parameter related to the rotor configuration can be studied by using this equation.

It is important to note that; the present analysis assumes the unbalance vectors lie in the same planes for all discs .However for the case when there is different unbalance planes of discs ,a spatial consideration for solving **Eq.(32)** must be made .This case is not dealt in the present analysis

2.1 Cambpell Diagram

The forward and backward whirling frequencies at a given spin speed can be calculated by using the homogenous parts of **Eqs. (26) and (27)** which are;

$$[K_z]\{q\}+[C_z]\{\dot{q}\}-\Omega[G]\{\dot{p}\}+[M]\{\ddot{q}\}=0 \quad (33)$$

$$[K_y]\{p\}+[C_y]\{\dot{p}\}+\Omega[G]\{\dot{q}\}+[M]\{\ddot{p}\}=0 \quad (34)$$

Since vibration is harmonic motion, one can assume the following solutions for *q* and *p*;

$$\{q\}=\{\hat{q}\}e^{i\omega\tau}, \{p\}=\{\hat{p}\}e^{i\omega\tau} \quad (35)$$

Where $\{\hat{q}\},\{\hat{p}\}$ are arbitrary constants .

Substituting **Eq. (35)** into **Eqs. (33) and (34**) and eliminating the arbitrary constants yield to the following characteristics determinant;

$$\begin{vmatrix} [K_z]+i\omega[C_z]-\omega^2[M] & -i\omega\Omega[G] \\ i\omega\Omega[G] & [K_y]+i\omega[C_y]-\omega^2[M] \end{vmatrix} = 0 \quad (36)$$

At a given rotor parameters **Eq.(36)** can be used to construct cambpell diagram .by plotting the backward and forward frequencies for selected modes against the spin speeds .

2.3 Finite element solution

For Finite element analysis ,ANSYS 14 software was employed . Three element types are selected to define the various rotor components which are;MASS21 element for discs, BEAM 188 element for shaft and COMBI214 element for Bearings.

The shaft is divided to 32 elements .The gyroscopic effect was considered by employing the rotating axis via the CORIOLIS and OMEGA commands .The HARMONIC ANALYSIS is used for evaluating the solution and plotting the results.

3-EXPERIMENTAL INVESTIGATION

The aim of the experimental work is carried to verify the present theoretical analysis. For this purpose, a model of rotor consisted of a two different size brass discs fitted on elastic steel shaft and sited on two identical journal bearings as shown in **Fig.3-a** was used. The specifications of the model are given in table(1) except that disc(1) was excluded .Disc(2) and (3) were located at 0.35 and 0.25m from the shaft right side end .The rotor is driven by an electrical motor with variable speed of (0-3000) RPM .In order to investigate the forward and backward whirl frequencies ,the motor has a facility of changing its speed directions .To reduce the undesired effect of the motor vibration which may interfere with the rotor response, a PVC coupling was used. A special attention was made for aligning the shaft with the

motor shaft and the bearings to insure center to center alignment which is necessary for reducing the misalignment effect on the response. A special mechanism was introduced to measure the response of the rotating shaft, since it is impossible to fit a pick up device directly on the rotating shaft .This mechanism consists of a small light rod slides vertically through a slot in the supported frame. A soft spring is used to insure continuous contact between the shaft and the slider rod. Finally the accelerometer pick up was mounted on the top of rod. The accelerometer was connected to the oscilloscope through a charger amplifier as shown in **Fig.3-c.**

The main task of the experimental work is to measure the forwarded and backward whirl frequencies. For this purpose, impact hummer test was used .In this test the rotor speed was assigned 0,200,400,600,800,1000 and 1200 RPM at clockwise and counterclockwise directions .For each speed an impact test was carried out .The time histories of the excited force and the response were recorded and analyzed by using SigView software package .The Fast Fourier Transformation (FFT) was performed from which the whirl frequencies were calculated .

4. RESULTS AND DISCUSSIONS

Although the present analysis is hold for any number of discs and bearings, However, an example of a rotor consists of elastic shaft carrying three different size discs and supported by two identical bearings was considered for the numerical analysis. The journal bearings has the following specifications; D=0.019170 m, L/d=1,c=0.1454mm.The oil lubricant is SAE 20 with μ =0.0562 N.s/m². For evaluating the bearing stiffness and damping, the value of Summerfield number was calculated from the above data and the graphs given by ,Lund, are employed. The numerical data of the model are listed in table .1

The validity and convergence of the present solution were checked by comparing with the ANSYS solution. MATLAB R2009 software was employed to solve Eq.(32) to evaluate the unbalance response. The number of modes of the present solution are varied from N=3 to 6. For the two methods the discs are located at ζ= 0.25, 0.5 and 0.75. The results of the two methods ,as well as, the percentage errors are presented in **Table 2.Table 2** shows that, the present solution has better convergence at N=5 where the percentage error is not exceeded (5 %) .Hence using five modes is quite sufficient for the accurate analysis.

Fig.4 shows the ANSYS simulation of the model. The unbalance response is displayed in figure. For the comparison purpose, the responses of the same model is plotted by using the present solution for N=3,4 and 5 and shown in **Fig.4**. As it is clear from these figures, the results of the two methods are in a good agreement especially when N approaches 5.

To investigate the effect of spin speed on the forward and backward frequencies for the lowest three modes, Campbell diagram is plotted in **Fig.5** .This diagram is plotted by using the two methods, again. As it is clear from these figures, that ,the agreements between the two solutions is good .

The main advantage of Cambpell diagram is to test the stability and evaluate critical speeds of the rotor .In order to inspect stability; the values of the natural frequencies are checked at the selected range of spin speeds. When their values changed from real to complex the rotor is regarded unstable. The speeds causing such a change are referred as Threshold speeds .It is found that the present rotor model is always stable at the selected speed range.

The critical speeds can be evaluated from cambpell diagram by plotting a straight line with slope=1(the solid line in **Fig.5** .The points of intersections between this line and the frequencies curves give the critical speeds .Referring to Fig.5 the critical speeds have the following values ; 630,660,780 and 1650 RPM .It is to be noted that, some of critical speeds cannot be detected from plotting the unbalance response curve since it consider the unbalance response for forward whirl speeds, only. Hence Cambpell diagram is more effective tool in designing rotors since it is able to detect wide range of critical speeds.

The orbit plot response of the model as it spin at 960 RPM is shown in **Fig.6.** As one can see from the plot that, the larger orbit path is found under the location of heaviest disc.

For further investigation , the effect of disc locating and arranging ,**Figs. 7,8 and 9** are created .In **Fig .7** the discs are allow to locate close together by assigning ζ=0.4,0.5 and 0.6.The unbalance response of this case is plotted. **Fig.7** indicates two information; firstly, the critical speeds decrease, secondly, one of critical speeds becomes insignificant (very small peak response) .This means that as the discs spacing decreased

the multi rotor behavior approach that of the single rotor behavior.

The effect of discs arrangements are investigated in **Figs.8 and 9** .In **Fig.8** the discs are arranged in increasing size order, whilst ,in **Fig.9** in decreasing order . Comparing the response of the two cases indicates that; reverting the order of discs sizes gives a slight change in the critical speeds which may be ignored .This may be reasoned due to the dynamical symmetry of the supporting bearings which give nearly identical elastic curve.

The theoretical and experimental results of the two discs model is shown in **Fig.10**.In this figure the forward and backward whirl frequencies are shown .As it is clear that the results are in a good agreements where the maximum error is not exceeding 11%.The deviation between the two results may be attributed to the measuring error ,effect of internal damping and bearings in isotropic .

4.CONCLUSIONS

In the present analysis, Galerkin method was used to evaluate the dynamical behavior of multi discs and bearing rotors. The present analysis can be used for any number of discs and bearings. All the rotor dynamic aspects; such as forward and backward whirl frequencies ,Cambpell diagram ,stability, critical speed and unbalance response can be evaluated by using the present method .

The validity and convergence of the present analysis was performed by comparing with the Finite element solution and experimental results . The numerical results of a sample of three disc rotor showed that; the solution has better convergence when only five modes are employed, and the maximum error is not exceeded 5% .Hence the computation time and labor can be saved. The experimental results showed good agreements in measuring the forward and backward whirl frequencies with maximum error is not exceeding 11%. The effects of disc locations and arrangements are investigated .It is found that closing the space between the discs tends to decrease the critical speeds values and diminish some of them .So that the multi discs rotor behaves as a single rotor However reverting the location of the discs has insignificant effect on the critical speeds since it cause a slight change.

5-REFERENCES

A. G. Holmes, C. M. Ettles and I. W. Mayes, 1978, *“The Dynamics of Multi-Rotor Systems Supported on Oil Film Bearings”*, J. Mech. Des., 100, 156 - 164.

A.S. Das, J.K.Dutt, 2012,“*A Reduced Rotor Model Using Modified SEREP Approach for Vibration Control of Rotors, Mechanical Systems and Signal Processing*” 26,167–180.

G. Genta, 2005,“*Dynamics Of Rotating Systems”*, springer.

J. Ding, 1997,“*Computation Of Multi-Plane Imbalance for a Multi-Bearing Rotor System”*, Journal of Sound and Vibration 205 (3), 364–371.

J. S. RAO ,1994,”*The Calculation of the Natural Frequencies of Multi-Disk-Rotor Systems Using the Influence Coefficient Method Including The Gyroscopic Effects”*, Mech. Mach. 7"heory (29). pp. 739-748.

J. W. Lund and K. K. Thomsen, 1978, *“A Calculation Method and Data for the Dynamic Coefficients of Oil-Lubricated”* Journal Bearings, Topics ‘In Fluid Film Bearing And Rotor Bearing System Design And Optimization, ASME Design Engineering ,New York.

L. Meirovitch, 1975, "*Elements Of Vibration Analysis"* Mcgraw-Hill, Inc.

M. Geradin, N. Kill, 1984, *“A New Approach to Finite Element Modeling Of Flexible Rotors*,” Engineering Computations, 52–64.

M. L. Adams &JR, 2010,“*Rotating Machinery Vibration, from Analysis to Troubleshooting”*, CRC press, Taylor & Francis group, second edition.

Q. Ding, A.Y.T. Leung, 2005 ,“*Experimental Study on Nonlinear Dynamic Behaviours of a Multi-Bearing Flexible Rotor System”*, Journal of Vibration and Acoustics—Transactions of the ASME, 127, (4),408–415.

R. D. Flack, R F. Lanes and P. S. Gambel, 1981,“*Effects Of Lubricant Viscosity on the*

Experimental Response of a Three-Mass Flexible Rotor in Two Types of Journal Bearings ,Wear", 67,201 – 216

Xie Wenhuia, Tang Youganga, Chen Yushub, 2008, *"Analysis of Motion Stability of the Flexible Rotor-Bearing System with Two Unbalanced Disks"*, Journal of Sound and Vibration 310, 381–393.

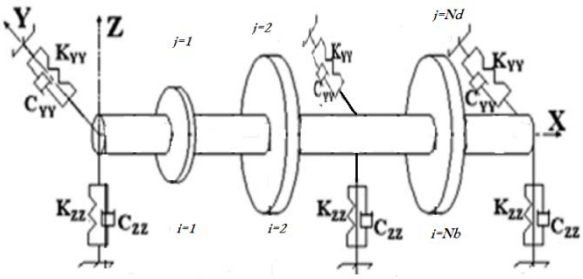

Figure 1. Multi discs and bearings model.

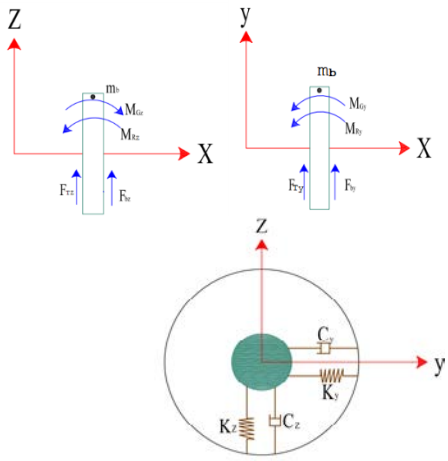

Figure 2. Disc and bearing modeling.

(a)

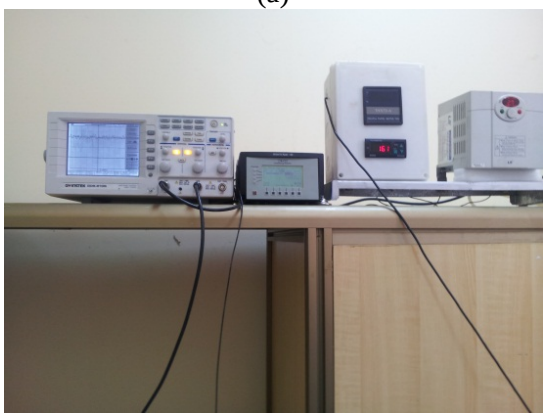

(b)

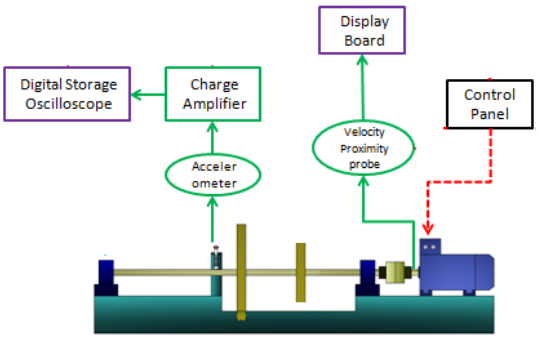

(c)

Figure 3. Experimental rig, instrumentations and connection block diagram**.**

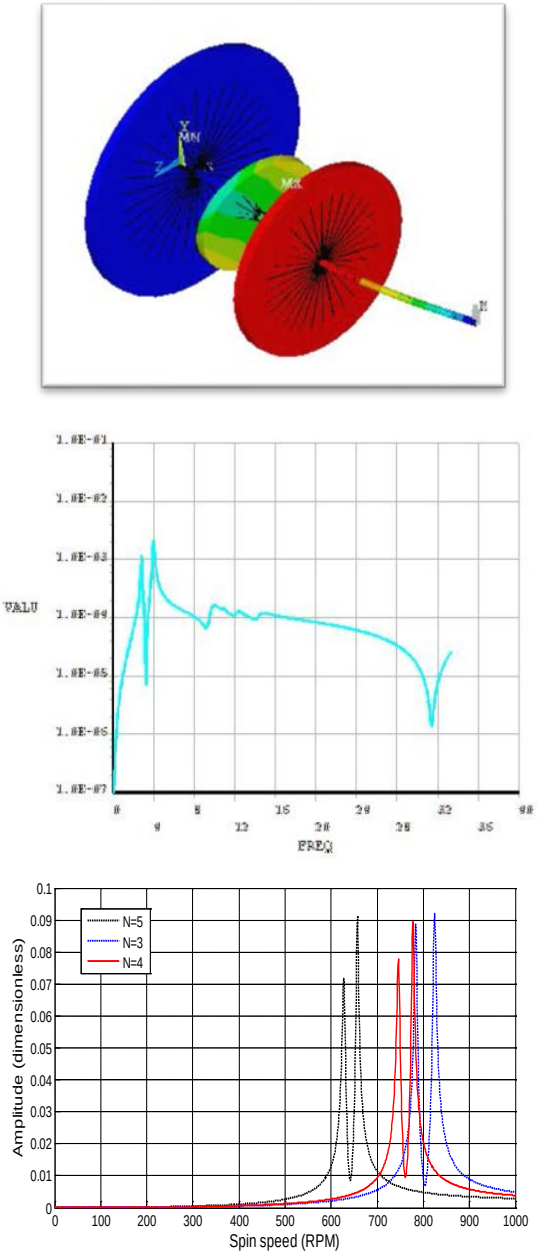

Figure 4. Model simulation , unbalance response by using ANSYS and the present method, for three discs rotor .

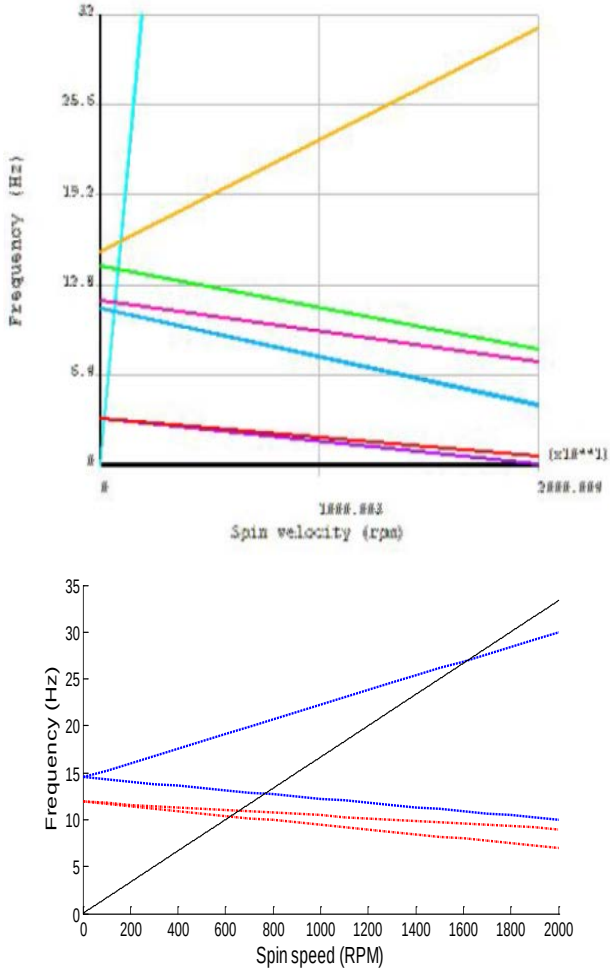

Figure 5. Cambpell diagram , by ANSYS and the present method.

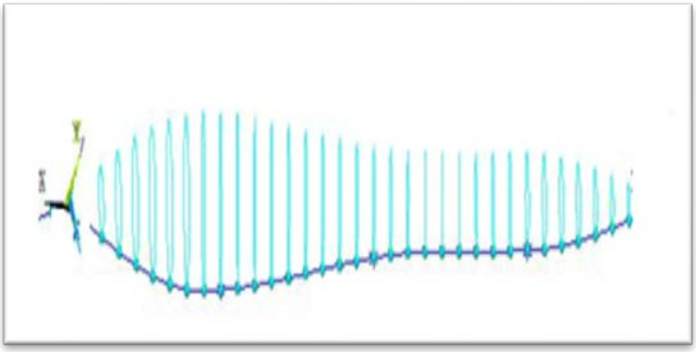

Figure 5. Orbit response of the three discs rotor spins at 960RPM.

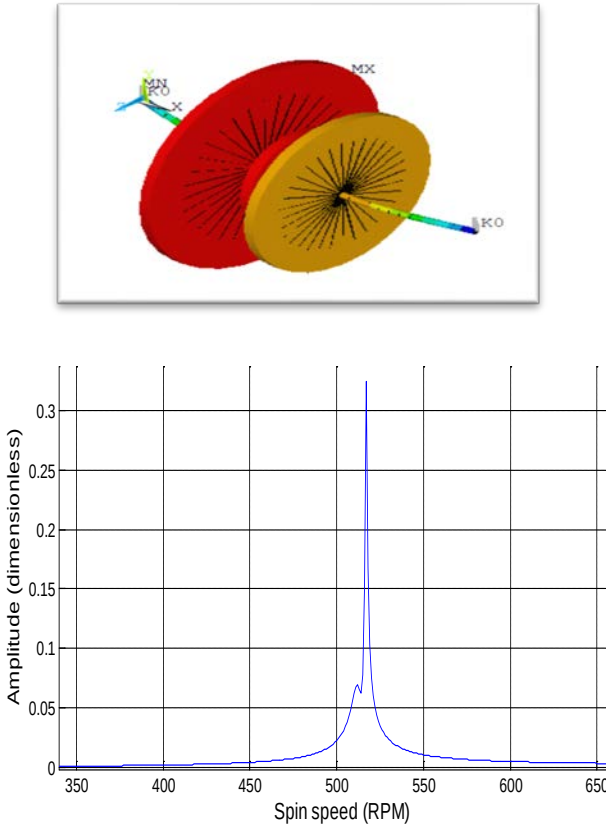

Figure 7. Model simulation and unbalance response for closing spaced discs case.

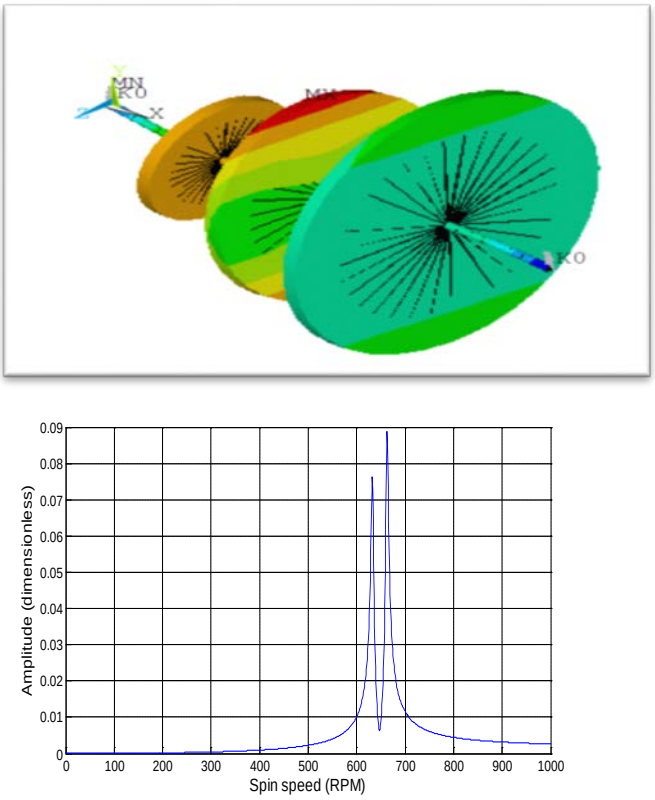

Figure 8. Model simulation and unbalance response of increasing order size discs case.

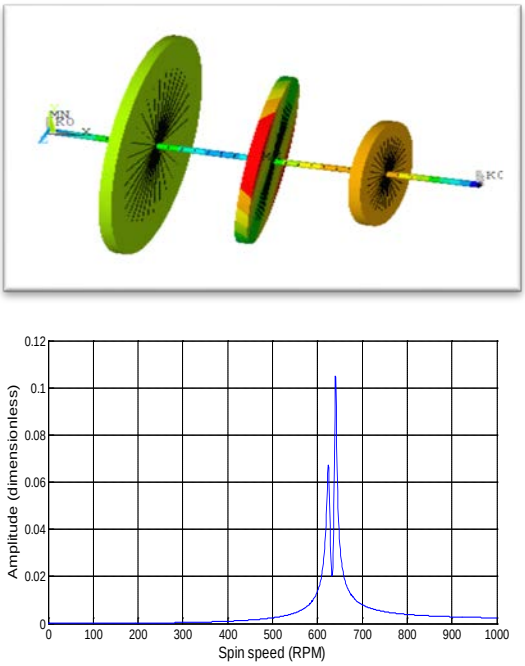

Figure 9. Model simulation and unbalance response of decreasing order size discs case.

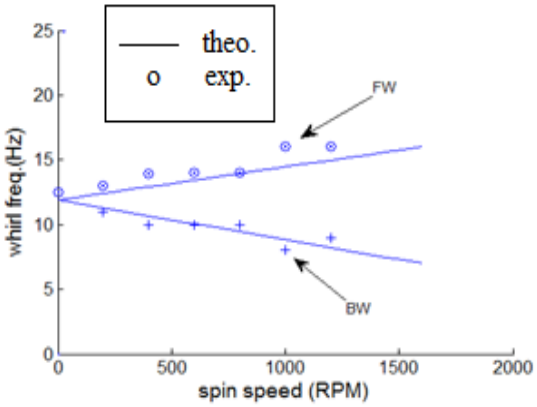

Figure 10. Theoretical and experimental whirl frequencies.

Table 1. Specifications of the theoretical and experimental models (in SI units).

Bearing(1)	Bearing (2)	Disc(1)
$Kxx_1=17.249x10^6$ $Kyy_1=1.294x10^6$ $Czz_1= 3.08x10^5$ $Cyy_1= 2.05x10^4$	$Kxx=17.249x10^6$ $Kyy =1.294x10^6$ $Czz= 3.08x10^5$ $Cyy= 2.05x10^4$	$d_1=0.35$ $t_1=0.013$ $\rho_1=8205$ $m_b=0.2$ r=0.05
Disc(2)	**Disc(3)**	**Shaft**
$d_2=0.167$ $t_2=0.019$ $\rho_2=8205$ $m_b=0.2$ r=0.05	$d_3=0.268$ $t_3=0.02$ $\rho_3=8205$ $m_b=0.2$ r=0.05	$L_s=1$ $d_s=0.019$ E=206x109 $\rho_s=7800$ damp=0.01

Table 2. Validity and convergence of the present.

S	Present solution								ANSYS
	N=3	E%	N=4	E%	N=5	E%	N=6	E%	
1	784	20.2	746	14.1	627	-3.8	623	-4.4	652
2	824	19.2	777	12.4	657	-4	653	-5.5	691

NOMENCLATURE

A	Shaft cross sectional area, m^2
C_{iz}	i th bearing damping coefficients, in z axis, N/m
C_{iy}	i th bearing damping coefficients, in y axis, N/m
c	Bearing clearance, m
D	Bearing diameter , m
ds	Shaft diameter, m
E	Modulus of elasticity, N/m^2
r	Disc eccentricity, m
I	Area second moment of inertia, m^4
F_{Zs}	Spring forces at z axis, N
F_{ys},	Spring forces at y axis, N
F_{zD}	Damping forces at z axis, N
F_{zI}	Damping forces at y axis, N
F_{zIb}	Imbalance forces at z, y axis, N
M_{zG}	Gyroscopic moments at z, y axis, $N.m$
M_{zI},	Inertial moments at z, y axis, $N.m$
I_p	Polar moment of inertia, $Kg.m^2$
I_T	Transverse moment of inertia, $kg.m^2$
K_{zi}	i th bearing stiffness, in z axis, N/m
K_{yi}	i th stiffness, in y axis, N/m
L	Bearing length, m
Ls	Shaft span length, m
m_d	Disc mass, kg
N	Mode number or RPM
p or $p(t)$	Generalized coordinate at y axis
μ,η	Dimensionless coordinates at z and y axis
λ	Eigen values of free-free beams
φ , Φ	

ζ	Dimensionless lateral coordinate
ρ	Density, *kg/m³*
μ	Oil viscosity, *Pa-sec*
τ	Dimensionless time
Ω	Disc spin speed, r/s
ω	Natural frequency, r/s

Elements of [A] and [B] ;

$$a_{s,r} = \int_0^1 \phi_s^{IV}(\zeta)\phi_r(\zeta)d\zeta = \int_0^1 \varphi_s^{IV}(\zeta)\varphi_r(\zeta)d\zeta \quad ,$$

$$a_{s,1+N} = \int_0^1 \phi_s^{IV}(\zeta)d\zeta = \int_0^1 \varphi_s^{IV}(\zeta)d\zeta$$

$$a_{s,2+N} = \int_0^1 \zeta\phi_s^{IV}(\zeta)d\zeta = \int_0^1 \zeta\varphi_s^{IV}(\zeta)d\zeta \quad ,$$

$$b_{s,r} = \int_0^1 \phi_s(\zeta)\phi_r(\zeta)d\zeta = \int_0^1 \varphi_s(\zeta)\varphi_r(\zeta)d\zeta$$

$$b_{1+N,r} = \int_0^1 \phi_r(\zeta)d\zeta = \int_0^1 \varphi_r(\zeta)d\zeta \ ,$$

$$b_{2+N,r} = \int_0^1 \zeta\phi_r(\zeta)d\zeta = \int_0^1 \zeta\varphi_r(\zeta)d\zeta$$

$$b_{s,1+N} = \int_0^1 \phi_s(\zeta)d\zeta = \phi_s(\zeta)d\zeta \ ,$$

$$b_{1+N,1+N} = \int_0^1 (1)d\zeta = \int_0^1 (1)d\zeta = 1 \ ,$$

$$b_{2+N,1+N} = b_{1+N,2+N} = \int_0^1 \zeta.d\zeta = 1/2 ,$$

$$b_{s,2+N} = \int_0^1 \phi_s(\zeta).\zeta.d\zeta = \int_0^1 \varphi_s(\zeta).\zeta.d\zeta$$

$$b_{2+N,2+N} = \int_0^1 \zeta^2.d\zeta = 1/3$$

Elements of matrix *H, L, T, V* and W;

$$h_{s.r} = \phi_r(\zeta_1)\phi_s(\zeta_1) = \varphi_r(\zeta_1)\varphi_s(\zeta_1)$$
$$h_{1+N,r} = h_{s,1+N} = \phi_s(\zeta_1) = \varphi_s(\zeta_1)$$
$$h_{1+N,1+N} = 1$$
$$h_{2+N,r} = h_{2+N,1+N} = h_{2+N,r} = h_{2+N,1+N} = h_{2+N,2+N} = 0$$

$$l_{s.r} = \phi_r(\zeta_3)\phi_s(\zeta_3) = \varphi_r(\zeta_3)\varphi_s(\zeta_3)$$
$$l_{1+N,r} = l_{s,1+N} = \phi_s(\zeta_3) = \varphi_s(\zeta_3)$$
$$l_{1+N,1+N} = 1$$
$$l_{2+N,r} = l_{2+N,1+N} = l_{2+N,r} = l_{2+N,1+N} = l_{2+N,2+N} = 0$$
$$t_{s.r} = \phi_r(\zeta_2)\phi_s(\zeta_2) = \varphi_r(\zeta_2)\varphi_s(\zeta_2) \ ,$$
$$t_{1+N,r} = t_{s,1+N} = \phi_s(\zeta_2) = \varphi_s(\zeta_2) \ , \ t_{1+N,1+N} = 1$$
$$t_{2+N,r} = t_{2+N,1+N} = t_{2+N,r} = t_{2+N,1+N} = t_{2+N,2+N} = 0$$

$$v_{s,r} = \phi_r'(\zeta_2)\phi_s'(\zeta_2) = \varphi_r'(\zeta_2)\varphi_s'(\zeta_2)$$
$$v_{s,1+N} = v_{s,2+N} = v_{1+N,r} = v_{1+N,1+N} = v_{1+N,2+N} = v_{2+N,r} = v_{2+N,1+N} = v_{2+N,2+N} = 0$$

$$w_{1,s} = \phi_r(\zeta_2) \quad , \quad w_{1,1} = 1 \quad , \quad w_{1,2} = \zeta_2$$

Vibration Analysis of Laminated Composite Plate under Thermo-Mechanical Loading

Prof. Dr. Adnan Naji Jameel
University of Baghdad
College of Engineering
Mechanical Engineering Dep
adnanaji2004@yahoo.com

Eng. Rasha Mohammed Hussien
University of Baghdad
College of Engineering
Mechanical Engineering Dep.
mechanicalflower99@yahoo.com

ABSTRACT

The present study focused mainly on the vibration analysis of composite laminated plates subjected to thermal and mechanical loads or without any load (free vibration). Natural frequency and dynamic response are analyzed by analytical, numerical and experimental analysis (by using impact hammer) for different cases. The experimental investigation is to manufacture the laminates and to find mechanical and thermal properties of glass-polyester such as longitudinal, transverse young modulus, shear modulus, longitudinal and transverse thermal expansion and thermal conductivity. The vibration test carried to find the three natural frequencies of plate. The design parameters of the laminates such as aspect ratio, thickness ratio, boundary conditions and lamination angle were investigated using classical laminated plate theory (CLPT) and Finite element coded by ANSYS, in addition to the design parameters of dynamic response such as load type with respect to time, x and y dimension and temperature value for simply supported symmetric cross ply. The main conclusion was the natural frequency could increase and decrease depending on the boundary conditions, thickness ratio, and lamination angle, the aspect ratio of the plate. Present of temperature could increase dynamic response of plate also depending on lamination angle, type of mechanical load and the value of temperature.

Keywords: composite laminated plate, natural frequency, dynamic response, classical laminated plate theory, ANSYS, thermo-mechanical load.

تحليل الاهتزازات للصفائح المركبة تحت تأثير احمال ميكانيكية حرارية

أ.د. عدنان ناجي جميل **مهندسة رشا محمد حسين**

الخلاصة:

هذه الدراسة ركزت بشكل رئيسي على تحليل الاهتزاز للصفائح المركبة معرضة للأحمال الحرارية و الميكانيكية أو دون أي تحميل (الاهتزاز الحر). ويتم تحليل الترددات الطبيعية والاستجابة الديناميكية عن طريق التحليل النظري، التحليل العددي والعملي (باستخدام المطرقة) لمختلف الحالات.في الجانب العملي تم تصنيع الصفائح المركبة المصنوعة من الالياف الزجاجية والبوليستر لايجاد الخواص الحرارية والميكانيكية مثل معامل يونك الطولي والعرضي و معامل القص والتمدد الحراري الطولي والعرضي و التوصيل الحراري.تم عمل اختبار الاهتزاز للعثور على الترددات الطبيعية الثلاثة للصفيحة. كما تم بحث عناصر تصميم شرائح مثل نسبة العرض إلى الارتفاع، ونسبة سماكة وشروط الحدود وزاوية التصفيح باستخدام النظرية الكلاسيكيةCLPT و طريقة العناصر المحددة المبرمجة باستخدام برنامج

ANSYS. بالإضافة إلى عناصر تصميم الاستجابة الديناميكية مثل نوع الحمولة المتغيرة مع الزمن،او احداثيات x وy وقيمة درجة الحرارة للصفائح المركبة المثبتة التثبيت البسيط simply supported المتماثلة.وكان الاستنتاج الرئيسي ان التردد الطبيعي يمكن ان يقل او يزيد تبعا لشروط الحدود، ونسبة سماكة، وزاوية التصفيح، ونسبة العرض إلى الارتفاع للصفيحة . وزيادة الاستجابة الديناميكية للصفيحة اعتمادا أيضا على زاوية التصفيح، ونوع الحمولة الميكانيكية وقيمة درجة الحرارة.

الكلمات الرئيسية: صفائح مركبة، الاهتزاز الطبيعي، الاستجابة الدينماكية، النظرية الكلاسيكية للصفائح الطباقية، حمل حراري ميكانيكي.

1. INTRODUCTION

1.1 General

During the last decades, needs for *composite materials* which contain two or more types of materials mixed together homogenously have appeared.

Composite materials have many advantages such as high strength with low weight compared with traditional engineering materials; furthermore, their properties can be controlled during mixing of their components to meet the suitable design requirements. Ref.[Reddy J.N.]
Study of vibration of thin plates is an extremely important area owing to its wide variety use of engineering applications. It is essential for a design engineer to have a prior knowledge of the first few modes of vibration characteristics before finalizing the design of a given structure.
Many researches had studied free vibration analysis and vibration of plate under mechanical or thermal or thermo-mechanical loading**.**
Dobyns, A.L., 1981, analysed simply supported orthotropic plates subjected to static and dynamic loading conditions presented the first shear deformation theory. Transient loading conditions considered included sine, rectangular, and triangular pulses.**Reddy, J. N.,1982,** presented two different lamination schemes, under appropriate boundary conditions and sinusoidal distribution of the transverse load. The exact solution was obtained by integrated numerically using Newmark's direct integration method. **Chorng-Fuh Liu and Chih-Hsing Huang,1996** performed a vibration analysis of laminated composite plates subjected to temperature change. The first order shear deformation theory of a plate is employed. The resulting finite element formulation leads to general nonlinear and coupled simulation equations and calculate the frequencies of vibration of a symmetric cross-ply plate. **Hui-Shen Shen, et.al**,**2003,** studied the dynamic response of shear deformable laminated plates exposed to thermo-mechanical loading and resting on a two-parameter elastic foundation. The formulation is based on higher order shear deformable plate theory and includes the plate foundation interaction and thermal effects due to temperature rise. Effects of foundation stiffness, plate side-to-thickness ratio, and temperature rise on the dynamic response are studied.
Metin Aydogdu and Taner Timarci,2007, presented numerical results for vibration frequencies of anti-symmetric angle-ply laminated thin square composite plates having different boundary conditions. The Ritz method, along with the displacement assumed in the form of simple polynomials, is applied to solve the problems.**Kullasup P. et al., 2010,** analysed Free vibration of symmetrically laminated composite rectangular plates with various boundary conditions by an extended Kantorovich method, in which a separable function to the dynamic-system energy equation is applied in order to reduce the partial differential equations to ordinary differential equations in the direction of x, y coordinates with a constant coefficient. The beam function is used as an initial trial function in the iterative calculation, which is employed to evaluate the natural frequency and force the final solution needed to satisfy the boundary conditions. **Suresh K. J. et al., 2011,** developed an analytical procedure is to investigate the free vibration characteristics of different laminated composite plates based on higher order shear

displacement model with zig-zag function. This function improves slope discontinuities at the interfaces of laminated composite plates. The related functions are obtained using the dynamic version of principle of virtual work or Hamilton's principle. The solutions are obtained using Navier's method.

The point of originality of the present work is how to derive the analytical solution of free vibration for composite laminated plates by classical laminated plate theory for the first time, by applied different type of boundary condition on the symmetric cross-ply composite laminated plates using levy solution. Then derived the equation of motion for transient vibration (with or without the temperature effect) and solving it by Newmark direct integration method. Thermal and mechanical properties, natural frequency for composite plate made from (glass-polyester) with fiber volume fraction (0.3) are determined experimentally.

Also Finite element coded by ANSYS14used in this thesis to find natural frequency and transient response of composite laminate plate.

2. ANALYTICAL SOLUTION (CLASSICAL LAMINATE PLATE THEORY)

2.1 Natural Frequency

2.1.1 Displacement

Classical lamination theory (CLPT) based on the Kirchhoff hypothesis based on assuming the straight line perpendicular to the mid surface before deformation remains straight after deformation which means neglecting shear strains and transverse normal strain and stress in the analysis of laminated composite plates. Ref.[Reddy J.N.]

$$u(x,y,t)=u_o(x,y,t)-z\frac{\partial w_o}{\partial x} \qquad \textbf{(1. a)}$$

$$v(x,y,t)=v_o(x,y,t)-z\frac{\partial w_o}{\partial y} \qquad \textbf{(1. b)}$$

$$w(x,y,t)=w_o(x,y) \qquad \textbf{(1. c)}$$

Where $\frac{\partial w_o}{\partial x}$, $\frac{\partial w_o}{\partial y}$ denote the rotations about y and x axis respectively.

u_o, v_o and w_o denote the displacement components along (x, y, z) directions respectively of a point on the mid-plane (i.e.…z=0).

2.1.2 Stress and strain

The total strains can be written as follows

$$\begin{Bmatrix}\varepsilon_{xx}\\ \varepsilon_{yy}\\ \gamma_{xy}\end{Bmatrix}=\begin{Bmatrix}\varepsilon_{xx}^{(0)}\\ \varepsilon_{yy}^{(0)}\\ \gamma_{xy}^{(0)}\end{Bmatrix}+z*\begin{Bmatrix}\varepsilon_{xx}^{(1)}\\ \varepsilon_{yy}^{(1)}\\ \gamma_{xy}^{(1)}\end{Bmatrix}$$

$$=\begin{Bmatrix}\frac{\partial u_o}{\partial x}\\ \frac{\partial v_o}{\partial y}\\ \frac{\partial u_o}{\partial y}+\frac{\partial v_o}{\partial x}\end{Bmatrix}+z*\begin{Bmatrix}-\frac{\partial^2 w_o}{\partial x^2}\\ -\frac{\partial^2 w_o}{\partial y^2}\\ -2*\frac{\partial^2 w_o}{\partial x\partial y}\end{Bmatrix} \qquad \textbf{(2)}$$

Where $(\varepsilon_{xx}^{(0)}, \varepsilon_{yy}^{(0)}, \gamma_{xy}^{(0)})$ are the membrane strains and $(\varepsilon_{xx}^{(1)}, \varepsilon_{yy}^{(1)}, \gamma_{xy}^{(1)})$ are the flexural (bending) strains, known as the curvatures [Reddy J.N.]. The transformed stress-strain relations of an orthotropic lamina in a plane state of stress are; for $\bar{Q}_{ij}$ see [Reddy J.N.]

$$\begin{Bmatrix}\sigma_{xx}\\ \sigma_{yy}\\ \sigma_{xy}\end{Bmatrix}_k=\begin{bmatrix}\bar{Q}_{11} & \bar{Q}_{12} & \bar{Q}_{16}\\ \bar{Q}_{12} & \bar{Q}_{22} & \bar{Q}_{26}\\ \bar{Q}_{16} & \bar{Q}_{26} & \bar{Q}_{66}\end{bmatrix}_k\begin{Bmatrix}\varepsilon_{xx}\\ \varepsilon_{yy}\\ \gamma_{xy}\end{Bmatrix} \qquad \textbf{(3)}$$

The resultant of inplane force *Nxx* ,*Nyy* and *Nxy* and moments *Mxx*, *Myy* and *Mxy* acting on a laminate are obtained by integration of the stress in each layer or lamina through the laminate thickness. Knowing the stress in terms of the displacement, we can obtain the inplane force resultants *Nxx*, *Nyy*, *Nxy*, *Mxx*, *Myy* and *Mxy*.

The inplane force resultants are defined as

$$\begin{Bmatrix}N_{xx}\\ N_{yy}\\ N_{xy}\end{Bmatrix}=\sum_{k=1}^{N}\int_{z_k}^{z_{k+1}}\begin{Bmatrix}\sigma_{xx}\\ \sigma_{yy}\\ \sigma_{xy}\end{Bmatrix}_k dz \qquad \textbf{(4.a)}$$

Where σ_x , σ_y and σ_{xy} are normal and shear stress.

$$\begin{Bmatrix} N_{xx} \\ N_{yy} \\ N_{xy} \end{Bmatrix} = \begin{bmatrix} A_{11} & A_{12} & A_{16} \\ A_{12} & A_{22} & A_{26} \\ A_{16} & A_{26} & A_{66} \end{bmatrix} \begin{Bmatrix} \varepsilon_{xy}^{0} \\ \varepsilon_{xy}^{0} \\ \gamma_{xy}^{0} \end{Bmatrix}$$

$$+ \begin{bmatrix} B_{11} & B_{12} & B_{16} \\ B_{12} & B_{22} & B_{26} \\ B_{16} & B_{26} & B_{66} \end{bmatrix} \begin{Bmatrix} \varepsilon_{xx}^{1} \\ \varepsilon_{yy}^{1} \\ \gamma_{xy}^{1} \end{Bmatrix} \qquad \textbf{(4.b)}$$

$$\begin{Bmatrix} M_{xx} \\ M_{yy} \\ M_{xy} \end{Bmatrix} = \sum_{k=1}^{N} \int_{z_k}^{z_{k+1}} \begin{Bmatrix} \sigma_{xx} \\ \sigma_{yy} \\ \sigma_{xy} \end{Bmatrix}_k z \, dz \qquad \textbf{(5.a)}$$

$$\begin{Bmatrix} M_{xx} \\ M_{yy} \\ M_{xy} \end{Bmatrix} = \begin{bmatrix} B_{11} & B_{12} & B_{16} \\ B_{12} & B_{22} & B_{26} \\ B_{16} & B_{26} & B_{66} \end{bmatrix} \begin{Bmatrix} \varepsilon_{xy}^{0} \\ \varepsilon_{xy}^{0} \\ \gamma_{xy}^{0} \end{Bmatrix}$$

$$+ \begin{bmatrix} D_{11} & D_{12} & D_{16} \\ D_{12} & D_{22} & D_{26} \\ D_{16} & D_{26} & D_{66} \end{bmatrix} \begin{Bmatrix} \varepsilon_{xx}^{1} \\ \varepsilon_{yy}^{1} \\ \gamma_{xy}^{1} \end{Bmatrix} \qquad \textbf{(5.b)}$$

Here, A_{ij} are the extensional stiffness, B_{ij} the coupling stiffness, and D_{ij} the bending stiffness.

$$A_{ij} = \sum_{k=1}^{N} (\bar{Q}_{ij})_k (z_{k+1} - z_k) \qquad \textbf{(6.a)}$$

$$B_{ij} = \frac{1}{2} \sum_{k=1}^{N} (\bar{Q}_{ij})_k (z^2{}_{k+1} - z^2{}_k) \qquad \textbf{(6.b)}$$

$$D_{ij} = \frac{1}{3} \sum_{k=1}^{N} (\bar{Q}_{ij})_k (z^3{}_{k+1} - z^3{}_k) \qquad \textbf{(6.c)}$$

2.1.3 Equation of motion

The equations of motion are obtained by setting the coefficient of δu_0 , δv_0 , δw_0 to zero separately

$$\frac{\partial N_{xx}}{\partial x} + \frac{\partial N_{xy}}{\partial y} = I_0 \frac{\partial^2 u}{\partial t^2} - I_1 \frac{\partial^3 w}{\partial x \partial t^2} \qquad \textbf{(7.a)}$$

$$\frac{\partial N_{xy}}{\partial x} + \frac{\partial N_{yy}}{\partial y} = I_0 \frac{\partial^2 v}{\partial t^2} - I_1 \frac{\partial^3 w}{\partial y \partial t^2} \qquad \textbf{(7.b)}$$

$$\frac{\partial^2 M_{xx}}{\partial x^2} + 2\frac{\partial^2 M_{xy}}{\partial x \partial y} + \frac{\partial^2 M_{yy}}{\partial y^2} + \hat{N}_{xx}\frac{\partial^2 w}{\partial x^2} + \hat{N}_{yy}\frac{\partial^2 w}{\partial y^2} + \hat{N}_{xy}\frac{\partial^2 w}{\partial x \partial y} = I_0 \frac{\partial^2 w}{\partial t^2} + I_1\left(\frac{\partial^3 u}{\partial x \partial t^2} + \frac{\partial^3 v}{\partial y \partial t^2}\right) - I_2\left(\frac{\partial^4 w}{\partial x^2 \partial t^2} + \frac{\partial^4 w}{\partial y^2 \partial t^2}\right) - q(x,y,t) \qquad \textbf{(7.c)}$$

Where

$$(I_0, I_1. I_2) = \sum_{k=1}^{N} \int_{z_{k-1}}^{z_k} \rho^{(k)} (1, z, z^2) dz \qquad \textbf{(8)}$$

$\rho^{(k)}$ being the material density of kth layer and q(x,y,t) is a dynamic force subjected on a system. For natural frequency q(x,y,t) and $\hat{N}_{xx}, \hat{N}_{yy}$ and $\hat{N}_{xy}$ equal to zero.

These equations of motion (7 a-c) can be expressed in terms of displacements (δu_0 , δv_0 , δw_0) by substituting the forces results from **Eqs. (4 ,5,8)** into Eq. (**7.a**) to**(7.c)** and get partial differential equations, then the analytical solution done by levy method as derived in[Reddy J.N.].

2.2 Dynamic Response

2.2.1 Equation of motion

In classical laminate plate theory, the equations of motion derived using the dynamic version of the principle of virtual displacements. The derivation and all equation for no temperature effect discussed in section (2.1). but the stress strain relations when there were temperature change is[9]

$$\begin{Bmatrix} \varepsilon_{xx} \\ \varepsilon_{yy} \\ \gamma_{xy} \end{Bmatrix} = \begin{Bmatrix} \varepsilon_{xx}^{(0)} \\ \varepsilon_{yy}^{(0)} \\ \gamma_{xy}^{(0)} \end{Bmatrix} + Z \begin{Bmatrix} \varepsilon_{xx}^{(1)} \\ \varepsilon_{yy}^{(1)} \\ \gamma_{xy}^{(1)} \end{Bmatrix}$$

$$= \begin{Bmatrix} \frac{\partial u_0}{\partial x} - \alpha_{xx} T_0 \\ \frac{\partial v_0}{\partial y} - \alpha_{yy} T_0 \\ \frac{\partial u_0}{\partial y} + \frac{\partial v_0}{\partial x} - \alpha_{xy} T_0 \end{Bmatrix} + Z \begin{Bmatrix} -\frac{\partial^2 w_0}{\partial x^2} - \alpha_{xx} T_1 \\ -\frac{\partial^2 w_0}{\partial y^2} - \alpha_{yy} T_1 \\ -2 * \frac{\partial^2 w_0}{\partial x \partial y} - \alpha_{xy} T_1 \end{Bmatrix}$$

eq. (9.a)

Eq. (2-21a) for linear varying of temperature i.e,[Reddy J.N.]

$$\Delta T = T_0(x,y,t) - zT_1(x,y,t) \qquad \textbf{(9.b)}$$

In present work the varying of temperature supposed uniform, thus **Eq. (2-21a**) became

$$\begin{Bmatrix}\varepsilon_{xx}\\ \varepsilon_{yy}\\ \gamma_{xy}\end{Bmatrix} = \begin{Bmatrix}\frac{\partial u_0}{\partial x} - \alpha_{xx}\Delta T\\ \frac{\partial v_0}{\partial y} - \alpha_{yy}\Delta T\\ \frac{\partial u_0}{\partial y} + \frac{\partial v_0}{\partial x} - \alpha_{xy}\Delta T\end{Bmatrix} + z\begin{Bmatrix}-\frac{\partial^2 w_0}{\partial x^2}\\ -\frac{\partial^2 w_0}{\partial y^2}\\ -2*\frac{\partial^2 w_0}{\partial x \partial y}\end{Bmatrix} \qquad \textbf{(9.c)}$$

α_x , α_y and $\alpha_{xy}$are thermal expansion coefficients defined

$$\alpha_{xx} = \alpha_{11}(\cos\theta)^2 + \alpha_{22}(\sin\theta)^2 \qquad \textbf{(10.a)}$$

$$\alpha_{yy} = \alpha_{11}(\sin\theta)^2 + \alpha_{22}(\cos\theta)^2 \qquad \textbf{(10.b)}$$

$$2\alpha_{xy} = 2(\alpha_{11} - \alpha_{22})\sin\theta\cos\theta \qquad \textbf{(10.c)}$$

$\alpha_{11}$and α_{22} Are longitudinal and transverse thermal expansions respectively. And $\theta$is the lamination angle.

The change in temperature defined

ΔT = *applied temperature – reference temperature*

Where reference temperature $T_{ref} = 25C^{\circ}$

The transformed stress-strain relations of an orthotropic lamina in a plane state of stress are; for$\bar{Q}_{ij}$

$$\begin{Bmatrix}\sigma_{xx}\\ \sigma_{yy}\\ \sigma_{xy}\end{Bmatrix}_k = \begin{bmatrix}\bar{Q}_{11} & \bar{Q}_{12} & \bar{Q}_{16}\\ \bar{Q}_{12} & \bar{Q}_{22} & \bar{Q}_{26}\\ \bar{Q}_{16} & \bar{Q}_{26} & \bar{Q}_{66}\end{bmatrix}_k \begin{Bmatrix}\varepsilon_{xx} - \alpha_{xx}\Delta T\\ \varepsilon_{yy} - \alpha_{yy}\Delta T\\ \gamma_{xy} - 2\alpha_{xy}\Delta T\end{Bmatrix} \qquad \textbf{(11)}$$

$\{N^t\}$ and $\{M^t\}$ are thermal stress and bending results, respectively

$$\begin{Bmatrix}N^t_{xx}, M^t_{xx}\\ N^t_{yy}, M^t_{yy}\\ N^t_{xy}, M^t_{xy}\end{Bmatrix} = \sum_{k=1}^{N}\int_{-h/2}^{h/2}\begin{bmatrix}\bar{Q}_{11} & \bar{Q}_{12} & \bar{Q}_{16}\\ \bar{Q}_{12} & \bar{Q}_{22} & \bar{Q}_{26}\\ \bar{Q}_{16} & \bar{Q}_{26} & \bar{Q}_{66}\end{bmatrix}\begin{Bmatrix}\alpha_{xx}\\ \alpha_{yy}\\ 2\alpha_{xy}\end{Bmatrix}(1, z)\Delta T dz \qquad \textbf{(12)}$$

The equation of motion is.

$$\begin{bmatrix}c_{11} & c_{12} & c_{13}\\ c_{12} & c_{22} & c_{23}\\ c_{13} & c_{23} & c_{33}\end{bmatrix}\begin{Bmatrix}u_0\\ v_0\\ w_0\end{Bmatrix} + \begin{bmatrix}m_{11} & 0 & 0\\ 0 & m_{22} & 0\\ 0 & 0 & m_{33}\end{bmatrix}\begin{Bmatrix}\ddot{u}_0\\ \ddot{v}_0\\ \ddot{w}_0\end{Bmatrix} = \begin{Bmatrix}0\\ 0\\ q\end{Bmatrix} + \begin{Bmatrix}f_1^t\\ f_2^t\\ f_3^t\end{Bmatrix}$$

eq. (13)

Where

$$f_1^t = \frac{\partial N_{xx}^t}{\partial x} + \frac{\partial N_{xy}^t}{\partial y} \qquad \textbf{(14.a)}$$

$$f_2^t = \frac{\partial N_{xy}^t}{\partial x} + \frac{\partial N_{yy}^t}{\partial y} \qquad \textbf{(14.b)}$$

$$f_3^t = -\left(\frac{\partial^2 M_{xx}^t}{\partial x^2} + 2\frac{\partial^2 M_{xy}^t}{\partial y \partial x} + \frac{\partial^2 M_{yy}^t}{\partial y^2}\right) \qquad \textbf{(14.c)}$$

These equations of motion (13) can be expressed in terms of displacements **(**δu_0 , δv_0 , δw_0) by substituting the forces results from **Eqs. (4,5,8,12,14 a-c**) into **Eq.(13)** and get partial differential equations, then the analytical solution done by Navier method as derived in ref.[Reddy J.N.].

After applying Navier method, Newmark's direct integration method done.

2.2.2 Newmark's direct integration method

The term "direct" means that prior to the numerical integration; no transformation of the equations into a different form is carried out. Many numerical integration methods are available for the approximate solution of such equations of motion. All the numerical integration methods have two basic characteristics. First, they do not satisfy the differential equations at all-time t, but only at discrete time intervals, say Δt apart. Secondly, within each time interval Δt, a specific type of variation of the displacement, velocity and acceleration is assumed. ref.[Rao V. Dukkipati]

In the Newmark direct integration method, the first time derivative $\{\dot{U}\}$ and the solution $\{U\}$ are approximated at (n+1) time step (i.e. at time $t = t_{n+1} = (n+1)\Delta t$ by the following expression (ref[7]).

$$\{\dot{U}\}_{n+1} = \{\dot{U}\}_n + \left[(1-\bar{\alpha})\{\ddot{U}\}_n + \bar{\alpha}\{\ddot{U}\}_{n+1}\right]\Delta t \quad \textbf{(15.a)}$$

$$\{U\}_{n+1} = \{U\}_n + \{\dot{U}\}_n \Delta t + \left[\left(\frac{1}{2} - \bar{\beta}\right)\{\ddot{U}\}_n + \bar{\beta}\{\ddot{U}\}_{n+1}\right](\Delta t)^2 \quad \textbf{(15.b)}$$

Where:

$\bar{\alpha}$ And $\bar{\beta}$: are parameters that control the accuracy and stability of the scheme, and the subscript n indicates that the solution evaluated at n^{th} time step (i.e. at time, t = t_n). The choice $\bar{\alpha} = 0.5$ and $\bar{\beta} = 0.25$ is known to give an unconditionally stable Scheme (average acceleration method), [Rao V. Dukkipati].

Solving from **Eq.(15.b)** for $\{\ddot{U}\}_{n+1}$ in term of $\{U\}_{n+1}$, the acceleration at time t_{n+1} is obtained:

$$\{\ddot{U}\}_{n+1} = a_0\left[\{U\}_{n+1} - \{U\}_n\right] - a_1\{\dot{U}\}_n - a_2\{\ddot{U}\}_n \quad \textbf{(16)}$$

The equilibrium **Eq.(13)** at time t_{n+1} is considered as:

$$[MA]\{\ddot{U}\}_{n+1} + [KS]\{U\}_{n+1} = \{R\}_{n+1} \quad \textbf{(17)}$$

Substituting from **Eq.(16)** into **Eq.(17)** and rearranging yields:

$$[\hat{M}]\{U\}_{n+1} = \{\hat{q}\}_{n+1} \quad \textbf{(18)}$$

Where:

$$[\hat{M}] = [KS] + a_0[MA] \quad \textbf{(19.a)}$$

$$\{\hat{q}\}_{n+1} = \{R\}_{n+1} + [M]\left[a_0\{U\}_n + a_1\{\dot{U}\}_n + a_2\{\ddot{U}\}_n\right] \quad \textbf{eq. (19.b)}$$

$$a_0 = \frac{1}{\bar{\beta}(\Delta t)^2} \quad , \quad a_1 = \frac{1}{\bar{\beta}(\Delta t)} \quad , \quad a_2 = \frac{1}{2\bar{\beta}} - 1$$

The first and second derivatives $(\dot{U}, \ddot{U})$ of $\{U\}$ at t_{n+1} can be computed from rearranging the expressions (15a-b):

$$\{\ddot{U}\}_{n+1} = a_0\left[\{U\}_{n+1} - \{U\}_n\right] - a_1\{\dot{U}\}_n - a_2\{\ddot{U}\}_n \quad \textbf{(20.a)}$$

$$\{\dot{U}\}_{n+1} = a_3\left(\{U\}_{n+1} - \{U\}_n\right) - a_4\{\dot{U}\}_n - a_5\{\ddot{U}\}_n \quad \textbf{(20.b)}$$

Where:

$$a_3 = \frac{\bar{\alpha}}{\bar{\beta}(\Delta t)} \quad , \quad a_4 = \left(\frac{\bar{\alpha}}{\bar{\beta}}\right) - 1$$

$$a_5 = \frac{\Delta t}{2}\left(\frac{\alpha}{\beta} - 2\right)$$

Once the displacements $\{U\}_{n+1}$ at time t_{n+1} are obtained by solving equation (18), the velocities $\{\dot{U}\}_{n+1}$ and accelerations $\{\ddot{U}\}_{n+1}$ are computed using **Eqs.(20.a)** and **(20.b),** respectively.

3. NUMERICAL ANALYSIS

3.1 Element selection and modeling

An element called shell281 as shown in **Fig.1** is selected which is suitable for analyzing thin to moderately thick shell structures. The element has eight nodes with six degrees of freedom at each node: translations in the x, y, and z axes, and rotations about the x, y, and z axes. It may be used for layered applications for modeling composite shells. It is include the effects of transverse shear deformation. The accuracy in modeling composite shells is governed by the first order shear deformation theory. The shell section allows for layered shell definition, options are available for specifying the thickness, material, orientation through the thickness of the layers.

Finite element method has been employed to analyze natural frequency and dynamic response. The model was developed in ANSYS 14.0 using the 225 (15*15) quadrate elements. The global x coordinate is directed along the width of the plate, while the global y coordinate is directed along the length and the global z direction corresponds to the thickness direction and taken to be the outward normal of the plate surface. There are 15 elements in the axial direction and 15 along the width (i.e. 4416 DOF). Convergence study is the reasons for

choosing the particular mesh used in this study. A modal analysis was performed on the model to calculate the natural frequency of the structure. The transient analysis was performed on the modal to calculate the dynamic response (the program used Newmark method).

3.2 Verification Case Studies

In the present study, Series of preselected cases are modeled to verify the accuracy of the method of analysis. The results are compared to analytical solution (Levy) and numerical solution (Finite element method).see **Table 1** and **Table 2.** For dynamic response see **Fig.2** (no temperature effect) and **Fig.3** (with temperature effect).

From these results, it is obvious that the methods of solution gives better results for both analytical and numerical solution.

4. EXPERIMENTAL WORK

In the present work, Five- purposes were investigated. First, to outline the general steps to design and fabricate the rectangular test models from fiber (E-glass) and polyester resin to form laminate composite materials. Second, the manufactured models are then used to evaluate the mechanical properties (E_1, E_2, G_{12}) without temperature change of unidirectional composite material. Third, measure thermal conductivity for fiber-polyester composite plate and polyester, measure the temperature dependence of mechanical properties (E_1, E_2, G_{12}) and coefficient of thermal expansion (CTE) of the composite plate.

Fifth, the vibration test can be done to calculate the fundamental natural frequency of composite laminate plate for different boundary conditions cross ply laminate plate.

4.1 Tensile Test

Each laminate was oriented in longitudinal, transverse and 45° angle relative to designated 0° direction to determine the engineering parameters E_1, E_2, G_{12}. Tensile test specimen include standard geometry according to ASTM (D3039/D03039M); and the mechanical properties for glass-polyester which obtained from tensile test as shown in **Table (3).**

4.2 Thermo-Mechanical Analyzer

Thermo-mechanical Analysis (TMA) determines dimensional changes of solids and liquids materials as a function of temperature and/or time under a defined mechanical force.

Irrespective of the selected type of deformation (expansion, compression, penetration, tension or bending), every change of length in the sample is communicated to a highly sensitive inductive displacement transducer (LVDT) via a push rod and transformed into a digital signal. The push rod and corresponding sample holders of fused silica or aluminum oxide can be quickly and easily interchanged to optimize the system to the respective application. **Figs.4 and 5.**

The dimension of sample is (5*20*4) mm. the thermal properties which obtain from this test shown in **Table 4.**

4.3 Thermal conductivity test

Thermal conductivity coefficient of specimens was measured by using Lee's disk method principle. Very often composite materials results in anisotropic media and their thermal conductivity change along the axes because of the presences of reinforcing fibers embedded in the matrix.

The rule of mixture accurately predicts the thermal conductivity of fiber reinforced composite in both directions, [Louay S. Yousouf]:

When the fibers are arranged in the longitudinal direction, then:

$$K_1^c = K_f * \upsilon_f + K_m * \upsilon_m \qquad \textbf{(21.a)}$$

When the fibers are arranged in the lateral direction:

$$K_2^c = \frac{K_f * K_m}{K_f * \upsilon_m + K_m * \upsilon_f} \qquad \textbf{(21.b)}$$

Fig. (6) represents the test apparatus (Lee's disk apparatus) with tested composite specimen and some accessories to measure the temperature of both sides of the composite specimen in which direction x, y, z.

The heater is switch on with (V = 6 Volts and I = 0.25 Amp.) to heat the brass disks (2,3). And the temperatures were recorded every (5 minutes) until reach to the equilibrium

temperature of all disks. The fibers were arranged in the lateral direction and in the longitudinal direction.

Fig. 7 shows the sample used to measure the thermal conductivity using the Lee's Disk method is in the form of a disk whose thickness $d_s$is small relative to its radius (r) with $(d_1 = d_2 = d_3 = 12.25\ mm)$. Using a thin sample means that the system will reach thermal equilibrium more quickly. When the fibers are arranged in the longitudinal direction(r=21mm) Coefficient of Thermal Conductivity k_1= 0.47068*(W/M°C)*

Ds=3.2 mm T_A=31.2C° T_B=34C° T_C=34C°

When the fibers are arranged in the transverse direction(r=21mm) Coefficient of Thermal Conductivity $k_2 = 0.33434$*(W/M°C)*

Ds=3.75 mm T_A=31 C° T_B=35.5C° T_C=35.5C°

And the thermal conductivity can be calculated experimentally by using the following equation, [5]:

$$K * \left[\frac{T_2 - T_o}{d_s}\right] = e * \left[T_o + \frac{2}{r} * \left(d_1 + \frac{1}{2} * d_s\right) * T_o + \frac{1}{r} * d_s * T_2\right] \quad \textbf{(22.a)}$$

And (e) can be evaluated from the following equation, [Louay S. Yousouf]:

$$I * V = \pi * r^2 * e * (T_o + T_3) + 2 * \pi * r * e * \left[d_1 * T_o + \frac{1}{2} * d_s * (T_o + T_2) + d_2 * T_2 + d_3 * T_3\right] \quad \textbf{(22.b)}$$

4.4 Vibration Test

The vibration test includes studying the first three frequencies for composite plate with different boundary condition four layers symmetric cross ply.

The dimensions of vibration plate samples used are, see **Fig. 8.**

a_t=a+$6cm(for\ supported)$

$b_t = b + 6cm(for\ supported)$

For S-S-S-S and S-C-S-C, $a\ and\ b$ equal to $20cm$,$a_t and\ b_t$ equal to 26

But for S-F-S-F $b = 20cm$ $a = 26cm$,$a_t and\ b_t$ equal to 26

The block diagram of the different instruments used for the measurements of natural frequencies is shown in **Fig.9.** And the whole instruments that used in this test shown in **Fig. 10.**

The vibration structure rig is composed of the following parts

(1) Frame Fixture: The composite laminate plate can be fixed according to the boundary conditions used a frame made from steel and supported (U-channel) made from steel to fix the composite plate.

(2) The impact hammer: model (086C03) (PCB Piezotronics vibration division), stiff steel mass with many tips. The hammer consists of an integral quartz force sensor mounted on the striking end of hammer head. The sensing element functions to transfer impact force in to electrical signal for display and analysis. Impulse force test hammer is adapted for adapts FFT analysis of structure behavior testing. Impulse testing of the dynamic behavior of mechanical structure involves striking the test object with the force-instrumented hammer, and measuring the resultant motion with an accelerometer. When can be used the hammer is knocked the composite plate strongly or lightly that is effect on the value of amplitude; but the frequency still constant.

(3) Accelerometer model (4371), accelerometer is a sensor that produces an electrical signal that is proportional to the acceleration of the vibrating component to which the accelerometer is attached. The accelerometer mounted to the plate by the screw which adhesive to the center of plate.

(4) Amplifier, type 7749, the amplifier measures the response signal from accelerometer and gives output signal to the digital storage oscilloscope. It is a low noise charge amplifier for use with piezoelectric accelerometers and other piezoelectric transducers. It offers a wide range of signal conditioning that makes it ideal for use in accelerometers calibration set-ups and for general purpose vibration measurements.

(5) Digital storage oscilloscope, modal GDS-810, has two input channels; this digital storage oscilloscope system can be driven with a computer. This device is used to display the response waves result, which extracted using accelerometer, for the

vibrated structures. Then analysis of response signal is read from digital storage oscilloscope to FFT function by using sig-view program to get the first three frequencies with different parameters studied.

5. RESULTS AND DISCUSSION

5.1 Experimental Results

The experimental results contain the first three frequencies in (HZ) for four layers symmetric cross ply for different boundary condition (SSCC, SSSS, SSFF) by using impact hammer the output signals appears on oscilloscope for each dynamic response which came from conditional amplifier which receives the dynamic response signal from accelerometer. Then analysis of response signal is read from digital storage oscilloscope to FFT function by using sig-view program to get the three frequencies of the plate. The experimental result gave good agreement when the analytical (CLPT with Levy method) and numerical (ANSYS) analysis compared with them maximum error is8.7%for analytical by CLPT and 7.99% for numerical by ANSYS 14.0. The result shown in **Table 5.**

The maximum natural frequency occurs when the boundary condition is SSCC then the frequency decrease when the B.C's became SSSS with percentage 42.3% and then decreases when it became SSFF with percentage 76.9%.

5.2 Theoretical Results Contain (Analytical and Numerical (ANSYS))

5.2.1 Frequency result

In this section discussed the effect of different parameter on fundamental natural frequency such as boundary condition, aspect ratio, thickness ratio for symmetric cross ply composite laminate plate. This result found by analytical method using CLPT with Levy method and numerically using ANSYS 14.0 program.

5.2.1.1 Boundary condition

From the results listed in **Table 6** it can be observed that the boundary conditions always effect on the fundamental natural frequency. It′s worth mentioning the natural frequency in SCSC and SCSS for cross ply and SSSS are higher than other cases because of B.C′S. effect.

5.2.1.2 Aspect ratio

Fig.(11) for SSSS and SSCC cross ply shows that the natural frequency decrease when a/b increase with high percentage reaches to 68.7%. On the other hand the maximum natural frequency in case SSCC symmetric cross ply is at a/b=0.5. While the minimum is at SSSS symmetric cross ply for a/b=2.5.

5.2.1.3 Thickness ratio

It is shown from **Fig.12** for SSSS and SSCC four layers symmetric composite plate, the natural frequency decrease when thickness ratio increase. It can be observed that the natural frequency is decrease with high percentage when b/h varies from 10 to 20 reach to (70.15%). Then, this percentage gets smaller when b/h varies from 20 to 50 the maximum percentage reach to (53.96%). Also here the maximum natural frequency when SSCC boundary condition and a/h=10.

5.2.2 Dynamic response

The present study focused mainly on the dynamic response behavior of composite laminated plates subjected to mechanical and thermo-mechanical loads of finite duration uniform (step, sine and ramp) and sinusoidal (step, sine and ramp) on the top surface of the plate for three cases of temperature (without temperature effect, T=50°C and T=100°C) . The step loading $q(x,y,t) = \bar{q}(x,y)$, ramp loading $q(x,y,t) = \bar{q}(x,y)t/t1$ and sinusoid loading$q(x,y,t) = \bar{q}(x,y)sin\pi t/t1$. For uniform distributed load $\bar{q}(x,y) = \frac{16}{nm\pi^2}$ and for sinusoidal distributed $\bar{q}(x,y) = q_o$. The amplitude of force is $q_o = 100\mathrm{N}/mm^2$ and the time of load applied on plate ist_1 =0.05sec. The dynamic response of central deflection of composite plate discussed for different parameter such as load condition, aspect ratio,

temperature value for symmetric cross ply for simply supported composite plate analytically by CLPT with Newmark direct integration method and numerical result by ANSYS.

5.2.2.1 Effect of load condition

Fig.13 and **Fig.14** represent the variation of central transverse deflection with time (dynamic response) for four layer symmetric cross-ply simply supported laminated plates under sinusoidal $(P(x,y) = qo\, sin(\pi x/a) sin(\pi y/b))$ and uniform $(P(x,y) = qo)$ variation loading, (step $q(x,y,t) = P(x,y)$,ramp loading $q(x,y,t) = P(x,y)\, t/t1$ and sinusoid loading q(x,y,t)=P(x,y) sinπt/t_1) for qo=100N/m^2 ,t_1=0.05 sec) without any temperature change solved by analytically by CLPT with Newmark direct integration method and (F.E.M) by ANSYS program. The deflection due to step loading higher in magnitude than the other loads with percentage reach to 91.96%, 97.4% from sine and ramp load, respectively, because the step load subjected suddenly with constant value with the time. Very good verification between CLPT with Newmark and FEM by ANSYS maximum error is12.9%. Maximum response for step load always occurs in the time of applying load (i.e. in the time less than t_1 after that the response became in negative sign and positive sign alternatively. for ramp load, the response increasing linearly with time until it reached to t_1 at this point the maximum response occurs, then the response became in negative sign and positive sign alternatively. For sine load the response behavior have the sine shape and the maximum response at $t_1/2$.

5.2.2.2 Effect of temperature change with varies load condition

Fig 15 to **Fig. 20** show the numerical result by ANSYS for dynamic response of central deflection of symmetric cross ply simply supported composite plate under different kind of load and different condition of temperature effect i.e. (T=25°C, T=50°C, T=100°C).The deflection increase with maximum percentage reaches to (58.47%) when temperature became 50°C and when the temperature reach to 100°C the response increase with higher percentage reaches to (200%) with respect to response without change in temperature.

5.2.2.3 Effect of aspect ratio

Fig. 21 shows the effect of the aspect ratio (a/b) on the deflection of the simply supported symmetric cross-ply laminated plates (b=200 mm) subjected to step sinusoidal loading without temperature change solved by F.E.M. From the results, increasing (a/b) ratio increasing the deflection of laminated plates. The increase in deflections is 92.4%, 92.8% for increasing aspect ratio (0.5 to 1.5) and (1.5 to 2) respectively.

6. CONCLUSION

This study considers the vibration analysis of symmetric cross-ply composite laminate plate with various B.C's. From the present study, the following conclusions can be made:

1-The Young and shear modulus decrease when temperature increases with high percentages reach to96.3% when temperature changes from (20 °C to 100°C) for longitudinal young modulus, for transverse young modulus is96.53% and for shear modulus is 91.1%. The longitudinal and transverse coefficient of thermal expansion also decrease when temperature increase with percentage 80% and73.7% respectively for the same temperature.

2- The boundary conditions effect on the natural frequency, the maximum frequency occurs when there were clamped in boundary condition of plate. The percentage of increasing the natural frequency when the B.C's change from SSSS to SSCC 45.4% and the percentage of increasing natural frequency when changing B.C's from SSFF to SSCC is 75.5% for symmetric cross ply.

3- The fundamental natural frequency of composite laminated plate is decreasing when a/b increase with high percentage reaches to 68.7%.

4- The natural frequency decrease when thickness ratio increases. It can be observed that the natural frequency is decrease with high

percentage when b/h varies from 10 to 20 reach to (70.15%). Then, this percentage gets smaller when b/h varies from 20 to 50 the maximum percentage reach to (53.96%).

5- The response due to step loading higher in magnitude than the other loads with percentage reach to 91.96%, 97.4% from sine and ramp load, respectively, because the step load subjected suddenly with constant value with the time.

6- The response increase with maximum percentage reaches to (58.47%) when temperature became 50°C and when the temperature reach to 100°C the response increase with higher percentage reaches to (200%) with respect to response without change in temperature. The reason behind that is there are two loads (mechanical and thermal) each of load cause the deflections (thermal and mechanical deflections) summation is the deflection of plate under thermo-mechanical loading. When the temperature increase the deflection increase with high percentage.

7- Increasing of aspect ratio (a/b) increasing the response of laminated plates. The increase in deflections reach to 92.4%, 92.8% for increasing aspect ratio (0.5 to 1.5) and (1.5 to 2) respectively for simply supported symmetric cross-ply laminated plates subjected to step sinusoidal loading without temperature change .

7. REFERENCES

- Chorng-Fuh Liu and Chih-Hsing Huang, 1996, "*Free Vibration of Composite Laminated Plates Subjected to Temperature Changes*" Computers & Structures, Vol. 60, pp. 95-10.

- Dobyns A. L.; *"Analysis of Simply Supported Orthotropic Plates Subjected to Static and Dynamic Loads"*, 1981,ALAA J., Vol. 19, No .3, p.p. 642-650.

- Hui-Shen Shen, J. J. Zheng and X. L. Huang, 2003,"*Dynamic Response of Shear Deformable Laminated Plates Under Thermomechanical Loading and Resting on Elastic Foundations*", Composite Structures, Vol. 60, pp. 57-66.

- Kullasup Phongsrisuk, Prasong Ingsuwan, Wetchayan Rangsri and Wiwat Klongpanich, "*Free vibration analysis of symmetrically laminated composite rectangular plates using extended Kantorovich method*" 2010, Maejo International Journal of Science and Technology ISSN 1905-7873, 4(03), 512-532.

- Louay S. Yousouf, *"Time Prediction of Dynamic Behavior of Glass Fiber Reinforced Polyster Composites Subjected to Fluctuating Varied Temperatures"* 2007, AL-Khwarizimi engineering Journal, vol5, no3,pp28-37(2009).
- Metin Aydogdu, Taner Timarci ,*"Free Vibration of Antisymmetric Angle-Ply Laminated Thin Square Composite Plates"* Turkish J. Eng. Env. Sci 31,243-249

- Rao V. Dukkipati*"Matlab an Introduction with Applications"* New age international publishers. ISBN(13):978-81-224-2920-6 (2010).
- Reddy J. N.; *"On the Solution to Forced Motions of Rectangular Composite Plates*" 1982, J. Applied Mechanics, Vol. 49, p.p. 403-408.

- Reddy J.N. *"Mechanics of Laminated Composite Plates and Shells: Theory and Analysis* ". 2ed; CRC Press 2004.

- Suresh Kumar J., Dharma Raju T. and Viaya Kumar Reddy K., *"Vibration Analysis of Composite Laminated Plates Using Higher Order Shear Deformation Theory with Zig-Zag Function*" 2011, Indian journal of science and technology vol.4 ,no.8,ISSN:0974-6846.

- "*Theory, Analysis, and Element Manuals"* ANSYS 13 Program.

8. NOMENCLATURE

Symbol	Description	Unit
a, b	Dimension of plate in x and y coordinate	m
A_{ij} , B_{ij} ,D_{ij}	Extensional stiffness, the coupling stiffness, and the bending stiffness	-
d_1, d_2, d_3	Thicknesses Of The Brass Disks	m
D_x	Thickness Of The Composite Specimen	m
E_1, E_2 , E_3	Elastic modulus of composite material	GPa
G_{12}, G_{23} , G_{13}	Shear modulus of composite material	GPa
h	Thickness	m
I	Ampere	Amp.
i	Imaginary Root = $\sqrt{-1}$	-
I_0, I_1, I_2	Mass moment of inertia	kg.m^2
k_1, k_2	Coefficient of Thermal Conductivity of composite material	*(W/m°C)*
k_f, k_m	Coefficient of Thermal Conductivity of fiber and matrix respectively	*(W/m°C)*
[MA]	Mass matrix	kg
M_{xx} , M_{yy} ,M_{xy}	Moment resultant per unit length	N.m/m
N	Total number of plate layers	-
Nxx, Nyy, Nxy	The resultant of in-plane force per unit length	N/m
$\bar{N}xx, \bar{N}yy, \bar{N}xy$	Applied edge force	N/m
q(x,y,t)	Dynamic force subjected on a system	N/m^2
$\bar{Q}_{ij}^{(k)}$	Transformed lamina stiffness	N/m
R	Vector of externally applied loads	N
r	Disk spacemen Radius	m
t	Time	min or s
Δt	Time Interval	min or s
t_1	The end time of load	sec
T	Temperature	C^0
ΔT	Temperature increment	C^0
T_A, T_B, T_C	Temperature across the sample sides	C^0
T_{ref}	Reference temperature	C^0
$U, \dot{U}, \ddot{U}$	Displacement , velocity and acceleration vectors	m, m/s, m/ s^2
u_o , v_o , w_o	Displacement components along (x,y,z) directions respectively	m
U_{mn} , V_{mn} , W_{mn}	Aamplitudes of (u_o , v_o , w_o) respectively	-
V	Voltage	Volt
V_f	Fiber volume fraction	-
V_m	Matrix volume fraction	-
w	Natural frequency	Hz
$\bar{w}$	Nondimensional frequency	Hz
x , y , z	Cartesian coordinate system	m
z	Distance from neutral axis	m
θ	Fiber orientation angle	Degree
α_1, α_2	Coefficient of thermal expansion of composite material	$(1/C^{-1})$ or $(1/K^{-1})$
ρ	Density	(kg/m3)
ϵ_{xx} , ϵ_{yy} , ϵ_{xy}	Strain components	m/m
σ_{xx} , σ_{yy} , σ_{xy}	Stress components	GPa

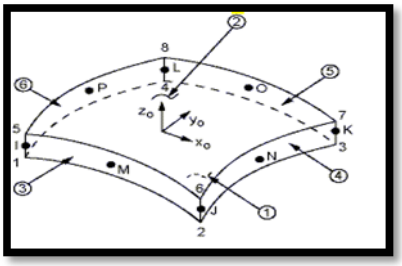

Figure . 1, Shell281 Geometry [ANSYS 13 Program]

Table 1. Dimensionless natural frequency $\bar{w} = wa^2\sqrt{\frac{\rho}{E_2 h^2}}$ of simply support symmetric cross ply laminates

a/h	[3] [HOSDT]	Present [ANSYS14.0] (Error %)	*E1/E2=40* *G12=G13=0.6E2* *G23=0.5 E2* *ν12=0.25* *a =b* *h=1* *ρ=1kgm^{-3}* *orientation* 0/90/0
5	10.263	10.12888 (1.3%)	
10	14.702	14.67395 (0.19%)	
20	17.483	17.45982 (0.13%)	
25	17.95	17.91815 (0.178%)	
50	18.641	18.62768 (0.0715%)	
100	18.828	18.79517 (0.174%)	

Table 2. Dimensionless natural frequency $\bar{w} = \frac{wb^2}{h}\sqrt{\frac{\rho}{E_2}}$ of anti-symmetric cross ply laminates

B.C'S	b/a	[9] CLPT(levy method)	present CLPT(levy method) (Error %)	*E1/E2=40* *G12=G13=0.6 E2* *G23=0.5 E2* *ν12=0.25* *a/h=10* *h=1m* *1kgm^{-3}=ρ* *orientation* 0/90
S-C-S-C	1	18.543	19.365(4.4 %)	
S-C-S-C	2	64.832	63.875 (1.48 %)	
S-C-S-C	3	137.71	140.728 (2.1 %)	
S-S-S-S	1	11.154	11.292 (1.24 %)	
S-S-S-S	2	30.468	31.749 (4 %)	
S-S-S-S	3	63.325	65.36 (3.11%)	
S-F-S-F	1	7.267	7.54 (3.6 %)	
S-F-S-F	2	7.267	7.32 (0.73 %)	
S-F-S-F	3	7.267	7.742093 (6.5 %)	

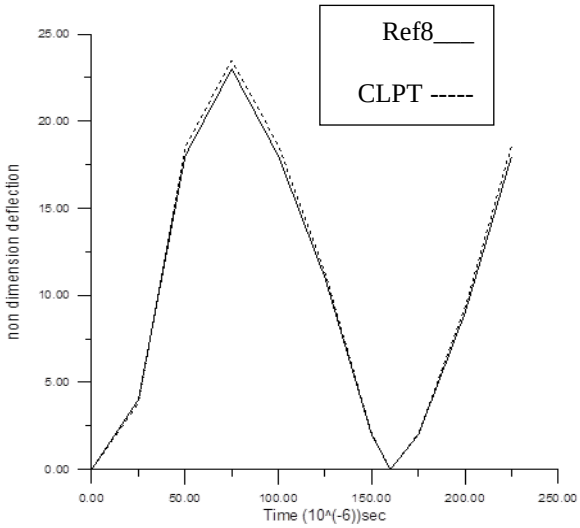

a1

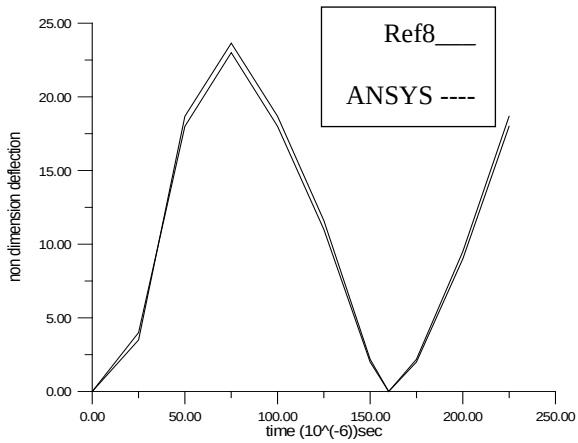

a2

Figure 2. Comparison of the present solution with the numerical solution of Reddy [8] of two-layer cross-ply (0/90) square plate under suddenly applied sinusoidal loading (a1-analytical with CLPT, a2-numerically with ANSYS).

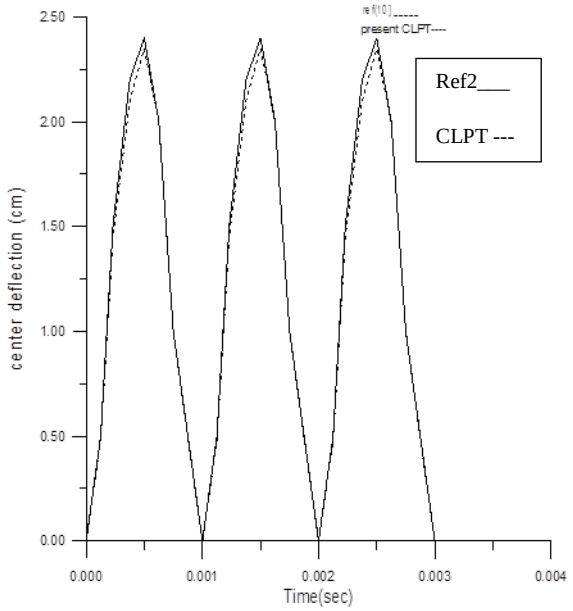

A1

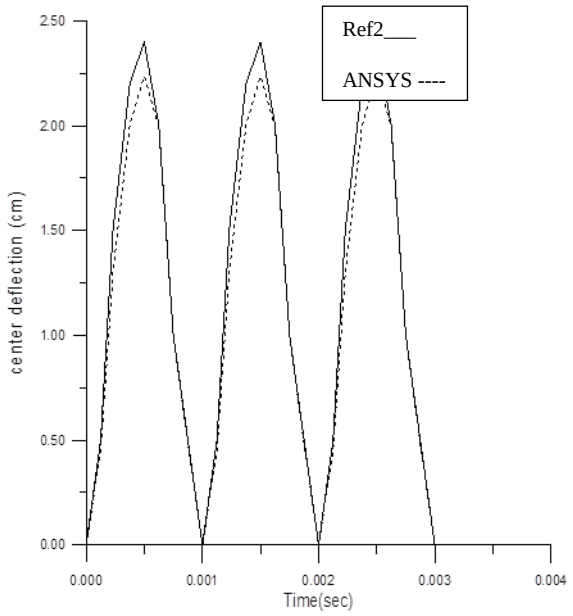

A2

Figure 3. Comparison of present study with Hui-Shen Shen et al [3] for laminated square plate under thermal loading condition at (Δ T = 200 C^0).

Table 3. Experimental unidirectional mechanical properties of fiber glass-Polyester with fiber volume fraction0.3 (Density ρ=1496.286 kg/m3).

property	Fiber-polyester composite plate
Young modulus E_1(Mpa)	22049.793
Young modulus E_2(Mpa)	4163.89
Shear Modulus G_{12}(Mpa)= G_{12}	1428.753
Shear Modulus G_{23} (Mpa)= G_{13}	1428.753

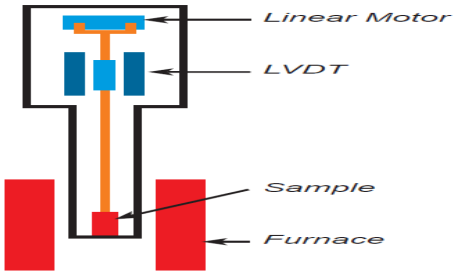

Figure 4. operating principle of TMA.

Figure 5. TMA PT1000 device.

Table4. Experimental value of mechanical and thermal properties of fiber –polyester composite plate for fiber volume fraction= 0.3 changed with temperature.

T C°	E_1 Mpa	E_2 Mpa	$G_{12}=G_{13}=G_{23}$ Mpa	α_1 E-6/K	α_2 E-6/K
20	24627.0	5588.04	1551.77	14.57	47.81
30	23343.30	4123.11	1618.65	9.03	31.7
40	21775.40	1550.22	2505.75	7.20	29.36
50	15219.80	1515.37	623.423	4.79	25.79
60	6475.41	566.8	114.2336	3.20	21.38
70	2990.82	458.59	113.535	3.18	15.60
80	2555.71	289.27	130.48	3.22	15.59
90	1471.90	210.49	158.83	3.08	15.19
100	903.90	193.84	138.48	2.91	12.58
110	741.31	191.75	131.74	2.75	11.57
120	674.40	187.53	125.23	2.57	10.47
130	644.70	186.51	122.56	2.48	9.34
140	629.01	185.19	117.59	2.45	7.67
150	612.02	182.66	107.81	2.44	5.28
160	597.61	181.88	100.28	2.44	4.19
170	592.41	173.50	95.414	2.44	3.90
180	592.22	164.55	95.04	2.45	3.88
190	591.02	163.91	85.71	2.46	3.66
200	590.57	153.3	83.64	2.47	3

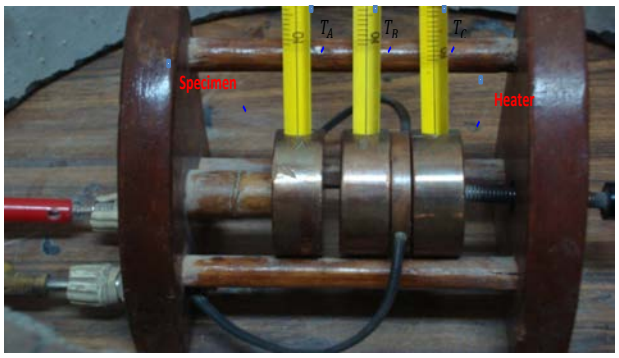

Figure 6. Lee's disk apparatus.

a- Thermal conductivity spacemen

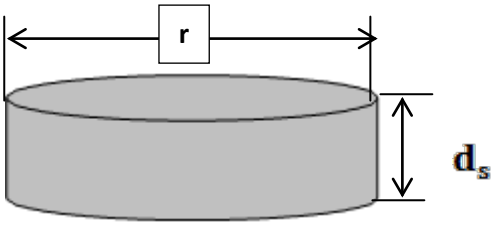

b- Dimension of thermal conductivity spacemen

Figure 7. Thermal conductivity spacemen dimension.

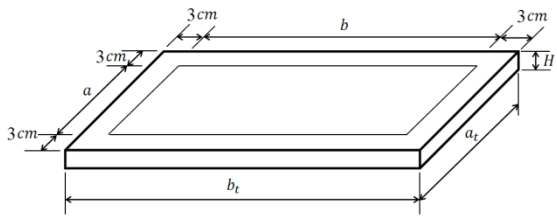

Figure 8. Dimensions of plate that used in vibration test.

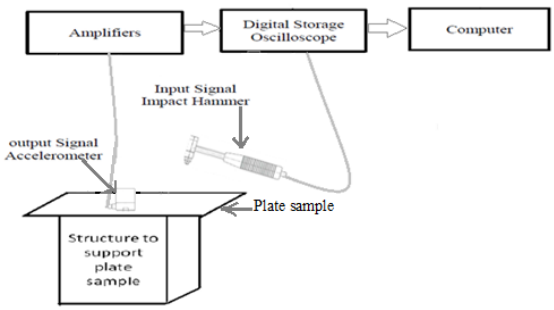

Figure9. Block diagram of vibration structure rig.

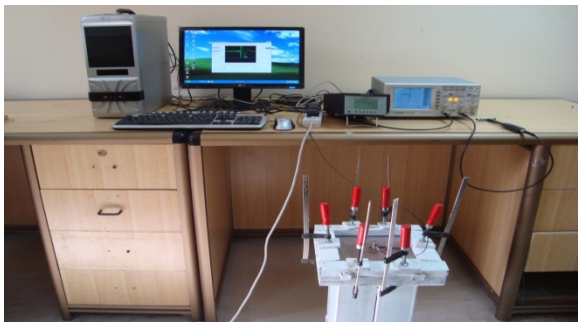

Figure 10. Rig and Vibration Test Machine of Composite Plate Structure.

Table 5. First three frequencies in (HZ) for four layers symmetric cross ply with different B.C's

B.C's	CLPT (Levy) (Error %)	Finite element ANSYS (Error %)	Experimental
SSCC	410.15**(2.2%)** 581.23**(3.5%)** 963.8**(2.5%)**	401.04**(0.10%)** 576.84**(4.2%)** 981.21**(0.71%)**	**401.461** **602.192** **988.21156**
SSSS	223.96**(3.2%)** 458.5**(1%)** 724.2**(4.3%)**	217.533**(6%)** 460.712**(0.6%)** 696.239**(7.99%)**	**231.479** **463.2736** **756.733**
SSFF	100.66**(8.7%)** 120.8**(2.3%)** 301.97**(2.9%)**	94.037**(1.5%)** 119.657**(3.2%)** 288.314**(1.7%)**	**92.644** **123.65** **293.36**

Table 6. Effect of boundary condition on natural frequency in (HZ) (0/90/90/0).

Boundary condition	Analytical Levy	F.E.M ANSYS (Error%)
S-C-S-C	410.15	**401.04 (2.2%)**
S-S-S-S	223.96	**217.533 (2.9%)**
S-F-S-F	100.66	**93.99 (6.6%)**
S-F-S-C	120.77	**124.66 (3%)**
S-C-S-S	304.5	**296.75 (2.5%)**
S-F-S-S	105.68	**105.7 (0.02%)**

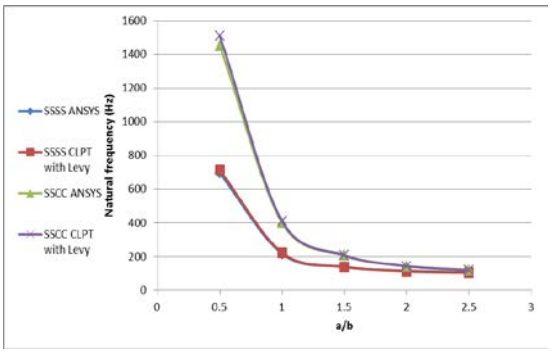

Figure 11. Effect of aspect ratio for symmetric cross plies on natural frequency.

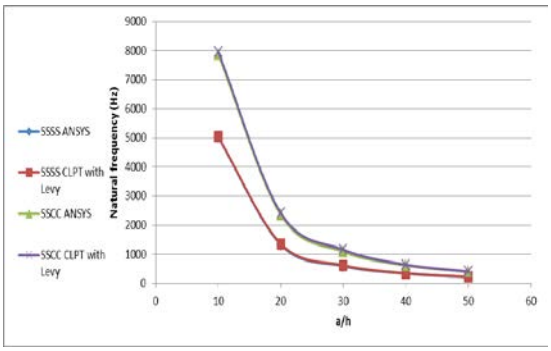

Figure 12. Effect of thickness ratio for symmetric cross plies on natural frequency.

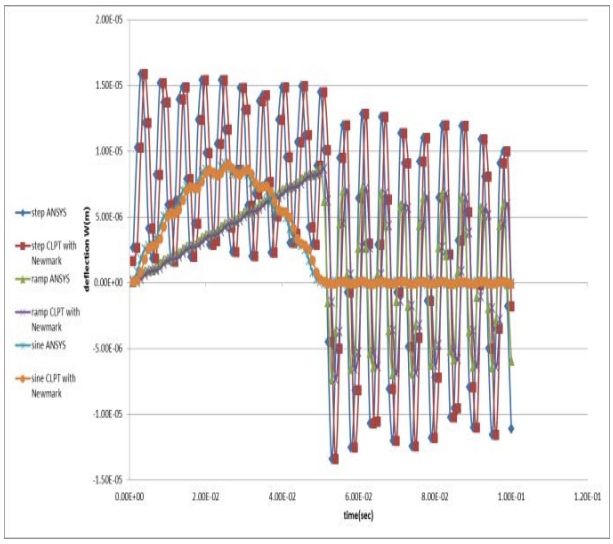

Figure 13. Central deflection of four layers symmetric cross-ply laminated plates for variant sinusoidal dynamic load without temperature change.

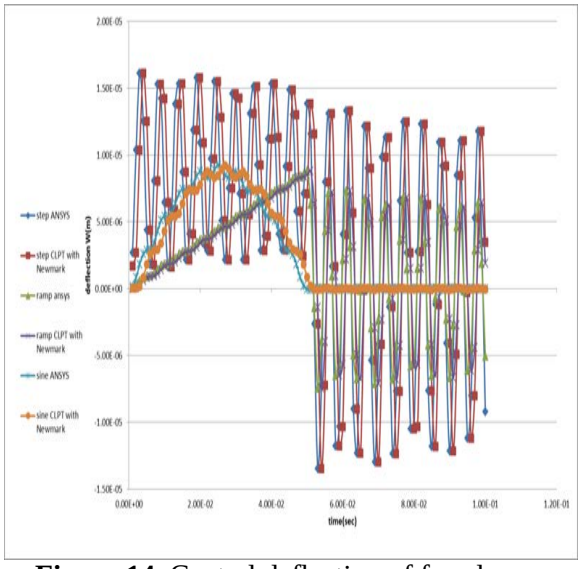

Figure 14. Central deflection of four layers symmetric cross-ply laminated plates for variant uniform dynamic load without temperature change.

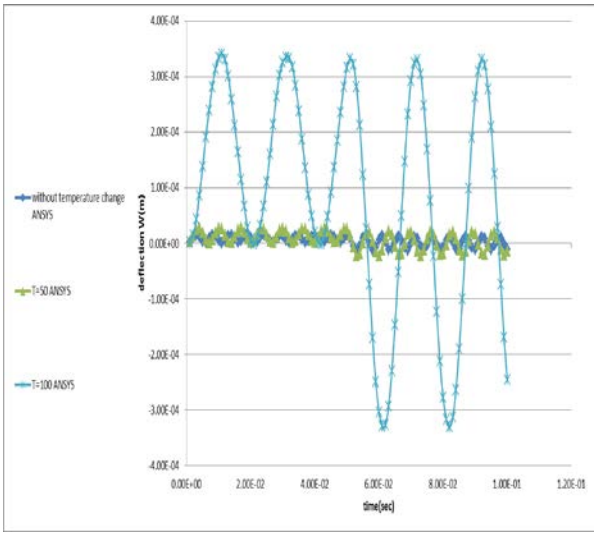

Figure 16. Central deflection of four layers symmetric cross-ply laminated plates for step sinusoidal dynamic load with temperature change.

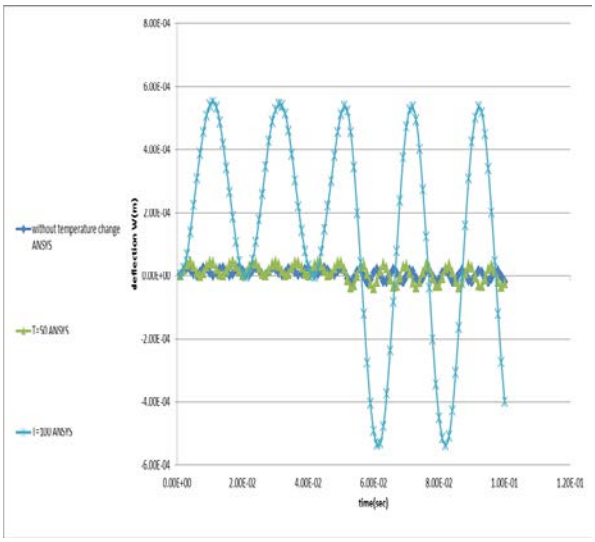

Figure 15. Central deflection of four layers symmetric cross-ply laminated plates for step uniform dynamic load with temperature change.

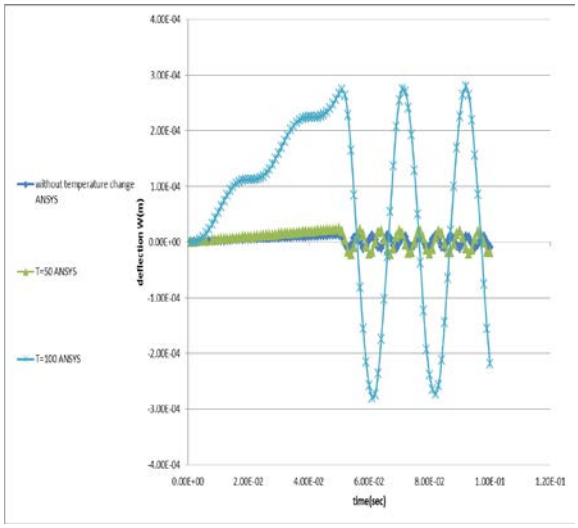

Figure 17. Central deflection of four layers symmetric cross-ply laminated plates for ramp uniform dynamic load with temperature change.

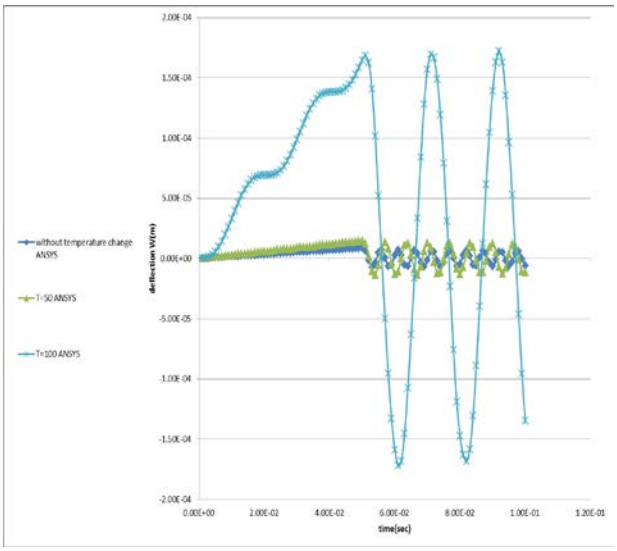

Figure 18. Central deflection of four layers symmetric cross-ply laminated plates for ramp sinusoidal dynamic load with temperature change.

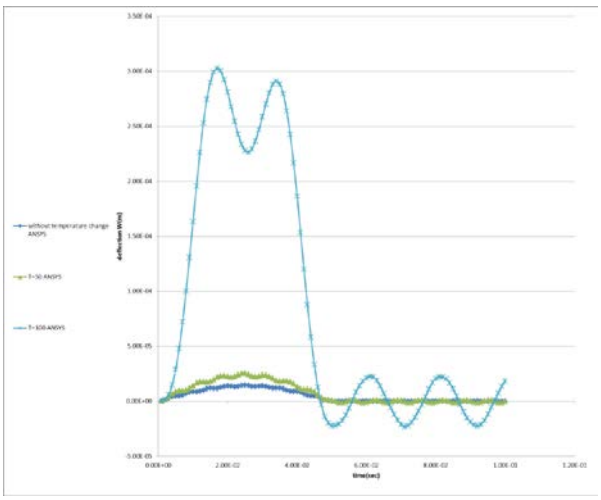

Figure 19. Central deflection of four layers symmetric cross-ply laminated plates for sine uniform dynamic load with temperature change.

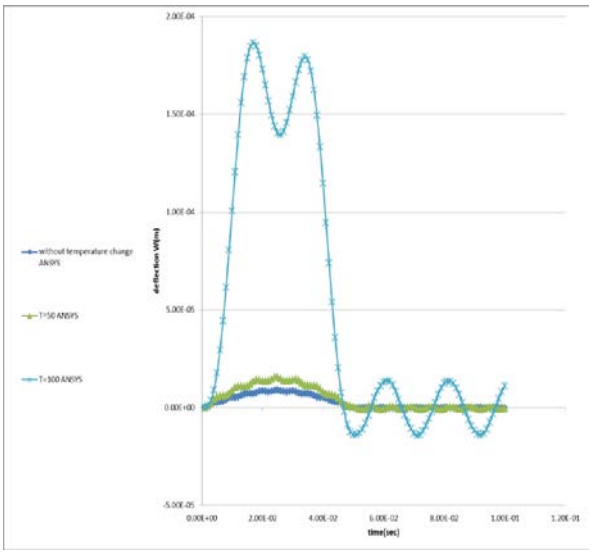

Figure 20. Central deflection of four layers symmetric cross-ply laminated plates for sine sinusoidal dynamic load with temperature change.

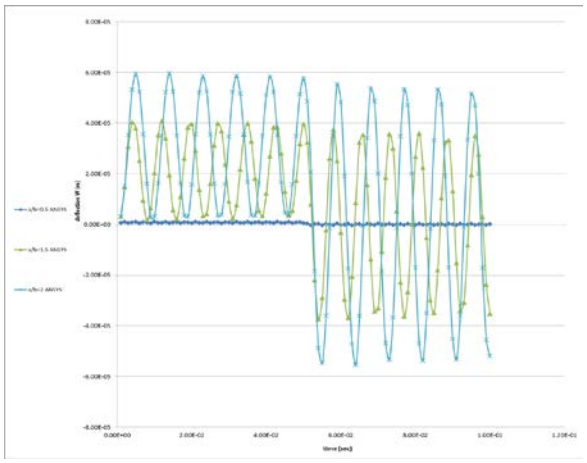

Figure 21. Effect of aspect ratio on central deflection of four layers symmetric cross -ply laminated plates for step sinusoidal dynamic load without temperature change.

Vibration Measurement and Analysis of knee-Ankle-Foot Orthosis (KAFO) Metal-Metal type

Dr.Ayad M. Takhakh
Mechanical Engineering Department- AL-Nahrain University
ayadtakak@yahoo.com

Dr.Jumaa S. Chiad
Mechanical Engineering Department- AL-Mustansirya University
jumaachaid@yahoo.com

Fahad Mohanad Kadhim
Mechanical Engineering Department- AL-Nahrain University
fahadmohanad988@yahoo.com

ABSTRACT

This paper deals with calculate stresses in Knee-Ankle-Foot-Orthosis as a result of the effect vibration during gait cycle for patient wearing KAFO .Experimental part included measurement interface pressure between KAFO and leg due to action muscles and body weigh on Orthosis. also measurement acceleration result from motion of defected leg by accelerometer .Results of Experimental part used input in theoretical part so as to calculate stresses result from applying pressure and acceleration on KAFO by engineering analysis program ANSYS 14.Resultes show stresses values in upper KAFO greater than lower KAFO that is back to muscles more effective in thigh part lead to recoding pressure higher than pressure in shank part.

Keywords: knee, ankle, foot, orthosis, pressure, stress, acceleration

قياس وتحليل الاهتزازات لمسند نوع قدم كاحل ركبة

د. اياد مراد طخاخ* **د. جمعة سلمان جياد**** **طالب الماجستير : فهد مهند كاظم***

*جامعة النهرين /كلية الهندسة /قسم الهندسة الميكانيكية
**الجامعة المستنصرية /كلية الهندسة /قسم الهندسة الميكانيكية

الخلاصة:

هذا البحث يتناول حساب الاجهادات المتولدة في مسند نوع قدم كاحل ركبة نتيجة تأثير الاهتزازات الحاصلة أثناء دورة المشي للمريض .يتضمن الجزء العملي قياس ضغط التداخل بين المسند والساق بسبب تأثير العضلات ووزن الجسم على المسند .كذلك قياس التعجيل الناتج من حركة الساق المصابة بواسطة جهاز قياس التعجيل (accelerometer) .تستعمل نتائج الجزء العملي كمدخلات في الجزء النظري ليتم حساب الاجهادات الناتجة من تسليط الضغط والتعجيل على المسند ببرنامج التحليل الهندسي ANSYS 14.اظهرت النتائج ان قيمة الاجهادات الناتجة في اعلى المسند عند عضلات الفخذ اعلى من الاجهادات الناتجة في منطقة الساق والسبب يعود الى قيمة الضغط المسجلة في منطقة الفخذ اعلى من الضغط في منطقة الساق .

الكلمات الرئيسية: قدم ، كاحل ، ركبة ، مسند، تعجيل ،ضغط ، اجهاد.

1. INTRODUCTION

An orthosis is a device that is applied to a part of the body to correct deformity, improve function or relieve symptoms of a disease. The word is derived from ortho, meaning straight [Alaa'SaeedHadi].

Orthoses added to the body to stabilize or immobilize a body part, prevent deformity, protect against injury or to assist with function. They can be divided into different types based on their intended function [CIGNA HealthCare].

The term KAFO is an acronym that stands for Knee-Ankle-Foot Orthoses and describes the part of the body that the device encompasses. The device extends from the thigh to the foot and is generally used to control instabilities in the lower limb by maintaining alignment and controlling motion. Instabilities can be either due to skeletal problems: broken bones, arthritic joints, bowleg, knock-knee, knee hyperextension or muscular weakness and paralysis [Jumaa S. Chiad].

Typically, KAFOs are extremely mechanically simple and often have few moving parts. This simplicity is accompanied by ease of donning and durability but leaves functional abilities only partially improved. Historically, KAFOs have locked the knee joint, providing stance phase stability while preventing knee motion during swing. Alternatively, KAFOs with an eccentric knee joint allow knee motion during swing but provide limited stability during stance. Either design results in inefficient gait[Jumaa S. Chiad].

These devices use a knee joint that is mechanically stable during the stance phase but releases at swing phase. The resulting gait is much smoother than the gait with a traditional KAFO where the knee remains locked throughout the entire gait cycle. Continued engineering development and creativity will be required for evolution of these designs into viable components for use by patients with knee instability during stance[Jumaa S. Chiad].

The human being in the environments of modern technology has to endure stresses of many and varied kinds of vibrations. These vibrations have significant effects on the physical and mental health. It has been observed that the stresses imposed by vibration have produced changes in the normal functions of the human body. The Whole body vibration can cause severe motion sickness which depends on the mechanical properties of the human body [AkeelZeki Mahdi].

2. EXPERIMENTAL PROCEDURE

The measurement occurred on girl under going from Polio in her left leg as a case study. The pathological subject is of age, weight, length and the residual palsy limb of 30years, 59kg, 156 cm, and 76 cm respectively.
so as to know the magnitude of stress that result from vibration in each position of knee Ankle Foot orthoses during dress up by patient must be measuring and calculate many necessary vibration data

1. Measure acceleration for KAFO by using portable acceleration sensor as shown in **Fig.1** in different position the sensor was located in
a. The center of ankle.
b. The mid of knee.
c. The mid of the thigh
The sensor was recording data, while patient was walking in her normal speed on the ground in straight way.

2. Measuring pressure: The pressure between the leg and knee Ankle foot orthotic was measured by using piezoelectric sensor as shown in **Fig.2** .The pole of sensor connected with multi-meter devise to obtain the magnitude of voltage that result from response of sensor through the stance phase explained in **Fig.3**. .The multi-meter and piezoelectric are interface with the computer and recording data as shown in **Fig. 4**. The pressure measured in shank and thigh region each position was divided into three parts longitudinal, in the middle and two parts on the terminal of the piece as shown in **Fig. 5**.The program of multi-meter giving maximum and minimum value of voltage with time Take maximum

value of this to be the pressure in this point .The procedure will be recurred to another part so as to obtain on the pressure values in all position that contact with muscles of leg as shown in **Fig. 6**. To convert the measurements to pressure, the following calibration steps must be done:

1. Using different disc masses of 50,100,….500gm
2. Put the gradual steps the masses over the pressure sensor and read the voltage from the multi-meter as shown
3. Develop the mass (or force) with voltage relationship.
4. Convert the force-voltage relation to pressure-voltage relation by dividing each force by the circular cross sectional area of sensor. The chart of calibration in **Fig. 7** is already now to using.

3. THE NUMEIRCAL ANLAYSIS

The finite element method (FEM) is now widely used in a variety of fields in engineering and science. Taking the advantage of the rapid development of digital computers with large memory capacity, as well as, fast computation. The method is recognized as one of the most powerful numerical methods because of its capabilities which include complex geometrical boundaries and non-linear material properties. In this work, FEM is with aid of ANSYS Workbench 14 software used as a numerical tool to determine the behavior of maximum stress [The Iron & Steel Society].

- Building the geometry as a model.
- Applying the boundary conditions load and obtaining the solution.
- Reviewing the results.

4. GRAPHING OF THE GEOMETRY

In this paper selection metal-metal knee ankle foot orthosis (KAFO) model was drawn by using CAD system (AUTOCAD) which processed according to an default pattern in three dimensions .The dimension was taken from the same KAFO that done on it measurement of experimental part. The aim of drawing models by AUTOCAD so as to use in ANSYS workbench program for modeling, meshing and defining boundary condition such as applied load. The models is illustrate in the **Fig. 8.**

5. MATERIAL SELECTION IN KAFO's

Various materials used in the manufacturing of KAFO depending on the type of KAFO such as (metal-metal, plastic-metal) and position of each section that building structure of KAFO like material used in the knee joint different from used in sole , the materials are: Stainless steel, Polypropylene and Aluminum

5.1. Stainless Steel

Stainless steel used for making the uprights side bars, knee joint system, ankle joint system and system shoe stirrup in of Metal – Metal KAFO as shown in **Fig. 8**. Stainless steel using in this sections because of the good characteristics like resistance to corrosion in many environments, their good mechanical properties over an extremely wide range of temperatures, and their superior resistance to oxidation and scaling at very high temperatures [The Iron & Steel Society], the mechanical properties of standard Stainless steel are listed in the **Table 2.**

5.2. Polypropylene

PP has low density and good flexibility and resistance to chemicals, abrasion and moisture, but decreased dimensional stability, mechanical strength, and resistance to UV (ultraviolet) light and heat [Maier C, & Calafut].Polypropylene used for making sole section of Metal – Metal KAFO, The mechanical properties of standard polypropylene are listed in the **Table 3.**

5.3. Aluminum:

Aluminum alloys 1200 were selected as the material for the calf band in the metal –metal KAFO in the thigh and shank section due to their light weight, high strength-to-weight ratio, corrosion resistance, and relatively low cost. , The mechanical properties of standard aluminum alloy 1200 are listed in the **Table 4**.

6. MESH OF THE MODEL

The meshing process has been done by choosing the volume, and then the shape of element was selected as tetrahedron (Automatic meshing), for metal-metal model as shown in **Fig. 9** contain total number of elements was (95298 elements) with total a number of nodes of (182108 nodes).

7. DEFINING THE ANALYSIS TYPE AND APPLYING LOAD

The boundary condition applying in the ANSYS Workbench software will be fixed support at the sole and the tip of the calf for both of shank and thigh segments. While, the interface pressure was distributed on the calf for both of shank and thigh segments shown in **Fig. 10**, and enters the values of acceleration measured in thigh, knee and Ankle shown in **Fig.11**.

8. RESULTS AND DISCUSSION

Observed by comparing the results of acceleration and frequency in the case of metal - metal knee ankle foot orthosis in **Table 1** to a person suffering from poliomyelitis disease find increase in the value of acceleration and frequency in knee joint this is due to more movement at knee joint comparing with ankle and thigh joints during gait walk cycle also it is very important to know that the knee joint is a bone region this is mean that there is no muscles working as a damper to reduce acceleration and frequency at this region according to this analysis acceleration and frequency increased in knee joint with about (62.3% and 46%) respectively comparing with ankle joint and with (30.19 %and 18.46%)respectively comparing with thigh joint.

All the readings of the interface pressure measurement are shown in **Fig. 5**.The difference between all these reading is related to value of pressure which is related to the activity of the muscles during which the pressure sensor is connected to measure the value of the interface pressure. The max value of IP in KAFO lower bands was recorded at gastrocnemius muscles with values of 28 Kpa While the max value of IP in KAFO upper band is recorded at biceps femoris and semitendinosus muscles with values of 58 Kpa.

Figs. 12 to14 show the general contour of Von Mises stress for KAFO resulted from the ANSYS 14 program. The figures also shows that the Max value of stress is recorded at the upper medial KAFO side with 23.6 Mpa in region of bar contact with Gracilis muscle, while the Max. Value of stress at upper lateral KAFO side is 5.2 Mpa at the illotibial band region. Also **Figs. 17 and 18** show that the Max value of stress is recorded at the lower lateral KAFO side with 2.49 Mpa in region of bar contact with soleus muscle, while the Max. value of stress at lower medial KAFO side is 1.62 Mpa at bar contact with peroneus longus muscle .**Figs.20-24** show the stress distribution in the uppers and lowers bands.it is clear that the Max. values of the stresses recorded in the upper bands is 6.5 Mpa exactly at the upper calf for thigh contact with semitendinosus muscles regions ,while the Max values of the stresses recorded in the lower band is 3.78 Mpa exactly at the upper calf for shank contact with gastrocnemius muscle regions .Results at figure(28) shows that the values of stresses at the upper KAFO bands (thigh) are greater than the lower KAFO bands (shank).This is certainly because of the values of pressure in the upper leg (thigh muscles)are higher than the pressure in shank muscles.

9. CONICLUSIONS

1- The max value of interface pressure in KAFO upper calf was recorded at semitendinosus muscles with values of 58 Kpa while the max value of interface pressure in KAFO lower calf was recorded at gastrocnemius muscles with values of 28Kpa.

2- The level of stresses in the upper KAFO thigh calf is greater than the lower KAFO shank thigh due to the high activities of the thigh muscles in comparison to shank muscles.

3- The maximum stress in the KAFO which was calculated numerically recorded at the bar contact with Gracilis muscle for Knee Ankle Foot Orthosis Aluminum.

4-Maximum value of frequency was recorded in knee joint with the value 6.5 Hz and maximum value of acceleration at knee joint about 5.578 m/s^2

Ankle	2.069	3.5
Knee	5.578	6.5
thigh	3.894	5.3

REFERENCES

- Alaa'SaeedHadi, 2007, "*Developing Guidelines for Improvement of Lower Limb Orthotic Health Services Through Assessment of Patients Attending Orthotic*" Workshops in Baghdad city

- CIGNA HealthCare,2008, "*Lower Limb Orthoses and Therapeutic Shoes*",

-Jumaa S. Chiad,2009 "*Analysis and Optimum Design of the Above Knee Prosthetic Socket*", Ph.D. Thesis in Mechanical Engineering, University of Technology.

- Jumaa S. Chiad and Bashar A. Bedaiwi,2012, "*Vibration Measurement and Analysis in The Blew Knee limb*" ASME International Mechanical Engineering, No.9-15.

-AkeelZeki Mahdi,2012, "*Design and Analysis of Knee Ankle Foot Orthosis (KAFO) for Paraplegia Person*" Thesis in Mechanical Engineering, University of Technology.

-The Iron & Steel Society,1999 "*Stainless Steel*".

-Maier C, & Calafut T.,1998, "*Polypropylene – the Definitive User's Guide and Data Book*", In: Woishnis, W. (Eds.), Plastics Design Library a Division of William Andrew Inc. New York.

Table1. Vibration data for metal KAFO.

Vibration data for the metal knee ankle foot orthosis		
Point	RMS Acceleration amplitude (m/s^2)	Frequency(Hz)

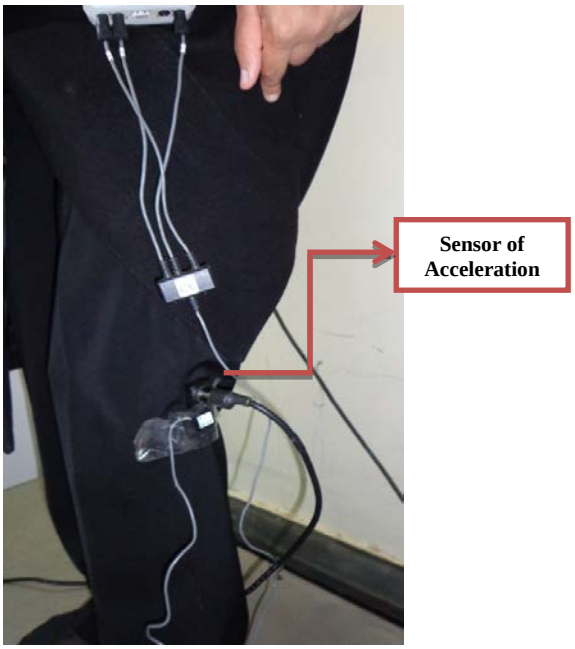

Figure 1. Acceleration sensor device.

Figure 2. The piezoelectric sensor.

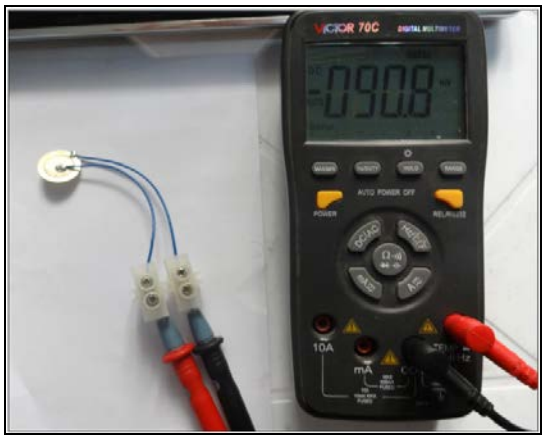

Figure 3. Pole of sensor connected with multi-meter devise.

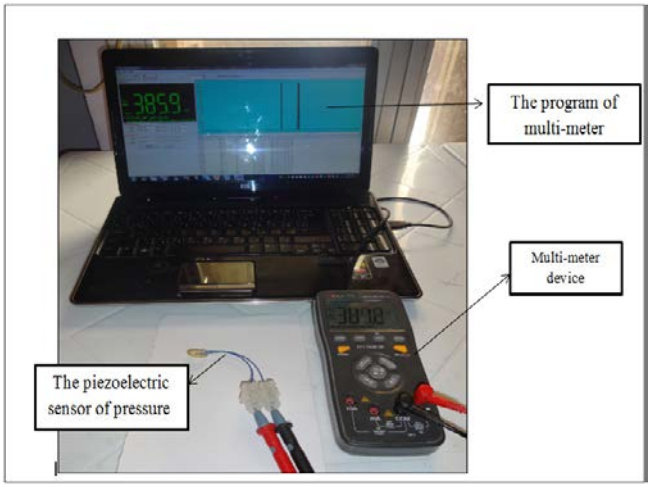

Figure 4. The multi-meter and piezoelectric are interface with the computer.

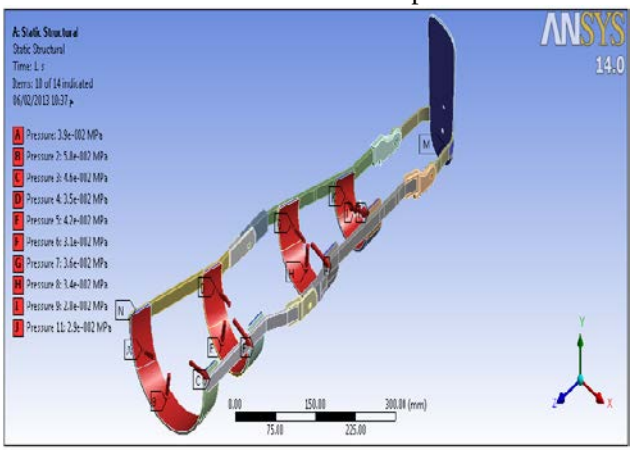

Figure 5. The model subjected to pressure load.

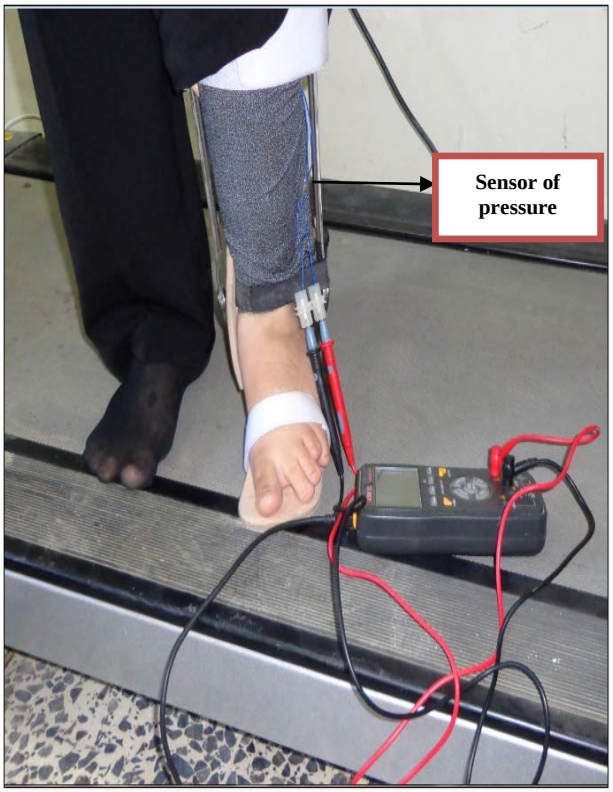

Figure 6. The pressure measured in shank region.

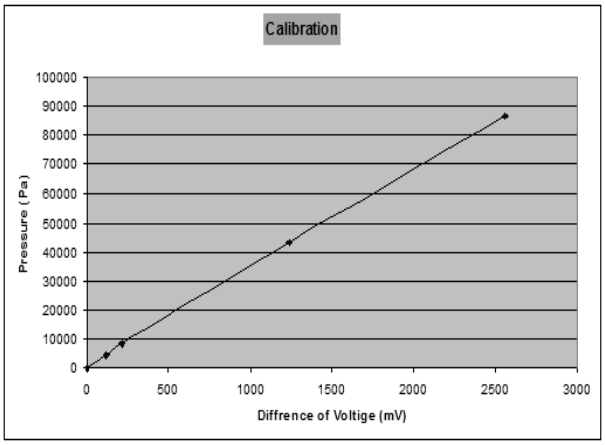

Figure 7. The calibration curve.

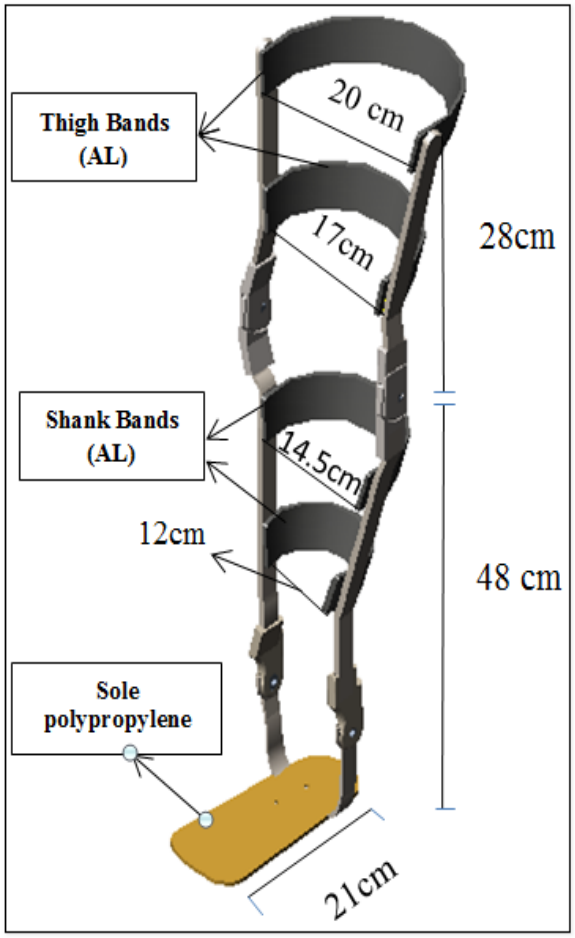

Figure 8. Graphing of the geometry and material selection in KAFO's.

Table 2. The mechanical properties of standard stainless steel.

Young's Modulus (GPa)	Poisson ratio	Density (kg/m^3)
210	0.3	7800

Table 3. The mechanical properties of standard polypropylene.

Young's Modulus (GPa)	Poisson ratio	Density(kg/m^3)
0.9	0.3	890

Table 4. The mechanical properties of aluminum alloy 1200.

Young's Modulus (GPa)	Poisson ratio	Density(kg/m^3)
70	0.3	2700

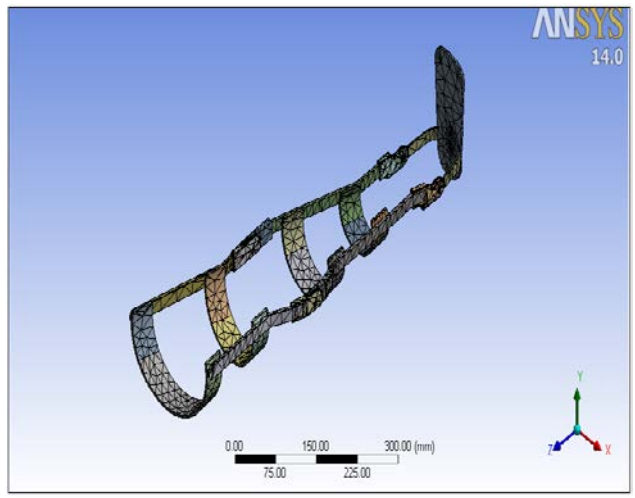

Figure 9. Mesh of the model.

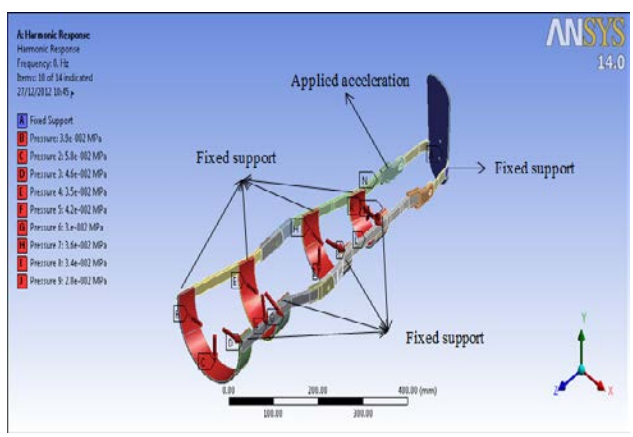

Figure 10. The model subjected to fixed support.

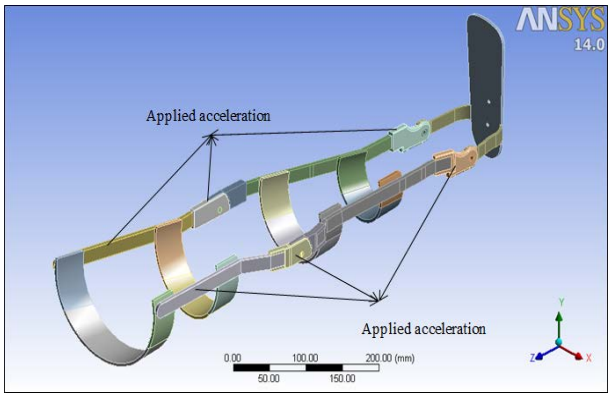

Figure 11. The model subjected to acceleration**.**

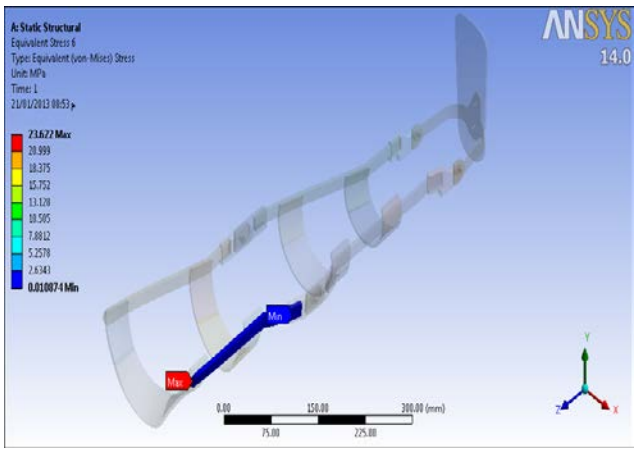

Figure 12. The Von-Misses stress due to loading boundary condition (IP) at bar contact with Gracilis muscle for KAFO Aluminum model.

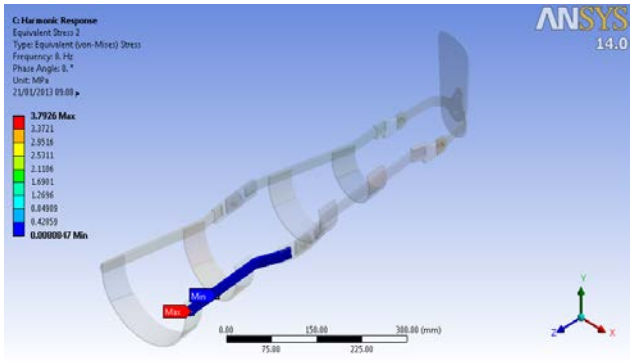

Figure 13. The Von-Misses stress due to harmonic body motion (acceleration) at bar contact with Gracilis muscle for KAFO Aluminum model.

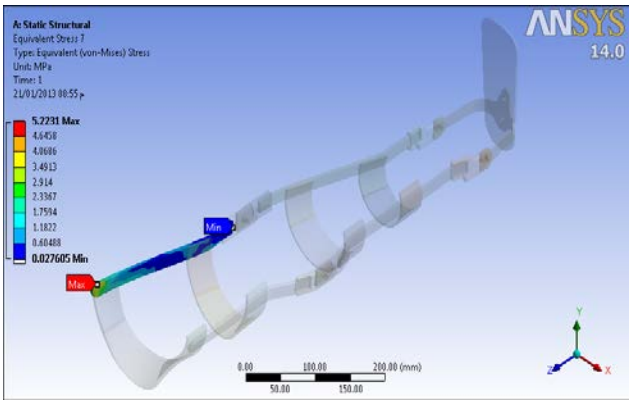

Figure 14. The Von-Misses stress due to loading boundary condition (IP) at bar contact with vastus lateralis muscle for KAFO Aluminum model.

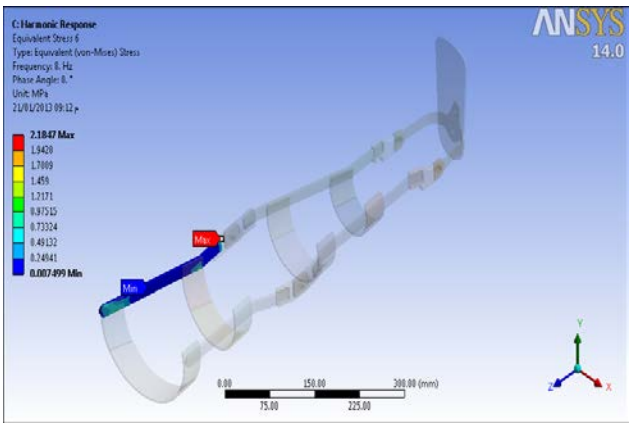

Figure 15. The Von-Misses stress due to harmonic body motion (acceleration) at bar contact with vastus lateralis muscle for KAFO Aluminum model

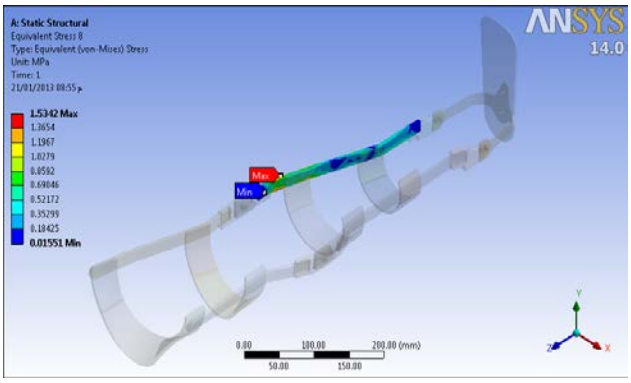

Figure 16. The Von-Misses stress due to loading boundary condition (IP)at bar contact with peroneus longus muscle for KAFO Aluminum model.

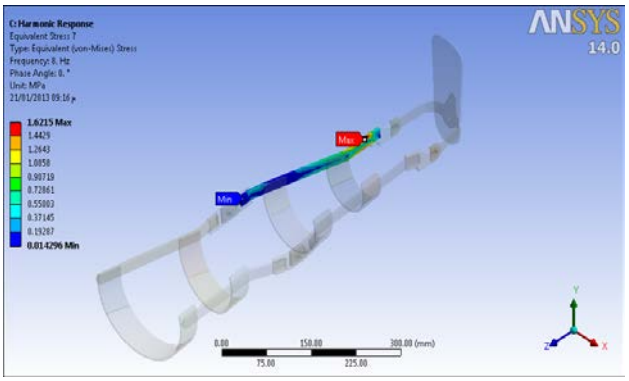

Figure 17. The Von-Misses stress due to harmonic body motion (acceleration) at bar contact with peroneus longus muscle for KAFO Aluminum model.

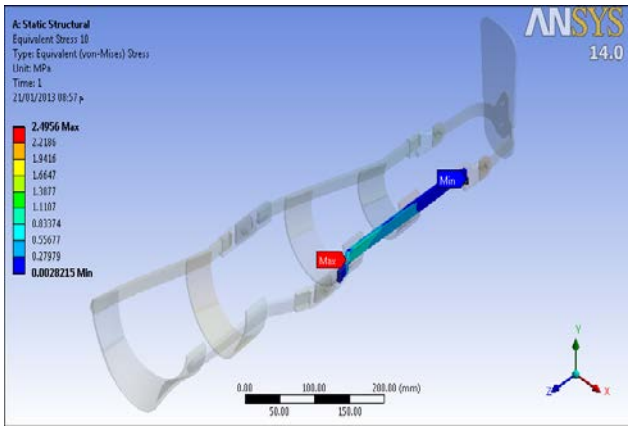

Figure 18. The Von-Misses stress due to loading boundary condition (IP) at bar contact with soleus muscle for KAFO Aluminum model.

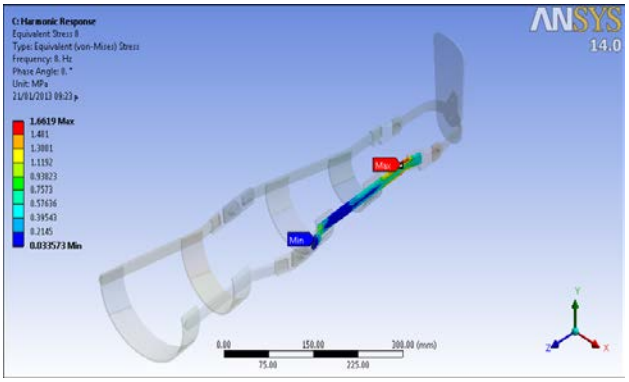

Figure 19. The Von-Misses stress due to harmonic body motion (acceleration) at bar contact with soleus muscle for KAFO Aluminum model.

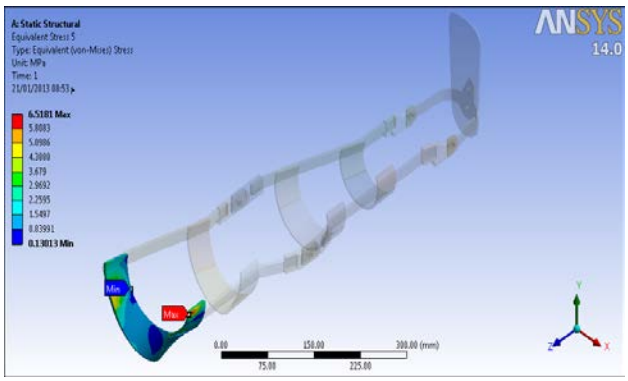

Figure 20. The Von-Misses stress due to loading boundary condition (IP) at upper calf for thigh contact with semitendinosus for KAFO.

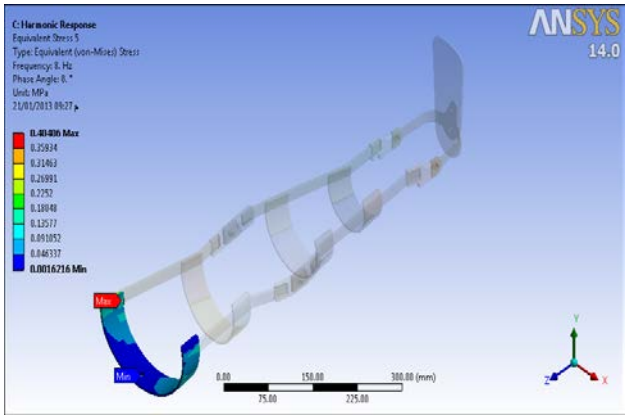

Figure 21. The Von-Misses stress due to harmonic body motion (acceleration) at upper calf for thigh contact with semitendinosus for KAFO.

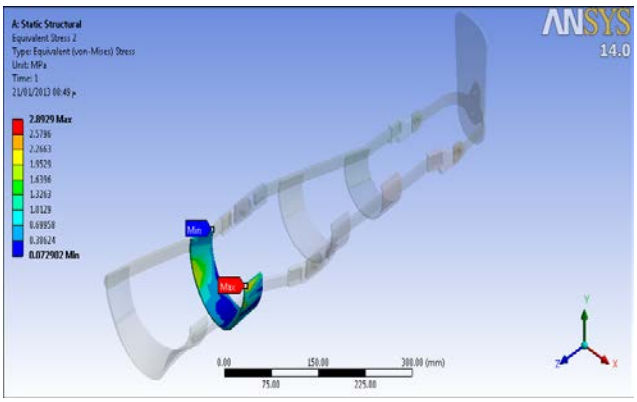

Figure22. The Von-Misses stress due to loading boundary condition (IP) at lower calf for thigh contact with semitendinosus for KAFO.

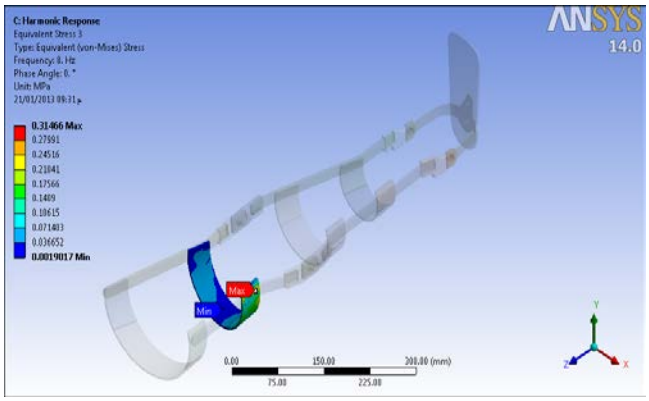

Figure 23 The Von-Misses stress due to harmonic body motion (acceleration) at lower calf for thigh contact with semitendinosus for KAFO.

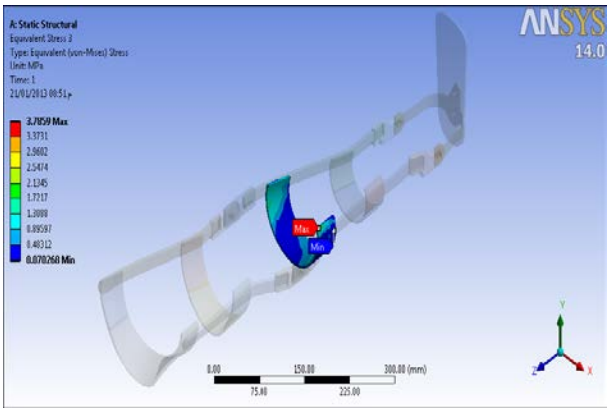

Figure 24. The Von-Misses stress due to loading boundary condition (IP) at upper calf for shank contact with gastrocnemius muscle for KAFO.

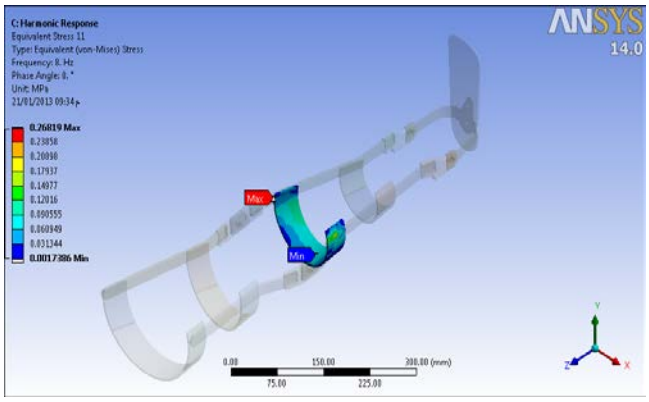

Figure 25. The Von-Misses stress due to harmonic body motion (acceleration) at upper calf for shank contact with gastrocnemius muscle for KAFO.

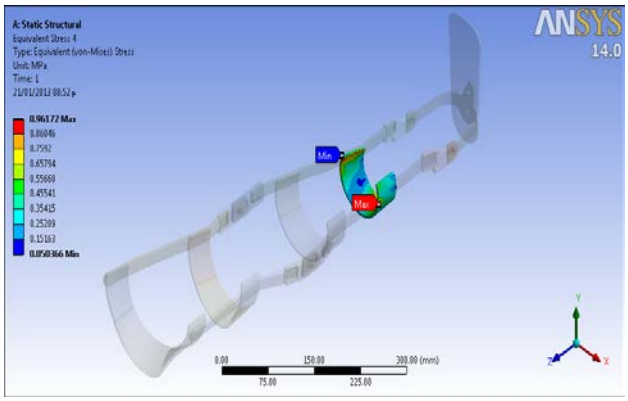

Figure 26. The Von-Misses stress due to loading boundary condition (IP) at lower calf for shank contact with gastrocnemius muscle for KAFO.

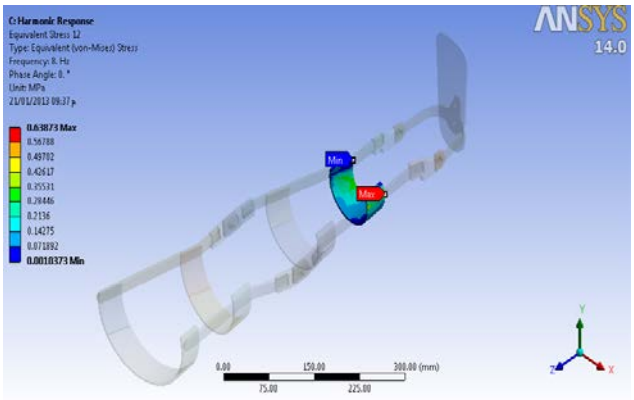

Figure 27. The Von-Misses stress due to harmonic body motion (acceleration) at lower calf for shank contact with gastrocnemius muscle for KAFO.

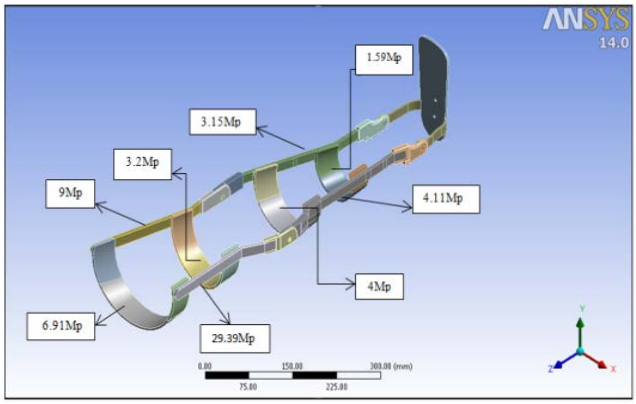

Figure 28. Total stress result from applied pressure and acceleration on the model.

FINITE ELEMENT EQUATION

The displacements are represented by the following equations:

$$u = C_{11} + C_{12}X + C_{13}Y + C_{14}Z$$
$$v = C_{21} + C_{22}X + C_{23}Y + C_{24}Z \qquad (1)$$
$$w = C_{31} + C_{32}X + C_{33}Y + C_{34}Z$$

Considering the nodal displacements, the following equations must be satisfied:

$$u = u_I \text{ at } X = X_I \quad Y = Y_I \text{ and } Z = Z_I$$
$$u = u_J \text{ at } X = X_J \quad Y = YJ \text{ and } Z = Z_J$$
$$u = u_K \text{ at } X = X_K \quad Y = Y_K \text{ and } Z = Z_K$$
$$u = u_L \text{ at } X = X_L \quad Y = Y_L \text{ and } Z = Z_L$$

Similarly, requirements must be satisfied:

$$v = v_I \text{ at } X = X_I \quad Y = Y_I \text{ and } Z = Z_I$$
$$v = v_J \text{ at } X = X_J \quad Y = YJ \text{ and } Z = Z_J$$
$$v = v_K \text{ at } X = X_K \quad Y = Y_K \text{ and } Z = Z_K$$
$$v = v_L \text{ at } X = X_L \quad Y = Y_L \text{ and } Z = Z_L$$

Also:

$$w = w_I \text{ at } X = X_I \quad Y = Y_I \text{ and } Z = Z_I$$
$$w = w_J \text{ at } X = X_J \quad Y = YJ \text{ and } Z = Z_J$$
$$w = w_K \text{ at } X = X_K \quad Y = Y_K \text{ and } Z = Z_K$$
$$w = w_L \text{ at } X = X_L \quad Y = Y_L \text{ and } Z = Z_L$$

Substitution of respective nodal values into **Eq. (1),** results in 12 equations and 12 unknowns:

$$u_I = C_{11} + C_{12}X_I + C_{13}Y_I + C_{14}Z_I$$
$$u_J = C_{11} + C_{12}X_J + C_{13}Y_J + C_{14}Z_J \qquad (2\text{-a})$$
$$u_K = C_{11} + C_{12}X_K + C_{13}Y_K + C_{14}Z_K$$
$$u_L = C_{11} + C_{12}X_L + C_{13}Y_L + C_{14}Z_L$$

Also,

$$v_I = C_{21} + C_{22}X_I + C_{23}Y_I + C_{24}Z_I$$
$$v_J = C_{21} + C_{22}X_J + C_{23}Y_J + C_{24}Z_J \qquad (2\text{-b})$$
$$v_K = C_{21} + C_{22}X_K + C_{23}Y_K + C_{24}Z_K$$
$$v_L = C_{21} + C_{22}X_L + C_{23}Y_L + C_{24}Z_L$$

And

$$w_I = C_{31} + C_{32}X_I + C_{33}Y_I + C_{34}Z_I$$
$$w_J = C_{31} + C_{32}X_J + C_{33}Y_J + C_{34}Z_J$$
$$w_K = C_{31} + C_{32}X_K + C_{33}Y_K + C_{34}Z_K \qquad (2\text{-c})$$
$$w_L = C_{31} + C_{32}X_L + C_{33}Y_L + C_{34}Z_L$$

Solving for the unknown C-coefficients, substituting the results back into **Eq.(1)**, and regrouping the parameters, obtained:

$$u = S_1u_I + S_2u_J + S_3u_K + S_4u_L$$
$$v = S_1v_I + S_2v_J + S_3v_K + S_4v_L \qquad (3)$$
$$w = S_1w_I + S_2w_J + S_3w_K + S_4w_L$$

The shape functions are:

$$S_1 = \frac{1}{6V}(a_I + b_IX + c_IY + d_IZ)$$
$$S_2 = \frac{1}{6V}(a_J + b_JX + c_JY + d_JZ) \qquad (4)$$
$$S_3 = \frac{1}{6V}(a_K + b_KX + c_KY + d_KZ)$$
$$S_4 = \frac{1}{6V}(a_L + b_LX + c_LY + d_LZ)$$

Where V, the volume of the tetrahedral element, is computed from:

$$6V = \det\begin{vmatrix} 1 & X_I & Y_I & Z_I \\ 1 & X_J & Y_J & Z_J \\ 1 & X_K & Y_K & Z_K \\ 1 & X_L & Y_L & Z_L \end{vmatrix} \qquad (5)$$

The a_I, b_I, c_I, d_I… d_L-terms are:

$$a_I = \det\begin{vmatrix} X_J & Y_J & Z_J \\ X_K & Y_K & Z_K \\ X_L & Y_L & Z_L \end{vmatrix} \qquad b_I = -\det\begin{vmatrix} 1 & Y_J & Z_J \\ 1 & Y_K & Z_K \\ 1 & Y_L & Z_L \end{vmatrix}$$
$$c_I = \det\begin{vmatrix} X_J & 1 & Z_J \\ X_K & 1 & Z_K \\ X_L & 1 & Z_L \end{vmatrix} \qquad d_I = -\det\begin{vmatrix} X_J & Y_J & 1 \\ X_K & Y_K & 1 \\ X_L & Y_L & 1 \end{vmatrix} \qquad (6)$$

The only six independent stress components are needed to characterize the general state of stress at a point. These components are:

$$[\sigma]^T = [\sigma_{xx}\ \sigma_{yy}\ \sigma_{zz}\ \tau_{xy}\ \tau_{yz}\ \tau_{xz}] \qquad (7)$$

Where σxx, σ_{yy}, and σ_{zz} are the normal stresses and τ_{xy}, τ_{yz}, and τ_{xz} are the shear-stress components. For the displacement vectors that measure the changes occurring in the position of a point within a body when the body is subjected to a load, it may be recall that the displacement vector $\vec{\delta}$ can be written in terms of its Cartesian component as:

$$\vec{\delta} = u(x,y,z)\,\vec{i} + v(x,y,z)\,\vec{j} + w(x,y,z)\,\vec{k} \tag{8}$$

The general state of strain is characterized by six independent components as given by:

$$[\varepsilon]^T = [\varepsilon xx \quad \varepsilon_{yy} \quad \varepsilon_{zz}\ \gamma xy\ \gamma yz\ \gamma xz] \tag{9}$$

Where ε_{xx} , ε_{yy} ,and ε_{zz} are the normal strains and γ_{xy} , γ_{yz} , and γ_{xz} are the shear-strain components. The relationship between the strain and the displacement is represented by:

$$\begin{gathered} \varepsilon_{xx} = \frac{\partial u}{\partial x} \qquad \varepsilon_{yy} = \frac{\partial v}{\partial y} \qquad \varepsilon_{zz} = \frac{\partial w}{\partial z} \\ \gamma_{xy} = \frac{\partial u}{\partial y} + \frac{\partial v}{\partial x} \qquad \gamma_{yz} = \frac{\partial v}{\partial z} + \frac{\partial w}{\partial y} \qquad \gamma_{xz} = \frac{\partial u}{\partial z} + \frac{\partial w}{\partial x} \end{gathered} \tag{10}$$

Equations (10) can be represented in matrix form as:

$$\{\varepsilon\} = LU \tag{11}$$

Where:

$$\{\varepsilon\} = \begin{Bmatrix} \varepsilon_{xx} \\ \varepsilon_{yy} \\ \varepsilon_{zz} \\ \gamma_{xy} \\ \gamma_{yz} \\ \gamma_{xz} \end{Bmatrix} \quad \text{and} \quad LU = \begin{Bmatrix} \frac{\partial u}{\partial x} \\ \frac{\partial v}{\partial y} \\ \frac{\partial w}{\partial z} \\ \frac{\partial u}{\partial y} + \frac{\partial v}{\partial x} \\ \frac{\partial v}{\partial z} + \frac{\partial w}{\partial y} \\ \frac{\partial w}{\partial x} + \frac{\partial u}{\partial z} \end{Bmatrix}$$

L is commonly referred to as the linear-differential operator.

Over the elastic region of material, there is also exists a relationship between the state of stressed and strains, according to the generalized Hook's law. This relationship is given by the following equations:

$$\begin{gathered} \varepsilon_{xx} = \frac{1}{E}\left[\sigma_{xx} - v(\sigma_{yy} + \sigma_{zz})\right] \\ \varepsilon_{yy} = \frac{1}{E}\left[\sigma_{yy} - v(\sigma_{xx} + \sigma_{zz})\right] \\ \varepsilon_{zz} = \frac{1}{E}\left[\sigma_{zz} - v(\sigma_{xx} + \sigma_{yy})\right] \\ \gamma_{xy} = \frac{1}{G}\tau_{xy} \qquad \gamma_{yz} = \frac{1}{G}\tau_{yz} \qquad \gamma_{zx} = \frac{1}{G}\tau_{zx} \end{gathered} \tag{12}$$

The relationship between the stress and strain can be expressed in a compact-matrix form as:

$$\{\sigma\} = [D]\{\varepsilon\} \tag{13}$$

Where,

$$\{\sigma\} = \begin{Bmatrix} \sigma_{xx} \\ \sigma_{yy} \\ \sigma_{zz} \\ \tau_{xy} \\ \tau_{yz} \\ \tau_{xz} \end{Bmatrix}$$

$$[D] = \frac{E}{1+v}\begin{bmatrix} \frac{1-v}{1-2v} & \frac{v}{1-2v} & \frac{v}{1-2v} & 0 & 0 & 0 \\ \frac{v}{1-2v} & \frac{1-v}{1-2v} & \frac{v}{1-2v} & 0 & 0 & 0 \\ \frac{v}{1-2v} & \frac{v}{1-2v} & \frac{v}{1-2v} & 0 & 0 & 0 \\ 0 & 0 & 0 & \frac{1}{2} & 0 & 0 \\ 0 & 0 & 0 & 0 & \frac{1}{2} & 0 \\ 0 & 0 & 0 & 0 & 0 & \frac{1}{2} \end{bmatrix}$$

$$\{\varepsilon\} = \begin{Bmatrix} \varepsilon_{xx} \\ \varepsilon_{yy} \\ \varepsilon_{zz} \\ \gamma_{xy} \\ \gamma_{yz} \\ \gamma_{xz} \end{Bmatrix}$$

For a solid material under triaxial loading, the strain energy Λ is:

$$\Lambda^{(e)} = \frac{1}{2}\int_V (\sigma_{xx}\varepsilon_{xx} + \sigma_{yy}\varepsilon_{yy} + \sigma_{zz}\varepsilon_{zz} + \tau_{xy}\gamma_{xy} + \tau_{xz}\gamma_{xz} + \tau_{yz}\gamma_{yz})dV \tag{14}$$

Or, in a compact matrix form,

$$\Lambda^{(e)} = \frac{1}{2}\int_V [\sigma]^T \{\varepsilon\} dV \tag{15.a}$$

Substituting for stresses in terms of strains using Hook's law, equation (14) can be written as:

$$\Lambda^{(e)} = \frac{1}{2}\int_V \{\varepsilon\}^T [D]\{\varepsilon\} dV \tag{15.b}$$

By using the four-node tetrahedral element to formulate the stiffness matrix. Recall that this element has four nodes, with each node having three translational degrees of freedom in the nodal x-, y-, and z-directions. The displacements u, v, and w in terms of the nodal values and are represented by:

$$\{u\} = [S]\{U\} \tag{16}$$

Where,

$$\{u\} = \begin{Bmatrix} u \\ v \\ w \end{Bmatrix}$$

$$[S] = \begin{bmatrix} S_1 & 0 & 0 & S_2 & 0 & 0 & S_3 & 0 & 0 & S_4 & 0 & 0 \\ 0 & S_1 & 0 & 0 & S_2 & 0 & 0 & S_3 & 0 & 0 & S_4 & 0 \\ 0 & 0 & S_1 & 0 & 0 & S_2 & 0 & 0 & S_3 & 0 & 0 & S_4 \end{bmatrix}$$

$$\{U\} = \begin{Bmatrix} u_I \\ v_I \\ w_I \\ u_J \\ v_J \\ w_J \\ u_K \\ v_K \\ w_K \\ u_L \\ v_L \\ w_L \end{Bmatrix}$$

Beginning by relating the strains to the displacement field and, in turn, to the nodal displacements through the shape functions. It is needed to take the derivatives of the components of the displacement field with respect to the x-, y-, and z- coordinates according to the strain-displacement relation, Eq.(11). The operation results in:

$$\begin{Bmatrix} \varepsilon_{xx} \\ \varepsilon_{yy} \\ \varepsilon_{zz} \\ \gamma_{xy} \\ \gamma_{yz} \\ \gamma_{xz} \end{Bmatrix} = \begin{bmatrix} \frac{\partial S_1}{\partial x} & 0 & 0 & \frac{\partial S_2}{\partial x} & 0 & 0 & \frac{\partial S_3}{\partial x} & 0 & 0 & \frac{\partial S_4}{\partial x} & 0 & 0 \\ 0 & \frac{\partial S_1}{\partial y} & 0 & 0 & \frac{\partial S_2}{\partial y} & 0 & 0 & \frac{\partial S_3}{\partial y} & 0 & 0 & \frac{\partial S_4}{\partial y} & 0 \\ 0 & 0 & \frac{\partial S_1}{\partial z} & 0 & 0 & \frac{\partial S_2}{\partial z} & 0 & 0 & \frac{\partial S_3}{\partial z} & 0 & 0 & \frac{\partial S_3}{\partial z} \\ \frac{\partial S_1}{\partial y} & \frac{\partial S_1}{\partial x} & 0 & \frac{\partial S_2}{\partial y} & \frac{\partial S_2}{\partial x} & 0 & \frac{\partial S_3}{\partial y} & \frac{\partial S_3}{\partial x} & 0 & \frac{\partial S_4}{\partial y} & \frac{\partial S_4}{\partial x} & 0 \\ 0 & \frac{\partial S_1}{\partial z} & \frac{\partial S_1}{\partial y} & 0 & \frac{\partial S_2}{\partial z} & \frac{\partial S_1}{\partial y} & 0 & \frac{\partial S_3}{\partial z} & \frac{\partial S_3}{\partial y} & 0 & \frac{\partial S_4}{\partial z} & \frac{\partial S_4}{\partial y} \\ \frac{\partial S_1}{\partial z} & 0 & \frac{\partial S_1}{\partial x} & \frac{\partial S_2}{\partial z} & 0 & \frac{\partial S_2}{\partial x} & \frac{\partial S_3}{\partial z} & 0 & \frac{\partial S_4}{\partial x} & \frac{\partial S_4}{\partial z} & 0 & \frac{\partial S_4}{\partial x} \end{bmatrix} \begin{Bmatrix} u_I \\ v_I \\ w_I \\ u_J \\ v_J \\ w_J \\ u_K \\ v_K \\ w_K \\ u_L \\ v_L \\ w_L \end{Bmatrix} \tag{17}$$

Substituting for the shape function using the relation of equation (4) and differentiating:

$$\{\varepsilon\} = [B]\{u\} \tag{18}$$

Where,

$$[B] = \frac{1}{6V} \begin{bmatrix} b_I & 0 & 0 & b_J & 0 & 0 & b_K & 0 & 0 & b_L & 0 & 0 \\ 0 & c_I & 0 & 0 & c_J & 0 & 0 & c_K & 0 & 0 & c_L & 0 \\ 0 & 0 & d_I & 0 & 0 & d_J & 0 & 0 & d_K & 0 & 0 & d_L \\ c_I & b_I & 0 & c_J & b_J & 0 & c_K & b_K & 0 & c_L & b_L & 0 \\ 0 & d_I & c_I & 0 & d_J & c_J & 0 & d_K & c_K & 0 & d_L & c_L \\ d_I & 0 & b_I & d_J & 0 & b_J & d_K & 0 & b_K & d_L & 0 & b_L \end{bmatrix}$$

And the volume V and the b-, c-, and d- terms are given by **Eqs. (5) and 6).** Substituting into the strain energy equation for the strain components in terms of the displacements, obtained:

$$\Lambda^{(e)} = \frac{1}{2}\int_V \{\varepsilon\}^T [D]\{\varepsilon\} dV = \frac{1}{2}\int_V [U]^T [B]^T [D][B][U] dV \tag{19}$$

Differentiating with respect to the nodal displacements yields:

$$\frac{\partial \Lambda^{(e)}}{\partial U_K} = \frac{\partial}{\partial U_K}\left(\frac{1}{2}\int_V [U]^T [B]^T [D][B][U] dV\right) \tag{20}$$

for K=1, 2,., 12

Evaluating of **Eq.(20)** results in the expression $[K]^{(e)}\{U\}$ and, subsequently, the expression for the stiffness matrix, which is:

$$[K]^{(e)} = \int_V [B]^T [D][B] dV = V[B]^T [D][B] \tag{21}$$

Where V is the volume of the element. Note that the resulting stiffness matrix will have the dimensions of 12x12.

The load matrix for a tetrahedral element is a 12x1 matrix. For a concentrated – loading situation, the load matrix is formed by placing the components of the load at appropriate nodes in a appropriate directions. For a distributed load, the load matrix is computed from the equation:

$$\{F\}^{(e)} = \int_A [S]^T \{P\} dA \tag{22}$$

Where $\{P\} = \begin{Bmatrix} p_x \\ p_y \\ p_z \end{Bmatrix}$

And A represents the surface over which the distributed-load components are acting. The surfaces

of the tetrahedral element are triangular in shape. Assuming that the distributed load acts on the I-J-K surface, the load matrix becomes:

$$\{F\}^{(e)} = \frac{A_{I-J-K}}{3}\begin{Bmatrix} p_x \\ p_y \\ p_z \\ p_x \\ p_y \\ p_z \\ p_x \\ p_y \\ p_z \\ 0 \\ 0 \\ 0 \end{Bmatrix} \tag{23}$$

The load matrix for distributed load acting on the other surface of the tetrahedral element is obtained in a similar fashion.

Place Identity in Defining Urban Space of Border Rivers in Historical City Centres

Dr. Mohammed Qasim Abdul Ghafoor Al Ani
Al Nahrain University – College of Engineering – Architecture Department - Baghdad- Iraq
PhD Instructor- Consulting Architect & Urban Designer E-mail: mohammedkassim66@yahoo.com

ABSTRACT

In the city, building space could transform to be as place, because architecture does not include only traditional values such as housing, human protection, stability, etc, but could carry other dimensions beyond the housing or building occupancy or develop urban design. Rivers had vision in motion as a way to show dynamic processes in its flowing slowly, which are simply measured in time and the life of citizens.

The research consider the river path in traditional cities as Alley connecting the spaces of the city ... old Baghdad was characterized by this property and it is look like Venice in the past, while traditional European cities were able to preserve this property till now, and capable to take transformation of the city with development projects inside it. These cities was distinguished by development of river edge as creating place along the river corridor and try to attract peoples who lived in, protect the natural environment along the river, as well as reflect the characteristics of the city along of the elevation of the river, and conserve the river banks as alley connected between urban spaces.

Baghdad which penetrates by Tigris River has maintained this feature until the middle of twentieth century. So now, the research can see the absence of specialized local studies, including The comprehensive development plan of the Baghdad city 2030 to study and Re design the spaces and places along river edge, this led to emerge research problem, in the absence of specific knowledge about identity of river space characteristics for identification of urban space in place of the Tigris River in downtown of Baghdad historical city center, in the urban development plans since the mid-twentieth century until now, and study design factors that contributed with disintegration of the space syntax relations in river elevation. Turning to the experience of historical European cities and how to deal with urban space to the edge of the river and created the identity of the place, especially the interface development experience the (Seine river in Paris, Thames River in London, Tiber River in Rome, Danube River in Vienna & Budapest, Vltava river in Prague) and study urban style in dealing with the river edge, in order to reach the elements which define the identity of each city. In order to reach the aim of research in redefining the identity of places for urban spaces overlooking to integrate the banks of Tigris River in the historical city centre of Baghdad, and the methods of linking the development of river front with the comprehensive development plan of the Baghdad city 2030.

Key words: waterfronts, historic architecture, urban design, urban renewal, development city center.

هوية المكان في تعريف الفضاء الحضري لحافات الأنهر في مراكز المدينة التاريخية

الدكتور محمد قاسم عبد الغفور العاني

الخلاصة

في المدينة، يمكن أن يحوّل الفضاء المبني إلى مكان, فالعمارة لا تشمل القيم التقليدية فقط كالسكن وتوفير الحماية للإنسان والاستقرار، الخ، وإنما من الممكن أن تحمل أبعاد أخرى تتجاوز السكن أو إشغال البناية أو السبب الحضري من التصميم. وتمتاز الأنهر بحرية الحركة في الرؤية, وهي وسيلة لإظهار الديناميكية والحيوية الموجود في هذه العمليات والتي هي ببساطة تقاس بالوقت.

يعتبر مسار النهر في المدن التقليدية بمثابة **زقاق رئيسي تفتح عليه فضاءات المدينة... واتسمت بغداد القديمة بهذه الخاصية** وكانت تبدو شبيهة بمدينة فينيسيا, بينما استطاعت المدن الأوروبية التقليدية بالمحافظة على هذه الخاصية, واستيعاب التحولات والتطورات المرحلية. وامتازت هذه المدن بأهداف تطوير الحافة النهرية المتمثلة في خلق ترابط على طول الممر النهري ومحاولة جذب العامة إلى النهر, والعمل على حماية البيئة الطبيعية على طول مسار النهر فضلاً عن دراسة الواجهة النهرية لتعبر عن خصوصية المدينة. وحافظت هذه المدن على اعتبار النهر كزقاق ومتصل حضري يربط ضفتيه. واستطاعت بغداد ونهر دجلة الذي يخترقها أن تحافظ على هذه الميزة لغاية أواسط القرن العشرين.

إن غياب الدراسات المحلية المتخصصة, وضرورة دعوة الدراسات المحلية ومنها المخطط الإنمائي الشامل لمدينة بغداد عام 2030 إلى دراسة الناحية التخطيطية والتصميمية للحافة النهرية ولد المشكلة البحثية, في **غياب المعرفة المحددة لهوية فضاء النهر وخصائص تعريف هوية المكان في الفضاء الحضري لنهر دجلة داخل مركز مدينة بغداد التاريخي في مخططات التنمية الحضرية منذ أواسط القرن العشرين ولحد الآن, ودراسة العوامل التصميمية التي ساهمت بتفكك العلاقات الفضائية في الواجهة النهرية.** وبالعودة إلى تجربة المدن الأوروبية وكيفية التعامل مع الفضاء الحضري لحافة الأنهر وخلق هوية للمكان, **وخاصة تجربة تطوير واجهة (نهر السين في باريس, نهر التايمز في لندن, نهر التيبر في روما, نهر الدانوب في فينا وبودابست, نهر فالتافا في براغ)** ودراسة الأنماط الحضرية في التعامل مع الحافة النهرية, من اجل الوصول إلى العناصر التي أعطت تعريف لهوية المكان لكل مدينة. من اجل الوصول إلى هدف البحث في **إعادة تعريف هوية المكان للفضاء الحضري المطل على نهر دجلة داخل مركز بغداد ألتأريخي, وأساليب ربط تطوير الواجهة النهرية بالمخطط الإنمائي الشامل لبغداد 2030** .

كلمات البحث: الواجهات النهرية، الهندسة المعمارية التاريخية, التصميم الحضري, التجديد الحضري, تطوير مركز المدينة.

1. INTRODUCTION

Water is important to the life and culture of human kind which led to rich practices of water harvesting and water storage/conservation reflected in the development of considerable variations in the forms of water structures, deep stepped basins. Amongst Living Cultural heritage, the performing and visual arts including painting and sculpture, folk, tribal art and handicrafts are significant. This unique environment along with the context of color, festivities and traditional way of life accumulate to become the incredibly rich heritage. That is "Baghdad", Despite its growth from a small princely town to an important heritage destination, it has retained the hierarchical relationship between the city and the people. Its heritage is very much a part of its daily life and constitutes the Baghdad river side of bright and colorful costumes, festivals and historic fine arts.

In recent years, the development of waterfront areas in the world has gradually become the hot spot. A lot of cities are enthusiastic about developing the waterfront areas. However, since the urban design renewal theory in Iraqi starts relatively late, it cannot thoroughly improve the waterfront environment. It is the urgent task of develop workers to attach great importance on the landscape ecology theory and draw on the advanced waterfront urban planning experience of foreign countries, combine the relevant scientific knowledge, start from the ecological environment of the whole city and respect the local culture so that the waterfront urban design may serve the city better. Moreover, they shall sum up a set of practical waterfront urban design theory. The research is carried out on the basis of this.

The absence of local specialized studies and invite local studies, including comprehensive development report to the need to study urban design side of river edge born problem in **the absence of planning standards research to the physical edges of the Tigris River in**

downtown Baghdad, and the emergence of **Western studies specialized in developing methodology planning research**, and the need for Western studies analysis of the design and planning study of applicability on the edge of river within the city of Baghdad.

The absence of a fact to the waterfront urban planning design of water as well as the absence of controls, and this was confirmed by the urban development project for the city of Baghdad 2030 (phase I – final report).

1 URBAN WATERFRONT OF THE CITY

1.1 Cities and the Water Relation

The first great cities on the whole are to be found in great river valleys and basins. Irrigation on the necessary scale seems to have been developed first of all in central Mesopotamia—between the Tigris and the Euphrates—from about 6000 BC. There the first city-scale developments were built in Sumer, at Uruk (c. 3500 BC), Ur (c. 3100 BC) and Eridu (c. 2750 BC). The presence of great rivers made irrigation possible.

Power naturally accrued to those who built and controlled the irrigation systems, not to mention the defenses. None of this could have been achieved without centralized planning. Small wonder then, that the first cities show evidence of social stratification and the development of craft specializations.

So, four things in the first place, made the city possible:

- The separation of the built-up area from the surrounding countryside, possibly by defensive walls.

- The development of irrigation systems for intensive agriculture.
- The development of power structures by which the irrigation systems, and other aspects of urban life, could be controlled—usually by kings and priests.
- The development of craft-specialties to serve not only the needs or the desires of the urban population but also as bases for trade.**Broadbent, 1990**.

So on Al-Mansur founded the rounded Baghdad city on the western side in (756-762 AC).

Since the ancient times, the urban development cannot live without water. The city depends on water and the water is the lifeline of urban life. The function of the water to the urban manifests its **ecological** adjustment function, the **ornamental** function, the **economical** function, the **cultural** function and **social** function. Many cities are formed along the water and thrive because of the water. The place with water around has always been the place where natural lives yearn for. Furthermore, the developed river system promotes the **transportation**, which further develops commodity circulation and commercial prosperity. **In such a way, cities are formed. People live along the water and water culture evolves.** The water holds the important status in the urban space environment. Both the ancient and modern cities home and abroad often primordially consider water source in its selection of the location. (Huang, 2011, P.1162)

Since cities were founded in these things, it is hardly surprising that cities ever since have been permeated by them or their equivalents. As for their physical design, cities and parts of cities have grown in two ways. The first is described by, **Alexander, 1964,** as **the natural way** in which people simply start building, as they still do in the shanty towns of the emerging world. And then there is **the artificial way** in which a master plan is prepared; streets laid out, squares and urban blocks on to which buildings are then placed according to some planners' sense of order. This contrast will recur many times in the research. So wills another contrast: between formality and informality. **The 'natural' city tends towards informality**, not to mention an apparent disorder **whilst the planners will want their conscious decisions to show**. Most planners aim for regularities of a kind which show that human minds have been at work; but some aim for a self-conscious irregularity of the kind we call Picturesque. This is largely about that contrast but of course it will have to be put into context. **Broadbent, 1990.**

The Importance of Urban Waterfront is a particular region of the city. It means the land or buildings which are adjacent to the city part of the water body such as the rivers, lakes and oceans, and it plays an important role in the city:

- The waterfront is a kind of scarce resources in the city, and it has great **economic value**. Usually, the Urban Waterfront has the **advantage of landscapes and traffic**, therefore it is **active in business and real estate activities, and the land price is higher** than some other regions. Waterfront building often represents the degree of the development of each city and the social image.
- The waterfront has unique community **cultural values.** Waterfront could supply the people's lives hydrophilic sites, and attract a large number of people and business to be gathered here to view, play, and enjoy the water. For example, the hydrophilic sites which are created along will make the management of the river towards to the functions of **leisure development**, using "water" as the starting point for the public to show the story of a city through the ages.
- The waterfront has the natural advantages of **climate and landscape value**, and it can regulate the local climate, cleaning up the environment, providing people with a high quality of life, **Hongyu, 2010**. Such as the European cities, it attracts numerous tourists to spend their holidays for its picturesque landscape and pleasant weather Waterfront can provide people with **health, leisure and quality of life**, but flooding is a major threat to its security. When we are enjoying the benefits of the waterfront, **the flood prevention and hazard reduction must be focused in urban design to ensure the safety of the waterfront**.

1.2 From space to achieve place in waterfront

A sense of a place of emotional gratification of components through living in a desirable and close itself and reflects the general concepts, goals and needs as a sense of support. The identity and cohesion of the community, keeps the place memories retains its value as image, and allows for a person to dream of quietly, and carries the imagination and memory for image formation. Hence the importance of the place and felt it was one of the factors that incorporate ideas and memories to create continuity factors.

The space could transform to be place, architecture does not include traditional values

just as housing and provide protection and stability but could carry other dimensions beyond the housing or building works or urban design.

The rivers have freedom of movement, vision in motion which is a way to show the dynamic processes in simply measured with time. The section river edge works as indicator used in design since the difference in water level, river edge influence shape and form design inorder to define the identity of the place.

The place is not abstract meaining, but is all made of real things and possess a moral and material, formal, sensory properties and symbolism are specific environmental identification constitutes the core of the place. The place product of many forces, **natural and social history**, and a **spatial property** create human environment satisfactory, either stages of sense of place: (**attention, sensation, feeling, perception, cognitive perception**).

1.3 Principles of the Place of Waterfront

The main feature of the waterfront area design trend to solve a series of complex and comprehensive problems; it refers to many areas of knowledge and technology. Waterfront has many functions in the city's natural systems and social systems, such as **water conservancy, transportation, recreation, urban image, and ecological function**, etc. Therefore, the waterfront project involves **shipping, river training, water reserves and supply, adjusting flood drainage, vegetation and animal habitat conservation, water quality, energy, urban security, architecture and urban design** and other aspects. Each city's rivers or the waterfront area has its own unique functional requirements and cultural characteristics, **Fig.1**. This determines the waterfront planning and landscape design should be a multi-angle designs which able to meet the characteristics of different cities. Urban waterfront landscape cultural design includes the reasonable functional of landscape visual aesthetic artistry and regional culture etc. The design achieves the **harmony between people and places**. Construction of urban waterfront areas should re-examine the city of this valuable resource based on new ideas, and carry out the waterfront urban design from the city's eco-systems, landscape systems, cultural systems and cultural factors. Among those cultural factors are particularly important, **Zhu, 2011**.

Along with the social and economical development, the construction and exploitation of the urban shore districts has become increasingly active, particularly since this century, many cities has carved in the development of the water shore area. Generally speaking, these efforts are fruitful. But problems also exist, as in **Huang, 2011**.

1.3.1 Social purpose

The **expansion of city changes the structure of urban fabric** and alienates people from the nature. So, the people lack the necessary and useful contact with the nature. As a result, the design of waterfront shall provide the chance for city dwellers to touch the nature and protect the present water culture in a city, fully excavate and continue the historical and cultural characteristics of a city, and carry forward the profound humanistic background and **shape the new images of a city**.

1.3.2 Ecology principle

Waterfront urban design is an important part of the open space of a city and the material carrier of the entertainment activity of city dwellers. As the compound area for the intersection of land, water and wetland, water can adjust the temperature and humidity of a city.

Ecology refers to the interactive relationship between the **living beings and environment**. To protect and develop the water resource of a city and provide city dwellers with a harmonious living environment is the responsibility that cannot be avoided by the city design. The waterfront landscape space shall provide the **link for the city to contact the nature**. Together with vegetation, water can improve the physical environment of a city, create a good ecological environment and shoulder the responsibility of adjusting the ecology of a city. So It is the **green corridor of a ci**ty and an important “base” for maintaining and establishing the biological diversity of a city.

1.3.3 Economic purpose

The waterfront space is not only a space for visiting and resting but also the material carrier of entertainment economy. Excellent waterfront space will **demonstrate the unique feature of a city** to the people, attract visitors from other places and rise people’s entertainment and consumption desire, therefore, promote the development of the tertiary industry, provide more employment opportunities for the dwellers and create more **wealth for the city.**

1.3.4 Respect regional culture

The urban elements for waterfront design shall give priority to the local features so as to display the regional character, Artful application will highlight the local characteristics; meanwhile, the local plants have the advantages of high survival rate and low maintenance cost. The hard composition elements of waterfront design such as the **bulding facade, shelters, street furnitures, bank, footpath, road pavement and decoration**, etc, **Fig. 1**. should also use local materials as much as possible. The local materials can bring very striking local characteristics and reflect the language of different from the common run. The design of benches, railing and indication board shall also adopt the symbols with the local features so as to show the extraordinary temperament of the city.

The modeling of waterfront shall reflect the local spirit. Therefore, the design should firstly understand the history and culture and excavate the deep historical connotation of the site. The waterfront usually embodies very rich historical memory. It seems that the **old stone bridge, ancient shipside, the building character and decoration patterns of the local folk house**, improve the vigor of waterfront and shape the new image of a city**.**

1.4 The Impact Factors on the Shaping Waterfront

Based on the affecting factors that planning and design of river edge, depending on the specificity of historic cities. These factors can be applied to river edge and waterfront:

1.4.1 City and water culture

The human feel with his entity about the place of memories associated with his passion and a meaningful for him, that human existence is through man's relationship to the world as meaning where the emotional and sentimental meanings leading to its **interaction with belonging to the place**.

Water is the origin of life. It is the substances that distribute the widest on the Earth. It is most important physical conditions people live on. It is closely linked with humanity's activity. The nation water culture is well-established. In the long-term production lifecycle, people have maintained a close relation with the water. From the initial worship of water, the awe to the water, the ancients had transmitted gradually to understand, exploit, utilize and appreciate water, and develop many philosophy, these thoughts are glittering throughout in the national culture that brands deeply in each heart's. And in the human development and evolution, people also express their understanding, therefore water culture with material and the spiritual wealth formed.

1.4.2 Preparation of alternative planning strategies

Show alternatives available to study the effects of planning and process planning design principles in the development of the river contain the following interface **Fig. 2**, **Nickels,2006** :

- **Linear Strategies**: it depends on the open space with a strong linear axis along the water edge and then publishes the spaces and events along the water edge. It emphasizes the strong interdependence between North and South.
- **The String of Pearls Strategies**: it depends on the nodes, and in this schema have five major nodes which bind the public spaces of the city with the edge of the water. This schema defines the events along the water's sites and main poolers, which note the relationship exists and its surroundings from the land.
- **The Bow Tie Strategies**: in this schema the focus of activity in the northern and southern edge with node status and these three are linked through a linear parks.

1.5 The Components of the Waterfront

The human factors of waterfront urban design should focus on the **combination of modernity and tradition** to embody the **spirit of local color and culture**. Although it is carrying out modern-style design, it cannot be completely to depart from the local culture and local humanistic history. There are two ways to deal with this issue. **Zhu, 2011**.

- In order to retain the traditional graphic patterns or the cultural spirit, it follows the traditional layout on the whole and presents a certain modern style and modern technology on handling the materials and pitch points.
- Another method is to abstract traditional modeling form and to use symbolic forms for migrating into the modern design in order to make people to receive the information and trace of history indistinctly.

The waterfront design can pass through the following aspects of the specific designed to enhance the cultural factors, as **measured factors of urban waterfront** and problem in its design:

1.5.1 Land Use

The entire visual order of a city is like an organism in that it is not made up of self contained parts. Interaction between the parts is continuous and essential to form a **coherent and legible urban environment'**. **Mixed land-use** along the waterfront can be classified as one which includes the palace complex, residential, commercial, religious and institutional uses. Although, the social/political climate of the formative years led to definitive patterns of land use and hierarchies in the built form, they have diluted due to changes over time. However, certain influences still remain. **Samant, 2010**.

1.5.2 Activities

The River City's history is linked closely by several aspects of the ancient events that were taking place on the river edge and ancient buildings and their functions and locations for river edge and old river edge location change and dealing with the current displacement. Contribute to events taking place on the river edge and recovery as well as the nature of actors influence in determining the nature of design and furnishing. **Casalino, 2005.**

Some cities neglect the local characteristics in the construction of the waterfront. They apply mechanically the success stories home and abroad, blindly pursuing the so-called modernization. The civic culture is formed after a long term accumulation, and the waterfront often is the carrier of its history and culture. Neglecting the historical background of the city will result in the absence of the special characteristic of the city and its **spatial identity**, destroying the unique image of the water shore city, affecting the extension the urban culture. **Huang, 2011.**

1.5.3 Landscape & Plant design

Plant design should take into account of the characteristics of the waterfront landscape, namely waterside. The best choice is the cultivation of hydrophytes, such as reed, flag leaf, water lily, iris pseudacorus, etc. These plants not only contribute to the **better environment**, but also **clean the waters**. Moreover, the growing season of plants should be concerned. Specifically, there are multiple seasonal cycles of plant in the same landscape, and this produces that the landscape has a corresponding plant in each season. However, we must choose the plants, which can match the date of the historical events, in designing some waterfront landscape of a memorial and historical of events. And this leads to the best view of the whole landscape in the activity's period. Therefore, plant is one of elements in the landscape system design and has an impact on it. (Zhu, 2011, P.6566).

1.5.4 Built Form

The place structure where the relationship between space and the viewer, or between elements as a set of relationships that appear in a specific point of time and place.

The historic area along city waterfront with its sense of place through its distinctive organic order, density, vernacular architecture and a built form that is recognizable as a singular entity. Built form is a result of evolution that has been guided by dominant determinants such as its **socio-economic hierarchy/structure**, **political and religious factors, climate, availability of materials and technology**. **Samant, 2010**.

1.5.5 Sidewalk design

The sidewalks along the river give opportunity to **bring the community to the waterfront**, and the successful experiences to convert a few areas to public space and promoting River environment without negative impact on them through design. As well as benefit from the extension of sidewalks in the foreground area increase River and deal with different levels provided site sitting River sessions and various optical sights, **Fig. 1**. Disconnect the movement area from seating and other events by creating two levels, one for movement and the other for other actors, as well as the use of different levels in **creating fun and diversity** of the views of the urban landscape.

In the process of the design, it is should be considered specific and various factors, such as paving design. It can use the representative image of signs or **historical signs**, and **paving brick or granite** to collage out the image texture on the floor. This can be applied to a large ground and a larger image. Another method can be applied to handle details. For instance, it collages with small stone on the corner line or a small ground. This produces that the overall design is novel and unique and harmonizes with the surrounding cultural environment. That not only riches the details of design but also enhances the depth of cultural connotation. **Zhu, 2011.**

1.5.6 Façade

Determines location based on vertical and horizontal elements, the **vertical elements are more effective** than horizontal levels in identifying where you can define space and create a sense of containment and moving in complete place perspective.

Continuous façade is formed along the river due to the positioning of various institutions, the relationship between them and the retaining wall. The elevation is dominated by the towering palace and fort walls but is also characterized by temple and domes and pavilions which are intricately carved with geometrical and floral patterns. **Samant, 2010.**

1.5.7 Public facilities design

Public facilities are an important component of the waterfront design. The feature of waterfront is closer people and water. In the design of public facilities, protective barrier is used in **protecting of seat and platform** where people can enjoy the waterscape and wood platform or wooden plank road also is used, **Fig.3**. Therefore, people can walk on the plank road, **close with water in the platform or play in the water**. Additionally, **pavilion** which is designed for visitors to rest, it's also commonly used in waterfront design. Pavilion not only takes fully into account the safety problem, but also pays attention to the cultural connotation in the design. According to the style of the overall design layout, it can use the corresponding style which can be a traditional style, simple modern style or a combination of traditional and modern elements which abstracts traditional symbols and uses modern methods to re-design, **Zhu, 2011.**

1.5.8 Streets and Squares

Represents a positional place relationship between ground place dimensions depending on the geometry and some researchers have linked between spot and area social and economic slide that occupy the place as well as events, **Fig. 2.**

The accessibility is an important index in measuring the development of the waterfront. In many urban waterfronts, we cannot see convenient **public pedestrian paths** to the water shore. With no enough **wide-open surfaces**, the water body is always **blocked by the buildings and walls**. Close to the water but seeing no water distances people and the water psychologically, **Huang, 2011**.

The street pattern was laid out to provide accessibility and create natural drainage on the hilly terrain. Depending on the usage, a **hierarchy in the street pattern** is observed in the area. The principle streets identified were bazaar streets with higher concentration of activities that were large in scale, **connecting important nodes, punctuated by small and large landmarks, and led from city gates and culminated at the important buildings, Samant, 2010.**

1.5.9 Parks

Parks along the water edge provides a unified identity to the edge. The most vital attribute of the success of the water edge is dealing with parks, designed with all the features and details. Park is working along the water edge and provides a **unified identity** to the edge, **Casalino, 2005.**

The concept of Greenway is various, but the general accepted concept is: The greenway is the land line network systems being planned, designed, and managed with ecological, recreational, cultural, aesthetic and many other functions, which is a **sustainable pattern of land-use**. The greenway is an open space usually along the construction of a natural corridor such as river banks, valleys, and mountains or along the recreation entertainment channel transformed by railway, a canal, a landscape road or other routes. Ahern summed up the characteristics of the **greenway**: The **shape of the contour line**; with connectivity; have versatility; to meet the requirements of sustainable development strategies; and the most important thing is that the greenway is the important supplement of the other non-linear landscape planning, by connecting to other non-linear system of Landscape Architecture to form an integrated whole, in order to the purpose of protection, rather than replace other planning. The design combine the greenway and waterfront together in order to make use of characteristics of greenway to improve the landscape and spatial design of waterfront, and at the same time to perfect flood control and disaster mitigation system, **Fig. 1**., **Hongyu, 2010**.

1.5.10 Monument & Art sculpture

The furnishing of waterfront elements need to know the monuments and street furniture in configure those spaces which depending on the nature and form of use.

Art sculpture can be a very good performance of the waterfront cultural characteristics. Sculpture generally divided into emboss and circular

engraver: emboss often used in walls, floors texture and the decoration of public facilities; circular engraver often used in the spacious plazas and wide lawns. The artistic form of sculpture can choose **typical historical stories**, myths, legends or characters as a theme. And then using the way of telling story can display artistically the cultural history of the region. In addition, sculpture can select **modern design methods** such as abstract geometric shapes and bright colors. It can harmonize well with the surrounding landscape, natural environment and local human culture, and this contributes to contrast the cultural atmosphere of the whole landscape. **Zhu, 2011.**

1.5.11 Slips

Means water bodies inside edge are successful means in **bringing people to the edge** and make it (cross gain connection) which is historically present naturally, **Fig. 4**. In modern designs it is dealing with this part of river edge through a small stalls and aquariums, toys as well as small parks and sometimes water Bank gateways of the city. **Burden, 2005.**

City should provide convenient transportation corridor that can enable the people to reach the water area and the sight-line corridor so that the waterfront urban design can be "available completely". The transportation system of urban waterfront area shall provide people with convenient transportation and attract people to the side of water. The transportation in the waterfront design shall **reduce the interference from motor vehicles** as much as possible so as to ensure the safety of walking and the quietness and beauty of environment. Street sight-line corridor shall provide more chances for the contact of man and nature, **Fig. 3**.

- The sight line in certain distance shall be ensured so that the visual contact between man and nature or humanistic landscape can be maintained and the beautiful sceneries **will not be blocked**.
- The water landscape should be **"penetrated" to the inner part of a city** as much as possible.
- The waterfront building should be designed to have the graded sense.
- By the side of water, some low-rise structures can be arranged and higher buildings should be far away from the water.

Furthermore, the arrangement should be arranged in picturesque disorder so as to get the best water visual angle. By the side of water, some friendly and safe water-playing space can be deployed so that people can play and enjoy water. **Huang, 2011.**

1.5.12 Under Bridge

The bridges and cross-pillar make the edge of the River in the usual impediments to traffic. So the area under the bridge (part of river edge) must be designed so as to allow the space under the bridge to **diverse uses** along the river and **link with neighboring** river edge parts. **Casalino, 2005.**

The space strategy of flood prevention as The waterfront area is rapidly developing in cities now, and its ability to flood prevention and hazard reduction has also been greatly improved. In order to contole on the area under bridge, there are major mitigation strategies of flood prevention and hazard reduction, and its principle includes that, solid fundamental, the formation of the level of the poor and the creation of a continuous channel. **Hongyu, 2010.**

1.5.13 Materials Choice

At present, many projects, especially the government projects, waterfront landscape design project like used the expensive material, such as **marble and granite**, etc. They are belonging of the natural exploitation, such materials for the maintenance and repair costs are also extremely expensive. Therefore, we encourage using regional materials, such as the regional **wood, brick and stone**. It is not only to save material costs including raw material costs and transportation costs, but also to **coordinate with the local geographic colors** and to accord with the regional aesthetic characteristics and culture. **Zhu, 2011.**

In the process of the design, it is should be considered specific and various factors, such as paving design. It can use the representative image of signs or **historical signs, and paving brick or granite** to collage out the image texture on the floor. This can be applied to a large ground and a larger image. Another method can be applied to handle details. For instance, it collages with small stone on the corner line or a small ground. This produces that the overall design is novel and unique and harmonizes with the surrounding cultural environment. That not only riches the details of design but also enhances the depth of cultural connotation. **Fig. 2, Zhu, 2011.**

1.5.14 Types of side retaining wall

The architecture and the flinty square in these areas block the soaking of the rain water and the supplement of the underground water. The cut straight of the river course and the concretes dikes destroy a dynamic natural landscape system. Although sometimes we take much count of the a forestation in the waterfront construction, we often simply replace the original rich flora with the artificial a forestation, which causes the water shore a forestation layers monotonous and destroys the diverse habitats. **Huang, 2011**.

The physical shape of water edge Divide to several types, each one of them have **unique personality**, either functionally be historical or environmental, as well as divided on the shape of that edge and physical river section where this deal affect and shape design features, such types observe in the following forms, some of which are with Boardwalk (Jetty extended) on the beach, and others are for hiking along the water, Some reuse old sidewalks located on the territory of the Park. And it all comes under the existing legislation and controls within the same edge. Help the sidewalks along the edge of the water to increase in size especially with ancient footpaths which rehabilitated for both purposes as piers and entertainment and events that do not conflict with extended downstream piers and its speed. **Burden, 2005.**

The physical section of river edge Divided into **Fig. 4**:

- **Tilt River edge**: it is easy in construction, but generates several problems including distancing human from the water and make a very sharp edge which **reduce the coherence** with the River, as well as shift vertical alleys to River to be parallel, so it make **bad connection** between city and river.
- **Vertical river edge**: strengthen interdependence between human and the river, using vertical elements like a wall works to identify the edge of the river, make projection masses overlap with a wonderful view to give the impression as alley. Overlapping masses and spaces, gardens and parks, entertainment places are all combined, gave the **good connection** between the river and the city.

2 CASE STUDIES

For the design of the edges of rivers, the research will choose some cities and way of dealing with the edges of rivers and waterfront, so explore the sense of place in their respective experience in accordance with the characteristics of the place, and will address the **(Tigris River within the historic city center of Baghdad, and Seine river in the historic center of Paris)** by applying **measured factors of urban waterfront** planning and design, by studying the case studies, the summary, conclusions, recommendations and proposals on the planning side and urban design of river waterfront.

2.1 Development of waterfront in new cities

Distinguished new cities by river edge development goals of creating a thread along the river corridor and try to attract to the river, to protect the natural environment along the River as well as the interface to reflect the specificity of River City, **Casalino, 2005** the study divides river edge into three sections for each Department has its own definition and style in design, and these handling sections are **Fig. 1**:

- **Riverbank Zone** where emphases is placed on environmental terms for the edge and protect it from erosion and to preserve the historical memory of the form and direction of movement of water, as well as the protection of biodiversity on the riverbank.
- Scope of the green route is the urban area means that at least 30 m confined between the edge of the river and the development, which use of design Landscape and garden uses that do not require the establishment of buildings **(Urban Greenway Zone**).
- **Development Zone** the area associated with the city and carried out construction and redevelopment as well as new development and diverse uses, as use zoning site providing components and elements of fields and gardens, river edge and how to deal with it, **Casalino, 2005.**

Development studies focused river edge in new cities on urban design for River waterfront, stressing the role of history and environment and transport as factors that require planning and handled according to design policies for each

range of zones. Schematic design side is concentrated along the Eastern facade of the New York City overlooking the River (Hudson), the historic importance and how to use them in connection with its surroundings through Visual motor connecting lines of the diagram, **Burden, 2005.**

2.2 Development of waterfront in historical cities

River edge is divided in historic towns and cities to different sections by its characteristics; design hand emphasizes the number of axes of the historical and environmental themes of the river, by highlighting the historical pillars on the river and its edge (such as bridges and historic sites), and use cultural and entertainment. Seek to develop an environment's edge and avoid damage, through the physical components of the river edge, **Burden, 2005**. The socially focused on how to deal with edge components through the generation of both:

- Active spaces represented by **movement spaces**.
- Quiet spaces (negative) of the **seating spaces**.

Emphasis was placed on both sides and relationship of the planning and urban design of edge, planning this tip around characters especially in historical perspective plus focus on socially side in the design through positive and negative spaces taking advantage in the provision of leisure and cultural services and attract the largest amount of people.

2.3 Waterfront of Seine River in Paris Historical city center

Since Paris City emerge with different close semantic organizations, It got one of the ancient tribes in the heart of the city, called Lutetia then Parissii and finally Paris has seen spot and inclusive planning processes have changed, altered and added a lot of morphological structure of the city, and as wide and rich urban operations.

The Seine river Traverses Paris, divided it by the (left and right), this Division has affected intellectual and social factors of Parisians — **right of capital and trade, left for culture, science and art** – and the kind of impact between the river and the city overlap between masses and spaces, giving different level of city street on the River. The kind of sense of place on the Seine River as it **represents one of the main roads** to watch Paris night and day through the many events and activities on it. Although this Division looks very simple but the impact in the development and growth of its population became part of their lifestyle, habits, and in the fabric of the entire city.(Carzou, 1982, P25-26). (Fig. 5)

2.3.1 The growth stage of waterfront inside Paris city

In the left bank there is intellectual life of the city center, a meeting of artists, writers and students. There is the first settlement of Parisii beyond the boundaries of the island, South of the river where the street St-Michel spread (which is historically belonging to the Romans) where all the buildings compact storage of masterpieces of Parisian heritage, as the University of Sorbonne and College Defrance wall on the Roman baths, and standing in the pantheon of modern Roman arena. **Carzon,1982** and **Table 1.**

Either the right bank means in Parisian society, thought, or political mettle with work only. At a time when the left bank acquired a Latin quarter with its schools and colleges, the right bank evolved as contrary. the central axis of the city extends naturally to end along the docks of the right bank. In the early nineteenth century the Halle's emerged as a counterpart to the Sorbonne, which requests from the opposite bank. And later demolished, giving place to Beaubourg and complex high-tech architecture of the Pompidou Centre, **Carzon,1982**.

The term survives, of course, in the Faubourgs St-Antoine, St- Germain and St-Honore in Paris. The merchants built their faubourgs, when they could, just outside the gates of the existing city where they would form secondary market places. As the merchants they became rich enough, and their faubourgs grew, so they too built walls or palisades. Which meant that others had to start new faubourgs outside theirs and thus the cities grew in concentric but irregular loops? So it was that close to the old ecclesiastical towns or feudal fortresses, mercantile agglomerations were constructed; **Broadbent, 1990** and **Fig. 5**.

2.3.2 The Haussmann new planning of Paris city

The most important experience changed the image of Paris is widely credited with see and reflects on the day of rich, semantic experience Baron (Haussmann) (1853-1882). His work in Paris had no such theoretical underpinning. It was a straight, **pragmatic solution to a highly**

practical problem, which Louis Napoleon put to him; of how to redevelop Paris, after the Revolution of 1848, in such a way that never again could the angry mob build barricades in the streets and lob missiles at the police from behind them, **Broadbent, 1990**. He concentrates instead on Haussmann's formidable skills of organization pointing out also that behind Haussmann's Plan there was the clear intention of focusing **'visually and functionally'** on the great monuments of Paris: the National Assembly, the Bourse, the Church of the Madeleine, the Panthéon, the Cathedral of Notre Dame, the enlarged Hôtel du Ville, the Arc de Triomphe, Garnier's new Opera House, the old Monastery of St Germain-des-Prés and so on.

And since the new railway stations of Paris were so peripheral these too were to be connected to make for more **efficient transport** between them and into the city. There were precedents for such planning in the era of the Baroque. (Broadbent, 1990, P.116)

Napoleon III, and the achievements of Baron Georges Haussmann that led to the **reintegration of the heart of Paris** and a strengthening of its interior structure on a scale commensurate with the forces of regional expansion. This reversal of the direction of energy, from outward explosion of the **avenues** and palaces of Louis Kings to the implosion of the connecting and life – giving **boulevards** of Haussmann, is one of the most dramatic in any city. Each development was devised and inspired by social and economic forces far different from those prevailing today, but each has **proved to be resilient**, to be capable of **providing a structure suited to modern needs**, **Bacon, 1978** and **Fig. 5.**

Haussmann created strong semantic relationships through Visual axes of broad boulevards, **linking significant Visual high points** in both built and non-built forms, he was intended to achieve three objectives through adoption of the Visual system, **Fig. 6**:-

- Produces the monument to spatial isolation and connects them to each other visually.
- Wipes and removes oldest and change everywhere to the images of modernity: space and light.
- Facilitates the move from station to station and from neighborhood to neighborhood.

Haussmann had derived the idea of the strong bond between the axis of the classic culture. As it is well known that the **emergences of holistic level** in the city by linking its parameters to the **visual axis** the most important baroque city properties. And with the need of Paris in urban growth phase for the type of structural adjustment, training new elements in the **Boulevards & Avenues**, which are dictated by the imperatives of links (in contradiction with the city focused on concepts such as **compartmentalization and overlap**).

So Haussmann's Boulevards by no means were designed for any kind of **intrinsic beauty**. They did indeed give long perspective views towards the major monuments and, with the various round points in front of or around they also speeded up the flow of traffic between them. But they also afforded the longest feasible sight-lines for Louis Napoleon's troops. As for the trees which seemed to humanize the boulevards it was they, above all, together with the great width of the boulevards themselves, that made barricade building difficult, **Fig. 6**.

Boulevard planning became the norm towards which most great European cities were developed, or redeveloped in the 1870s, **Broadbent, 1990** and **Table 1.**

2.4 Waterfront of Dijla River in Baghdad Historical City Center

The historical city of Baghdad chose it location on the river. In the ancient the beautiful urban design along the river and the **connected two sides (Karkh & Rusafa)** has formed the urban pattern. Thus the Baghdad city becomes alive with the water, and the water charms because of the urban inverted reflection. The city and the water shine on each other, wherein the unique urban reflection culture is formed.

Perceptions of the old city and river edge, Built on the schematic side through the roles of history and environment in a street movement's relationship with the river and its edge, where the **streets perpendicular to the river and not paralleled** by through alleys, and **linking important architectural icons and monuments** of the River through the incision extended alleys.

To provide initial scenarios to deal with the planning of river edge of Baghdad according to history (environment, planning standards, movement problem) need in-depth studies of the policies to deal with waterfront urban design. Focusing on the planning of the waterfront alone Tigris River in central Baghdad, which depende on land use according history and technology, as a basis for waterfront design **without any effect**

to the historical architectural values (archaeological & heritage), **Table 1**.

2.4.1 The situation of waterfront inside Baghdad city

Tigris River is one of the most important monuments of Baghdad city, where the River runs through this historic city from North to South. The length of the **Tigris River in Baghdad (52,300) km** starting from the tourist island of Baghdad in the Tarmiyah area to the south of Diyala River estuary.

It features within the city there are a number of bends and twists as well as three distinct Islands (tourist island of Baghdad and Al Aaras Island and Abu Rmeal island), these Permanent islands which divide the river bottom to unequal parts. **Euphrates Center, 1998**. Flowing water levels change over time, so emerged from a process of **coatings for the Tigris River**, which began at the **end of the 1990s**.

The width Changes of the River in the center of the city to be the limits of **190 meters in the rectum**. To be cut relatively narrow in this part, and an advanced development should be good type protection of the banks of the to prevent erosion in the upper parts of this section. **Euphrates Center, 1988.**

2.4.2 Rusafa Development project - Japanese Consultants JCP in 1984

The study focused on planning terms based on the historical side of the region in the planning of several aspects, reviving old traffic hubs and connect them with the modern movement as metro areas, as well as on **historic buildings the river edge and revive it.**

The markets represent an essential element of traditional urban life for Baghdad. The target is to **reintegrate the architectural value of the market system and restore the central axis**, for example the direction beginning on the river side nearly the Al Shohadai bridge till al-Kilani mosque, **JCP, 1984.**

However, this study came in the urban planning aspect and not to the river edge, as well as it did not address the urban design of River waterfront.

2.4.3 Karkh development project - office of alusi technical advice in 1982

The study focused on planning terms based on a number of factors working in the **social, economic and historic as well as traffic and transport,** the study was an evaluation of all criteria within a chart.

The project is based on the development of Karkh on the traditional **opening of the market to the river** with a large interface and coming in some parts inside to relive the most powerful river, **Alusi, 1982.**

2.4.4 Baghdad Municipality; Integrated capital development plan of Baghdad 2015, 1998

The report addresses the review and update of studies and designs developed by foreign institutions to re develop the city of Baghdad. This report addressed the waterfront in two chapters: Chapter IV-III **(waterfront in the City Center).**

It offers to the waterfront of River in the city centre and the area between Bab Al-Mu'azzam District Bridge to Aljamuria Bridge on the South, highlighting the most important disadvantages of City River and relation of movement and edge design (waterfront) contains the following:

- The **absence of open spaces** bordering the River dedicated to public use, recreation and tourism.
- **Absence of pedestrian corridors** as there are streets in the river bank (as in the Abu Noas) overlooking the River.
- **Lack of clear focus of traffic links between open spaces for historic buildings** overlooking the River.
- **Lack of clear architectural style** leading to confusion in the elevation of waterfront.

With regard to section III study indicates **neglect the river and design of waterfront in several levels** including **access and openness to the river and the absence of an informed and transfer to river edge**, about **abuses function of river and waterfront**, **Baghdad Municipality, 1998.**

2.4.5 Kirkpatrick , Scott Wilson: Baghdad comprehensive transport study: 1982

The study focused on the **movement of various kinds and the relationship** between those different types, but **did not clarify the relationship with the river traffic and the performance edge** that was to transport goods or persons as tourists and daily transportation and organization shape and its relationship with other transaction types. So it point to the absence of a river where the use of river traffic controls in

their stations and their interdependence with other traffic types, **Kirkpatrick, 1982.**

2.4.6 Ministry of irrigation, preventing edge of Digjla river, 1998

River edge investment process is one of the most important means, by which edge is preserved and maintained. through previous studies and study the edge of the Tigris River, the process of maintaining the stability of the river course is important not only in the process of preserving the River, but to develop its edge and maintain static areas have managed to deal with various types of physical as well as the **preservation of the natural environment of the erosion and sediment** to water streams and affecting agriculture.

So, emerged from the Tigris River finishing at the end of 1990s which was a comprehensive study with a view to **identifying a refinement** to the Tigris River in Baghdad, identify abuses occurring and the impact of the abuse on the line and examine the absorption of the River to flood the vicissitudes of time.

The study included many axes to define discipline line the river within the city and the results of studies that attributed the discharge is expected when it pass (35, 30 m) in the South and North of Baghdad sites (31, 34 m) and (37, 70 m), respectively, **Euphrates Center, 1998.**

2.4.7 Comprehensive development planning Baghdad 2030 - Qateeb & Alame and PCI Japanese consultants - 2010

The objective of the project development plan of the city of Baghdad, deal this city as an integrated **environment includes all aspects of social, economic, environmental, administrative**, and other aspects, beyond the current building to meet the needs of their citizens.

Includes a series of **strategic interventions in the fabric** of the city, take into account the relationship between the center of Baghdad and its immediate environment, as well as between the city of Baghdad and its suburbs adjacent to it, especially for projects that are currently being implemented there.

The functions of the draft comprehensive development plan for the city of Baghdad in 2030, consists of and focusing on the following elements: (land use, planning, management of growth, The environment, Natural resources in and outside the city, entertainment, social resources, The historical and cultural resources, Housing. Transport, Infrastructure services, The development of the economy, Guiding principles for urban design).

Although the Comprehensive development planning Baghdad 2030 complete the three stages and prepare for fourth stage, but it is important for a new study for developing of greater Baghdad, and **historical city center and waterfront treatments which till now not appears with details**. (Qateb, 2010, CD Rom)

3 CONCLUSIONS

- According to the result gain from (table 1), The emergence of many problems on the level of urban planning and urban design for reality of river edge in Baghdad, which faced waterfront of Baghdad historical city center, needed to taken in the studies especially in the Comprehensive development planning Baghdad 2030.
- During the historical city urban design, it should make scientific and reasonable layout on near-water environment, creating conditions for reaching each good performance for city; coordinate the normal operation between human construction and natural ecology, setting up a balanced ecological system; pay attention to the mutual connection between city and water, making water system involved in the city environment; respect local culture, create local character, and the harmonious water environment between human and water.
- Produce many facilities in the Baghdad water edge as public domain for everyone to use them as equal, without distinction of party at the expense of the other, and is open at all times. Encourage people to increase their pass throw water edge by creating attractive elements for different slides.
- Create linkages along Tigris river waterfront and continuity with the surroundings edge of land, water and urban context (Karkh & Rusafa).
- Affect physical shape of river edge and the section on the feasibility form of usage and design result. The vertical edge best than Tilt edge in creating Visual and motion connection as follows between the city and the River (the River work as alley), with control of water level.
- In the contemporary society, the roles and missions of urban waterfront urban design should be not just creating and promoting the aesthetic quality of urban environment, but

also integrate the local human environment, ecological quality and the public awareness. This creates that cultural landscape and its promotion will become an effective approach to contribute to better material life and spiritual life of citizens.

- Promote activities of the walk on the river edge to the city and create a set of visual communication points during public space and distribution of furniture, lighting and landscaping.
- Take advantage of sidewalks in river edge and more space to deal with different levels providing River sessions of shelters and ceiling with various visual sights.
- Bridges and pillar located across the River in the usual impediments to traffic, so the area under the bridge (part of river edge) must be designed, so as to allow the space under the bridge to diverse uses along the river and link with neighboring river edge parts, and providing means of access to river boats.
- There are many established and temporary Islands did not invest well on the level of urban planning and urban design to develop of the Baghdad city.
- One of the big problems is the establishment of river edge as car parking which cut the human connection with the river.
- Lack of open spaces and overlooking the river for recreation and tourism, because of the lack of clarity of the main axes of movement up to this space.
- There are many irregular anchors on the edge of Tigris river , which not connected with other types of movement, so for the revival of river transport requires the characterization and the duties of the transport and link it with other types of transport through the study of traffic
- Tigris river suffer from significant pollution due to throw various and waste accumulation.
- The locating waterfront away from the edge of River (15) meter from the river without any investment or building or even to provide the possibility of intervening to avert the danger of flooding and the forbidden River led to many problems including the weak building view on the River and connecting with context of city.
- The wide width of Tigris river and problems of water level control increased the separation of both edges of the Al Rusafa and Al-Karkh. In Baghdad's old layout there was interaction between the city and the River through the visual and motional axes and flowing into the River, and through the overlapping blocks and spaces with Riverbed. Which is lacking at the present time, bringing a sense of place for the Tigris River is very weak and seeing River only when crossing bridges.

4 RECOMMENDATIONS

- Cancelling the law of not allowing development in areas where the proportion of Tilt edge 20% gradient and the proposed design to keep them as green areas only, generating problems in the River facade on the urban context of the city.
- Establish organization to solve problems in the construction of the Iraqi waterfront area. Like Common problems are monotonous content, formulate style and non-innovative landscape because of the limited understanding of the designers and finance issues of local government.
- Solve problems of the waterfront urban design which is being built in the most of cities, it only regarded as a project, focusing on certain utilitarian values such as architecture, urban design, social requirement, economical requirement, flood control, water transport, irrigation, etc. It is not involved in the public space design systematically and scientifically, but also lack of considerations of people's physical and psychological needs. This leads to alienate, blunt, cold, non-innovative in design. Moreover, in some developed cities, the government has put a lot of money in the construction of the waterfront area for more reasonable and modernized design. However, this design is lack of local cultural characteristics, and not be able to enrich the historical and human spirit on the basis of functions, which causes the method of copying and formulating, lacking connotation and vitality.
- Iraqi's ancient people focused on "water body" concept and believed. Therefore, the city's location and layout were associated with water. Nowadays, on the re-construction of old waterfront area, we have to face the problems of transformation of buildings and water environment in this region. The most important of urban waterfront cultural design should protect and re-use all round the existing historic buildings.

5 REFERENCES

- Alous, Maath; Muller, Manfred, 1982: "*Al Karkh Redevelopment Study: Baghdad Municipality"*.
- Bacon, Edmund, 1978 : "*Design of Cities*" Thomas and Hudson, London, England.
- Baghdad municipality, Baghdad University, 1998, "Urban Development Project for the City of Baghdad 2015": the first phase, Baghdad municipality.
- Broadbent, Geoffrey, 1990, "*Emerging Concepts in Urban Space Design";* Van Nostrand Reinhold, London.
- Burden, Amanda, 2005, "*Transforming the East River Waterfront"*, the city of new York, department of design.
- Casalino, Denise,2005, "*Chicago River Corrido"*, Department of Planning and Development .
- Carzou , J.m ; Paris,1982, Larousse , France.
- Euphrates Center, 1998, "*Fine Tune of the Tigris River Banks",* the first stage, Euphrates Center to study designs of irrigation projects, Ministry of agriculture and irrigation.

- Euphrates Center, 1988, "*Refinement of the Tigris River in Baghdad: Euphrates Center for Studies and Designs of Irrigation Projects*", Department of studies and projects, Ministry of agriculture and irrigation, Iraq.

- Hongyu 1, Zhao, Ruhai 2, Yu, 2010, "*Urban Waterfront Greenway System for Flood Prevention and Hazard Reduction",* 2010 Second IITA International Conference on Geosciences and Remote Sensing, Harbin Institute of Technology Shenzhen Graduate School, Shenzhen, CHINA, p.185- 189. IVSL.

- Huang, Jiangwen, 2011," *Landscape Design of Urban Waterfront"*, Design Department, Guilin University of Electronic Technology. Guilin, Guangxi, China, p.1162-1164. IVSL.

- JCP, Japanese consultant, 1984, "*Al Rusafa Redevelopment Project"*: Baghdad Municipality.
- Kirkpatrick , Scott Wilson, 1982, *Baghdad Comprehensive Transport Study*.

- Nickels, Greg, 2006, "*Seattle's Central Waterfront Concept Plan"*. Department of Planning and Development.
- Qateb and Alame, 2010 "*The Comprehensive Development of the city of Baghdad in 2030*", CD Rom, Baghdad Municipality, Baghdad, Iraq.
- Samant, S,2010, "*Reflections on Water: Architectural Manifestations in the Historic and Cultural Quarter along Lake Pichola in Udaipur";* Department of the Built Environment, University of Nottingham, UK, p. 27-32. IVSL.
-
- Zhu, Jie, 2011, "*Urban Waterfront Landscape Cultural Design Studies*", Institute of Urban Design Wuhan University Wuhan,China, p. 6564- 6567. IVSL.

Table 1: Comparative factors of waterfront between two cities, **Author, 2013**.

		Measured factors	Measured cities	
			Baghdad	**Paris**
3.5 The components of the waterfront	*3.5.1*	*Land Use*	Privet or without facilities	Public facilities
	3.5.2	*Activities*	Not attractive facilities	Attractive facilities
	3.5.3	*landscape & Plant design*	Not cooperated with urban design	Trees as part of urban design
	3.5.4	*Built Form*	As wall without penetration	As wall with penetration
	3.5.5	*Sidewalk design*	Not available	Available
	3.5.6	*Façade*	Set back from edge of the river	There are cantilevers somewhere on edge of the river
	3.5.7	*Public facilities design*	car parks & markets	Streets and culture facilities
	3.5.8	*Streets and Squares*	Separated from river	Intersection with river
	3.5.9	*Parks*	No parks	Open parks overlook with river
	3.5.10	*Monument & art sculpture*	Rare available	Available everywhere
	3.5.11	*Slips*	No equipments make integration between human and water	Many equipments make integration between human and water
	3.5.12	*Under bridge*	Negative and useless space	Space as part of waterfront
	3.5.13	*Materials choice*	Entering new artificial materials with brick	Still using stone as traditional material
	3.5.14	*Types of side retaining wall*	Tilt retaining wall	Vertical retaining wall

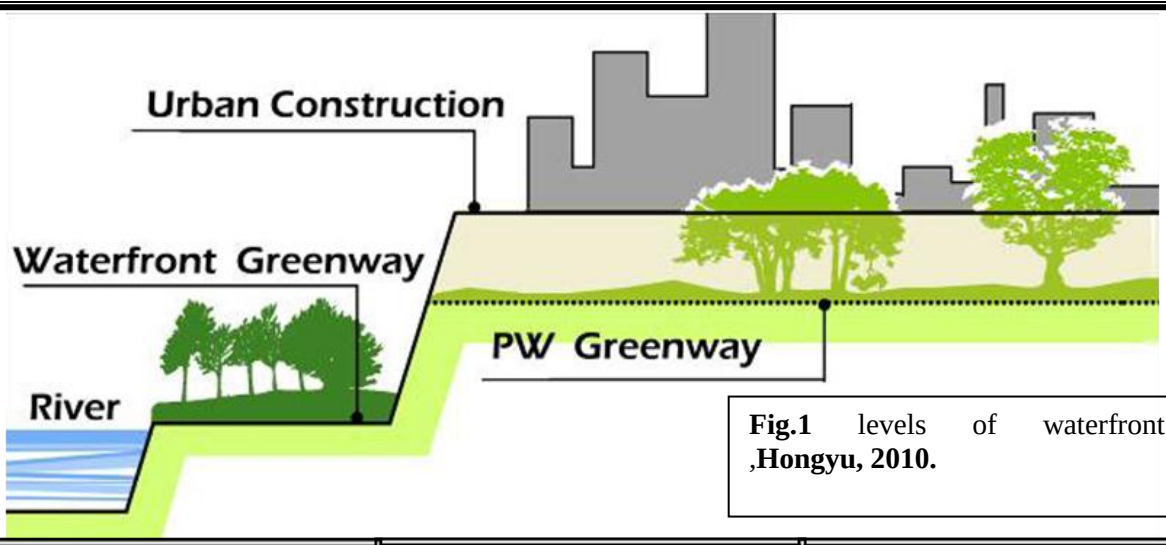

Fig.1 levels of waterfront ,**Hongyu, 2010.**

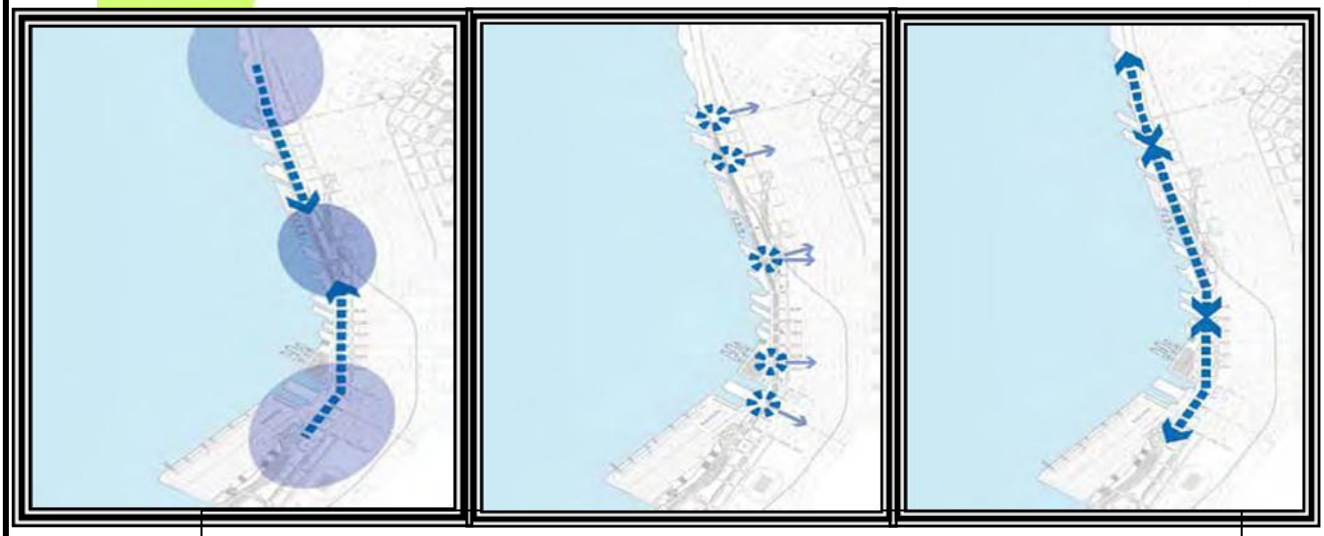

Figure 2. Alternative planning strategies of waterfront, **Nickels, 2006**.

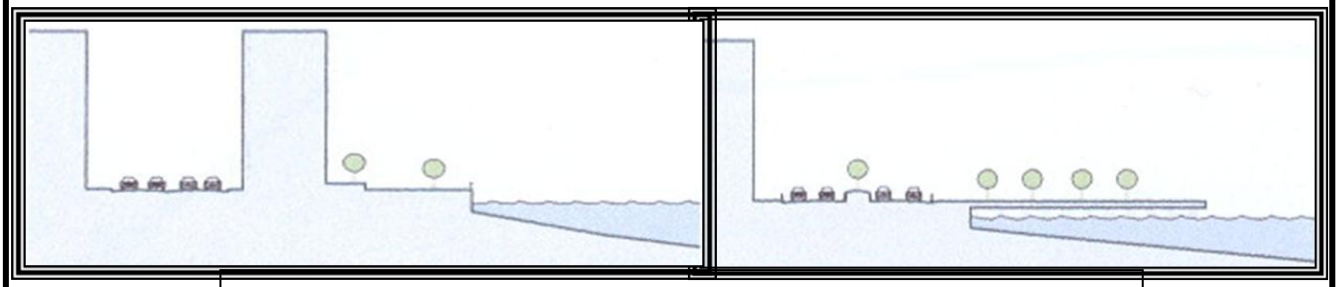

Figure. 3 The river edge and its relation with water, **Burden, 2005**.

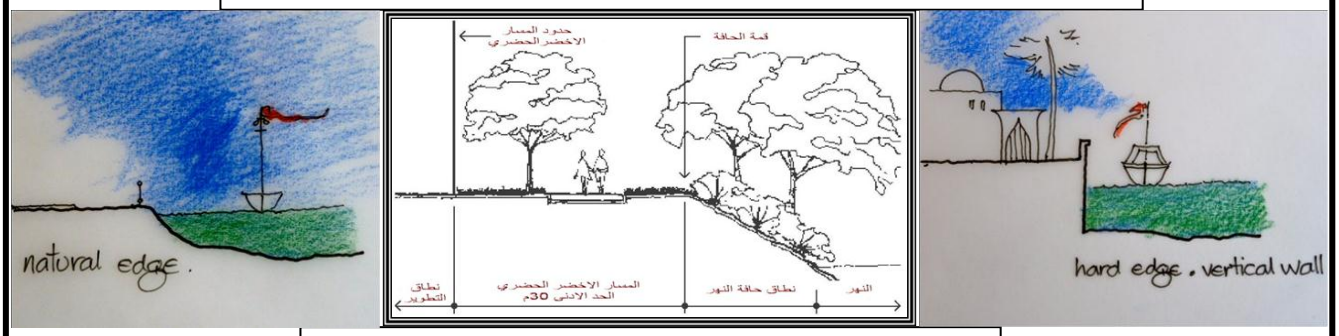

Figure4. Types of river edge**, Casalino, 2005.**

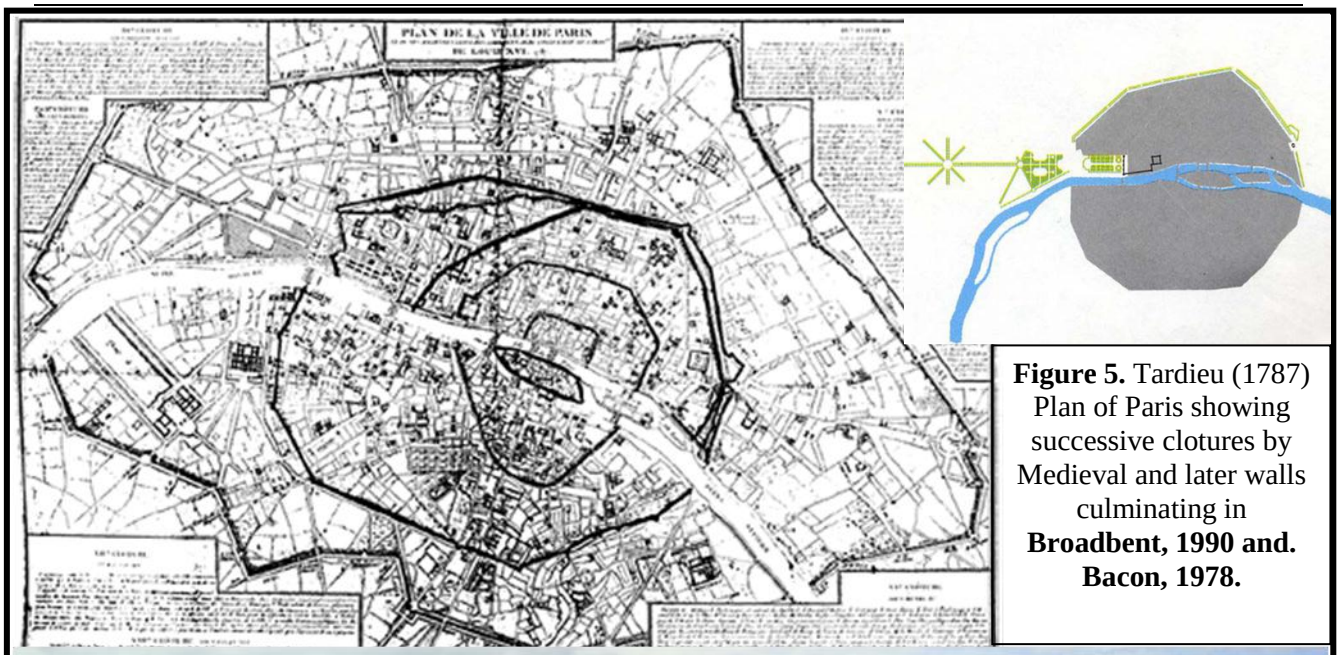

Figure 5. Tardieu (1787) Plan of Paris showing successive clotures by Medieval and later walls culminating in **Broadbent, 1990 and. Bacon, 1978.**

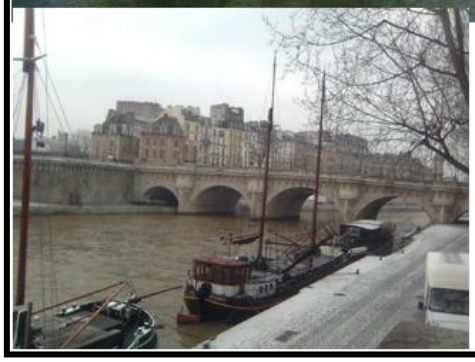

Figure 6. Paris waterfront treatments with vertical retaining wall edge and public facilities, **Author, 2010.**

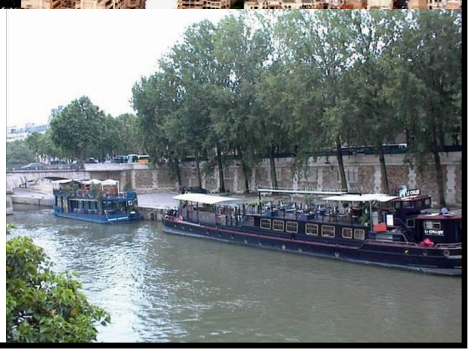

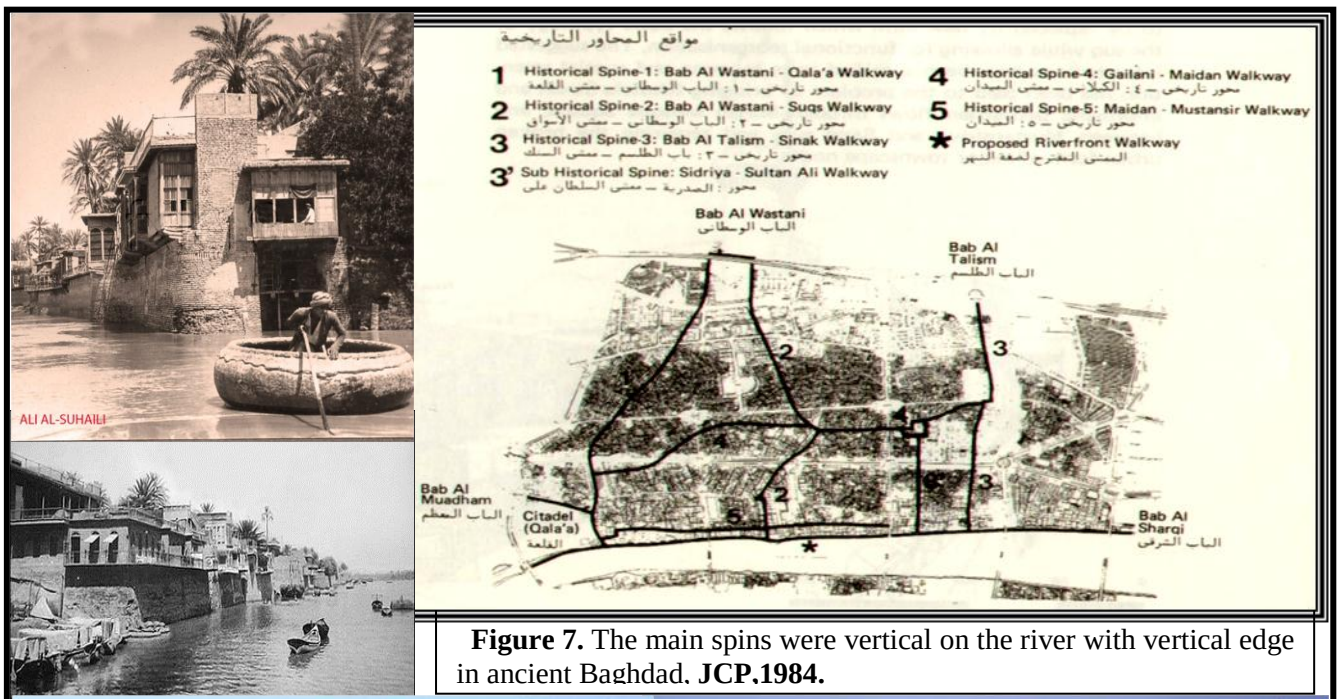

Figure 7. The main spins were vertical on the river with vertical edge in ancient Baghdad, **JCP,1984.**

Figure 8. Baghdad waterfront treatments with tilt retaining wall edge and neglected public facilities without clear paths**, Author, 2010.**

قائمة المحتويات

القسم العربي: